LEABHARLANN CHOLÁISTE NA TRÍONÓIDE, BAILE ÁTHA CLIATH | TRINITY COLLEGE LIBRARY DUBLIN
Ollscoil Átha Cliath | The University of Dublin

Terms and Conditions of Use of Digitised Theses from Trinity College Library Dublin

Copyright statement

All material supplied by Trinity College Library is protected by copyright (under the Copyright and Related Rights Act, 2000 as amended) and other relevant Intellectual Property Rights. By accessing and using a Digitised Thesis from Trinity College Library you acknowledge that all Intellectual Property Rights in any Works supplied are the sole and exclusive property of the copyright and/or other IPR holder. Specific copyright holders may not be explicitly identified. Use of materials from other sources within a thesis should not be construed as a claim over them.

A non-exclusive, non-transferable licence is hereby granted to those using or reproducing, in whole or in part, the material for valid purposes, providing the copyright owners are acknowledged using the normal conventions. Where specific permission to use material is required, this is identified and such permission must be sought from the copyright holder or agency cited.

Liability statement

By using a Digitised Thesis, I accept that Trinity College Dublin bears no legal responsibility for the accuracy, legality or comprehensiveness of materials contained within the thesis, and that Trinity College Dublin accepts no liability for indirect, consequential, or incidental, damages or losses arising from use of the thesis for whatever reason. Information located in a thesis may be subject to specific use constraints, details of which may not be explicitly described. It is the responsibility of potential and actual users to be aware of such constraints and to abide by them. By making use of material from a digitised thesis, you accept these copyright and disclaimer provisions. Where it is brought to the attention of Trinity College Library that there may be a breach of copyright or other restraint, it is the policy to withdraw or take down access to a thesis while the issue is being resolved.

Access Agreement

By using a Digitised Thesis from Trinity College Library you are bound by the following Terms & Conditions. Please read them carefully.

I have read and I understand the following statement: All material supplied via a Digitised Thesis from Trinity College Library is protected by copyright and other intellectual property rights, and duplication or sale of all or part of any of a thesis is not permitted, except that material may be duplicated by you for your research use or for educational purposes in electronic or print form providing the copyright owners are acknowledged using the normal conventions. You must obtain permission for any other use. Electronic or print copies may not be offered, whether for sale or otherwise to anyone. This copy has been supplied on the understanding that it is copyright material and that no quotation from the thesis may be published without proper acknowledgement.

ON THE MOLECULAR GENETICS OF HEREDITARY DEGENERATIVE RETINOPATHIES

A Thesis Submitted to the University of Dublin for the Degree of Doctor of Philosophy

by

TRINITY COLLEGE
0 2 JUN 2004

Aileen Mary Aherne
Department of Genetics
University of Dublin
Trinity College

PhD Thesis

October 2003

TRINITY COLLEGE
02 JUN 2004
LIBRARY DUBLIN
THOSIS
7967
7506

DECLARATION

This thesis has not been previously submitted to this or any other university for examination for a higher degree. The work presented here is entirely my own except where noted. This thesis may be made available for consultation within the university library. It may be photocopied or lent to other libraries for purposes of consultation.

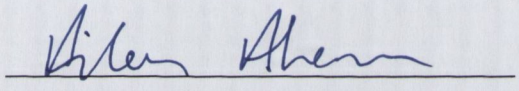

Aileen Aherne

31st October, 2003.

❖ *Acknowledgements* ❖

Thanks firstly to my supervisor Pete for his constant support and guidance and for giving me the opportunity to work in such a great lab. Massive thanks have to go to Avril, who has basically taught me everything! Thanks so much Avril for reading my thesis, for the never-ending help and discussions and for being such a good friend since day one of my PhD. There are so many people to thank in the lab-I hope I don't forget anyone. Special thanks have to go to Niamh, Brian and Sophie who were so kind and welcoming when I first started in the lab and have been great friends ever since. Thanks to Jane, Paul, Marian, Mary and Sophia for all their help and support. The entire Ocular genetics gang have been wonderful, so thanks to Fiona, Alison, Helena, Therese, Alex, Danny, Gearoid, Sarah, Sylvia, Arpad, Mandy and all the other members of the lab, past and present, everyone has helped in some way. A special mention for our honorary lab member Carmel, who has left us but has not been forgotten, thanks for all the chats and pints! There are so many more people to thank in the Genetics department, too many to mention, but thank you all.

I would like to thank all our collaborators who have contributed to the work described in this thesis, especially Steve Daiger and Sara Bowne in Texas who have been really helpful for many discussions on RP10. Thanks to Paul Engel in UCD who was extremely helpful with the enzyme activity work, and to the many members of the lab who have helped with different techniques, especially Sarah for help with tissue culture, Fiona for help with the Westerns and Mary for help with cloning work. Thanks also to the clinicians who provided DNA samples for analysis and we are especially grateful to all the families who participated in these studies.

On a personal level I have to thank all my friends who have been so understanding (and generous) over the last four years, my fantastic cousins Claire and Nicola, my good friends Shox, Sullie and Ollie and the whole Galway crew, too many to name. Special thanks to my best friend Catherine, who I've known for over 22 years now -who would have thought we'd finish our PhDs within two weeks of each other! Thanks to my housemates past and present, especially Karen and Corina for putting up with me over the years. My family and extended family have been particularly amazing and supportive, especially my sisters Emer and Molly, the best sisters a girl could have, and not forgetting my brother Patrick. Last of all, but most importantly, thanks to my wonderful parents, who have always supported and encouraged me in whatever I wanted to do. Thanks for everything Mum and Dad, I'll repay you some day!

TABLE OF CONTENTS

	Page
Title page	I
Declaration	II
Acknowledgements	III
Table of contents	IV
List of tables	X
List of figures	XII
Summary	XVI
Publications	XVIII
Abbreviations	XIX

CHAPTER 1: GENERAL INTRODUCTION 1

1.0 INTRODUCTION 2

1.1 THE EYE AND VISION 3

1.1 1 The eye 3

1.1.2 The retina 3

1.1.3 The photoreceptors 5

1.1.4 Visual transduction 6

1.1.5 The retinoid cycle 8

1.2 HEREDITARY DISEASES OF THE RETINA 10

1.2.1 Retinitis pigmentosa 10

1.2.1.1 Syndromes incorporating RP 11

1.2.2 Leber congenital amaurosis 12

1.2.3 Cone dystrophies 12

1.2.4 Congenital stationary night-blindness 13

1.2.5 Macular dystrophies 14

1.3 IDENTIFICATION AND ANALYSIS OF RETINAL DEGENERATION GENES 17

1.3.1 Identification of disease-causing genes 17

1.3.2 Characterisation and screening of candidate genes 19

1.3.3 Elucidation of disease mechanisms in retinal disease 20

1.3.3.1 Methods of studying disease mechanisms in retinal disease 21
1.3.3.2 Mouse models 22
1.3.4 Proposed mechanisms of retinal degeneration 24
1.3.5 Therapy of inherited retinal disease 25
1.4 THE AIMS OF THIS THESIS 28

CHAPTER 2: ANALYSIS OF MITOCHONDRIAL DNA SEQUENCE IN ATYPICAL USHER PATIENTS 29

2.1 INTRODUCTION 30
2.1.1 Introduction 30
2.1.2 Usher syndrome 30
2.1.3 Genetics of Usher syndrome 31
2.1.4 Family ZMK 32
2.1.5 The mitochondrion 33
2.1.6 Mitochondrial mutations and disease 34
2.1.7 Mitochondrial mutations affecting tRNA genes 35
2.1.8 Mitochondrial tRNA mutations involving RP and/or deafness 37
2.1.9 The aim of the study 38
2.2 MATERIALS AND METHODS 39
2.2.1 PCR Amplification 39
2.2.2 Agarose gel electrophoresis 39
2.2.3 Purification of PCR products 40
2.2.4 Automated sequencing 40
2.2.5 Direct sequencing 41
2.3 RESULTS 42
2.3.1 Mitochondrial tRNA screening in Usher patient DNAs 42
2.3.2 PCR amplification and sequencing reactions 45
2.3.3 Mitichondrial tRNA variants identified 47
2.4 DISCUSSION 48
2.5 CONCLUSION 49

CHAPTER 3: COMPARATIVE MICROARRAY ANALYSIS OF WILD-TYPE AND *RHO-/-* RETINAS 50

3.1 INTRODUCTION 51

3.1.1 Introduction 51

3.1.2 Rhodopsin knockout mouse 51

3.1.3 Microarray analysis 52

3.1.4 Studies on global gene expression in the retina 54

3.1.5 Microarray analysis for disease gene discovery 56

3.1.6 Validation of microarray studies 57

3.1.7 The aim of the study 58

3.2 MATERIALS AND METHODS 59

3.2.1 RNA extraction 59

3.2.2 cRNA preparation 59

3.2.3 CHIP analysis 59

3.2.4 Data analysis and selection of candidate genes 60

3.2.5 Databases used in analysis of microarray data 61

3.2.6 Quantitative RT-PCR analysis 61

3.3 RESULTS 62

3.3.1 Microarray based transcriptional analysis of wild-type and *Rho*$^{-/-}$ retinas 62

3.3.2 Quantitative PCR analysis 63

3.3.3 Differentially expressed genes that map to retinopathy loci 65

3.3.4 Genes showing significant changes in transcription level in *Rho*$^{-/-}$ retinas 68

3.3.5 General features of down-regulated genes 72

3.3.6 General features of up-regulated genes 74

3.4 DISCUSSION 76

3.5 CONCLUSION 78

CHAPTER 4: THE STORY OF RP10

Candidate gene screening and identification of disease-causing mutation within the IMPDH1 gene 79

4.1 INTRODUCTION 80

4.1.1 Introduction 80

4.1.2 Clinical features of retinitis pigmentosa 80

4.1.3 Diagnosis of retinitis pigmentosa 82

4.1.4 Genetics of retinitis pigmentosa 83

4.1.5 Autosomal dominant RP 84

4.1.6 Autosomal recessive RP 87

4.1.7 X-linked RP 88

4.1.8 A locus for adRP on chromosome 7q31 (RP10) 89

4.1.9 Identification of candidate RP10 genes 91

4.1.9.1 Human genome resources 92

4.1.9.2 Rhodopsin knockout mouse 93

4.1.9.3 Expressed sequence tags (ESTs) 94

4.1.10 Methods used in screening candidate RP10 genes 95

4.1.11 The aim of the study 96

4.2 MATERIALS AND METHODS 97

4.2.1 PCR for DHPLC analysis 97

4.2.2 Extraction of RNA from mouse retinas 97

4.2.3 Reverse transcriptase PCR (RT-PCR) 98

4.3 RESULTS 99

4.3.1 Identification of candidate RP10 genes 99

4.3.2 Analysis of candidate gene expression in the retina 100

4.3.3 Screening candidate RP10 genes 101

4.3.4 GRIP-domain gene 103

4.3.4.1 Screening the GRIP-domain gene 105

4.3.5 Cyclophilin-like gene 106

4.3.6 Zinc-finger gene 107

4.3.7 Blue cone opsin gene (OPN1SW) 107

4.3.8 Inosine monophosphate dehydrogenase, type 1 (IMPDH1) gene 108

4.3.8.1 Screening IMPDH1 in family FA-84 108

4.3.8.2 DHPLC analysis of IMPDH1 exon 7 109
4.4 DISCUSSION 112
4.5 CONCLUSION 114

CHAPTER 5: MOLECULAR MECHANISMS IN IMPDH1-BASED RETINITIS PIGMENTOSA 115

5.1 INTRODUCTION 116
5.1.1 Introduction 116
5.1.2 IMPDH1 mutations identified in retinitis pigmentosa 117
5.1.3 IMPDH sequence conservation across species 118
5.1.4 Function of IMPDH 118
5.1.5 IMPDH protein structure 120
5.1.6 IMPDH enzyme activity 121
5.1.7 *Impdh1*$^{-/-}$ knockout mouse model 122
5.1.8 Molecular methods for analysis of protein function and properties 122
5.1.9 The aim of the study 123
5.2 MATERIALS AND METHODS 124
5.2.1 Preparation of competent cells 124
5.2.2 Transformation of XL-1 Blue cells 124
5.2.3 Plasmid DNA isolation 125
5.2.3.1 Boiling minipreps 125
5.2.3.2 Maxipreps 125
5.2.4 Construction of pET15b-IMPDH1 vector 126
5.2.5 Site-directed mutagenesis 126
5.2.6 Expression of wild type and mutant His-tagged IMPDH1 in *E.coli* 127
5.2.7 Purification of His-tagged IMPDH1 127
5.2.8 Protein quantification 128
5.2.9 SDS-PAGE analysis and Coomassie blue staining 128
5.2.10 Enzyme activity assay of recombinant IMPDH1 proteins 128
5.2.11 Construction of mammalian expression vectors 129
5.2.12 Mammalian cell culture techniques 130
5.2.13 Transient transfection of mammalian cells 130

5.2.14 β-galactosidase assay for assessment of transfection efficiency 131
5.2.15 Isolation of cellular compartment protein fractions 131
5.2.16 Western blot analysis of protein extracts 132
5.3 RESULTS 133
5.3.1 Expression of wild-type and mutant IMPDH1 proteins in *E. coli* 133
5.3.2 IMPDH1 enzyme activity assay 134
5.3.3 Analysis of wild-type and mutant IMPDH1 in mammalian cells 136
5.3.4 Computer modelling studies on IMPDH1 137
5.3.5 *Impdh* expression in the mouse retina 138
5.3.6 Retinal structure and function in *Impdh1*$^{-/-}$ mice 139
5.4 DISCUSSION 141
5.5 CONCLUSION 144
5.6 FUTURE WORK 145

REFERENCES 146

APPENDIX A: Stock solutions 175
APPENDIX B: Primer sequences 182
APPENDIX C: Cloned and/or mapped genes causing retinal diseases (adapted from the RetNet database) 187

LIST OF TABLES

Page

Table 2.1. (A) Clinical summary of 19 atypical Usher samples in which all tRNA genes were screened for mutations. 44

Table 2.1. (B) Available clinical data for additional DNA samples screened for C12258A and T4336C variants only. 44

Table 2.2. Location of 22 tRNA genes in the mitochondrial genome and amplification primer names. 46

Table 2.3. Variants in mitochondrial tRNA gene sequences identified in a study of atypical Usher patient DNAs. 47

Table 3.1. Validation of fold changes observed for a number of genes in the microarray analysis using relative quantitative RT-PCR. 64

Table 3.2. Differentially expressed genes identified in a comparison between wild-type and *Rho*$^{-/-}$ mouse retinas, that map to known human retinal degeneration loci. 67

Table 3.3. (A) Genes showing down- regulation of expression in a microarray comparison between Wild-type and *Rho*$^{-/-}$ mouse retinas. 69

Table 3.3. (B) Genes showing up-regulation of expression in a microarray comparison between Wild-type and *Rho*$^{-/-}$ mouse retinas 70

Table 3.4. Functional groups of genes showing differential expression in a microarray comparison between wild-type and *Rho*$^{-/-}$ mouse retinas. 71

Table 4.1. Thirteen loci for autosomal dominant RP. 86

Table 4.2. RP10 candidate genes screened using DHPLC analysis. 111

Table 5.1. Spectrum of IMPDH1 substitutions identified in RP patients. 117

Table 5.2. Previously reported enzyme activity measurements for IMPDH. 121

Table 5.3. Specific enzyme activities and kinetic constants calculated for IMPDH1 wild-type and mutant enzymes. 135

LIST OF FIGURES

Figure 1.1. Histological cross section through a mouse retina.

Figure 1.2. Schematic representation of neuronal cell types in the retina.

Figure 1.3. Diagram of a photoreceptor cell in the human retina.

Figure 1.4. Schematic representation of visual transduction.

Figure 1.5. Diagrammatic representation of the retinoid cycle.

Figure 2.1. Diagrammatic representation of the mitochondrial gene map.

Figure 2.2. Representation of the cloverleaf structure of mitochondrial tRNA $^{Leu(UUR)}$.

Figure 2.3. Automated sequence analysis of mitochondrial tRNA genes in atypical Usher patient DNA samples.

Figure 2.4. Direct sequence analysis of mitochondrial tRNA genes in atypical Usher patient DNA samples.

Figure 3.1. Retinal histology of wild-type (Wt) and *Rho*$^{-/-}$ mice.

Figure 3.2. Comparison between the number and extent of genes up-regulated from wild-type to *Rho*$^{-/-}$ retina, and those down-regulated.

Figure 3.3. Quantitative PCR analysis comparing expression of *GAPDH* in Wild-type (Wt) and *Rho*$^{-/-}$ mouse retinal cDNA.

Figure 3.4. Quantitative PCR analysis comparing the expression of the *IMPDH1* gene in Wild-type (Wt) and *Rho*$^{-/-}$ mouse retinal cDNA.

Figure 4.1. Fundus photography of a normal and RP retina.

Figure 4.2. ERG analysis of normal and RP retinas.

Figure 4.3. Visual field testing in normal and RP patients.

Figure 4.4. Pedigree for the adRP family FA-84.

Figure 4.5. Schematic illustration of the RP10 region on chromosome 7q31.

Figure 4.6. The RP10 locus on chromosome 7q31-32 as viewed using the UCSC Human Genome Browser.

Figure 4.7. The RP10 region as viewed using the Human Genome Browser (July 2003 release).

Figure 4.8. A view of the RP10 locus using the Ensembl Genome Browser.

Figure 4.9. RT-PCR on RNA extracted from wild-type and *Rho*$^{-/-}$ mouse retinas.

Figure 4.10. Summary of results obtained following BLAST homology analysis of the *Ensembl*-predicted GRIP-domain gene.

Figure 4.11. PCR analysis of a human retinal cDNA library to detect expression of a candidate GRIP-domain gene.

Figure 4.12. RT-PCR analysis on RNA extracted from wild-type and *Rho*$^{-/-}$ mouse retinas to detect expression of GRIP- domain gene.

Figure 4.13. Melting curve report for the GRIP-domain gene exon 1-2.

Figure 4.14. DHPLC analysis of exon 1-2 of a candidate GRIP-domain gene.

Figure 4.15. Automated sequence analysis of exon 1-2 of the GRIP-domain gene in DNA from family FA-84.

Figure 4.16. Schematic representation of the *IMPDH1* gene exon structure.

Figure 4.17. Automated sequence analysis of exon 7 of the *IMPDH1* gene.

Figure 4.18. Clustalw alignment showing partial nucleotide and protein sequences of IMPDH from different species.

Figure 4.19. Melting curve predicted by WAVEmaker software for *IMPDH1* exon 7 sequence.

Figure 4.20. DHPLC analysis of *IMPDH1* exon 7 PCR products from Family FA-84.

Figure 4.21. Automated sequence analysis of *IMPDH1* exon 7 in an FA-84 individual showing a pathogenic mutation and polymorphic variant.

Figure 5.1. Alignment of IMPDH protein sequences from a range of organisms.

Figure 5.2. Schematic representation of the guanine nucleotide biosynthetic pathway.

Figure 5.3. Structure of human Type II IMPDH tetramer.

Figure 5.4. Diagrammatic representation of the pET-15b bacterial expression vector.

Figure 5.5. Automated sequencing of wild-type, Arg224Pro and Asp226Asn IMPDH1 cDNA sequences.

Figure 5.6. SDS-PAGE analysis with Coomassie staining of total cell protein (TCP) extracts from *E. coli* cells over-expressing IMPDH1 protein.

Figure 5.7. SDS-PAGE analysis of total cell lysates from E.coli expressing IMPDH1 proteins at 37°C.

Figure 5.8. SDS-PAGE analysis of His-tag purified IMPDH1 protein (WT) extracts.

Figure 5.9. SDS-PAGE analysis of *E.coli* soluble cell lysates before and after His-tag purification.

Figure 5.10. Expression and purification of IMPDH1 protein in *E.coli.*

Figure 5.11. Graphs showing enzyme activity reaction rates of wild-type and mutant IMPDH1 proteins.

Figure 5.12. Graphs showing Km[NAD] measurements.

Figure 5.13. Diagrammatic representation of the pcDNA3.1/His C mammalian expression vector.

Figure 5.14. Automated sequence analysis of the pcDNA3.1/His C vector with insertion of IMPDH1 cDNA sequence.

Figure 5.15. Positive transfection control in HEK293T mammalian cells.

Figure 5.16. Analysis of wild-type and mutant IMPDH1 proteins expressed in HEK293T cells.

Figure 5.17. Computer molecular modelling studies of IMPDH1.

Figure 5.18. ERG analysis in *Impdh1*$^{-/-}$ mice.

Figure 5.19. Light micrographs of retinal sections from *Impdh1*$^{-/-}$ mice.

SUMMARY

The central aim of this thesis was the elucidation of the underlying molecular pathologies of inherited diseases of the retina. The main focus of study concentrates on the molecular genetics and disease mechanisms in retinitis pigmentosa (RP), a hereditary disease in which photoreceptor cells of the retina degenerate, eventually leading to blindness in affected individuals.

Usher syndrome is a disease segregating RP and sensorineural deafness. Previous studies in a large family segregating Usher-like symptoms identified a disease-causing heteroplasmic C12258A transversion in the second serine tRNA mitochondrial (*MTTS2*) gene (Mansergh *et al.,* 1999). In this study, automated sequencing analysis was used to screen all 22 mitochondrial tRNA sequences in a cohort of atypical Usher syndrome individuals, in order to investigate the frequency of mitochondrial tRNA mutations in the molecular pathology of Usher syndrome. A number of variants from the consensus mitochondrial DNA sequence were identified, but none that were novel or that could be regarded as disease-causing. The C12258A mutation was not identified in any additional patients segregating blindness and/or sensorineural deafness, suggesting it may be a relatively rare cause of Usher syndrome.

The third chapter describes the results from a large comparative microarray analysis, which was carried out to compare the transcriptional profiles of approximately 6,000 genes in the retinas of wild-type (Wt) mice with those carrying a targeted disruption of the rhodopsin gene (*Rho*$^{-/-}$). The *Rho*$^{-/-}$ mouse represents an animal model in which the degeneration of the photoreceptor cell layer is complete, enabling a comparison between mouse retinas with and without photoreceptor cells. This revealed a series of transcripts, in which levels were elevated or reduced in the retinas of *Rho*$^{-/-}$ mice, some of which were derived from genes known to map at retinopathy loci. Subsequently, a number of analyses were carried out including the identification and screening of potential candidate retinopathy genes, validation of microarray results using quantitative real-time PCR and functional group classification of those genes showing the greatest changes in expression levels. A number of interesting observations were made in the analysis of differentially regulated genes. Many that showed down-regulation in degenerating *Rho*$^{-/-}$ retinas were genes that function in apoptotic or intracellular signalling cellular pathways, while approximately half of those genes

shown to be transcriptionally activated in degenerating retinas encode proteins of either the extra-cellular matrix or the structural cytoskeleton of the cell.

The remaining two chapters describe a large study that was carried out on the initial identification and subsequent analysis of a novel RP gene. Previous linkage analysis on a large Spanish family, called FA-84, segregating autosomal dominant RP, resulted in the localisation of an adRP gene (RP10) to chromosome 7q31.3 (Jordan *et al.*, 1993). Identification and characterisation of candidate RP10 genes involved analysis of the emerging human genome sequence and the use of novel gene prediction and expression databases, as well as homology searching tools. This analysis led to the characterisation and screening of a number of candidate genes that mapped to within the RP10 region. One gene mapping to the RP10 locus, *IMPDH1,* was predicted following the previously described microarray analysis, to show higher levels of expression in the photoreceptor cells of the retina, and therefore was adopted as a strong candidate for the RP10 gene. A screen of the *IMPDH1* gene in DNA from family FA-84 individuals revealed an Arg224Pro substitution, that segregated in affected individuals only. This substitution was not identified in unaffected or control individuals and was highly conserved amongst species, providing strong evidence that mutations within the *IMPDH1* gene cause the RP10 form of RP.

Following on from the discovery that mutations within the IMPDH1 gene cause adRP, studies were undertaken to evaluate the effects of two adRP mutations identified in large RP10 families, on the properties and activity of the IMPDH1 enzyme. IMPDH1 catalyses the conversion of inosine monophosphate (IMP) to xanthosine monophosphate (XMP), which is the rate limiting step in guanine nucleotide biosynthesis. Wild-type and mutant IMPDH1 proteins were over-expressed in bacterial cells, purified and their activity levels were measured spectrophotometrically. No dramatic difference in enzyme activity was detectable between wild-type and mutant IMPDH1 proteins. However, a difference in solubility was detected between wild-type and mutant IMPDH1 proteins following their expression in a mammalian cell culture system, which suggests abnormal protein folding and aggregate formation are a feature of mutant proteins. Histological and functional studies in *Impdh1*$^{-/-}$ mouse retinas revealed a relatively mild retinal disease phenotype and preserved photoreceptor structure in these mice, which suggests a probable dominant-negative effect of the IMPDH1 mutations studied. These observations may form the basis of a novel therapeutic approach in respect to this form of RP.

PUBLICATIONS ARISING FROM WORK DURING THIS THESIS

Kennan, A., Aherne, A., Palfi, A., Humphries, M., McKee, A., Stitt, A., Simpson, D.A., Demtroder, K., Orntoft, T., Ayuso, C., Kenna, P.F., Farrar, G.J. and Humphries, P. (2002) Identification of an IMPDH1 mutation in autosomal dominant retinitis pigmentosa (RP10) revealed following comparative microarray analysis of transcripts derived from retinas of wild-type and *Rho(-/-)* mice. *Hum Mol Genet*, **11**, 547-557.

Aherne, A., Kennan, A., Bowne, S.J., Daiger, S.P., Engel, P.C., Farrar, G.J., Kenna, P.F., and Humphries, P. (2003) Functional analysis of mutations in IMPDH1 gene implicated in RP10 form of Retinitis Pigmentosa. ARVO Meeting Poster Presentation, May 2003; E. abstract **44**, 3564.

Kennan, A., Aherne, A., S.J., Daiger, S.P., Farrar, G.J., Kenna, P.F., and Humphries P. (2003) On the role of IMPDH1 in retinal degeneration. In *Retinal Degenerations.* LaVail, M.M., Hollyfield, J.G. & Anderson, R.E. Eds. Kluwer Academic/Plenum publishers, New York, pp. 13-18.

Aherne A., Kennan A., Kenna, P.F., McNally, N., Lloyd, D.G., Alberts, I.L., Kiang, A.S., Humphries, M.M., Ayuso C., Engel, P.C., Gu, J.J., Mitchell, B.S., Farrar, G.J., and Humphries, P. (2004) On the molecular pathology of neurodegeneration in IMPDH1-based retinitis pigmentosa. *Hum Mol Genet*, **13**, 641-650.

ABBREVIATIONS

AdRP	Autosomal dominant retinitis pigmentosa
ACN	Acetonitrile
AD	Alzheimer's disease
ALS	Amylotrophic lateral sclerosis
AMD	Age-related Macular Dystrophy
ANT	Adenine nucleotide translocator
ArRP	Autosomal recessive retinitis pigmentosa
Arg	Arginine
Asn	Asparagine
Asp	Aspartic Acid
ATCC	American Type Culture Collection
ATP	Adenosine tri-phosphate
BBS	Bardet-Biedl syndrome
CBS	Cystathionine β-synthase
cDNA	Complementary DNA
CEPH	Centre d'Etude du Polymorphisme Humain
cGMP	Cyclic guanosine monophosphate
cM	Centimorgan
CMV	Cytomagalovirus
CNS	Central nervous system
CORD	Cone-rod retinal dystrophy
CPEO	Chronic progressive external opthalmoplegia
CSBN	Congenital stationery night-blindness
DHPLC	Denaturing high performance liquid chromatography
DMDF	Diabetes mellitus and deafness
dNTP	Di-nucleotide triphosphate
DTT	Dithiothreitol
EDTA	Ethylenediamine tetra acetic acid
ECG	Electrocardiography
ECM	Extra-cellular matrix
EMG	Electromyography
ERG	Electroretinography
EST	Expressed sequence tag
ETC	Electron transport chain
FFM	Fundus flavimaculatus
GDP	Guanosine diphosphate
GMP	Guanosine monophosphate
GTP	Guanosine triphosphate
HCl	Hydrochloric acid
HEK	Human Embryonic Kidney
His	Histidine
HPRT	Hypoxanthine phosphoribosyl transferase
IMP	Inosine monophosphate
IMPDH	Inosine monophosphate dehydrogenase
ISH	*In situ* hybridisation
KSS	Kearns Sayre syndrome
LB	Luria broth
LCA	Leber congenital amaurosis

LHON	Leber hereditary optic neuropathy
Leu	Leucine
LOD	Log of the odds
Lys	Lysine
MELAS	Mitochondrial encephalomyopathy, lactic acidosis and stroke-like episodes
MERFF	Myoclonic epilepsy and ragged-red fibre syndrome
MM	Mitochondrial myopathy
mRNA	Messenger RNA
mtDNA	Mitochondrial DNA
NAD	Nicotinamide adenine dinucleotide
NADH	Nicotinamide adenine dinucleotide, reduced
NARP	Neuropathy, ataxia and retinitis pigmentosa
NCBI	National Centre for Biotechnology Information
NHGRI	National human genome research institute
OMIM	Online Mendelian Inheritance in Man
ORF	Open reading frame
OXPHOS	Oxidative phosphorylation
PBS	Phosphate buffered saline
PCR	Polymerase chain reaction
PD	Parkinson's disease
PDE	Phosphodiesterase
PKC	Protein kinase C
Pro	Proline
RCS	Royal college of surgeons
RD	Retinal degeneration
RDS	Retinal degeneration slow
RHO	Rhodopsin
RFLP	Restriction fragment length polymorphism
ROS	Rod outer segment
RP	Retinitis pigmentosa
RPE	Retinal pigment epithelium
RT-PCR	Reverse transcriptase-PCR
S.A.	Specific Activity
SDS	Sodium dodecyl sulphate
SDS-PAGE	SDS-Polyacrylamide gel electrophoresis
SNP	Single nucleotide polymorphism
SSCP	Single stranded conformational polymorphism
STGD	Stargardt disease
STS	Sequence tagged site
TEAA	Ttiethylammonium acetate
TIGR	The Institute of Genomic Research
tRNA	Transfer RNA
UCSC	University of California, Santa Cruz
UTR	Untranslated region
UV	Ultraviolet
xlRP	X-Linked RP
XMP	Xanthosine monophosphate
YAC	Yeast artificial chromosome

CHAPTER 1

GENERAL INTRODUCTION

1.0 INTRODUCTION

The primary purpose of this Ph.D. thesis was the identification and analysis of genes associated with retinal degenerative diseases, in particular retinitis pigmentosa. The identification of mutations within novel genes that cause retinal disease in individuals, is generally followed by functional analysis of novel proteins within the context of a normal retina, and hence elucidation of the molecular mechanisms that bring about a retinal degenerative phenotype. The discovery and characterisation of genes that are essential to normal retinal functioning, increases our comprehension of the complex molecular pathways that exist in the retina to enable vision processes. More importantly, the identification of the primary cause of disease is essential to accurate disease diagnosis in affected individuals, possible pre-natal or pre-clinical testing of individuals and is especially important in the development of specific and effective therapies for the treatment of debilitating retinal degenerative diseases, for which no therapy currently exists.

The purpose of this introductory chapter is to give an overview of the structural organisation and visual processes of the retina as a background to studies described in subsequent chapters. The clinical heterogeneity of retinal disease is introduced with a brief description of well-characterised diseases that involve retinal degeneration, and in particular the death of photoreceptor neurons. A full description of the clinical and genetic features of two diseases, retinitis pigmentosa and Usher syndrome, the molecular genetics of which are investigated in this thesis, will be presented in subsequent chapters. An overview is also given of some common methods used in the identification and characterisation of novel genes associated with retinal degenerative disease, and potential avenues that can be explored in an effort to establish disease mechanisms and in the development of therapies.

1.1 THE EYE AND VISION

1.1.1 The eye

The eye is responsible for focusing light on the retina, which in turn translates it into electrical and neurochemical signals enabling vision. It is an elongated sphere that consists of three layers, the sclera, the choroid and the retina. The sclera is the opaque white protective coat of the retina that is continuous with the cornea, a transparent layer at the front of the eye. The choroid is the middle layer containing many blood vessels that supply the photoreceptors, and the inner layer, the retina, contains the sensory epithelium of the eye. Towards the front of the eye the choroid thickens and forms the ring-shaped ciliary body, which becomes a thin, circular muscular diaphram called the iris, that regulates the size of the opening of the eye, the pupil. The lens is attached to the ciliary body by ligaments that hold and adjust its shape, focusing light onto the retina. The lens also divides the cavity of the eye into two chambers. The aqueous humour is a watery solution that fills the chamber between the cornea and the lens, and the vitreous humour is a viscous gelatinous material that fills the large cavity behind the lens. The optic nerve transmits nerve impulses to the brain and exits from the back of the eye.

1.1.2 The retina

The retina is a delicate multi-layered tissue containing many types of neural cells. The layers of the retina can be visualised by microscopy, and include the retinal pigment epithelium (RPE), outer nuclear layer, outer plexiform layer, inner nuclear layer, inner plexiform layer and ganglion cell layer (Fig. 1.1). The outermost layer of the retina is the RPE, which consists of a single layer of pigmented cells, firmly attached to the basal lamina of Bruch's membrane. The RPE is required for normal photoreceptor outer segment development and is the site of regeneration of the visual pigment chromophore, 11-*cis* retinal, following its isomerization by light. The RPE is also involved in the phagocytosis and digestion of shed outer segment discs, absorption of

scattered light by the melanin granules and the transport of nutrients and metabolites through the extra-retinal blood barrier (Djamgoz *et al.,* 1995).

The primary neurons in the visual pathway are the photoreceptors, which (with their axonal processes and synapses) constitute the outer segments of the rods and cones, the outer nuclear layer and the outer plexiform layer (Dowling, 1987). The photoreceptor layer of rod and cone cells consists of inner and outer segments, with the outer segments embedded in the interphotoreceptor matrix, just internal to the RPE. The outer nuclear layer contains the cell bodies of photoreceptor cells while the external limiting membrane, located just below the inner segments is a histologically identifiable attachment site between the photoreceptors and the Muller cells (Fig. 1.2 & Fig. 1.3). The outer plexiform layer marks the junction of the photoreceptor neurons and the second-order neurons in the retina, which are the bipolar and horizontal cells. The inner nuclear layer consists of closely packed nuclei of bipolar cells, horizontal cells, amacrine cells, interplexiform cells and supportive Muller cells (Fig. 1.1 & Fig. 1.2). Horizontal cells transform visual information received from photoreceptors, and form a network of fibres that integrate the activity of the photoreceptor cells by means of lateral communication. Bipolar cells synapse with amacrine and/or ganglion cells, in transmission of the visual signal. Muller cells are the principle glial cells of the retina and they conserve the structural alignment of its neuronal elements, as they extend from the outer to the inner limiting membranes (Fig. 1.2) (Djamgoz, 1995). The amacrine cells spread laterally and extend processes to adjacent amacrine or bipolar cells, and their axons synapse with ganglion cells. Interplexiform cells are similar to amacrine cells but they extend processes into both synaptic layers (outer and inner plexiform layers) (Ogden, 1989). The inner plexiform layer marks the synaptic junction of the second order neurons and the third order neurons, the ganglion cells. The ganglion cells each produce a single axon that converge together and exit from the eye as the optic nerve.

To enable vision, light rays must pass through the ganglion cell layer and the inner layers of the retina to reach the photoreceptor cells at the back of the retina, where it is transformed into an electrochemical event. The photoreceptors are located on the outer surface because of their high energy requirements, which demands that they are in close proximity to the RPE and underlying blood supply in the choroidal layer, that provides essential nutrients and oxygen (Stone *et al.,* 1999b). The visual stimulus passes through photoreceptor synapses to the complex circuitry of bipolar and

horizontal cells through to the amacrine and ganglion cells, and is finally transmitted to the brain via the optic nerve (Fig. 1.2).

The specialised regions of the retina include the optic disk, the area centralis containing the macula and fovea, and the peripheral retina. The optic disk is an area without photoreceptors, where the axons of ganglion cells leave the eye to form the optic nerve, and is often referred to as the blind spot. The area centralis, or central retina, is characterised by a ganglion cell layer that is more than one cell thick, at the centre of which lies the fovea (Ogden, 1989). The macula lutea, an oval zone of yellow colouration due to the presence of the carotenoid pigments lutein and zeaxanthin, lies within the central retina, and extends above and below the fovea. The macula is suggested to function both as an optical filter by absorbing blue light and to play a role in protection against light-dependent damage (Nussbaum *et al.,* 1981; Sies *et al.,* 2003). At the centre of the fovea, the layers of the retina are thinner so that a central concave indentation, the foveola is produced, which represents the area of highest visual acuity in the retina, due partly to the presence of closely packed cone photoreceptors (Ogden, 1989). The peripheral retina increases the field of vision and is divided into four regions, the near periphery, the mid-periphery, the far periphery and the ora serrata, which marks the most anterior region of the retina where the photoreceptor layer ceases and it continues as the unpigmented epithelium of the ciliary body (Ogden, 1989).

1.1.3 The photoreceptors

Rod and cone photoreceptor cells are specialized neurons of the vertebrate retina that function in the primary events of vision. Rod cells are highly sensitive to light and operate under dim lighting conditions, while cones are less sensitive and function in bright light and in colour vision. There are approximately 100 million rod cells and 5 million cone cells in the human retina (Curcio *et al.,* 1990). The two types of photoreceptors are generally arranged in a mosaic pattern, exhibiting an organized architecture with cones rather evenly spaced surrounded by rings of rods. Individual variations in the density of both rods and cones occur in different regions of the retina. Cone density is highest in the fovea and falls rapidly outside the fovea to a fairly even density in the peripheral retina, while the highest rod densities are located along an elliptical ring centred at the macula (Ogden, 1989). Rod density declines rapidly

towards the rod-free central fovea, and also slowly declines towards the retinal periphery (Curcio *et al.,* 1990).

Photoreceptors are highly polarized cells, which consist of an outer segment, an inner segment and a synaptic terminal (Fig. 1.3). Cone cells taper in width from the inner to the outer segment, while in rod cells the outer segment is longer and cylindrical. The outer segments are embedded in the interphotoreceptor matrix, just internal to the RPE, and are the light-sensitive portion of the cell (Djamgoz *et al.,* 1995). They contain an elaborate system of stacked membranous discs that consist of outer rims and central lamellar regions. The rims are believed to contain proteins critical for the development and maintenance of outer segment structure such as peripherin-RDS and ROM1, whereas disc lamellas contain the visual pigment and other molecules required for phototransduction (Clarke *et al.,* 2000). The outer segment discs are constantly renewed at a predicted rate of 10% per day (Clarke *et al.,* 2000). As old discs are phagocytosed by the RPE, they are replaced by newly formed discs that migrate from near the base of the outer segment (Ogden, 1989). The membranes of outer segment discs in rod cells contain the visual pigment rhodopsin, while cone cells have three different types of cone visual pigment corresponding to blue, green and red opsin, that are maximally sensitive to different wavelengths of light. The inner and outer segments of the photoreceptor are joined by a connecting cilium, which contains motor and cytoskeletal proteins such as myosin VIIA, that are believed to be required for the trafficking of rhodopsin, and other essential proteins, into the outer segments from the inner segments and nuclei (Williams, 2002). The inner segment of rods and cones contains organelles such as mitochondria and golgi apparatus which constitute the photoreceptor metabolic machinery. The nuclei of the photoreceptor cells are responsible for the distinct outer nuclear layer of the retina, while the synaptic body constitutes the outer plexiform layer where it forms synapses with the secondary neurons of the retina (Fig. 1.3).

1.1.4 Visual transduction

Visual transduction is the mechanism by which incoming light is processed and visual images are sent to the brain via the optic nerve. The phototransduction process exhibits an enzyme cascade including a visual pigment (rhodopsin), a GTP-binding protein

(transducin) and an enzyme that hydrolyses cGMP (cGMP-phosphodiesterase) (Fig. 1.4) (Kawamura, 1995).

In the rod outer segment (ROS) membrane, cGMP binds to a cation channel (cGMP-gated channel) in the dark, and keeps it open allowing Na^+ and Ca^{2+} ions to flow into the ROS. Under these conditions of high levels of cGMP, the cell is in its depolarised state and there is constant release of the glutamate transmitter from the synaptic region of the photoreceptor cell (Molday, 1998). Following light absorption, rhodopsin, a seven transmembrane-helix G protein-coupled receptor, is activated by conversion of the 11-*cis* retinal chromophore bound form of rhodopsin to its all-*trans* isomer. This reaction leads to the formation of Meta II rhodopsin or R^* which causes activation of the visual cascade, brought about by exposure of the G protein binding sites of rhodopsin, thus permitting the binding of transducin (Molday, 1998). A transducin molecule then transmits the photoreception signal from rhodopsin to cGMP-phosphodiesterase (PDE). This is initiated when activated rhodopsin (R^*) catalyzes the exchange of GDP for GTP on the α-subunit of the transducin molecule and, with this exchange, transducin converts into the active form. The photoreception signal generated by a rhodopsin molecule is amplified greatly during activation of transducin, with one R^* generating about 700 activated transducin molecules (Kawamura, 1995). The activated GTP-bound form of transducin in turn activates cGMP-PDE, which brings about the hydrolysis of cGMP to 5'-GMP. One PDE can hydrolyse up to 1000 cGMP molecules, demonstrating further amplification of the signal (Kawamura, 1995). The rapid decrease in intracellular cGMP levels causes the cGMP-gated channels to close and the rod cell becomes hyperpolarized (Molday, 1998). When the channels are closed, glutamate release at the synaptic region is inhibited and Ca^{2+} levels in the outer segment are decreased. The hyperpolarisation of the cell brings about curtailment of glutamate release and results in the transmission of an electrical signal, via synaptic junctions, through the various layers of the retina and on to the brain, via the optic nerve.

After photoexcitation, the photoreceptor cell returns to its dark state by the shutdown of the visual cascade system and resynthesis of cGMP, mediated by a calcium feedback mechanism (Djamgoz, 1995). Activated rhodopsin is phosphorylated by rhodopsin kinase and then bound by arrestin, which prevents further interaction with transducin (Molday, 1998). Transducin and PDE are inactivated by the hydrolysis of

GTP to GDP on the transducin α-subunit, by its intrinsic GTPase activity (Molday, 1998). Guanylate cyclase, the enzyme responsible for the synthesis of cGMP from GTP, is activated by the decrease in intracellular Ca^{2+} after photoexcitation. As the cGMP concentration increases, the cGMP-gated channels re-open, and the photoreceptor cell is returned to its depolarised state (Fig. 1.4).

The visual cascade that operates in cone photoreceptor cells has not been studied in as much detail as the rod visual transduction pathway, but the two phototransduction cascades are basically similar. It has been found that signal amplification is lower in cones, while phosphorylation of the visual pigment, one of the shut-off mechanisms of the phototransduction cascade, appears to be much faster. This may explain the lower light sensitivity and briefer photoresponse characteristic of cone photoreceptor cells (Tachibanaki *et al.,* 2001).

1.1.5 The retinoid cycle

Regeneration of 11-*cis*-retinal, which is also known as the retinoid or visual cycle, is a complex process involving several enzymes and retinoid binding proteins in both the rod photoreceptor and the RPE (Reviewed by Bessant *et al.,* 2001). Retinol (Vitamin A) is transported to the retina via the circulation, where it moves into the RPE. If needed, it is isomerised to form 11-*cis*-retinol, which is subsequently oxidised to form 11-*cis* retinal (Fig. 1.5). Retinal is the essential biochemical initiator in the complex process of vision, and in the rod photoreceptor 11-*cis* retinal is covalently bound to the visual pigment, rhodopsin (Garriga & Manyosa, 2002). Absorption of a photon of light by rhodopsin at the beginning of the visual transduction cascade catalyses the isomeration of 11-*cis* retinal to all-*trans* retinal, which results in its release. Once released all-*trans* retinal is transported by ATP-binding cassette transporter (ABCR) out of the rod outer segment discs (Bessant *et al.,* 2001). All-*trans* retinal is converted to all-*trans* retinol by a rod-specific dehydrogenase (t-RDH), and it is then transported across the interphotoreceptor matrix to the RPE, bound to interphotoreceptor retinoid binding protein (IRBP). In the RPE, all-*trans*-retinol, bound to cellular retinoid binding protein (CRBP), is esterified by lecithin retinal acyl transferase (LRAT) to produce an all-*trans*-retinyl ester. This ester is transformed to 11-cis retinol by all-trans-retinyl

ester isomerohydrolase (RPE65), which is then regenerated back to 11-cis retinal by 11-cis-retinol dehydrogenase (c-RDH). 11-*cis* retinal can be shuttled back to a rod photoreceptor cell by cellular retinaldehyde binding protein (CRALBP) to complete the visual cycle by binding to rhodopsin (Fig. 1.5).

1.2 HEREDITARY DISEASES OF THE RETINA

Inherited retinal dystrophies are a major cause of progressive visual impairment often leading to blindness and represent the most prevalent cause of blindness amongst working populations in developed countries. They represent a very large and extremely clinically and genetically heterogenous group of disorders. Genetic heterogeneity refers to mutations within different genes causing the same disease, allelic heterogeneity arises from different mutations in the same gene causing either the same disease or different diseases, and clinical heterogeneity refers to a situation where the same mutation results in different symptoms in different individuals, even within the same family. Mutations responsible for human retinal disease have been identified in virtually every protein that participates in either the photoactivation or the recovery process of visual transduction, and a number of mutations have also been identified that affect the protein products of genes involved in the retinoid cycle described earlier in this chapter.

Retinal dystrophies can affect primarily rod photoreceptor cells, as is the case in retinitis pigmentosa, or can primarily affect the cone cells as is seen in cone dystrophies. Cone-rod dystrophies affect both populations of cells and macular dystrophies affect both populations also, but specifically within the macular region. A comprehensive list of retinal dystrophies, and details of genes and mutations associated with each type is available from the RetNet database (http://www.sph.uth.tmc.edu/Retnet/, a copy of which is available in Appendix C).

1.2.1 Retinitis Pigmentosa

Retinitis Pigmentosa (RP) is the name given to a set of hereditary retinal diseases in which photoreceptor cells degenerate. They have a number of clinical features in common which include night blindness, a gradual loss of peripheral visual field, and the eventual loss of central vision. A progressive deterioration of retinal function is revealed by electroretinographic (ERG) analysis, in which the electrical signals generated by the retina in response to flashes of light, are reduced in amplitude and

delayed in response times (Humphries *et al.,* 1992). Usually, the rod photoreceptors which govern dim light vision, are affected early in the disease, hence the onset of night blindness at an early age. This gradually leads to more extensive tissue degeneration including the death of cone cells and characteristic retinal pigmentary deposits.

RP can be inherited by autosomal dominant, recessive, x-linked or mitochondrial inheritance patterns. It is extremely genetically heterogenous, and to date up to 32 genes have been implicated in disease pathology (http://www.sph.uth.tmc.edu/Retnet/). The products of a number of these disease-associated genes can be placed in general categories of phototransduction proteins; such as rhodopsin and PDE; structural proteins, for example peripherin-RDS and ROM1; proteins involved with retinal recycling, for example RPE65 and CRALBP and proteins involved with the regulation of gene expression such as cone-rod homeobox (CRX) and neural retina leucine zipper (NRL) (Bessant *et al.*, 2001). There also exists a number of recently identified RP genes that have an unknown function in the retina, and genes such as pre mRNA-splicing factors, which exhibit widespread expression patterns. A detailed description of RP, clinical symptoms, diagnosis and genes involved in its molecular pathology, is presented in Chapter 4.

1.2.1.1 Syndromes incorporating RP

RP is also exhibited as one of a number of symptoms in certain hereditary syndromes. One of these is Usher syndrome, which is a genetically heterogeneous disease, characterised by progressive RP, accompanied by varying severities of sensorineural deafness and vestibular dysfunction (Keats & Corey, 1999). Usher syndrome is recessively inherited and to date seven disease-associated genes have been characterised. Many of the Usher genes identified function as extracellular matrix, cytoskeletal or cell adhesion proteins such as myosin 7A and cadherin-like gene 23 (Farrar *et al.,* 2002). A detailed description of the Usher syndromes is presented in Chapter 2.

A second syndrome that includes retinal degeneration is Bardet-Biedl syndrome (BBS), a genetically heterogeneous autosomal recessive disorder. This disease also involves obesity, polydactyly, hypogenitalism, mental retardation and renal anomalies (Heckenlively, 1988). Six BBS genes have been cloned to date but many encode proteins of unknown function (www.sph.uth.tmc.edu/Retnet/). Results from a recently cloned gene, BSS8, suggest that BBS is probably caused by a defect at the basal body

of ciliated cells, such as the connecting cilium of photoreceptor cells, causing their dysfunction (Ansley *et al.*, 2003). A number of rare syndromes that are not discussed here also exist, which incorporate symptoms of pigmentary retinopathy along with a range of other clinical symptoms.

1.2.2 Leber Congenital amaurosis

Leber congenital amaurosis (LCA) is the most severe form of inherited retinal dystrophy and is characterised by blindness or severe visual impairment from birth. LCA is the most prevalent cause of blindness in children in the developed world, and the uncomplicated form of disease is diagnosed as bilateral congenital blindness, with a diminished or absent electroretinogram (ERG) (Heckenlively, 1988). Juvenile and early onset RP are distinguished from LCA by a later age of onset, night blindness and a relatively good central visual acuity (Cremers *et al.*, 2002). Six genes have been implicated in LCA to date, which are all exclusively or predominantly expressed in the retina, but display functional diversity. Many LCA genes have also been associated with other forms of retinal disease such as *CRX*, which is also associated with dominant RP, *RPE65*, which has also been identified in recessive RP and retinal-specific guanylate cyclase (*GUCY2D*) which has also been associated with dominant cone-rod dystrophy (Sohochi *et al.*, 1998; Morimura *et al.*, 1998; Kelsell *et al.*, 1998). The protein products of LCA-associated genes have varied functions and include a retinal-specific transcription factor CRX, a protein predicted to be involved with retinal protein folding or trafficking, denoted AIPL1, a guanylate cyclase, involved in the conversion of GTP to cGMP during phototransduction (GUCY2D) and RPE65, which is involved in the retinal cycling in the RPE (Cremers *et al.*, 2002).

1.2.3 Cone dystrophies

Cone dystrophies manifest initially with loss of central visual acuity (discrimination) and colour vision. They do not generally affect peripheral vision unless the rod system is also involved, in which case the disease manifests itself as a cone-rod dystrophy. In patients with a cone degeneration, all three types of cone photoreceptors die, while the

rod photoreceptors generally remain alive and functional (Rivolta *et al.,* 2002). In the absence of cone cells, vision is mediated exclusively by rod cells and is called achromatopsia. There is no rod counterpart to cone degeneration because rod photoreceptor degeneration is always accompanied by a secondary loss of cone photoreceptors, as in RP (Rivolta *et al.,* 2002). The boundaries separating some of the diagnostic categories of retinal disease are not distinct, and some patients with a rapid loss of cones and a slower loss of rods may be diagnosed with either cone-rod dystrophy or RP, mainly due to the fact that the end-point of both types of degeneration is indistinguishable. In some instances, different mutations arising within the same gene can result in the clinical features of RP, cone dystrophy, cone-rod dystrophy or LCA, as has been found following the analysis of the CRX and AIPL1 genes in patients suffering from these diseases (http://www.sph.uth.tmc.edu/Retnet/).

Genes implicated in cone dystrophy include guanylate cyclase activating protein 1A (*GUCA1A*), which is involved in visual transduction processes, and 11-*cis* retinol dehydrogenase 5 (RDH5), an enzyme that participates in the visual cycle (http://www.sph.uth.tmc.edu/Retnet/). Two genes associated with cone-rod dystrophy only to date have been identified as rab3A-interacting molecule (RIM1) and the *C.elegans* homolog, UNC119, both of which localise to photoreceptor ribbon synapses (Johnson *et al.,* 2003; Kobayashi *et al.,* 2000).

One inherited retinal disease, the enhanced S-cone syndrome (ESCS), manifests a gain in function of photoreceptors, and exhibits excess cone cell proliferation. ESCS is an autosomal recessive retinopathy in which patients have an increased sensitivity to blue light (S-cone function) and visual loss, with night blindness occurring from early in life, varying degrees of colour vision, and retinal degeneration (Haider *et al.*, 2000). The one gene associated with ESCS to date, is called nuclear receptor subfamily 2 group E3 (NR2E3), and encodes a retinal nuclear transcription factor, that functions in regulation of human cone photoreceptor development and differentiation (Haider *et al.,* 2001; Milam *et al.*, 2002).

1.2.4 Congenital stationary night-blindness

Congenital stationary night blindness (CSNB) is characterised by normal daytime vision but very poor vision in dim light, and patients can manifest associated ocular

symptoms such as myopia, hyperopia, nystagmus and reduced visual acuity (Pusch *et al.*, 2000). The disease is caused by rod photoreceptors that are not sensitive to dim light or that require an abnormally long time to adapt to dim light. Patients usually have a full complement of rod and cone photoreceptors, but there may be a defect in how photoreceptor signals are transmitted to inner retinal neurons (Rivolta *et al.*, 2002). Many of the genes implicated in CSNB are also associated with RP and include rhodopsin, the alpha subunit of rod transducin, PDE and RPGR (http://www.sph.uth.tmc.edu/Retnet/).

Two genes in which mutations have been identified only in CSBN patients are rhodopsin kinase, which has been associated with Oguchi type CSNB and is involved in rhodopsin inactivation, and nyctalopin (NYX), which is an extracellular glycosylphosphatidyl (GPI)-anchored member of the small leucine-rich proteoglycan protein family (Yamamoto *et al.*, 1997; Pusch *et al.*, 2000). It has been suggested that mutant nyctalopin disrupts developing retinal interconnections involving the bipolar cells (Bech-Hansen *et al.*, 2000). CSBN mutations have also been found in an L-type voltage-gated calcium channel (CACNA1F), which presumably causes a decrease in neurotransmitter release from photoreceptor presynaptic terminals (Strom *et al.*, 1998).

1.2.5 Macular dystrophies

The inherited macular dystrophies comprise a heterogeneous group of disorders characterised by central visual loss and atrophy of the macula and underlying RPE. There is considerable clinical and genetic heterogeneity, with evidence of macular dystrophies showing autosomal dominant, autosomal recessive, x-linked recessive and mitochondrial inheritence. While progress has been made in uncovering the molecular basis of monogenic macular disease, little progress has been made in the elucidation of a genetic component in age-related macular degeneration (AMD), the leading cause of blind registration in the developed world (Michaelides *et al.*, 2003).

Stargardt macular dystrophy (STGD) is the most commonly inherited macular dystrophy with a prevalence of 1 in 10,000 and a recessive mode of inheritance (Michaelides *et al.*, 2003). It displays a variable phenotype but most cases present with central visual loss in early teens, with white flecks at the level of the RPE visible on opthalmoscopy and subretinal deposition of lipofuscin-like material. When the retinal

flecks are seen without atrophy the term fundus flavimaculatus (FFM) is often used to describe the phenotype (Michaelides *et al.,* 2003). A number of mutations causing STGD have been found in the retinal ATP-binding cassette transporter (*ABCR* or *ABCA4)* gene, which localises to the rims of outer segment discs and is involved in retinoid transport in the visual cycle (Allikmets *et al.,* 1997b; Azarian & Travis, 1997). Over 400 different mutations have to date been identified within the ABCR gene, which have also been associated with a large number of retinal degenerative diseases including recessive RP, recessive fundus flavimaculatus and recessive cone-rod dystrophy (Jaakson *et al.,* 2003).

There are a number of relatively rare forms of dominantly inherited macular degenerative disease. Some dominantly inherited Stargardts-like phenotypes exist which generally exhibit a milder phenotype and later onset than recessive forms. Mutations in the elongation of very long fatty acids (*ELOVL4)* gene which as the name suggests, encodes a photoreceptor-specific component of the fatty acid elongation system, have been associated with this form of disease (Zhang *et al.,* 2001). Other forms of dominant macular disease include Best disease also known as vittelliform macular dystrophy (VMD), which is characterised by a classic round yellow subretinal macular deposit caused by accumulation of lipofuscin-like material within and beneath the retinal pigment epithelium, and is associated with a progressive loss of central vision (Petrukhin *et al.,* 1998). Best disease is caused by mutations affecting the protein product of the *VMD* gene, bestrophin, which is localised to the RPE and functions as a novel, transmembrane, oligomeric chloride channel (Sun *et al.,* 2002). Sorby's fundus dystrophy is a rare autosomal dominant macular dystrophy which has been associated with mutations in the tissue inhibitor of metalloproteinase-3 (*TIMP3*) gene, a gene that plays a pivotal role in extracellular matrix remodelling (Weber *et al.,* 1994).

Another form of dominant macular disease, Doyne honeycomb retinal dystrophy (Malattia leventinese), has been associated with a predicted extracellular matrix glycoprotein called EGF-containing fibrillin-like extracellular matrix protein 1 (EFEMP1) (Stone *et al.,* 1999a). This form of macular disease is characterised by drusen-like deposits similar to those seen in AMD. It has been suggested that misfolding and aberrant accumulation of EFEMP1 may cause drusen formation and cellular degeneration, which plays an important role in the etiology of this form of macular dystrophy and possibly also AMD (Marmorstein *et al.,* 2002). Despite the

prevalence of AMD, its etiology and pathogenesis are poorly understood and are complicated by the predicted involvement of environmental factors as well as a genetic component. A number of large scale genome scans and screening of macular dystrophy-associated genes have been undertaken in AMD patient cohorts, but very few genes has been definitively shown to confer increased risk for AMD to date (Michaelides *et al.,* 2003). A number of groups have reported possible involvement of the *ABCR* gene in AMD (Allikmets *et al.,* 1997a; Shroyer *et al.*, 2001). In addition, a recently identified gene called Hemicentin-1, which is similar to the EFEMP1 gene, has been implicated as the ARMD1 gene following linkage analysis in a large family (Schultz *et al.,* 2003).

1.3 IDENTIFICATION AND ANALYSIS OF RETINAL DEGENERATION GENES

Identification of causative genes associated with retinal degenerative diseases represents an essential first step in understanding the molecular pathology of these disorders, and the design of therapies, including possibly gene therapies. Since the first disease-associated genes were isolated in the early 1980s, huge advances have been made in the elucidation of the genetic basis of almost all human diseases. A number of different approaches and techniques are now available for use in disease gene identification studies. Originally candidate genes were chosen based on knowledge of their biochemical properties or function in the context of a particular disease phenotype, or through subtractive cloning techniques. These techniques are relatively limited however, and since the sequence of the human genome has become available, novel disease-associated genes are generally identified using a combination of positional and candidate cloning.

1.3.1 Identification of disease-causing genes

The most common approach for isolating genes that predispose to a particular disease is positional cloning, in which disease genes are identified using only knowledge of their approximate chromosomal location. Initially, a disease gene is mapped to a chromosomal region by linkage analysis, attractive candidates in the region are surveyed, and finally mutational analysis points to the correct gene. Prior to the generation of physical human genomic sequence maps, genetic maps were developed that were based on the frequency with which selected genetic markers are co-inherited in a population. Genetic maps are essential to genetic linkage studies and contain information about the order of genes and genetic markers on a particular chromosome. Physical maps represent the actual distance in base pairs between genetic markers or genes on a chromosome and a complete (or almost complete) physical map of each chromosome is now available, resulting from the completion of the human genome sequencing project.

The mapping of human disease genes depends on the use of polymorphic markers, the most commonly used of which are microsatellite markers. Microsatellites are di-, tri- and tetra-nucleotide repeats that are distributed throughout the human genome and are highly variable. A huge number of polymorphic genetic markers have been identified in all regions of the human genome, the sequence, order and location of which can be viewed in detailed genetic maps that are available in online databases. If a particular marker has multiple possible alleles it is highly informative, because it is more likely that maternal and paternal genotypes will differ and therefore the parental origin of a specific allele can be determined in the offspring. The specific order of these genetic markers was originally elucidated using the principle of homologous recombination. In other words, the greater the degree of genetic recombination or crossover between markers, the greater the genetic distance between them (Strachan & Read, 1999). These genetic mapping principles are used in linkage analysis. After collecting DNA samples from family members, the genotype for each individual is obtained using a number of polymorphic markers. If a disease gene and marker are located close to one another, all affected individuals will possess the same allele. To assess the significance of linkage, a statistical test known as the log of the odds (LOD) score is used, which is a calculation of the likelihood that loci are linked, or are not linked, and is generally determined with the aid of computer software. Evidence in favour of linkage is generally accepted when a positive LOD score of 3 or more is obtained (Strachan & Read, 1999). Once linkage is established, the disease interval containing a causative gene can be narrowed, usually by looking for conservation of linked marker alleles in affected individuals across a region (haplotype conservation). Fine mapping of the disease interval may be performed by isolating and testing additional markers contained within the region of interest. When flanking markers are found for which all meioses are informative and non-recombinant, linkage analysis comes to a halt. More than any other factor, the size of the candidate region determines the work required in the identification of a disease-associated gene, so every effort should be made to define as small a candidate region as possible, especially if the candidate region is particularly gene-rich.

1.3.2 Characterisation and screening of candidate genes

Once a linkage has been established between a disease gene and a particular region of a chromosome, it is necessary to analyse the gene content of the predicted disease interval in detail. Owing to the initial and subsequent releases of the draft sequence of the human genome since 2001, and the huge advances that have been made in the development of physical genetic maps and gene prediction databases, physical mapping of disease intervals has become considerably less labour intensive. The generation of clones across an interval has largely become redundant, as the sequences of assembled contigs is now freely available through accessing a number of human genome databases, a detailed description of which is given in Chapter 4. Any gene that maps to within a disease interval may be considered a candidate for the disease gene, but a prioritisation of genes is often required for mutation screening, and is generally based on the pattern of expression and/or function of a gene in the context of the disease under investigation. In some cases novel genes must be sought using database searches, sequence analysis tools and screens of cDNA libraries to determine the expressed sequence of an as yet uncharacterised gene. Most genes are identified by defining a candidate gene on the basis of both its chromosomal location and its functional properties (the positional candidate approach).

In the case of retinal disease gene identification, suitable candidate genes would naturally be expected to show expression in the retina. This is generally established by analysing retinal EST databases, through amplification of the expressed sequence of a candidate gene in retinal cDNA libraries or following *in situ* hybridisation analysis on retinal sections. Candidate genes may also be adopted on the basis of a close functional relationship with a gene previously identified as being involved in retinal disease. Subtractive cDNA cloning strategies have also been used to isolate retinal-enriched cDNA sequences, which can then be characterised. This method selects for genes that are highly expressed in the retina, and a number of candidate retinal disease-associated genes have been identified using this technique (den Hollander *et al.,* 1999b; Inana *et al.,* 1997). The recently developed application of large-scale transcriptional profiling of retinal tissue using microarray or SAGE analysis, has resulted in the isolation of a number of candidate diseases for involvement in retinal dystrophies. These methods of analysis will be described in detail in Chapter 3. Briefly, a comparative analysis of transcripts derived from wild-type mice and those in which the photoreceptor cells of

the retina have degenerated can be used to identify genes that may be more highly expressed in the photoreceptor cell layer. The corresponding human chromosomal location of differentially expressed genes can be determined, and if these genes are found to localise to previously mapped human degenerative loci, they may be regarded as retinal disease candidates (Kennan *et al.,* 2002; Blackshaw *et al.,* 2001).

Once suitable candidate genes are identified that map to within a particular disease interval, the coding sequence of the gene can then be screened for potential pathogenic mutations. A number of high-throughput methods are available, such as single stranded conformational polymorphism analysis (SSCP) and denaturing high performance liquid chromatographic (DHPLC) analysis. In general, the most accurate method of screening is sequencing, but it is often also the most expensive option. Disease-causing mutations in a particular gene can manifest as missense and nonsense point mutations, deletions, insertions, or disruption to a splice site or promoter region of the gene. Following the identification of a disease-causing mutation within a novel gene, it is critical to provide more evidence that a mutation is pathogenic (and not simply a polymorphic variant) by demonstrating that it co-segregates with affected individuals, disrupts the protein sequence and is not present in unaffected individuals or population controls. Strong supporting evidence is provided if additional gene mutations are found in affected individuals from other families, that exhibit similar disease symptoms. Additional supporting evidence is also provided if the position of an identified sequence change shows a high level of conservation amongst species, or in some cases, highly homologous proteins.

1.3.3 Elucidation of disease mechanisms in retinal disease

Identification of a disease mutation provides the first insight into the molecular cause of disease, but understanding the pathogenesis of a disorder, especially in the complex cellular environment of the retina, is a far more daunting task. Almost all of the genes that were originally implicated in retinal degenerative diseases encoded proteins with a direct involvement in visual transduction processes, the visual cycle or structural proteins of the photoreceptors. In recent times however, the number of genes and mutations identified in association with retinal dystrophies has risen rapidly, and many genes have been identified which have a completely unknown function in the retina

and/or often show expression in many other tissues of the body. A particular disease-causing mutation can cause its phenotypic effect through a dominant-negative effect, exerted by the presence of mutant protein, or disease can arise due to haploinsufficiency, resulting from the lack of normal functional protein. The disease mechanism involved in the pathogenesis of each disease gene, or even each individual mutation within a gene, can differ, depending on the functional or structural alterations to the resulting protein. Hence, at least in the case of retinal disease research, functional analysis on the effects of disease mutations on a particular protein is really only in the early stages.

1.3.3.1 Methods of studying disease mechanisms in retinal diseases

A number of different research avenues can be explored in the elucidation of disease mechanisms in the retina, such as expression analysis, biochemical analysis, protein interaction and co-localisation studies, protein modelling and animal model studies. Often the first avenue of investigation following the identification of a novel disease-associated gene is the determination of its expression pattern in the retina. This is generally determined by *in situ* hybridisation or immunocytochemical analysis, which can often provide an indication as to the normal function of the protein product of a gene. For example, a gene that shows expression in the connecting cilium may have a predicted structural function, or alternatively may have a role in the trafficking of essential proteins, such as rhodopsin, into and out of the outer segments, as was found in the case of the myosin VIIA gene product (Liu *et al.,* 1997a).

Once the probable role of a gene has been established, functional analysis or intracellular immunolocalisation studies of disease–associated proteins can be carried out. This is often done by expression of mutant protein (usually corresponding to a mutation previously identified in retinal disease patients) in a suitable cell culture system. Investigation into the properties of mutant proteins in cell culture systems can reveal intracellular mislocalisation of mutant protein or differences in solubility leading to the formation of aggresomes, as has been previously demonstrated by the aberrant localisation of mutant pre-mRNA splicing factor and rhodopsin proteins within human cultured cells (Deery *et al.,* 2002; Saliba *et al.,* 2002). Computer protein modelling studies can also be carried out to predict possible protein structural perturbations brought about by the presence of disease-causing mutations.

Pathogenic mutations can often disrupt the biochemical properties or activity of retinal proteins or enzymes, particularly those involved in visual transduction or visual cycle processes. This can be investigated following the expression of a particular protein, by using a particular assay for functional activity measurements in the protein of interest. Biochemical analysis of the LCA protein, guanylate cyclase revealed that mutations within the catalytic domain of the protein result in the complete inability of the mutant cyclases to hydrolyze GTP into cGMP in vitro (Rozet *et al.,* 2001). In contrast, missense mutations lying in the extracellular domain of guanylate cyclase can result in proteins that exhibit normal catalytic activity, but still cause the same LCA phenotype, possibly resulting from mis-folded protein (Rozet *et al.,* 2001).

Alterations to protein structure or disruption to protein-protein interactions brought about by pathogenic mutations, can be investigated using protein interaction screens such as yeast two-hybrid or co-localisation studies. Pathogenic mutations can affect the interactions, either between subunits of the same protein or interaction with another protein that is essential for its proper functioning. For example, RP-causing mutations in a rod cyclic nucleotide-gated channel gene (CNGA1) were found to cause disruption to intersubunit interactions, which prevents the formation of functional ion channels (Trudeau & Zagotta, 2002). Yeast two-hybrid studies have been employed in the identification of candidate proteins that interact physiologically with the ubiquitously-expressed retinitis pigmentosa GTPase regulator (RPGR) protein, in an attempt to explain the retinal pathology, in particular retinitis pigmentosa, brought about by mutations within the *RPGR* gene. This study resulted in the identification of an RPGR-interacting protein (RPGRIP), which is expressed specifically in the connecting cilium of rod and cone photoreceptors (Boylan & Wright, 2000; Hong *et al.,* 2001). Mutations within the RPGR gene have been identified that disrupt the interaction of RPGR with RPGRIP, a protein with the essential function of anchoring RPGR in the photoreceptor connecting cilia (Zhao *et al.,* 2003). It was subsequently found that mutations within the RPGRIP gene are also associated with retinal disease, and mutations within this gene have been implicated in Leber's congenital amaurosis (Dryja *et al.,* 2001).

1.3.3.2 Mouse models

There are limitations when using cell culture systems for gene and protein functional analysis studies, because such systems do not represent a true model organism with its

associated intricate cell systems and circuitry. The analysis and use of animal models of retinal degeneration have been extremely valuable in the study of human disease genes, providing a living system that manifests similar diseases to those affecting humans. A number of natural animal models of retinal degeneration exist, the first, and most extensively studied natural mouse model, was the *rd* mouse which is a recessive model of RP, caused by a mutation in the beta subunit of rod cGMP-phosphodiesterase (Bowes *et al.,* 1990). Natural models of retinal degeneration in dogs, cats, and chickens also exist, most of which represent recessive forms of disease (Reviewed by Chader, 2002). These models can assist in the identification of novel genes associated with retinal diseases in humans, as demonstrated by the characterisation of the mutated *Mertk* gene in the RCS rat, the human ortholog of which was subsequently found to be mutated in RP patients (Gal *et al.,* 2000).

In recent times progress in genetic engineering has led to the generation of a large number of transgenic animals, mostly mice, which carry constructs that lead to disruption or overexpression of genes implicated in human retinal degenerative diseases, thereby mimicking the human form of disease. Mouse models constitute a powerful and adaptable tool for determination of function of a particular novel gene in the retina by its targeted disruption or deletion. A mouse carrying a targeted disruption of the rhodopsin gene features in a number of studies described in this thesis, as it represents a mouse model in which all photoreceptors die within the first three months of life (Humphries *et al.,* 1997). A mouse model has recently been generated carrying a targeted disruption of the *RP1* gene, which had been previously implicated in autosomal dominant RP, in an attempt to elucidate its function. The *Rp1*$^{-/-}$ mouse displayed morphologically abnormal outer segments and mislocalized rhodopsin, which therefore suggested that RP1 is required for normal outer segment formation, and may play a role in rhodopsin transport (Gao *et al.,* 2002).

As well as representing models of degeneration, knockout mouse models provide suitable backgrounds for the generation of mice expressing mutant transgenes, that lead to phenotypic retinal degeneration. The study of transgenic mice is extremely useful, because these animals produce a simulation of the progression of human autosomal dominant form of retinal disease, and also enable investigation into the effects of specific gene mutations on retinal function and histology. The first transgenic mouse model of retinal disease to be generated, was that expressing rhodopsin Pro23His, which results in a rapid retinal degeneration (Olsson *et al.,* 1992). A number

of additional transgenic animal models have been made, including a transgenic pig expressing the mutant rhodopsin Pro347Leu transgene (Petters *et al.,* 1997). The porcine model possesses a retina more similar in size and composition to human than a mouse retina, and is therefore better suited to pre-clinical testing of novel therapies (Petters *et al.,* 1997). Transgenic and natural retinal degeneration animal models are essential to the elucidation of both retinal degeneration mechanisms and the development and testing of novel therapies for the treatment of retinal disease.

1.3.4 Proposed mechanisms of retinal degeneration

The above examples demonstrate the complexities that can arise in the functional analysis of retinal degeneration proteins, raising the possibility that mutations within the same protein can cause disease in a number of different ways, through loss of activity, mis-folding and aggregation, or possible disruption to the essential interactions either between the subunits of an oligomeric protein or with other essential regulatory proteins. The ultimate outcome of the presence of the numerous pathogenic mutations described in this review, is the death of photoreceptor neurons. While it is perhaps easy to imagine why mutations in a photoreceptor-specific gene, such as rhodopsin, could cause a retinal degeneration, it is considerably more difficult to imagine why mutations affecting a widely-expressed gene, such as a pre-mRNA splicing factor, cause death of photoreceptor cells only. The identification of novel disease-causing mutations is an essential first step towards understanding disease pathology, but much additional, and often more demanding study is involved in the elucidation of the exact function of a particular protein within the retina, and a mechanism or pathway of retinal degeneration. Photoreceptor cells appear to be more vulnerable to mutation of their proteins than any other cell of the body, which is evidenced by the large number of genes and mutations associated with their degeneration. Factors which may increase photoreceptor vulnerability include their highly specialised structure and function, their high energy requirements and lack of self-protective mechanisms (Stone *et al.,* 1999b).

A number of retinal degeneration disease mechanism studies have concentrated on rhodopsin mutations. In one study involving the production of structurally abnormal rhodopsin, cell death is predicted to result from the toxicity of misfolded mutant proteins to the photoreceptor neuron or defects in retranslocation of mutant protein

(Saliba *et al.,* 2002). Other reports suggest that rod cell death is triggered by mislocalised rhodopsin that causes the stimulation of normally inaccessible signalling pathways (Alfinito & Townes-Anderson, 2002). In effect, the disease mechanism caused by mutations in different genes, or even different mutations within the same gene, may be specific to each individual genetic alteration.

Apoptosis is the term used to describe the gene-regulated death of target cells. This form of cell death utilises complex signalling pathways that include induction of a proteolytic cascade involving proteases called caspases and ultimately the formation of apoptotic bodies that are phagocytosed by neighbouring cells (Reme *et al.,* 2000). Although several potential mechanisms for the degenerative process in retinal diseases have been proposed, a clear and detailed explanation, other than the fact that retinal cell death may go through an apoptotic pathway, has not yet been provided (Portera-Cailliau *et al.,* 1994; Reme *et al.*, 2000). Apoptosis is considered the 'final common death pathway' converging from a variety of primary defects in the retina, but it remains largely unknown how these disturbances actually initiate apoptosis. Although much progress has recently been made in the identification of the genetic component of retinal disease, there is still some way to go before the biochemical mechanisms by which each gene mutation initiates retinal degeneration, are elucidated. The elucidation of these molecular mechanisms through studies in cell culture systems or animal models, is essential for the future development of suitable therapies.

1.3.5 Therapy of inherited retinal diseases

No effective therapy currently exists for the treatment of RP or for most other inherited retinal dystrophies. There is some evidence that administration of large doses of vitamin A to RP patients may slow the progression of disease, but not to any great extent (Berson *et al.,* 1993). In addition, a number of artificial retinal implants, both subretinal and epiretinal, are currently under development. An artificial silicon retinal microchip implanted subretinally into RP patients has recently been reported to improve visual function, with subjective improvements to perception of brightness, contrast, color, movement, shape, resolution, and visual field size, without any significant safety-related adverse affects (Chow *et al.,* 2004). In another study, visual perception of light has been reported in a previously blind RP patient who received an epiretinal implant

(stimulation of ganglion calls), with reports of the patient seeing spots of light and also possibly direction of movement (Humayun *et al.,* 2003). However, further technological advances and larger clinical trials are required to further evaluate the safety and efficacy of these treatment methods.

Ultimately, the most important aspect of animal model research will be their usefulness for the demonstration of efficacy and safety of novel treatments under study for inherited retinal degeneration diseases. A number of potential treatments are currently being investigated which include the use of novel pharmacological agents, cell transplantation of RPE or stem cells and gene therapy (Reviewed by Bessant *et al.,* 2001). While progress has been made in all of these therapeutic fields, perhaps most attention to date has been focused on the development of gene therapies, which involve the correction of an underlying genetic defect in a patient and/or introduction of a functional copy of a gene to cells. A number of different gene therapy strategies are currently under investigation, but it may be necessary to tailor specific therapies to the particular genetic and biochemical defect in each individual in order to secure success. Ribozymes (mRNA cleaving molecules) or interfering RNA molecules can be specifically designed to identify and cleave mutant RNA while leaving wild-type intact, but they must be designed to target each individual mutation that causes retinal disease, and therefore are unlikely to be viable in economic terms. One method developed to circumvent the extreme genetic heterogeneity exhibited in RP is to use mutation-independent suppression-replacement strategies for dominant mutations (Millington-Ward *et al.,* 1997; O'Neill *et al.,* 2000). These strategies involve the use of ribozymes or RNA interference, for the simultaneous down-regulation of both mutant and wild-type transcripts of a particular gene, by targeting a neutral polymorphism rather than a rare mutation, thereby removing the disease-causing and wild-type transcripts. This is combined with the provision of a replacement functional gene, which escapes ribozyme suppression because of the introduction of a subtle alteration to the gene sequence, but that still encodes wild-type protein. Another potential avenue of therapy is the targeting of genes controlling the cellular apoptotic pathway, since it is predicted to be similar in most forms retinal degenerations. There is a danger however, that preventing apoptosis may not be possible in the long term, without the removal of the damaging genetic mutation (Reme *et al.,* 2000).

The development of safe and efficient delivery systems is essential to the eventual success of gene therapy technology. Most therapies under development use a

system of viral delivery vectors, and a number of laboratories have now demonstrated in animal models the safe, efficient and long-term delivery of genes to photoreceptor cells using viral vectors (Flannery *et al.,* 1997; Bennett *et al.,* 1999). Some recent success in the development of therapies includes the restoration of visual function or preservation of the retina in autosomal recessive forms of degenerative retinopathy, including the Briard dog model of Leber congential amaurosis and the RCS rat, following AAV-mediated delivery of therapeutic genes to retinal tissues (Acland *et al.,* 2001; Smith *et al.,* 2003). Long term preservation of the retina in a rat model of autosomal dominant RP expressing an engineered mutation within the rhodopsin gene has also been reported, following a single sub-retinal injection of an AAV vector expressing a gene encoding a hammerhead ribozyme and targeting the mutated transcript (LaVail *et al.,* 2000).

There are of course many risks involved with the development of gene therapies, as well as important social and ethical issues that need to be addressed. To date the actual treatment of diseases using the technique of gene therapy has met with little success and many technical obstacles, mainly concerned with delivery methods, have yet to be overcome. Nevertheless, there is great hope that effective treatments for people suffering from retinal dystrophies will be available in the not too distant future.

1.4 THE AIMS OF THIS THESIS

The primary aim of this thesis was the identification and characterisation of genes associated with retinitis pigmentosa and associated syndromes. An initial analysis of mitochondrial gene sequences in Usher syndrome individuals is presented in Chapter 2, with the aim of establishing the frequency of mitochondrial mutations in individuals suffering from this disease. The third chapter focuses on a large scale comparative transcriptional analysis of the mouse retina, using microarray analysis to compare the global expression of genes in mouse retinas with and without photoreceptor cells. This study resulted in the identification of a number of candidate genes that mapped to retinopathy loci and also revealed many potentially significant, differentially expressed transcripts. Chapter 4 contains a description of candidate gene analysis in a large autosomal dominant RP family, which resulted in the identification of the *IMPDH1* gene as the causative gene in the RP10 form of disease. Investigations into the functional properties of mutant IMPDH1 proteins and potential disease mechanisms in this form of RP are presented in Chapter 5.

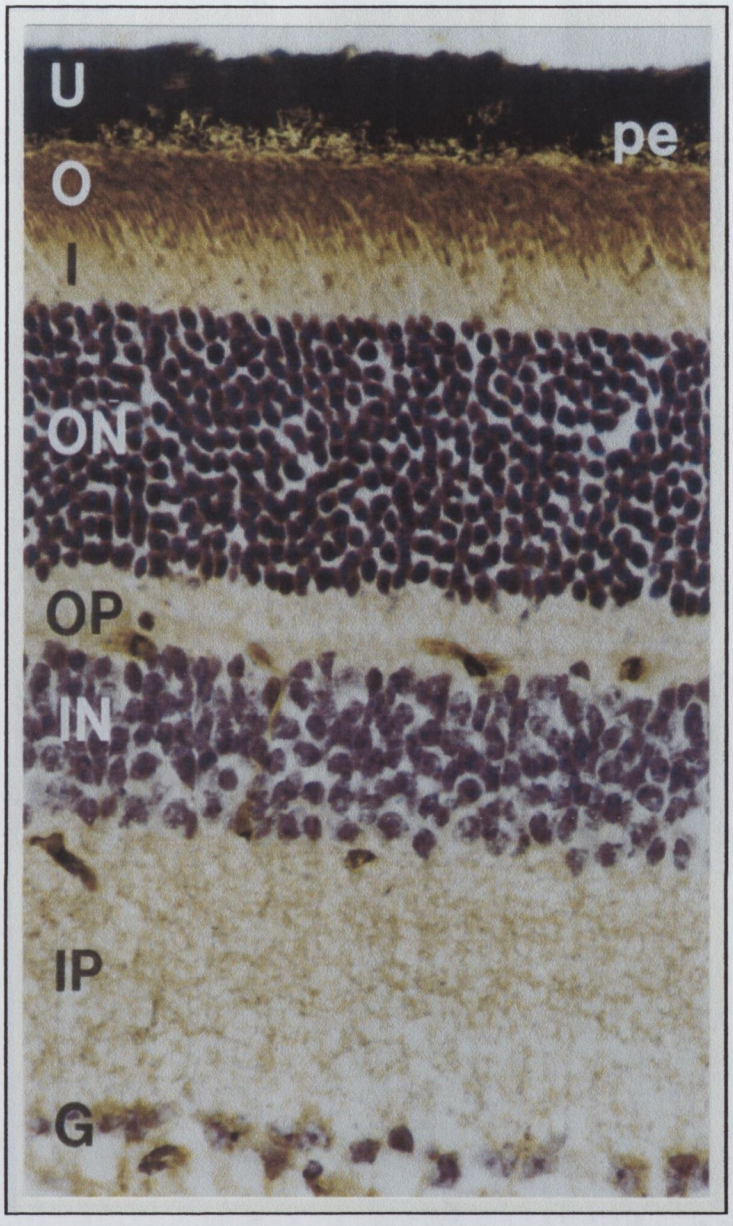

Figure 1.1. Histological cross section through a mouse retina stained with hemotoxylin and eosin. The following cellular and synaptic layers are shown: pe, retinal pigment epithelium; O, outer segments of photoreceptor cells; I, inner segments of photoreceptor cells; ON, outer nuclear layer; OP, outer plexiform layer; IN, inner nuclear layer; IP, inner plexiform layer; G, ganglion cell layer.

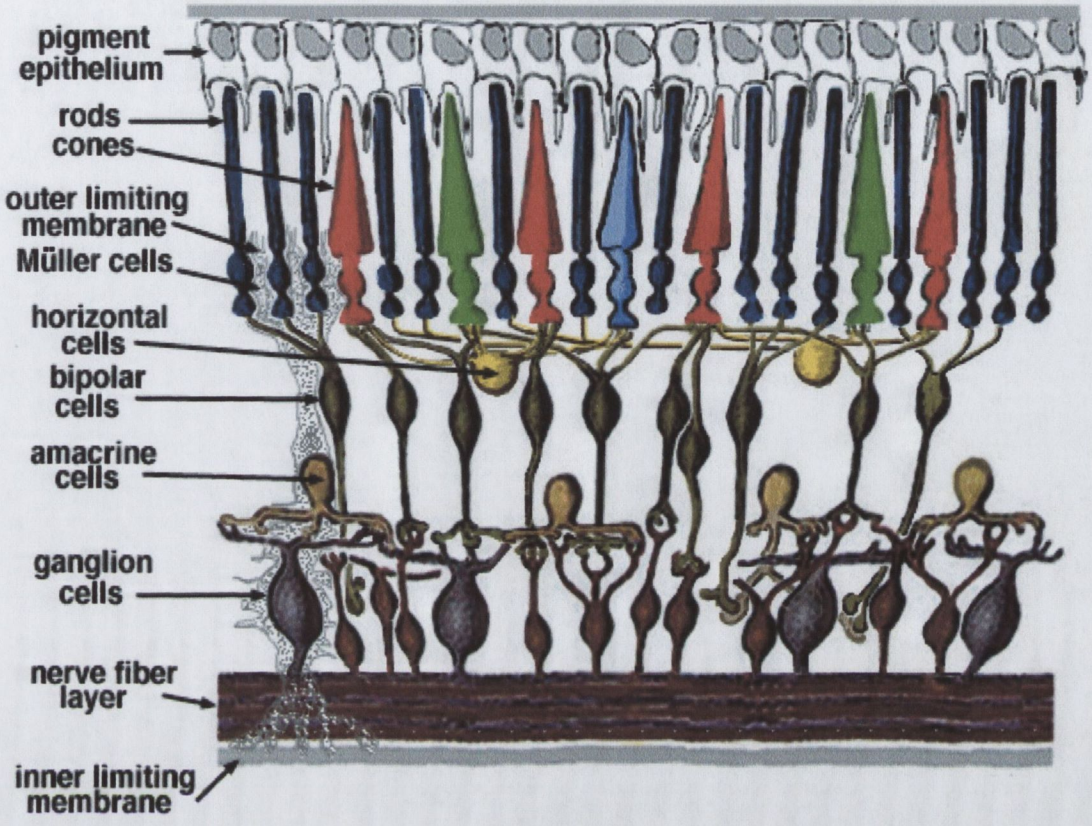

Figure 1.2. Schematic representation of neuronal cell types and their interactions in the retina. The photoreceptor rod and cone cells detect the visual signal in the form of light, which causes them to become hyperpolarised and transmit a signal to the brain via a complex circuitry of neuronal cells. The signal first travels through horizontal and bipolar cells, it is then transmitted to amacrine and ganglion cells, and finally exits through the axons of ganglion cells which make up the nerve fibres of the optic nerve. (Taken from http://webvision.med.utah.edu/)

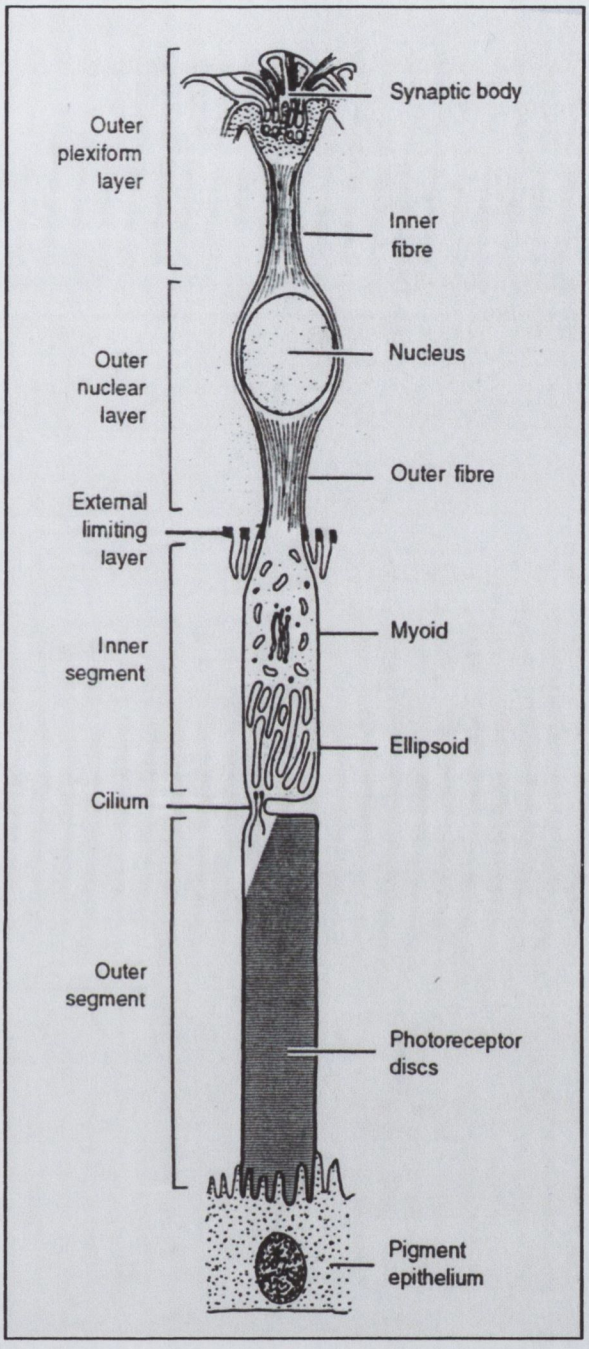

Figure 1.3. Diagrammatic representation of a rod photoreceptor cell in the human retina. (Modified from Newell, 1982)

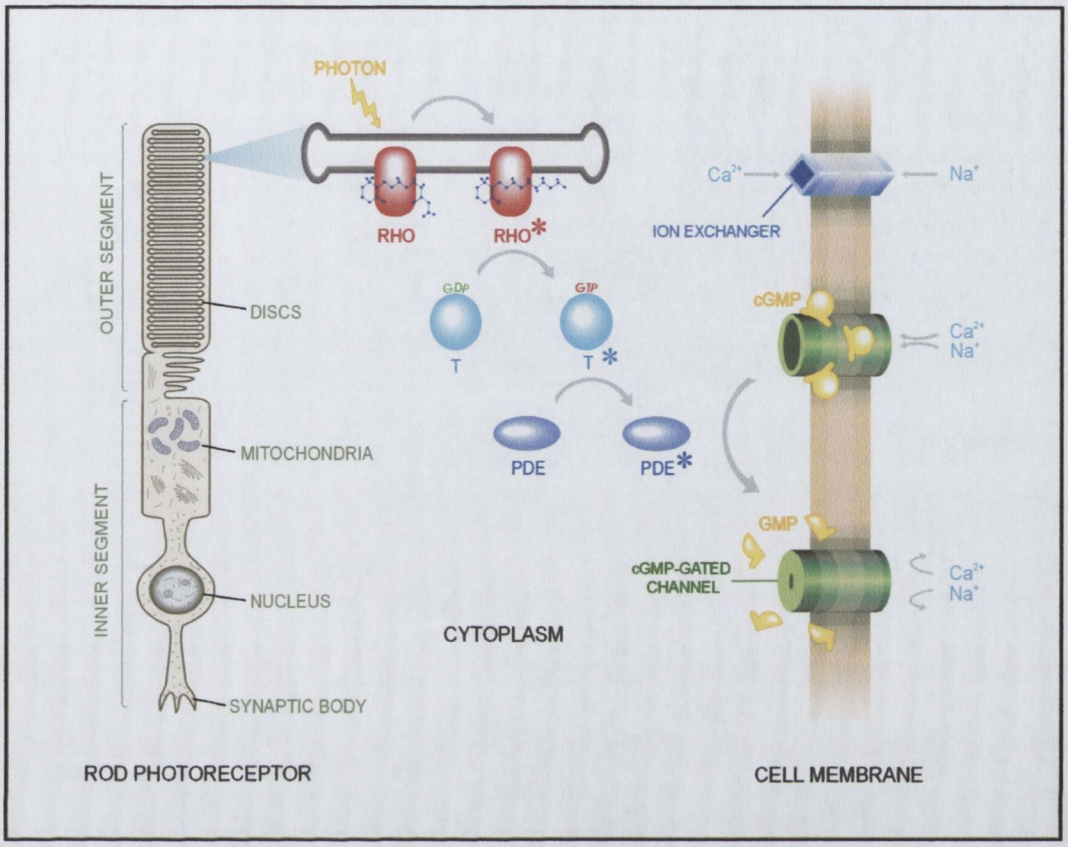

Figure 1.4. Schematic representation of visual transduction. Molecules involved in the transmission of the visual signal include RHO, Rhodopsin; T, Transducin; PDE, cGMP-Phosphodiesterase. * denotes activated molecules.

(Diagram supplied by Dr. Avril Kennan)

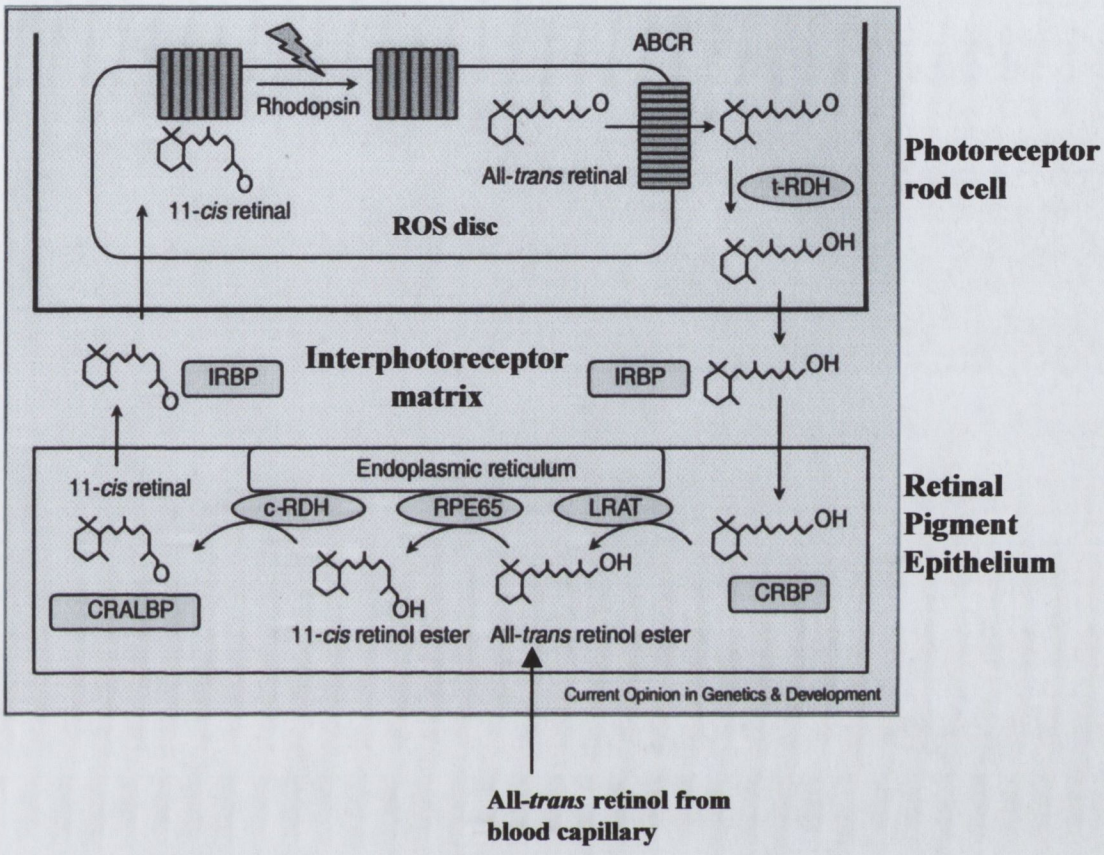

Figure 1.5. Diagrammatic representation of the retinoid cycle.

The 11-*cis*-retinal chromophore is bound to rhodopsin, and is converted to all-*trans* retinal upon activation of rhodopsin. It is transported by ABCR out of the ROS disc, converted to all-*trans* retinol, and transported to the RPE. In the RPE, all-*trans* retinol is esterified to form an all-*trans* retinol ester. This ester is transformed to 11-*cis* retinol ester by RPE65 and then to 11-*cis* retinal to complete the cycle.

ABCR, ATP-binding cassette transporter; t-RDH, rod specific dehydrogenase; IRBP, interphotoreceptor binding protein; CRBP, cellular retinoid binding protein; LRAT, lecithin retinol acyl transferase; RPE65, All-*trans*-retinyl ester isomerohydrolase; c-RDH, 11-*cis*-retinol dehydrogenase; CRALBP, cellular retinaldehyde binding protein. (Adapted from Bessant *et al.*, 2001)

CHAPTER 2

ANALYSIS OF MITOCHONDRIAL DNA SEQUENCE IN ATYPICAL USHER PATIENTS

2.1 INTRODUCTION

2.1.1 Introduction

Usher syndrome (USH) refers to a group of diseases involving both progressive RP and sensorineural deafness. Family ZMK is a previously described Irish pedigree segregating progressive sensorineural hearing loss and retinitis pigmentosa, symptoms similar to Usher syndrome (Kenna *et al.,* 1997). The disease–causing mutation in this family was identified as a C12258A transversion in the second serine tRNA mitochondrial (*MTTS2*) gene (Mansergh *et al.,* 1999). The aim of this study was to screen additional atypical Usher syndrome patient DNAs to investigate whether there is a greater involvement of mitochondrial tRNA mutations in the molecular pathology of Usher syndrome.

A background on the clinical and genetic aspects of Usher syndrome is presented here, along with a description of the genes that have been associated with this disease to date. An overview of the mitochondrion and its role in disease is given, particularly diseases caused by mutations identified within mitochondrial tRNA genes that involve RP and/or sensorineural deafness. Results from a screen of the 22 mitochondrial tRNA genes in atypical Usher syndrome patient DNA samples are presented, along with a discussion on the potential significance of any variants identified.

2.1.2 Usher syndrome

The prevalence of Usher syndrome is currently estimated to be 3.8-4.4 cases per 100.000 live births (Boughman *et al.,* 1983; Rosenberg *et al.,* 1997; Ahmed *et al.,* 2003). While many syndromes are known to affect both hearing and vision, Usher syndrome is the most common genetic cause of deafness and blindness amongst school age children (Ahmed *et al.,* 2003). Usher syndrome is inherited in an autosomal recessive fashion and is genetically and clinically heterogeneous. Clinically distinct sub-types of Usher syndrome have been distinguished by age at onset, rate of

progression, presence or absence of vestibular involvement causing balance defects and severity of symptoms. Patients with Usher syndrome type 1 (USH1), the most severe Usher subtype, have severe to profound congenital hearing impairment, vestibular dysfunction, and retinal degeneration beginning in childhood (Keats & Corey, 1999). Patients with USH2 have moderate to severe hearing impairment, normal vestibular function, and later onset of retinal degeneration. USH3 is found most frequently amongst Finnish patients who exhibit progressive hearing loss, onset of RP at puberty or later and variable vestibular dysfunction (Keats & Corey, 1999; Ahmed *et al.,* 2003). Some patients affected by Usher syndrome display atypical clinical symptoms and cannot easily be categorized into any of the above subtypes (Ahmed *et al.,* 2003).

2.1.3 Genetics of Usher Syndrome

To date, eleven different Usher syndrome loci have been mapped, and seven disease-causing genes have been cloned (http://www.sph.uth.tmc.edu/Retnet/). The first gene to be associated with Usher syndrome was myosin VIIA (MYO7A) in which over 35 pathogenic mutations have been identified to date (Weil *et al.,* 1995; Ahmed *et al.,* 2003). Mutations in the MYO7A gene most frequently cause USH1B, but different mutant alleles can also cause non-syndromic hearing impairment, and one USH3 phenotype has been described (Liu *et al.,* 1997b; Keats & Corey, 1999). MYO7A is an unconventional member of the large superfamily of myosin motor proteins that move on cytoplasmic actin filaments (Keats & Corey, 1999). It localises to the photoreceptor connecting cilia where it is believed to be involved in rhodopsin trafficking (Liu *et al.,* 1997a; Williams, 2002). Mutations in a novel cadherin-like gene, the intercellular adhesion protein CDH23, have been implicated in USH1D (Bolz *et al.,* 2001) and a mutation in protocadherin 15 has also been described in Usher syndrome type 1F (Ahmed *et al.,* 2001). Genes for four additional loci have been identified as, USH1C, USH2A, USH3A and USH1G, which encode harmonin, usherin, clarin-1 and SANS respectively (http://www.sph.uth.tmc.edu/Retnet/). Harmonin contains PDZ protein domains which are known to mediate protein localisation and signalling (Verpy *et al.,* 2000), while usherin has laminin epidermal growth factor and fibronectin type III domains, and is predicted to encode a novel basement membrane protein (Eudy *et al.,* 1998; Bhattacharya *et al.,* 2002). Clarin-1 and SANS are the most recently identified

Usher genes, about which little is known. Clarin-1 is a 4-transmembrane protein with a possible role in hair cell and photoreceptor synapses (Adato *et al.,* 2002) while SANS has been shown to associate with harmonin (Weil *et al.,* 2003). Interactions between four USH1 proteins; MYO7A, harmonin, cadherin 23 and SANS have been demonstrated, and it is thought that the transmembrane complex formed by their interactions is involved in the development and cohesion of the stereocilia, which make up the hair cell bundle of inner ear sensory cells (Boeda *et al.,* 2002; Siemens *et al.,* 2002; Weil *et al.,* 2003). It is possible these genes may also have a role in the connecting cilium of photoreceptors, in a similar manner to Myosin 7A.

Therefore, it appears that many of the genes identified as being involved in Usher syndrome to date play a role in the maintenance and structural integrity of the extracellular matrix or cytoskeleton of the cell.

2.1.4 Family ZMK

Family ZMK is a large Irish kindred segregating progressive sensorineural hearing loss and RP together with a very mild muscle myopathy. These symptoms are almost identical to those found in USH3 (except for the symptoms of myopathy) and the pattern of inheritance in this family is compatible with autosomal dominant, X-linked dominant or maternal inheritance (Kenna *et al.,* 1997). The retinopathy in this family is typical of retinitis pigmentosa, but the age of onset and severity is extremely variable, ranging from early 20's to early 60's in affected individuals. Audiometric analysis showed a moderate to severe sensorineural deafness with evidence of 'recruitment', which is marked distortion and physical discomfort precipitated by loud noise. Two individuals in the family also suffered from moderate to severe mental handicap. Electrocardiography (ECG) and electromyography (EMG) testing was carried out on four affected individuals, and a muscle biopsy was carried out on one individual. ECG changes were noted in all individuals tested, while EMG demonstrated short, small motor unit action potentials consistent with myopathy. The muscle biopsy was examined by electron microscopy, and showed an abnormally high number of mitochondria beneath the sarcolemmal membrane (for a complete description of clinical symptoms in this family, see Kenna *et al.*, 1997).

A linkage to chromosome 9q was originally suggested in this family, but the wide variation in disease symptoms between family members, together with an observation of subclinical myopathy, suggested that the disease could be mitochondrially inherited (Mansergh *et al.,* 1999). Following a screen of the entire mitochondrial genome, a C→A transversion at position 12258 in the gene encoding the second mitochondrial serine tRNA (MTTS2) was found to be heteroplasmic in affected family members (Mansergh *et al.,* 1999). There were no precedents for the precise combination of symptoms observed in this family, but there are examples of mitochondrial disorders that manifest either progressive hearing loss or a retinopathy (Mansergh *et al.,* 1999). The C12258A mutation probably disrupts the amino acid-acceptor stem of the tRNA serine molecule, affecting aminoacylation of the tRNA and thereby probably reducing the efficiency of miochondrial translation. This study had significant implications for the etiologies of various retinopathies and forms of hearing loss, especially the various forms of Usher syndrome (Mansergh *et al.,* 1999). A study was therefore carried out to investigate the possible involvement of this mutation in 19 additional atypical Usher syndrome patients, but none were found to harbour the C12258A mutation (Kennan, 1999). In addition, there has been no report since, of any Usher syndrome patients segregating this mutation.

2.1.5 The Mitochondrion

The mitochondria are organelles present in the cell cytosol that fulfil most of the cells energy requirements. The typical human cell contains several hundred mitochondria, which have a double membrane structure. The outer membrane is smooth, while the inner membrane is highly folded with a large surface area that accommodates the mitochondrial energy-generating oxidative phosphorylation (OXPHOS) apparatus (Wallace *et al.,* 1996). The OXPHOS complexes are each composed of a number of polypeptides, most of which are encoded by the nuclear DNA, which are synthesised in the cytosol and then imported into the mitochondria. The OXPHOS protein complexes include the electron transport chain (ETC) components, ATP synthase and the adenine nucleotide translocator (ANT). Briefly, the energy available from combining oxygen with the reactive electrons carried by compounds such as NADH or $FADH_2$, is harnessed by the electron-transport chain, which pumps protons out of the

mitochondrial matrix to create a transmembrane electrochemical proton gradient (Alberts *et al.,* 1983). This gradient is, in turn, used by the ATP synthase complex to synthesise ATP. The energy-carrier ATP is then transported to the cytosol by the ANT, where it is exchanged for ADP (Wallace *et al.,* 1996).

Human mitochondrial (mt) DNA is a 16.6 kb double-stranded, circular genome, located within the mitochondrial matrix and present in hundreds of copies per cell (Wallace *et al.,* 1996). The mtDNA codes for 37 genes, 22 of which specify transfer RNAs (tRNAs) that are required for mitochondrial protein synthesis and two specify ribosomal RNAs (rRNAs). Only 13 genes encode polypeptides, all of which are components of the respiratory chain-OXPHOS system (Fig. 2.1) (Schon, 2000). The 22 mitochondrial tRNAs can interpret the entire genetic code through the use of modified wobble codon rules (Schon, 2000). Human mtDNA is maternally inherited being transmitted through the oocyte's cytoplasm at fertilisation (Wallace *et al.,* 1996).

2.1.6 Mitochondrial mutations and disease

Mitochondrial mutations have been shown to cause a wide variety of degenerative diseases, most of which have a delayed onset and a progressive course. The mtDNA mutation rate is much higher than that of nuclear genes, which is reflected in the extensive mtDNA polymorphism frequency, and is probably due to an oxidative environment (Wallace *et al.,* 1996; Florentz & Sissler, 2001). When a mutation arises in a cellular mtDNA, it creates a mixed intracellular population of mutant and normal molecules known as heteroplasmy. During cell division, the wild-type and mutant mtDNAs are randomly distributed into daughter cells. Over time the percentage of mutant mtDNAs in different cell lineages can drift towards either pure mutant or normal (homoplasmy), a process known as replicative segregation (Wallace *et al.,* 1996). As the percentage of mutant mtDNAs increases, the cellular energy capacity declines, and eventually falls below the minimum output threshold necessary for normal tissue function. Beyond this point disease symptoms appear and become progressively worse (Wallace *et al.,* 1999). The inheritance and expression of heteroplasmic mutations are highly variable, often producing markedly different symptoms among members of the same family

Pathogenic mtDNA mutations include both base substitutions and rearrangement mutations. The base substitutions can be sub-divided into missense mutations that affect the protein-coding genes and those that affect the rRNA or tRNA genes, which have global effects on mitochondrial protein synthesis (Wallace, 1999). Those that alter the protein-coding genes affect a specific respiratory complex such as the polypeptides of the electron transport chain or the ATP synthase complex (Wallace *et al.,* 1996). Examples of resulting diseases include Leber hereditary optic neuropathy (LHON), which is a maternally inherited form of central vision loss, that is associated with mtDNA pathogenic point mutations affecting different subunits of complex I of the ETC (Wallace, 1999). Neuropathy, ataxia and retinitis pigmentosa (NARP) is often associated with mutations in the mitochondrial ATPase 6 gene (Holt *et al.,* 1990). One mutation at position 8993G causes NARP when present in a small percentage (<75%) of mtDNAs, but when present in a higher percentage (>95%) of mtDNAs it can cause Leigh's syndrome, which is an early-onset disease that is frequently lethal (Wallace, 1999). Leigh's syndrome is associated with ataxia, hypotonia, spasticity, developmental delay and subsequent regression.

Diseases resulting from large scale mtDNA re-arrangements or deletions include Chronic Progressive External Opthalmoplegia (CPEO) and Kearns-Sayres Syndrome (KSS) (Wallace *et al.,* 1996). These diseases present with mitochondrial myopathy including opthalmoplegia and ptosis, and a subset have cardiac defects, renal problems, diabetes mellitus and other symptoms. The pathogenicity of mtDNA deletions is almost certainly due to the fact that they invariably remove tRNA genes that are required for translation of mtDNA-encoded mRNAs (Schon, 2000).

2.1.7 Mitochondrial mutations affecting tRNA genes

Approximately 77% of the coding capacity of the mitochondrial genome is allocated to the 13 protein-coding genes, with the remainder coding for the rRNA and tRNA genes. It is therefore surprising that two-thirds of the 115 pathogenic point mutations in mtDNA described to date are located in genes required for mitochondrial protein translation, with the vast majority located in the tRNA genes (Schon, 2000; http://www.mitomap.org/). All mitochondrial tRNAs are approximately 70 nucleotides in length and their general structure can be represented in a cloverleaf pattern in which

about half the nucleotides are base paired and which contains an amino acid acceptor stem and an anticodon recognition loop (Fig. 2.2) (Stryer, 1995).

Pathogenic mutations in the mitochondrial protein synthesis genes can produce a complex array of symptoms. They typically affect the translation of all 13 mtDNA-encoded polypeptides, resulting in generalised OXPHOS deficiencies (Schon, 2000). In severe cases the mutations are heteroplasmic and frequently cause central nervous system (CNS) abnormalities as well as mitochondrial myopathy with ragged red fibres, an association referred to as mitochondrial encephalomyopathy (Wallace, 1999). CNS manifestations can include sensorineural hearing loss, epilepsy, stroke-like episodes and progressive dementia (Wallace, 1999). The most commonly mutated tRNA gene is the $tRNA^{Leu(UUR)}$ gene, in which 16 pathogenic mutations have been identified, that are randomly distributed throughout the tRNA structure, suggesting that each of the domains are equally susceptible to mutation (Fig. 2.2) (Florentz & Sissler, 2001). These mutations can cause a variety of diseases such as mitochondrial encephalomyopathy, lactic acidosis and stroke-like episodes (MELAS), maternally inherited diabetes mellitus and deafness (DMDF), mitochondrial myopathy (MM), CPEO as well as a number of other rare disorders (http://www.mitomap.org/). The most common substitution in $tRNA^{Leu(UUR)}$ has been identified at position 3243, which has been associated with the diseases MELAS, DMDF, MM and CPEO (Schon, 2000). The second most frequently mutated tRNA gene is $tRNA^{Lys}$, which is often associated with myoclonic epilepsy associated with ragged-red fibers syndrome (MERFF) (Wallace *et al.*, 1996).

Milder mitochondrial protein synthesis mutations are often homoplasmic and only affect the CNS. One example is the $tRNA^{Gln}$ gene mutated at position 4336, which is consistently homoplasmic and has been associated with late-onset Alzheimer's disease (AD) and Parkinson's disease (PD) (Shoffner *et al.,* 1993; Egensperger *et al.,* 1997). The 4336 mutation appears to define a mtDNA lineage with a predisposition to AD and PD. There are many more examples of disease–causing tRNA mutations detailed in the Mitomap database (http://www.mitomap.org/). There have been as many polymorphic, non-pathogenic variants as pathogenic mutations in tRNA genes described in the literature, which have been found in almost all 22 mitochondrial tRNA genes. Despite the accumulation of information about the positions of a large number of mutations within tRNA genes, it is not possible to identify simple basic features such as position of mutation in a tRNA gene (stem or loop) or degree of conservation, that

would make possible the prediction of pathogenicity of new mutations (Florentz & Sissler, 2001).

2.1.8 Mitochondrial tRNA mutations involving RP and/or sensorineural deafness

In addition to the C12258A mutation identified in family ZMK, a number of additional substitutions have been associated with mitochondrially inherited deafness or RP, but no individuals have yet been identified with identical symptoms. The C12258A mutation has been identified in a family with diabetes mellitus, deafness, cerebellar ataxia and cataracts to varying degrees of severity (Lynn *et al.,* 1998). The same mutation was also identified in one additional individual in a screen of eleven patients displaying symptoms of maternally-inherited diabetes with one or more features of mitochondrial disease. This individual segregating the 12258A mutation had diabetes, cerebellar ataxia, bilateral nerve deafness and cataracts in three generations (Choo-Kang *et al.,* 2002). These findings demonstrate further the clinical heterogeneity resulting from mitochondrial mutations, and raises the possibility that a nuclear or separate mitochondrial modifier gene may be involved in either or both forms of disease.

A novel heteroplasmic G12183A mutation in the $tRNA^{His}$ gene has recently been reported, in which two members of the family had progressive bilateral sensorineural retinal and inner ear impairment, while one had severe pigmentary retinopathy, sensorineural deafness, testicular dysfunction, muscle hypertrophy and ataxia (Crimi *et al.,* 2003). These symptoms are similar to those previously observed in family ZMK, which supports a more substantial association of Usher syndrome–like diseases with mitochondrial mutations. A number of tRNA substitutions have been associated with sensorineural hearing loss with three separate mutations identified in the tRNA Serine (UCN) gene at positions 7445, 7510 and 7511 (Reid *et al.,* 1994; Hutchin *et al.,* 2000; Sue *et al.,* 1999). The existence of modifier loci has again been suggested in some reports of families segregating the T7511C mutation, which display variable disease phenotype, and where severity of disease does not correlate with levels of heteroplasmy (Chapiro *et al.,* 2002).

In summary, pathogenic mtDNA point mutations and rearrangements have been associated with a striking variety of multisystemic as well as tissue-specific human

diseases, but the genotype/phenotype relationship is complex and poorly understood. The existence of possible nuclear modifier genes that may affect the severity or alter the clinical manifestation of mitochondrially-inherited diseases cannot be ruled out. A candidate modifier nuclear locus on chromosome 8 has been identified in maternally inherited deafness associated with the A1555G mutation in the 12S rRNA gene (Bykhovskaya *et al.,* 2001). It is interesting to note that a previous candidate gene linkage to chromosome 9q in family ZMK may also represent a possible modifier locus (Kenna *et al.,* 1997).

2.1.9 The aim of the study

Usher syndrome has been mapped to eleven different loci, and seven disease-associated genes have been cloned to date. It is possible that mutations within the mitochondrial genome are responsible for more cases of Usher syndrome than has been previously predicted, in particular atypical cases displaying unusual symptoms. Additionally, some families with Usher syndrome do not show linkage to any previously mapped loci, suggesting further genetic heterogeneity. A number of mutations in mitochondrial tRNA gene sequences have previously been detected in individuals suffering from retinitis pigmentosa and sensorineural deafness, sensineural deafness only and syndromes incorporating one or both symptoms. The aim of this study was therefore to screen mitochondrial tRNA genes in atypical Usher syndrome patients, in order to investigate the frequency of mitochondrial mutations in relation to diseases incorporating both retinitis pigmentosa and sensorineural deafness.

2.2 MATERIALS AND METHODS

All reagents were purchased from Sigma-Aldrich (Ireland) Ltd., and primers were purchased from Sigma-Genosys unless stated otherwise.

2.2.1 PCR amplification

In a standard PCR reaction, 0.1-0.5 μg of DNA template was added to 5 μl of 10x PCR reaction buffer (Appendix A.1), 100 μM dATP, dTTP, dCTP and dGTP (Boehringer-Mannheim), 25 pmol of forward and reverse primers and 1.25U *Taq* polymerase in a total volume of 50 μl. Following initial denaturation at 94°C for 5 minutes, PCR amplifications were carried out for 30-40 cycles with denaturation at 94°C for 30 seconds to 1 minute, followed by primer annealing at 55°C-63°C for 30 seconds to 1 minute and extension at 72°C for 1 min 20 seconds. PCR reactions were carried out on a DNA engine PTC-200 (MJ Research) using a heated lid to prevent evaporation.

Most oligonucleotide primers were chosen using the primer3 program which designs primer pairs based on their Tm (primer melting temperature), and inter- or intra-complementarity (http://www-genome.wi.mit.edu/cgi-bin/primer/primer3_www.cgi). Certain conditions were modified depending on the particular PCR reaction. A magnesium curve was generally carried out using a final concentration of 1.0-2.5 mM $MgCl_2$ in PCR 1x buffer, to determine the optimum concentration for a particular set of primers. The annealing temperature initially used was T_m of primers minus 5°C, but the temperature was increased if necessary to improve primer specificity. The extension time was increased for larger fragments. PCR reactions were carried out in 25, 50 or 100 μl volumes, and reagent volumes and concentrations were scaled up or down accordingly.

2.2.2 Agarose gel electrophoresis

Agarose gels were made by adding 1-2% agarose (Gibco BRL) in 1x TAE buffer (Appendix A.2), and heating in a microwave until completely dissolved. 1 μl of ethidium bromide was added per 30 ml agarose solution and gel was poured. Loading

dye (Appendix A.2) was added to PCR products and they were visualised following electrophoresis of 1-5µl on an agarose gel run in 1x TAE buffer at 100 volts.

2.2.3 Purification of PCR products

Sepharose columns were used for purification of PCR products to remove traces of primer and enzyme for subsequent reactions. Columns were prepared by adding 20 µl of glass beads in TE into the bottom of a 0.5 ml eppendorf tube, in the base of which a small hole had been pierced. The tube was filled with CL-6B sepharose (Pharmacia), placed in a collection vial, and spun in a bench-top centrifuge for 2 minutes at 2000 rpm. The PCR reaction (usually 50 µl) was added onto the surface of the column. The column was transferred into a 1.5 ml eppendorf as the collection tube, and spun again at 2000 rpm for 2 minutes.

For some sequencing reactions PCR products were purified using Qiaquick PCR purification columns (Qiagen) according to manufacturers' instructions. For direct sequencing, PCR products were incubated with 5 µl of 200 µg/ml proteinase K (Sigma) for one hour at 55°C.

2.2.4 Automated sequencing

Concentration of PCR products was estimated by eye following electrophoresis of 1 µl on a 1.5% agarose gel. Approximately 250 ng of PCR product and 5 pmols of sequencing primer were added to 8 µl reaction mix from the Dye terminator cycle sequencing ready reaction kit (Perkin Elmer), and the final volume was made up to 20 µl with dH_2O. Sequencing PCR reactions were carried out in an MJ Research Inc. PCR block, according to the manufacturers' protocol. The reactions were then precipitated by adding 50 µl ethanol and 3 µl 3M sodium acetate pH 5.2, vortexing samples, and placing samples at –20°C for 30 minutes. Samples were then spun in a centrifuge at 13,200 rpm for 15 minutes. Pellets were washed with 70% ethanol. Samples were allowed to dry completely and were then resuspended in 3.5 µl suspension buffer (100 µl formamide, 20 µl 25 mM EDTA, pH 8.0). Resuspended samples were briefly heated

to 94°C for 2 minutes and then snap chilled on ice. Samples were loaded onto an ABI 373A Genetic Analyzer (Perkin Elmer) and sequencing was carried out according to manufacturers' instructions. Sequence data was collected using ABI data analysis and collection software. Automated sequencing was also carried out on an ABI 310 Genetic Analyzer (Perkin Elmer, Shelton, Connecticut) using Big Dye Terminator chemistries and a similar protocol. These sequencing samples were resuspended in Template Suppression Buffer (Perkin Elmer) prior to denaturation (Perkin Elmer).

2.2.5 Direct sequencing

Sequencing primers were labelled by incubating 5 pmol primer with 0.1U of T4 polynucleotide kinase (Biolabs), 1 µl of 10x T4 polynucleotide kinase buffer and 3 µl Ci [gamma-32P] dATP in a total volume of 10 µl, for at least an hour at 37°C. The mixture was then heat denatured at 94°C for 5 minutes. The DNA template was denatured at 94°C for 5-7 minutes with 2 µl of the labelled primer. The mixture was chilled on ice and held for 2 minutes. 2 µl of sequenase (USB) diluted 1 in 8 was added followed by 8 µl of sequencing buffer (Appendix A.1) and solution was mixed well. 4.4 µl of this DNA/primer mixture was added to each of four tubes containing 3 µl of the G, A, T or C dideoxy termination mixes (USB) held at 37°C. These mixtures were then incubated at 37°C for at least 10 minutes after which time 5 µl formamide loading dye (Appendix A.2) was added. A drop of paraffin oil was added to prevent evaporation and samples were denatured at 94°C for 5 minutes and placed on ice. 3-4 µl was loaded into the wells of an 8% non-denaturing polyacrylamide gel (Appendix A.2) for analysis and run in 1x TBE (Appendix A.2) buffer. Results were visualised by exposing dried gels to x-ray film.

2.3 RESULTS

2.3.1 Mitochondrial tRNA screening in Usher patient DNAs

Previous research carried out in this lab on a large family segregating RP and sensorineural deafness (symptoms resembling Usher syndrome), identified a novel disease-causing mutation within a mitochondrial tRNA gene (Mansergh *et al.*, 1999). A C→A transversion at position 12258 in the gene encoding the second mitochondrial serine tRNA, (*MTTS2*), was found to be heteroplasmic in affected family members. The aim of the current study is to investigate the extent to which mitochondrial tRNA mutations might be responsible for disease symptoms in other atypical cases of Usher syndrome, sporadic RP and/or sensorineural deafness.

Nineteen atypical Usher patient DNAs were acquired from Dr. William Kimberling, Boystown National Research Hospital, Omaha, NE, USA. These individual DNAs were carefully chosen from a large stock of Usher DNA samples. Families showing clear-cut Mendelian inheritance were excluded, and all DNAs chosen for analysis were from small families for which the mode of inheritance could not be defined or were isolated cases of the disease. These samples were screened previously for the C12258A mutation by Dr. Avril Kennan but this mutation was not detected in any individual (Kennan, 1999). Therefore, the aim of this study was to screen the coding sequence of the remaining 21 mitochondrial tRNA genes for possible disease-causing mutations. There was limited clinical data supplied for some of these individuals but any available information is presented in Table 2.1A.

A further 11 Usher DNA samples were provided by Dr. David Birch, Retina Foundation of the Southwest, Dallas, TX, USA. In addition, four atypical Usher DNA samples from patients segregating RP, hearing problems and other symptoms were received from Dr. Carmen Ayuso, Fundacion Jimenez Diaz, Madrid, Spain, as well as a number of Usher syndrome-like DNA samples which were provided by Dr. Paul Kenna, Ocular Genetics Unit, Trinity College Dublin (Table 2.1 B). These DNA samples were received by Dr. Kenna from a number of clinicians who suspected mitochondrial inheritance in patients that showed symptoms similar to those observed in the original family ZMK (Mansergh *et al.*, 1999). All patient DNA samples screened were from

families in which disease pedigree was compatible with mitochondrial inheritance, with a number of individuals displaying symptoms of mental retardation or muscular abnormalities.

In total, 27 additional DNA samples were screened for the C12258A mutation previously identified in family ZMK. These 27 samples were also screened for a variant at position 4336 in the $tRNA^{Gln}$ gene (Table 2.1). In screening for these two variants, the resulting PCR products also incorporated additional tRNA sequences which were subsequently screened, and included the complete tRNA sequences of Ile, Gln, Met, His, Ser2 and Leu2 (Table 2.2).

Table 2.1. (A) Clinical summary of 19 atypical Usher samples in which all 22 tRNA genes were screened for mutations

Family No.	No. of affected individuals	Clinical Symptoms
1	2	RP early and stabilised. Progressive and rapid hearing loss. RP in cousin with normal hearing.
2	1	Mental retardation, peripheral atrophy of RPE, facial dysmorphism.
3	1	Atypical Usher syndrome
4	1	Atypical Usher II syndrome, severe hearing loss since birth
5	2	Atypical Usher syndrome
6	1	Atypical Usher syndrome, cerebellar ataxia and pyramidalism
7	2	Atypical complex Usher type. One individual mild mental retardation, severe RP, skin and teeth problems. Other individual mild RP, asymmetrical progressive hearing loss
8	1	Atypical Usher syndrome
9	3	Atypical Usher syndrome
10	1	Atypical Usher syndrome.
11	1	Atypical Usher syndrome. Father and 3 siblings reported deaf.
12	1	Atypical Usher syndrome
13	1	Atypical Usher syndrome
14	1	Atypical Usher syndrome. RP at age 40, hearing aid at 40, mild retardation.

Table 2.1. (B) Available clinical data for additional DNA samples screened for C12258A and T4336C variants only.

15	1	Usher 2
16	1	Usher 2, heart problems, strabismus
17	2	Usher 1,
18	1	Atypical Usher 2, one sibling has hearing loss
19	1	Usher 2
20	1	Usher
21	1	Usher 2
22	1	Usher 2
23	1	RP isolate
24	1	Usher 2
25	1	Night blindness, progressive deafness, mental retardation
26	1	Night blindness, progressive deafness
27	1	Night blindness, progressive neurosensorial asymmetric deafness, partial focal seizures
28	1	Night blindness, delayed neural development, progressive deafness, distal muscular atrophy and ataxia.
29	3	RP, sensorineural hearing loss, maternal inheritance
30	2	RP, progressive hearing loss
31	4	Atypical Usher syndrome
32	2	RP, progressive hearing loss
33	1	RP, progressive hearing loss

Family DNA's 1-14 received from Dr. William Kimberling, Boystown National Research Hospital, Omaha, NE, USA.
Family DNA's 15-24 received from Dr. David Birch, Retina Foundation of the Southwest, Anderson Vision Research Centre, Dallas, TX, USA.
Family DNA's 25-28 received from Dr. Carmen Ayuso, Fundacion Jimenez Diaz, Clinica de Nuestra Senora de la Conception, Madrid, Spain.
Family DNA's 29-33 were acquired by Dr. Paul Kenna Ocular Genetics Unit, Trinity College Dublin and Royal Victoria Eye and Ear hospital, Adelaide Road, Dublin.

2.3.2 PCR amplification and sequencing reactions

The mitochondrial genome contains coding sequence for 22 tRNA genes, each approximately 70 nucleotides in length. Since many of the genes lie adjacent to each other on the mitochondrial chromosome, 13 sets of primer pairs were sufficient to amplify all 22 tRNA coding regions (Table 2.2). PCR conditions were optimised for all primer pairs and PCR reactions were carried out on the 19 atypical Usher DNA samples listed in Table 2.1A. The PCR products were subjected to automated sequencing and resulting sequences were analysed and compared to the published consensus sequence (http://www.mitomap.org/) using the computer program 'Genejockey'. Any variants that were found to be of particular interest, were sequenced manually to detect low levels of heteroplasmy if present.

Table 2.2. Location of 22 tRNA genes in the mitochondrial genome and amplification primers. (Individual primer sequences available in Appendix B.1).

tRNA (MTT)	Mitochondrial DNA Start site	Amplification Primers	
		Forward	Reverse
Phe (F)	577	Mt501F	Mt711R
Val (V)	1602	Mt1531F	Mt1781R
Leu 1 (L1) UUA/G	3230	Mt3151F	Mt3356R
Ile (I) Gln (Q) Met (M)	4263 4329 4402	Mt4189F	Mt4523R
Trp (W) Ala (A) Asn (N)	5512 5587 5657	Mt5451F	Mt5772R
Cys (C) Tyr (Y)	5761 5826	Mt5701F	Mt5942R
Ser 1 (S1) UCN Asp (D)	7445 7518	Mt7369F	Mt7639R
Lys (K)	8295	Mt8207F	Mt8418R
Gly (G)	9991	Mt9917F	Mt10150R
Arg (R)	10405	Mt10337F	Mt10521R
His (H) Ser 2 (S2) AGU/C Leu 2 (L2) CUN	12138 12207 12266	Mt12067F	Mt12389R
Glu (E)	14674	Mt14611F	Mt14793R
Thr (T) Pro (P)	15888 15955	Mt15806F	Mt16076R

N = Any nucleotide U,C,A or G.
Note: Some sets of primers span more than one tRNA gene.

2.3.3 Mitochondrial tRNA variants identified

A number of variations from the consensus mitochondrial sequence were observed in the initial analysis of all 22 tRNA sequences in 19 atypical Usher DNA samples. Five polymorphic variants were identified at positions 5823, 7521, 10463, 12236, and 15928 in one individual only, but which have previously been detected in normal populations at high frequency (http://www.mitomap.org/). Three additional sequence variants were identified, at positions 4336, 12308 and 15924 (Fig. 2.3), which have previously been associated with various diseases, but many of these associations are unconfirmed (http://www.mitomap.org/). The variants at position 4336 and 15924 were analysed using direct sequencing methods to detect possible heteroplasmy, but all variants appeared to be homoplasmic (Fig. 2.4). Further details of variants identified are outlined in Table 2.3 below. A total of 27 additional patient DNAs were screened for the C12258A mutation, but it was not detected in any samples. These samples were also screened for the T4336C variant, which was identified in one additional individual's DNA.

Table 2.3. Variants in mitochondrial tRNA gene sequences identified in a study of atypical Usher patient DNAs.

Variant nt position	No. of DNA samples	Family Number (Table 2.1)	tRNA gene	Homo-plasmy	Hetero-plasmy	Disease assoc-iation	Frequency in Normal Controls (%)	Status
4336 (T-C)	2/46	4, 28	tRNA Gln	+	+	AD+PD	0.4	Unclear
12308 (A-G)	7/46	2, 3, 11, 29, 33	tRNA Leu(CUN)	+	-	CPEO	16	P.M.
15924 (A-G)	1/19	3	tRNA Thr	+	-	LIMM	10.7	P.M.

AD+PD, Alzheimers and Parkinsons disease; CPEO, Chronic Progressive External Opthalmoplegia; LIMM, Lethal Infantile Mitochondrial Myopathy; nt, nucleotide.

Status refers to the classification assigned to a particular polymorphic variant in the mitomap database (http://www.mitomap.org/):

'P.M.' indicates that some published reports have determined these variants to be polymorphic.

'Unclear' indicates that more than one independent group has reported the pathogenicity of this mutation but others dispute these findings.

2.4 DISCUSSION

Despite extensive investigation into the association between mitochondrial tRNA variants and disease, it is difficult in many cases to establish whether a variant is truly disease-causing or simply a neutral polymorphic variant. A variant at position 4336 (A to G on reverse strand) in the tRNA Glutamine gene, has been identified in two atypical Usher patient DNAs out of 46 samples examined in the current study (4.3%). This moderately-conserved variant has previously been associated with the neurodegenerative diseases Alzheimer's Disease (AD) and Parkinson's Disease (PD) (Shoffner *et al.,* 1993; Hutchin & Cortopassi, 1995), and is generally found to be homoplasmic, but incidences of heteroplasmy have also been reported (Sternberg *et al.,* 2001). One group has reported that approximately 5.2% of AD and PD patients harboured this mutation compared to 0.7% of age-matched controls (Shoffner *et al.,* 1993). A second group screened AD and PD patients for mitochondrial mutations, and their results also supported the hypothesis that the mitochondrial A4336G mutation represents a risk factor for AD and PD (Egensperger *et al.,* 1997). A more recent paper has reported increased risk of sensorineural hearing loss and migraine in patients with the A4336G mutation (Finnila *et al.,* 2001). This group reported the 4336 mutation in patients with matrilineal sensorineural hearing impairment, at a frequency of 3.6% compared to 0.63% of controls. Other reports however do not support an association between the 4336 variant and AD or PD, or report inconclusive findings (Simon *et al.,* 2000; Mayr-Wohlfart *et al.,* 1997; Edland *et al.*, 2002).

It has been proposed that mutations of mitochondrial genes may interact with nuclear or environmental factors and may predispose individuals to an increased risk of developing neurodegenerative diseases (Finnila *et al.,* 2001). The variant at position 4336 could represent one of these modifying factors. It may be of benefit to carry out further analysis of this variant in RP and/or sensorineural deafness patients to investigate, if any, its role in neurosensory disease but it is unlikely any solid conclusions could be drawn about it's involvement unless it was found in a relatively high percentage of individuals.

It is not known if the other two variants identified in atypical Usher patients at positions 12308 and 15924 are disease-related, but they are unlikely to be of

significance because of the relatively high frequency at which they are found in the normal population. The variant at position 12308 in the tRNA $^{Leu\ (CUN)}$ gene which was identified in 15% of patients in the current study, has previously been associated with chronic progressive external opthalmoplegia (CPEO) (Lauber *et al.,* 1991), but it has also been reported at high frequency in normal controls (up to 16%) (van den Ouweland *et al.,* 1992). The variant at position 15924 in the tRNA^{Thr} gene has previously been associated with lethal infantile mitochondrial myopathy (LIMM), but since initial reports, it has also been found in a number of normal control individuals (Brown *et al.,* 1992). These two variants lie in relatively conserved sites of the mitochondrial genome, but it has been shown in a number of studies that even evolutionarily conserved regions in mitochondrial tRNA genes can exhibit a significant polymorphism in humans (van den Ouweland *et al.,* 1992).

The C12258A substitution originally identified in Family ZMK has not been identified in any of the 46 additional atypical Usher DNA samples analysed to date. This substitution may occur very infrequently in cases of Usher syndrome as it has only ever been identified in two families as well as in one isolated individual, and in only one of these families were the disease symptoms similar to Usher syndrome (Mansergh *et al.,* 1999; Lynn *et al.,* 1998).

2.5 CONCLUSION

Pathogenic mutations in mitochondrial tRNA genes do not appear to be a common cause of atypical Usher syndrome. An entire screen of tRNA sequences in 19 atypical Usher DNAs did not identify any previously reported pathogenic mutation nor any previously undescribed possible disease-causing variant. Three of the variants identified in this study have been associated with disease, but are unlikely to be the primary disease-causing mutations in the individuals screened, due to the severity of disease symptoms and the presence of these variants in the general population.

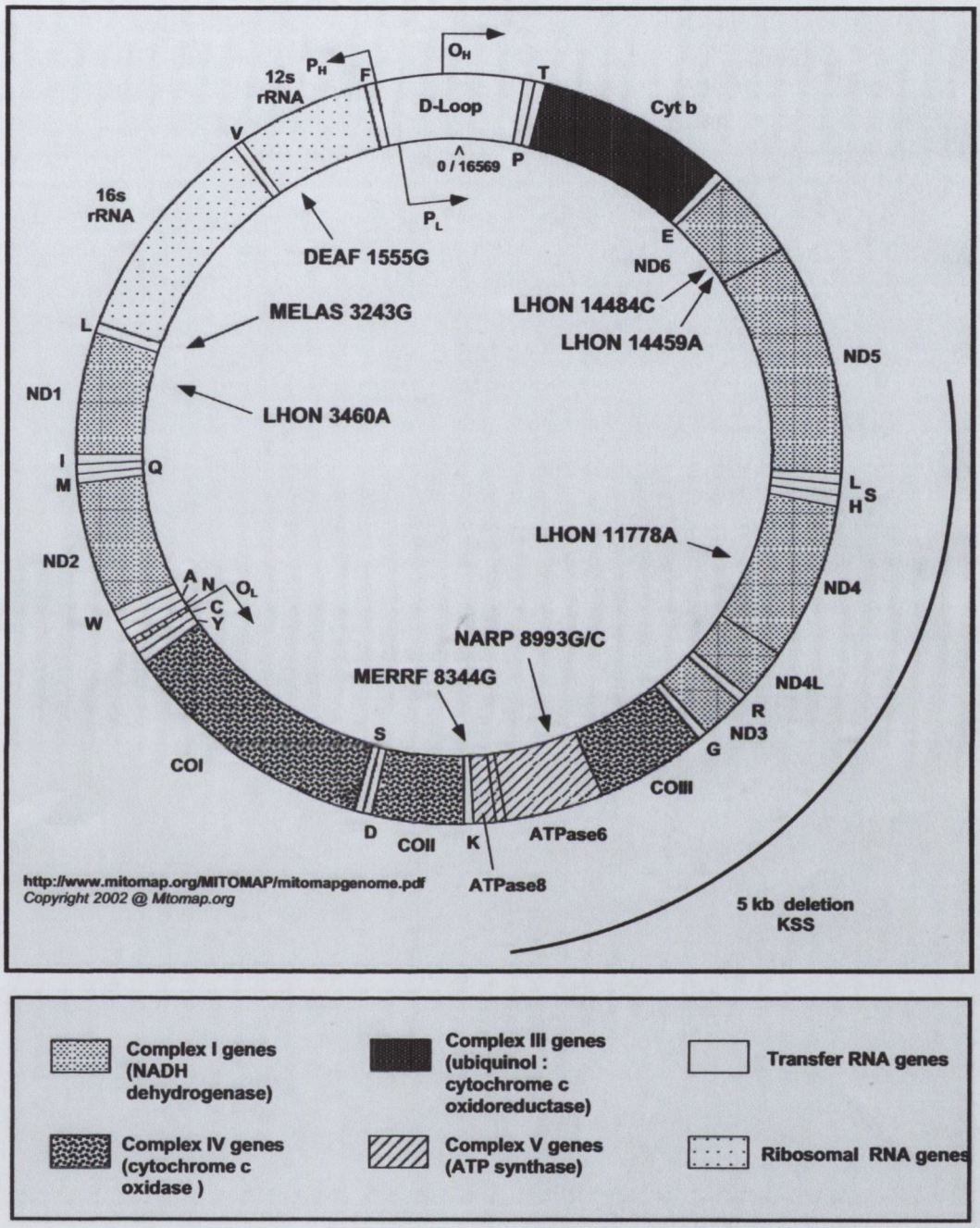

Figure 2.1. Diagrammatic representation of the human mitochondrial gene map.

The general function of each gene is identified by a shaded pattern. The 22 tRNA genes, 2 rRNA genes and 13 polypeptide-coding regions contained in the mitochondrial genome are shown. The nucleotide location of a number of well-established mutations and their disease association is also shown.

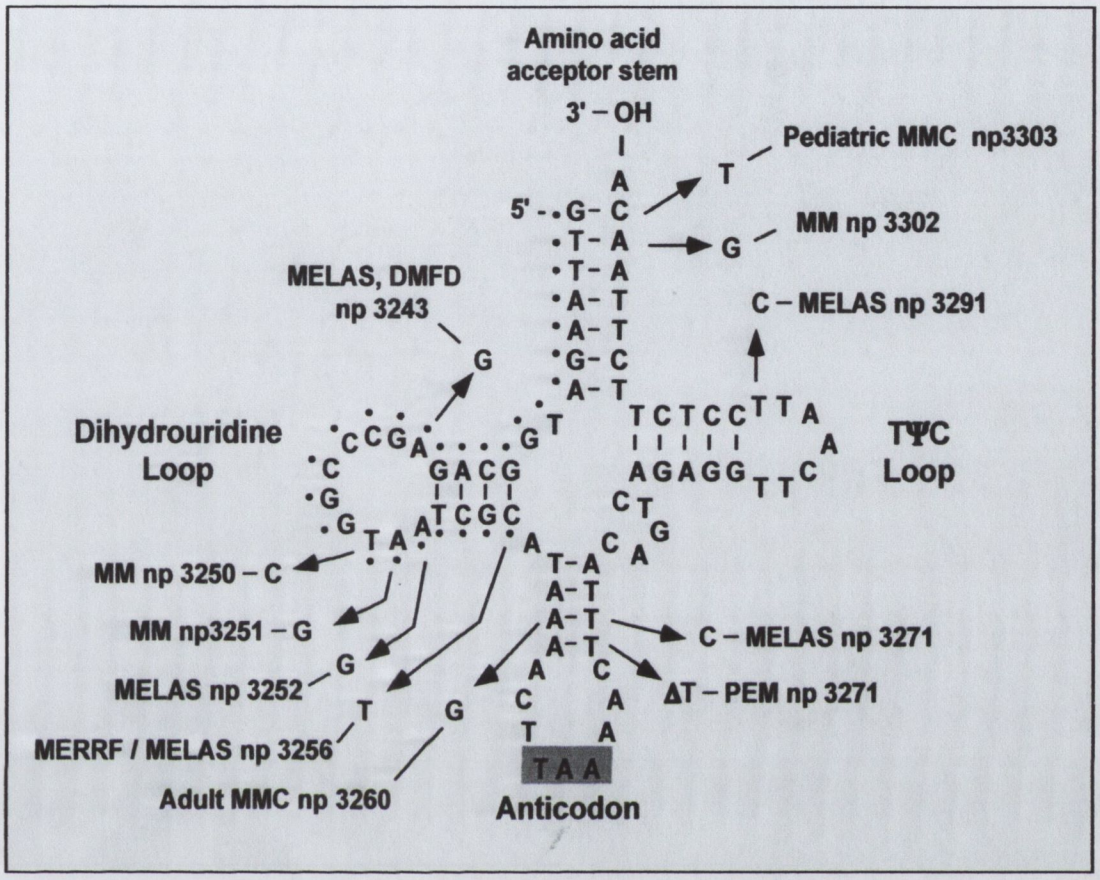

Figure 2.2. Representation of the cloverleaf structure of mitochondrial tRNA $^{Leu(UUR)}$ showing a selection of pathological mutations identified to date. Disease-causing mutations are randomly distributed throughout the structural domains of the tRNA gene, and can encompass a variety of clinical presentations. The mitochondrial transcription terminator binding site is indicated by the black dots. (Figure adapted from Wallace *et al.*, 1996 and http://www.mitomap.org/MITOMAP/tRNAleu.pdf)

MELAS, Mitochondrial myopathy, encephalopathy, lactic acidosis, and stroke-like episodes; MM, Mitochondrial myopathy; DMDF, Diabetes mellitus and deafness; MMC, Maternal myopathy and cardiomyopathy; MERFF, Myoclonic epilepsy associated with ragged-red fibers; PEM, Progressive encephalopathy; np, nucleotide position.

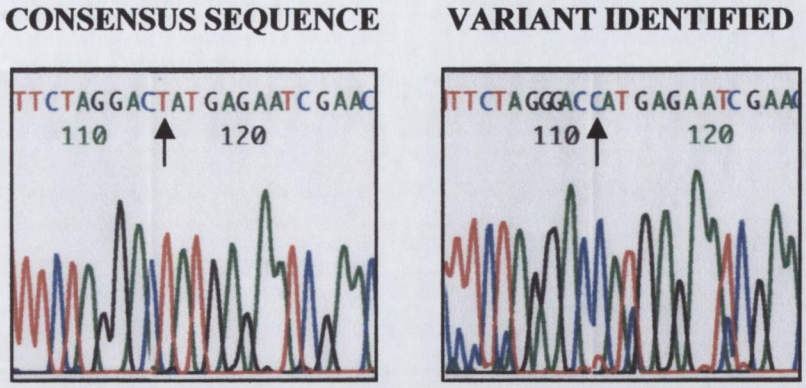

A Mitochondrial T4336C variant identified in 2 out of 46 Usher DNAs

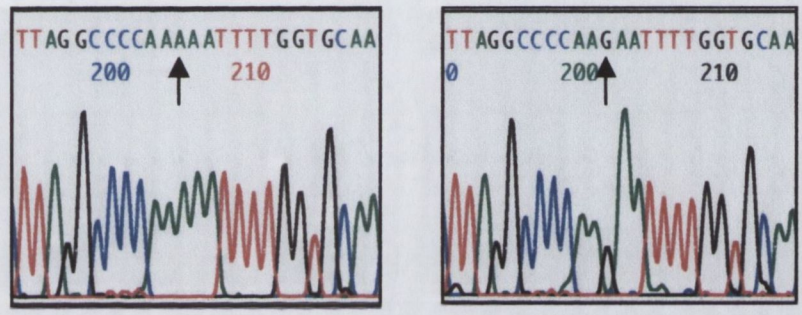

B Mitochondrial A12308G variant identified in 7 out of 46 Usher DNAs

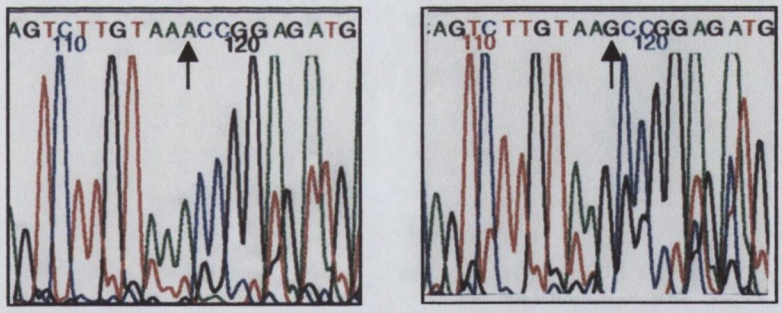

C Mitochondrial A15924G variant identified in one of 19 Usher DNAs

Figure 2.3. Automated sequence analysis of mitochondrial tRNA genes in atypical Usher patient DNA samples. **(A)** Sequence analysis of the normal consensus sequence shown alongside an Usher syndrome patient segregating a T4336C variant, **(B)** normal consensus sequence and an Usher sample that showed the A12308G variant and **(C)** normal sequence and an Usher syndrome patient showing the A15924G variant.

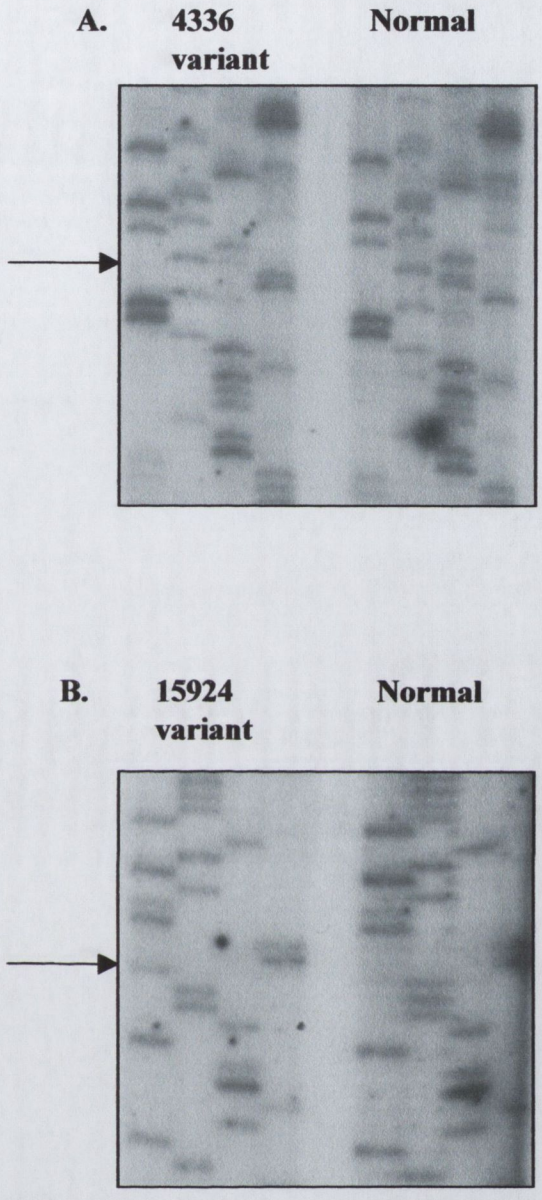

Figure 2.4. Direct sequence analysis of mitochondrial tRNA genes in atypical Usher patient DNA samples. **(A)** Usher patient showing a T-C variant at position 4336 alongside a normal individual. **(B)** Usher patient showing an A-G variant at position 15924 alongside a normal individual. Both variants appear to be homoplasmic. The four gel lanes for each individual have been loaded in the order G A T C.

CHAPTER 3

COMPARATIVE MICROARRAY ANALYSIS OF WILD-TYPE AND *RHO*$^{-/-}$ MOUSE RETINAS

3.1 INTRODUCTION

3.1.1 Introduction

DNA microarray analysis is an extremely powerful tool in the global analysis of gene expression patterns. This chapter describes the results obtained following a large microarray experiment carried out using commercially available Affymetrix genechips. The aim of this analysis was to compare the transcriptional profiles of approximately 6,000 genes in the retinas of wild-type (Wt) mice with those carrying a targeted disruption of the rhodopsin gene (*Rho*$^{-/-}$). This revealed a series of transcripts, in which levels were elevated or reduced in the retinas of *Rho*$^{-/-}$ mice, some of which were derived from genes known to map at retinopathy loci. One of the down-regulated genes, *IMPDH1*, was found to map to the RP10 locus which is discussed in detail in Chapter 4. Quantitative RT-PCR was used to verify the up- or down-regulation of a selection of transcripts showing differential expression.

An investigation into the function of genes showing altered expression patterns was undertaken, and a discussion of the functional gene groups that may be of significance in the degenerating retina is presented. We suggest that those genes observed to be differentially expressed between Wt and *Rho*$^{-/-}$ retinas may represent candidate disease-associated genes in hereditary retinal degenerations.

3.1.2 Rhodopsin knockout mouse

A mouse carrying a targeted disruption of the rhodopsin gene (*Rho*$^{-/-}$) was generated by Dr. Marian Humphries and colleagues in 1997. *Rho*$^{-/-}$ mice do not elaborate rod outer segments, and they lose their photoreceptor cell layer over 3 months. At 24 days, the number of nuclei in the outer nuclear layer (ONL) of *Rho*$^{-/-}$ mouse retinas is similar to that of wild-type mice, by 48 days the ONL is reduced to about half of its original width, and by 90 days, there remains only a single cell thickness in the ONL (Fig. 3.1). There is no rod ERG response detectable in 8-week old animals (Humphries *et al.*, 1997). Thus, at 90 days the degeneration is essentially complete. It has been

demonstrated that the severity of retinal degeneration is influenced by the nature of the genetic background upon which the mutation is expressed. Retinas from *Rho*$^{-/-}$129Sv mice degenerate structurally and functionally more rapidly than those of *Rho*$^{-/-}$C57/BL6 mice (Hobson *et al.,* 2000; Humphries *et al.,* 2001). In the *Rho*$^{-/-}$129Sv strain, all rod photoreceptors are lost at four months of age, and while residual cell bodies of cones persist, ERG analysis has shown that these cells are non-functional (Humphries *et al.,* 2001; Toda *et al.,* 1999). For the microarray analysis described in the current study, only mice on the 129Sv background were used, which minimises any potential gene expression differences that would occur between different strains of mice.

The *Rho*$^{-/-}$ mouse provides a model that enables a comparison of transcriptional profiles in mouse retinas with and without functional photoreceptors. Elevations or reductions in expression of transcripts from the *Rho*$^{-/-}$ retinas are likely to be a reflection of the destruction of primary retinal neurons, and/or of a response by remaining retinal cells toward the degenerative processes taking place.

3.1.3 Microarray analysis

Microarray or gene chip experiments allow the simultaneous study of thousands of genes or mRNAs under various physiological and pathological states. Microarray analysis allows a global analysis of gene expression to be undertaken, providing information on expression patterns and possibly identifying interactions between genes. The gene sequence which is used in microarray chips is derived from expressed sequences of genes which were originally identified through sequencing of 5' and 3' ends of randomly selected cDNA library clones. These stretches of sequence are called expressed sequence tags (ESTs), which are then deposited in an expressed sequence database such as the Genbank database at the NCBI (http://www.ncbi.nlm.nih.gov/Genbank/) or The Institute of Genomic Research (TIGR) EST database (http://www.tigr.org). Overlapping and homologous sequences are clustered together to generate sequence sets called 'Unigene' sets, that each represent the transcription product of a particular gene. The sequence information in these EST clusters is then used to construct microarray chips.

The study of gene expression by DNA microarray technology involves the immobilisation of DNA sequences corresponding to known genes, onto glass chips.

The technology for cDNA-based microarrays is based on an approach whereby cDNA clones, usually PCR products of sequences obtained from EST databases, are amplified and are robotically printed or spotted onto slides (Watson & Akil, 1999). Different fluorophores (generally Cy3- and Cy5-dUTP) are used to label cDNAs from control or reference samples. The labelled cDNAs are mixed together, prior to hybridisation to the array. Relative amounts of a particular gene transcript in the two samples are determined by measuring the signal intensities detected for both fluorophores, and calculating signal ratios.

On GeneChip® arrays, such as those from Affymetrix Inc., oligonucleotides are synthesised directly on the chip itself in parallel, resulting in the addition of an A, C, T, or G nucleotide to multiple growing chains simultaneously. A given gene is represented by 11-20 different 25-mer oligonucleotides, which are unique to each gene. For each probe designed that is perfectly complementary to a target sequence, a partner probe is generated that is identical except for a single mismatch in its centre, in an approach called the Perfect Match/Mismatch probe strategy (Lipshutz *et al.*, 1999). These probe pairs allow the quantitation and subtraction of signals caused by non-specific cross-hybridisation. Labelled cDNA or cRNA targets derived from the mRNA of an experimental sample are then hybridised to the probes attached to a solid support. The difference in hybridisation signals between the Perfect Match and Mismatch probes, as well as their intensity ratios, serve as indicators of specific target abundance. Both cDNA microarrays and GeneChip array types are analysed using specialised fluorescent image analysis systems, that measure the hybridisation intensities for each individual probe set. Oligonucleotide arrays have a number of advantages over cDNA arrays. They can be generated directly for sequence information without the need for physical intermediates such as cDNAs or PCR products, and large number of probes are used, which can be designed specifically to unique regions of a particular gene, thereby reducing cross-hybridisation. In comparison, cDNA arrays are more versatile because array probe sets can be added or removed relatively easily.

Many different applications of microarrays have also been developed in recent times. Commercially available GeneChips for gene expression experiments have become larger and more advanced, and now contain probe sets for a number of genomes including human, mouse, rat, *E.coli*, Arabidopsis, Drosophila and *C. elegans*. The GeneChip® Human genome U133 array (Affymetrix) can now analyse the expression of over 47,000 transcripts including 38,500 well-characterised human genes,

while the most recent mouse genome expression set, the GeneChip® mouse expression array 430A set (Affymetrix) analyses the expression level of over 39,000 transcripts including over 34,000 well substantiated mouse genes (Affymetrix data sheets; http://affymetrix.com/index.affx). While GeneChips were originally used for gene expression analysis experiments, a more recent application is the analysis of whole genomes, by tracking single nucleotide polymorphisms (SNPs) (Cutler *et al.,* 2001). The GeneChip® HuSNP Array (Affymetrix) enables whole genome surveys, by simultaneously tracking nearly 1,500 genetic SNP variations dispersed throughout the genome. These arrays can be used in familial linkage studies that aim to map human hereditary diseases, detection of chromosomal re-arrangements, and also in analysis of variants associated with complex diseases. Recent studies have demonstrated that global patterns of allelic imbalance (loss or gain of at least one allele) can be discerned by allelotyping of tumors with new-generation SNP arrays, which may identify important cancer genes associated with disease progression (Hoque *et al.,* 2003; Primdahl *et al.,* 2002). The use of custom microarrays, both cDNA and oligonucleotide, is also growing in popularity. Custom arrays can be used for expression analysis of a particular subset of chosen genes, or custom resequencing arrays can be generated, which can be used to detect genetic variation in a large number of selected candidate genes (up to 30,000 base pairs), in one single experiment. DNA microarrays are extremely valuable tools but can be expensive to employ, especially if the use of specialised or custom arrays is required.

The Affymetrix genechip used in this study was one of the first murine chips to be made commercially available. It was called the Murine Genome Mu11K array set and represented approximately 6,000 sequences in the Mouse Unigene database. A microarray experiment was designed which involved the use of this chip to analyse the differential expression of genes in retinas of wild type 129Sv mice with those of *Rho*$^{-/-}$ 129Sv mice (Kennan *et al.,* 2002).

3.1.4 Studies on global gene expression in the retina

Researchers have recently begun to analyse the retinal transcriptome (pattern of expression of all genes in the retina) using high-throughput molecular and computational tools. Microarray experiments on gene expression patterns in the retina

have been carried out by a number of groups. One of the first microarray studies on retinal tissue was carried out using a cDNA microarray containing 960 gene probes to analyse gene expression in the *Crx*$^{-/-}$ mouse, and thereby identify the transcriptional network controlled by the retinal-specific transcription factor CRX (Livesey *et al.*, 2000). More recent studies have included microarray analysis of gene expression in the aging human retina, in which it was found that pathways involved in stress response and energy metabolism play key roles in retinal aging (Yoshida *et al.*, 2002). Other groups have reported gene expression profiles of light-induced apoptosis in arrestin/rhodopsin kinase-deficient mouse retinas and analysis of gene expression in the developing mouse retina (Choi *et al.*, 2001; Diaz *et al.*, 2003).

A large research effort has concentrated on the identification of genes and expressed sequence tags (ESTs) isolated from the retina and the RPE, many through computational analysis of databases such as Unigene, or through subtractive library analysis (Malone *et al.*, 1999; Sinha *et al.*, 2000; Yu *et al.*, 2003). Expression analysis in the retina has also been investigated using serial analysis of gene expression (SAGE), which is a sequence-based approach that identifies the genes that are expressed in a particular sample and quantifies their level of expression (Velculescu *et al.*, 1995). A large SAGE analysis of over 500,000 tags derived from developing and mature mouse retinas has been performed, which resulted in the identification of 264 uncharacterized genes, that were specific to, or highly enriched in rod photoreceptor cells (Blackshaw *et al.*, 2001). The same group also carried out a large SAGE study to measure the relative levels of expression of the genes expressed in the human peripheral retina, macula, and retinal pigment epithelium (RPE) (Sharon *et al.*, 2002). It is estimated from analysis of the current Unigene clusters, SAGE tags and ESTs, that a complete transcriptome of the human retina will consist of approximately 25,000 sequences (Swaroop & Zack, 2002). While a large number of ESTs have been identified that are expressed at higher levels in the retina, many of these are uncharacterised and only a limited number of cell-type specific or preferentially expressed genes (less than a hundred) have to date been characterised for the neural retina (Swaroop & Zack, 2002). Future characterisation of novel SAGE tags and ESTs should result in the identification of many more genes that are preferentially expressed in the retina. Another major use of a comprehensive retinal gene catalog is the production of custom microarrays specifically containing retinal gene probes. A custom cDNA microarray for human retinal gene expression has recently been produced which contains over 10,000 gene sequences, and will likely be

used for comparing expression profiles between normal and diseased human retinas (Chowers *et al.*, 2003).

Extensive amounts of data are generated in large scale expression analysis experiments, and a major challenge exists in the analysis of results in order to interpret observed expression differences. In addition, results from EST data mining, SAGE analysis and microarray data do not always agree with each other and have often produced very different results (Swaroop & Zack, 2002). There is some controversy over inconsistency between methods used in the analysis of microarray data, but the recent adoption of common standards and ontologies for the management and sharing of microarray data should be of considerable benefit (Stoeckert *et al.*, 2002). In an effort to consolidate information for data-mining efforts, a number of retinal expression databases have been developed such as the NEIBank database created by the National Eye Institute, which includes EST data for several human eye cDNA libraries (http://neibank.nei.nih.gov/index.shtml).

The microarray analysis described in this study gives an insight into the gene expression patterns of a normal and a degenerated retina, and provides some clues into the processes that are occurring in the retina immediately after photoreceptor degeneration.

3.1.5 Microarray analysis for disease gene discovery

While positional cloning projects have been greatly facilitated by the availability of human genome maps and sequence data, the application of expression profiling to disease gene identification is also growing in importance. Several approaches to disease gene identification using techniques such as microarray analysis have previously been suggested, but few have actually achieved this goal. The simplest approach involves the comparison of expression levels directly between two tissue types or samples, as demonstrated in the current study comparing a diseased ($Rho^{-/-}$) versus normal (Wt) tissue. Alternatively, statistical and cluster analysis of microarray results may reveal new, previously uncharacterised signalling pathways associated with a target disease gene (Meltzer, 2001). As mentioned previously, SNP chips could also be used for large-scale genome analysis in gene mapping experiments. In a novel diagnostic use of microarray technology, a genotyping microarray for the large retinal

disease-associated gene, *ABCR*, has recently been developed. This microarray includes approximately 400 disease-associated sequence changes and other variants currently described within the *ABCR* gene, enabling simultaneous detection of all known *ABCR* variants (Jaakson *et al.,* 2003).

The current study, which involves the comparison of transcriptional profiles of wild-type and *Rho*$^{-/-}$ mouse retinas, was one of the first to use the results from microarray analysis for the identification of a disease-associated gene. At the same time as this study was reported, the large SAGE experiment by Blackshaw and colleagues described previously, identified a large number of genes that appeared to be preferentially expressed in photoreceptors, by comparing the SAGE tags derived from a control mouse retina with that of mice lacking the *Crx* gene. The authors estimated that up to 86 of the human orthologs of these genes, including *IMPDH1*, mapped to within intervals containing uncloned retinal disease genes, and were thus identified as possible retinal disease candidates (Blackshaw *et al.,* 2001). The identification of a novel deafness-associated gene, μ-crystallin, has also been reported following microarray analysis of gene expression in human cochlea and vestibule tissue (Abe *et al.,* 2003). Further analysis of a number of genes identified as being preferentially-expressed in the retina may, in the future, point to additional novel genes involved in retinal degenerative diseases.

3.1.6 Validation of microarray studies

The results obtained following microarray analysis experiments, are usually validated by measuring the expression level of a selection of predicted differentially expressed genes, using an alternative experimental technique. In many instances this validation is done by real-time or quantitative RT-PCR analysis. The microarray results showing changes in levels of transcript detected between wild-type and *Rho*$^{-/-}$ mouse retinas in the current study, were validated by quantification of changes in gene expression using the Roche LightCycler® system. The amplification of candidate genes can be analysed quantitatively by adding the fluorescent dye SYBR Green I to the PCR reaction, which binds to the minor groove of the DNA double helix. In solution, the unbound dye exhibits very little fluorescence, but fluorescence is greatly enhanced upon DNA-binding. As PCR amplification progresses, a greater number of dye molecules bind to

the newly synthesized DNA. If the reaction is monitored continuously, the increase in fluorescence can be viewed in real time. The final quantity of dsDNA detected can be directly related to the starting concentrations present in a particular sample. This is an appropriate method of looking at the up/down-regulation of genes between different tissue samples because it detects very minor changes in expression levels, and is reproducible. A house-keeping gene such as GAPDH or β-actin is usually analysed to normalise RNA or cDNA concentrations between different samples being examined, prior to calculation of relative expression levels.

Other methods can also be used in the direct measurement or validation of microarray findings such as Northern blotting, which measures relative quantities of RNA, and Western blotting to measure protein levels. *In situ* hybridisation studies are often carried out to measure cell or region specificity of mRNA transcripts.

3.1.7 The aim of the study

The aim of this study was to compare the transcriptional profiles of wild-type mouse retinas, with *Rho-/-* retinas which lack photoreceptor cells, in an attempt to identify genes that are preferentially expressed in the photoreceptor cell layer and gain an insight into the processes that are occuring in the degenerating retina. A number of genes showing considerable differences in transcript levels between samples were identified. The corresponding human chromosomal location of these genes was established to see if any mapped to known retinal degeneration loci, which resulted in the identification of a number of possible candidate retinal degeneration genes. Any genes that showed a decrease in levels of expression in $Rho^{-/-}$ retinas were predicted to play an important role in the functioning of photoreceptor cells. A functional analysis of both up- and down-regulated gene products was undertaken to determine whether expression patterns between particular functional groups of genes could be established.

3.2 MATERIALS AND METHODS

3.2.1 RNA extraction

Mice were initially generated carrying a targeted disruption of the rhodopsin gene using 129Sv-derived manipulated stem cells and C57BL/6J blastulas (Humphries *et al.*, 1997). Founders on the mixed 129/C57 background were backcrossed through a minimum of twelve successive generations onto essentially pure C57BL/6J and 129Sv genetic backgrounds. The latter were used in the current investigation. Total RNA was isolated by Dr. Arpad Palfi from pooled retinas of two sets of 10, four month old, 129Sv wild type and 129Sv *Rho*$^{-/-}$ mice by the method of Chomczynski and Sacchi.

3.2.2 cRNA preparation

cRNA preparation and microarray analysis was carried out in Aarhus Denmark in a collaboration with Dr. Karin Demtroder and Dr. Torben Orntoft. Reverse transcription was performed on 12 μg of total RNA for 1 hr at 42°C using a T7-oligo $(dT)_{24}$-primer and Superscript II RT (Gibco, Life Technologies, Rockville , MD). Second strand cDNA synthesis was done for 2 hours at 16°C using *E.coli* DNA Pol I, DNA Ligase and RNAseH (Gibco, Life Technologies), followed by incubation in NaOH/EDTA for 10 min at 65°C in order to degrade rRNA and tRNA. After phenol-chloroform extraction transcription was performed for 6 hr at 37°C using the Bioarray high-yield RNA transcript labeling kit with Bio-16-UTP and Bio-11-CTP nucleotides (Enzo Diagnostics, Farmingdale, NY). cRNA samples were purified with the RNeasy kit (Qiagen, Crawley, UK) followed by fragmentation for 35 min at 95°C.

3.2.3 CHIP-analysis

Samples were analyzed on GeneChips® (Affymetrix, USA), where perfect match and mismatch are defined by an algorithm. To check the quality of each sample with regard

to housekeeping genes GAPDH and β-actin, 15 μg of labeled cRNA was run on Test2-CHIPs (Affymetrix, Inc., Santa Clara, CA). Murine expression chips "Mu11K subB" (Affymetrix) containing 6595 datasets were hybridized with 15 μg labeled cRNA for 16 hr at 45°C under rotation. Mu11K subB-chips were stained in an Affymetrix Fluidics station using SAPE (Streptavidin/Phycoerythrin) followed by staining with an anti-streptavidin antibody and SAPE. Chips were scanned with a HP-Laserscanner and data were analyzed with the Microarray Suite Software (Affymetrix). Each microarray was scaled to "150" for normalization and then analyzed as previously described in detail (Thykjaer *et al.*, 2001).

3.2.4 Data analysis and selection of candidate genes

Four comparison analyses were obtained by comparing expression data of each wild-type versus each *Rho*$^{-/-}$ sample using Affymetrix Software (Microarray Suite 4.0, Microdatabase 2.0 and Datamining Tool 2.0). After deletion of 55 Affymetrix spike-controls the remaining 6540 datasets derived from subB-Genechip analysis were sorted according to stringent criteria. 144 datasets were excluded from analysis because the absolute call was absent on all GeneChips® and 5497 datasets were excluded because the difference call was not changed in all four comparisons. A ranking based on difference calls was done on the remaining 899 datasets. Genes were then excluded in cases where 3 of 4 comparisons were not changed or 2 of 4 comparisons were not changed, accompanied by one decreased and one increased comparison. The 420 remaining genes showing an increase or decrease in at least 2 of 4 comparisons were regarded as potential candidates. 275 genes were up-regulated and 145 were down-regulated in the *Rho*$^{-/-}$ mouse retinas. Of these candidates, 57 genes were up-regulated and 62 genes were down-regulated more than 3-fold. 85 of these genes changed more than 3-fold in at least three comparisons and were regarded as the most interesting candidate genes (33 up- and 52 down-regulated, and of these 21 genes were up- and 42 were down-regulated in all four comparisons).

3.2.5 Databases used to in analysis of microarray data

Datamining was performed to obtain functional information and expression patterns of all 85 genes that showed differential expression levels, and involved the use of the following databases; Locuslink (http://www.ncbi.nlm.nih.gov/LocusLink/), Unigene (http://www.ncbi.nlm.nih.gov/entrez/query.fcgi?db=unigene)and Refseq (http://www.ncbi.nlm.nih.gov/RefSeq/), as well as extensive literature searches (http://www.ncbi.nlm.nih.gov/entrez/query.fcgi?db=PubMed).
Candidate retinal disease loci were identified using the Retnet database (http://www.sph.uth.tmc.edu/Retnet/), and interval flanking markers were confirmed using the Human Genome Browser (http://genome.ucsc.edu/cgi-bin/hgGateway), and Ensembl Genome Browser (http://www.ensembl.org/) databases.

3.2.6 Quantitative RT-PCR analysis

Primers for each gene were designed using the Primer3 program and spanned exon/intron boundaries if possible (Appendix B.2). The ideal product size was about 200 bp. All primers for use on the Lightcycler were HPLC purified. First strand cDNA synthesis was carried out using 2 μg of total RNA from the original pooled wild-type and *Rho*$^{-/-}$ RNA samples prepared by Dr. Arpad Palfi. cDNA was prepared by adding 4 units Omniscript RT (Qiagen) and 1 μM random primers. Quantitative PCR was performed on a Roche LightCycler using a Quantitect PCR kit (Qiagen) according to manufacturers' instructions. This system uses SYBR green to fluorescently label double-stranded DNA as the PCR reaction progresses. Serial dilutions of cDNA from 1/10 to 1/10,000 were used to generate standard curves of crossing cycle number versus the logarithmus of concentration for the gene of interest. A linear regression line calculated from the standard curves allowed relative transcript levels in both cDNA samples to be determined. Values were normalised to the relative amounts of a housekeeping gene GAPDH present in the same cDNA preparations. A melting curve analysis was also carried out after each amplification step, which provides confirmation that specific PCR products were formed in the reaction.

3.3 RESULTS

3.3.1 Microarray-based transcriptional analysis of wild-type and *Rho*$^{-/-}$ retinas

Microarray studies were performed on RNA extracted from the retinas of wild-type 129Sv mice and *Rho*$^{-/-}$ 129Sv mice, at four months of age. Wild-type (Wt) retinas are normal in appearance at 4 months, but rod photoreceptors are absent from the retinas of *Rho*$^{-/-}$ mice at this age and cone photoreceptor function is completely ablated (Humphries *et al.*, 1997). Four GeneChips® (Affymetrix Inc.) were used in total; two were hybridised with Wt retinal cRNA and two with *Rho*$^{-/-}$ cRNA. RNA from the retinas of 10 mice was extracted by Dr. Arpad Palfi, and pooled for each of the four RNA samples used in the analysis. Pooled samples were used to minimise the effects of variability that may occur between individual animals. Four different comparisons were made between the different cRNA samples; Wt1/*Rho*$^{-/-}$1, Wt2/*Rho*$^{-/-}$2, Wt1/*Rho*$^{-/-}$2 and Wt2/*Rho*$^{-/-}$1. Following analysis, 420 genes showed increased or deceased expression in at least 2 of 4 comparisons and therefore these genes were considered highly likely to show real differential expression between wild-type and *Rho*$^{-/-}$ mice. The GeneChip hybridisations and initial analysis were carried out by Karin Demtroder and colleagues, Aarhus, Denmark.

Photoreceptors are essentially absent from the *Rho*$^{-/-}$ retina at 4 months and therefore there is less RNA present in a single mutant retina than in the wild type. As mRNA levels were compared between the same concentrations of retinal RNA it was predicted that, as a result of compensation for the lack of photoreceptor RNA, non-photoreceptor layers would be over-represented in the *Rho*$^{-/-}$ sample. This prediction was borne out by the 107 genes showing a moderate increase in expression (1.7 to 2.5-fold) between wild-type and *Rho*$^{-/-}$ retinas, compared to only 38 with an equivalent decrease. The 228 transcripts that showed an average increase of >1.5-fold in at least 2 of 4 comparisons and the 131 that showed an average decrease of >1.5-fold in at least 2 of 4 comparisons were further analysed. Classification of these genes into categories of average fold change in expression levels between wild type and *Rho*$^{-/-}$ retinas illustrated the greater numbers of moderately increased genes and dramatically decreased genes

(Fig. 3.2). This analysis was carried out by Dr. David Simpson, Queens University Belfast.

Of these transcripts, only those that had an average change of ≥3-fold in 3 or 4 comparisons were selected for further analysis leaving a total of 74 different candidates, 44 of which showed decreased expression in the *Rho*$^{-/-}$ retinas and 30 of which showed increased expression. By choosing these parameters, the large number of moderately increased genes observed are not included in the analysis. An average fold change was calculated for each gene with altered expression. The fact that the hybridisation was performed in duplicate, and that in cases where a gene was represented by more than one probe set, a very close correlation was observed between the expression levels reported, indicates a high level of reliability of data within these levels of change.

3.3.2 Quantitative PCR analysis

In order to validate the transcriptional variation observed following microarray analysis, a number of genes showing either up- or down-regulation at the transcriptional level were analysed using relative quantitative RT-PCR. It should be noted that the terms up- and down-regulation refer to the relative transcript levels in equal amounts of RNA from Wt and *Rho*$^{-/-}$ retinas. The same Wt and *Rho*$^{-/-}$ RNA samples that were used in the microarray study were used for quantitative PCR analysis. This analysis was also carried out by Dr. Avril Kennan. Dilutions were made of both cDNA samples (as detailed in materials and methods) and a standard curve was generated by the Lightcycler software, taking the Wt cDNA dilutions as standards. The RNA was initially normalized using the GAPDH house-keeping gene, which showed an average 1.7-fold increase in expression in Wt cDNA (Fig. 3.3). The fold-change result obtained for each subsequent gene tested in the same cDNA samples had to be corrected by this factor. Genes chosen for further analysis were the β-subunit of rod cGMP phosphodiesterase, peripherin/rds, hexokinase II, high mobility group 2 (*HMG2*), testican, a gene homologous to myosin regulatory light chain 2 (*LC2*) and *IMPDH1*. Results are shown for quantitative PCR analysis of the *IMPDH1* gene. *IMPDH1* was found to show an average 5.8-fold decrease in transcript levels in *Rho*$^{-/-}$ retinas

compared to Wt following microarray analysis. A 4-fold decrease in expression was obtained following quantitative PCR analysis (Fig. 3.4).

The change in expression levels observed for genes according to the microarray results spanned a range from 4.8-fold to 276-fold (Table 3.1). This allowed the reliability of both large and moderate fold changes seen in the chip data to be tested. The fold changes calculated from the quantitative RT-PCR experiments, while not always matching the array results in terms of precise calculations, showed agreement for the direction of the change in all cases. The observed changes in transcript level were, in general, less in magnitude for the RT-PCR than for the chip, but all results were nevertheless within the significant range with a lowest fold change of 2 for the gene homologous to *LC2* and a highest fold change of -123 for the β-subunit of rod cGMP phosphodiesterase.

Table 3.1. Validation of fold changes observed for a number of genes in the microarray analysis using relative quantitative RT-PCR.

Gene Name	Average microarray fold change	Average RT-PCR fold change
Peripherin-RDS	-12	-58
PDE6B	-276	-123
Hexokinase 2	-6	-4
HMG2	-6	-6
IMPDH1	-5.8	-4
Testican	+8	+3
Cathepsin S precursor	4	4
Homologous to myosin LC2	5	2

3.3.3 Differentially expressed genes that map to retinal degeneration loci

The locations of genes encoding transcripts significantly up- or down-regulated in degenerating *Rho*$^{-/-}$ retinas were compared with the known locations of human retinopathy causing loci which have previously been identified by linkage mapping (http://www.sph.uth.tmc.edu/Retnet/home.htm). Nine of the genes identified in this study map at the exact locations of retinopathy loci and therefore may arguably represent disease candidates (Table 3.2). One gene in particular, *IMPDH1*, was down-regulated 5-8-fold in the *Rho*$^{-/-}$ retina according to microarray analysis, a down-regulation that was confirmed by quantitative RT-PCR. The human homolog of *IMPDH1* mapped to within the flanking markers of the RP10 disease interval (Jordan *et al.*, 1993). *IMPDH1* was immediately regarded as a strong disease candidate for this form of RP and the subsequent screening of the gene in affected RP10 individuals revealed pathogenic mutations associated with disease. Full details of this analysis are discussed in Chapter 4.

In addition, two genes that also showed decreased expression levels in *Rho*$^{-/-}$ retinas following microarray analysis, were subsequently screened for disease-causing mutations by students under my supervision. The *CDR2* gene was down-regulated by over 6-fold in the *Rho*$^{-/-}$ retina according to microarray data, and was found to map to the recessive RP22 locus on chromosome 16 (Finckh *et al.*, 1998). CDR2 is believed to down-regulate c-Myc, a nuclear transcription factor regulating cell growth and cell cycle progression (Okano *et al.*, 1999). It was suggested that disruption of CDR2 may lead to inappropriate cell cycle signalling and may mediate neuronal apoptosis in the retina. This gene was screened by Shane Dillon for mutations in DNA from two affected members of two consanguineous recessive RP families. These were the original family DNAs that were used for the RP22 linkage analysis, and were received from Dr Andreas Gal, Hamburg, Germany (Finckh *et al.*, 1998). The second gene, *MEF2C*, showed a down-regulation of –6.8-fold in *Rho*$^{-/-}$ retinal tissue according to microarray data, and was found to map to a region on chromosome 5q14 that contains a locus for Usher syndrome, type 2 (Pieke-Dahl *et al.*, 2000). MEF2C functions as a transcription factor and is a member of the MADS family of transcription factors that regulate developmental processes (Shore & Sharrocks, 1995). It is involved in cell signalling pathways and also has a suggested role in apoptotic pathways (Okamoto *et al.*, 2002). The coding region of the *MEF2C* gene was screened by Stephen Kelly, in

individuals from ten USH2C families received from Dr William Kimberling, Boystown National Research Hospital, Omaha, NE, USA (Pieke Dahl *et al.,* 2000). Both genes were screened using automated sequencing. No sequence variations were detected in the coding regions of either gene, *CDR2* or *MEF2C*, in the individuals tested. However, a more complete analysis will be required to finally exclude the genes for disease involvement, in view of the fact that deletions were not screened for (deletion of complete exons would not have been detected), nor was an analysis undertaken to screen for mutations in the promoter regions.

Table 3.2. Differentially expressed genes identified in a comparison between wild-type and *Rho*$^{-/-}$ mouse retinas, that also map to known human retinal degeneration loci. Locus information obtained from Retnet (http://www.sph.uth.tmc.edu/Retnet/home.htm).

Gene name	Average fold-change	Human homolog chromosomal location	Retinal disease locus and flanking markers
Zinc finger protein A20	-12.45	6q23.3	6q25-q26; Dominant retinal-cone dystrophy 1 Deletion mapping, no marker data.
Cerebellar degeneration-related protein 2 (CDR2)	**-18.02/ -6.6**	**16p12.2**	**16p12.1-p12.3; Recessive RP (RP22) D16S287-D16S420**
Hexokinase 2	-7.4/-4.72	2p12	2p11-p16; Recessive RP (RP28) D2S1337-D2S286
Myocyte specific enhancer factor 2C (MEF2C)	**-6.8**	**5q14.3**	**5q14.3-q21.2; Usher syndrome, type 2 D5S428-D5S433**
High mobility group 2	-6.03	4q34.1	4q32-34; Recessive RP (RP29) D4S621-D4S2417
Inosine monophosphate dehydrogenase type 1 (IMPDH1)	**-5.77**	**7q31.3**	**7q31.3; Dominant RP (RP10) D7S2471-D7S530**
Ecto-5-prime nucleotidase (Cd73)	-3.7	6q14.3	6q12-6q16; Recessive Leber congenital amaurosis D6S1551-D6S1694
CD44 antigen	+3.03	11p13	11p13-p12; Dominant familial exudative vitreoretinopathy GATA34E08-D11S4102
Amyloid beta (A4) precursor protein	+3	21q21.3	21q21; Usher syndrome, type 1 D21S1905-D21S1913

3.3.4 Genes showing significant changes in transcription level in *Rho*$^{-/-}$ retinas

Predictably, 8 genes involved in the visual transduction cascade were shown to be significantly down-regulated in *Rho*$^{-/-}$ retinas, in comparison to wild-type. These included genes encoding the photoreceptor-specific α, β, and γ subunits of rod transducin, the β and γ subunits of rod cGMP phosphodiesterase, peripherin/rds and recoverin. The average fold change between the 4 comparisons varied for these genes, but all were decreased in the *Rho*$^{-/-}$ retina by between 6.9- and 276-fold in their expression levels according to the microarray data.

All genes showing elevations or reductions of >3-fold in expression levels in microarray comparisons of wild type and *Rho*$^{-/-}$ retinas are listed in Table 3.3 and proteins encoded by such genes have been placed into functional groups in Table 3.4. It is of interest to note that a number of proteins with anti-apoptotic functions are shown to be down-regulated in the degenerating retinas of *Rho*$^{-/-}$ mice. Evidence accrued to date suggests that apoptosis may be a general mechanism of photoreceptor cell death in mutation-induced retinopathies. In addition, a surprisingly large number of those genes shown to be transcriptionally activated in degenerating retinas encode proteins either of the extra-cellular matrix or the cytoskeleton. The potential significance of these findings are discussed.

Table 3.3. (A) Genes showing down-regulation of expression levels by ≥ 3-fold in a microarray comparison between Wild-type and *Rho*$^{-/-}$ mouse retinas. Genes are listed in order of decreasing fold-change value and corresponding chromosomal locations of human gene orthologs are given. For genes present on the microarray twice, two values for fold change are presented.

Genbank Accession Number	Average Fold-Change Decrease	Gene Name	Human Chromosomal location
Genes showing an average fold-change of ≥ -3x in all 4 comparisons			
X55968	-276	Rod cGMP PDE beta-subunit	4p16.3
M25513	-214/-225	Rod transducin alpha subunit	3p21.31
X60664	-39.15	Rod cGMP PDE alpha-subunit	5q33.1
X66196	-32.97	Recoverin	17p13.1
Y00746	-19.75	Rod cGMP PDE gamma-subunit	17q25.3
AA087559	-18.45/-4.72	Alkaline phosphatase 2	1p36.12
M64228	-18.25	Mouse potassium channel protein (Shab)	20q13.13
AA051446	-18.02/-6.6	Cerebellar degeneration-related protein 2	16p12.2
X66983	-12.95/-6.6	Rck for protein kinase	6p24.2
X14770	-12.5	Retinal degeneration slow (rds)	6p21.1
U19463	-12.45	Zinc finger protein A20	6q23.3
U29055	-10.8	G protein (transducin) beta-1	1p36.33
AA059557	-8.38	Similar to uridine kinase	20q13.33
Y11666	-7.4 /-4.72	Hexokinase II	2p12
U38495	-6.9	Rod transducin gamma subunit	7q21.3
L13171	-6.8	Myocyte-specific enhancer factor 2	5q14.3
X84797	-6.68	Hematopoietic specific protein 1	3q13.33
J03482	-6.5	Histone H1, member 2	6p22.2
Z46757	-6.03	High mobility group 2 protein	4q34.1
AA061266	-5.88 /-5.7	Oxysterol binding protein like 1	22q12.2
U00978	-5.77	Type I inosine monophosphate dehydrogenase	7q31.3
AA163305	-5.65/-5.47	Serum/glucocorticoid regulated kinase (Sgk)	6q23.2
L20343	-4.63	L-type calcium channel beta 2a	10p12.31-33
U34277	-4.4	Platelet activating factor acetylhydrolase	6p12.3
L00919	-4.13	Protein 4.1	1p35.3
Y00051	-3.9	Neural cell adhesion molecule	11q23.1
W63974	-3.9	Protein phosphatase 2A, reg. subunit B, βisoform	5q32
U37353	-3	Protein phosphatase 2A, reg. subunit B γ isoform	14q32.31
X87817	-3.88	Ulip/ dihydropyrimidinase-like 3	5q32
X14972	-3.88 /-3.3	Adaptor-related protein complex 2	11p15.5
Y12650	-3.7	Hereditary haemochromatosis-like protein	6p22.2
L12059	-3.7	Ecto-5'-nucleotidase (Cd73)	6q14.3
W62420	-3.6	ADP-ribosylation factor 4-like	17q21.31
U28342	-3.32	Immunoglobulin heavy chain variable region	14q32.33
L02914	-3.08	Aquaporin 1	7q14.3
Genes showing an average fold-change of ≥−3x in 3 of 4 comparisons			
U19880	-8.52	D4 dopamine receptor gene	11p15.5
AA098332	-7.65	5'-AMP-activated protein kinase, beta chain	12q24.23
U95167	-6.07	Transient receptor potential cation channel (trp)1	3q23
AA062247	-4.78	Homologous to transcription factor IIF, beta subunit	13q14.12
X90778	-3.88	Histone H2B, testis	6p22.2
AA089097	-3.35	START domain containing 7	2q11.2
U07159	-3.25	Acetyl-Coenzyme A dehydrog,, medium chain	1p31.1
W77226	-3.13	ADP-ribosylation-like protein 3	10q24.32
AA103047	-3.13	Homologous to ADP-ribosylation factor-like protein 2	3q11.2

Table 3.3. (B) Genes showing up-regulation of expression levels by ≥ 3-fold in a microarray comparison between Wild-type and *Rho*$^{-/-}$ mouse retinas. Genes are listed in order of decreasing fold-change value and corresponding chromosomal locations of human gene orthologs are given. For genes present on the microarray twice, two values for fold change are presented.

Genbank Accession Number	Average Fold-Change Increase	Gene Name	Human Chromosomal location
Genes showing an average fold-change of ≥ +3x in all 4 comparisons			
X61800	+9.75	CCAAT/enhancer binding protein delta	8q11.21
X07411	+8.28	Adipocyte p27 protein/ carbonyl reductase 2	17q25.3
X92864	+7.95	Testican (Spock1)	5q31.1
X58861	+6.65	Complement C1Q, alpha chain	1p36.12
W13739	+5.93	Homologous to pterin-4-alpha-carbinolamine dehydratase	5q31.1
W71543	+4.82	Homologous to myosin regulatory light chain 2	20q11.23
X06368	+4.35	c-fms proto-oncogene	5q33.1
U43541	+4.27	Laminin beta 2	3p21.31
X00496	+4.05	Mouse la-associated invariant chain (CD74)	5q33.1
AA146437	+3.98 /+3.85	Cathepsin S	1q21.2
AA059700	+3.88/+3.1	Beta 2-microglobulin	15q21.1
X70854	+3.73	Fibulin 1	22q13.31
Y10386	+3.65	Complement C1 inhibitor (Serping1)	11q12.1
X57337	+3.58	Procollagen C-proteinase enhancer protein	7q22.1
X62600	+3.52	CCAAT/enhancer binding protein beta	20q13.13
W12941	+3.25	Interferon-induced transmembrane protein 3	11p15.5
V00835	+3.1	Metallothionein-1	16q12.2
X66081	+3.03	CD44 antigen precursor	11p13
AA067929	+3	Amyloid beta (A4) protein precursor	21q21.3
Genes showing an average fold-change of ≥+3x in 3 of 4 comparisons			
AA023669	+16.58/+3.4	Homologous to heat shock 27 kDa protein	7q11.23
X15475	+8.43	Peripherin	12q13.12
X15789	+6.93	Cellular retinoic acid binding protein 1	15q25.1
AA044561	+5.75	Homologous to phosphoenolpyruvate carboxykinase	14q11.2
AA137902	+4.42	Na+/K+-transporting ATPase beta-3 chain	3q23
AA003323	+4.05	Filamin A	Xq28
X14194	+3.9	Nidogen (Entactin)	1q42.3
X99807	+3.75	Selenoprotein P, plasma 1	5p12
X58251	+3.63	Procollagen type 1alpha 2 chain	7q21.3
Y00305	+3.42	Voltage-gated potassium channel protein 1	12p13.32
X66449	+3.38	S100 Calcium binding protein A6 (calcyclin)	1q21.3

Table 3.4. Functional groups of genes showing differential expression in a microarray comparison between wild-type and *Rho*$^{-/-}$ mouse retinas.

GENE NAME	GENE FUNCTION
FUNCTIONAL GROUPS SHOWING DECREASED EXPRESSION IN *RHO*-/- RETINAS	
Intracellular Signal Transduction	
Cerebellar degeneration-related 2	Transcriptional co-repressor
Rck protein kinase	Ser/thr protein kinase involved in cell cycle regulation
Zinc finger protein A20	Inhibits NF-kappaB & TNF-induced apoptosis
Myocyte-specific enhancer factor 2C	Transcription factor, neurogenesis
Hematopoietic specific protein 1	Transcription factor
Sgk	Ser/thr protein kinase, cell survival
Protein phosphatase 2A	Ser/thr phosphatase, cell growth/division
Ulip protein	May mediate signals involved in axonal outgrowth
ADP-ribosylation factor 4-like	Small GTP-binding protein (ARF family)
D4 dopamine receptor gene	Large G protein coupled receptor
5'-AMP-activated protein kinase	Metabolic sensor for AMP and ATP levels
ADP-ribosylation-like protein 3	Small GTP-binding protein (ARF family)
Homologous to ARF-like protein 2	Small GTP-binding protein (ARF family)
Ion Channel/ Plasma Membrane Proteins	
Potassium channel protein (Shab)	Voltage-gated potassium ion channel
Transient receptor protein (trp) 1	Non voltage-sensitive store-operated Ca^{2+} channel
Calcium channel beta 2a subunit	Voltage-gated calcium channel
Neural cell adhesion molecule	Cell-cell signalling, neuron adhesion
Alpha-adaptin C	Found in coated vesicles of plasma membrane
Aquaporin 1	Molecular water channel protein
DNA Processing and Assembly	
Uridine Kinase	Pyrimidine ribonucleoside kinase
Histone H1 gene	Compact DNA into nucleosomes
High mobility group 2	Increases transcription
Ecto-5'-nucleotidase (Cd73)	Catalyses cAMP into AMP
Transcription factor IIF, beta subunit	Binds to RNA polymerase II
Histone H2B, testis	Compacts DNA into nucleosomes
FUNCTIONAL GROUPS SHOWING INCREASED EXPRESSION IN *RHO*-/- RETINAS	
Extracellular Matrix (ECM)/ Cytoskeleton	
Testican	Proteoglycan- cell adhesion, migration, proliferation
Laminin beta 2	Basement membrane constituent
Cathepsin S	Cleaves elastin, degradation of ECM
Fibulin 1	Glycoprotein incorporated into a fibrillar ECM
Procollagen C-proteinase enhancer	Cleavage of type I procollagen, ECM maintenance
Procollagen type I, alpha 2 chain	Fibrillar collagen family of ECM proteins
Entactin/ nidogen	Binds type IV collagen and laminin
CD44 antigen	Glycoprotein with a role in matrix adhesion
Beta2-microglobulin	Cell surface amyloid protein
Amyloid beta (A4) precursor	Membrane associated glycoprotein
Homololog ous to myosin regulatory light chain 2	Structural protein of muscle
Peripherin	Intermediate filament protein
Homologous to filamin A	Crosslinks actin filaments to membrane glycoproteins
Heat shock protein 27kDa	Inhibits actin polymerisation, stabilises protein structures
Immune Response	
CCAAT/Enhancer binding protein	Transcriptional activator of genes involved in immune responses
Complement C1Q subcomponent	Component of the serum complement system
Mouse la-associated invariant chain	Invariant polypeptide of MHC class II antigen-associated
Complement C1 inhibitor	Regulates complement activation

3.3.5 General features of down-regulated genes

Transcripts derived from a number of genes not previously associated with vision processes or visual defects were decreased significantly in the *Rho*$^{-/-}$ retina, and a number of common gene functions were observed (Table 3.4). Approximately 36% of these genes are involved in intracellular signaling, and are known to play a variety of roles in the cell. They include receptors, GTP-binding proteins, protein kinases, protein phosphatases and transcription factors. A number of these genes function in the signaling pathways that ultimately lead to apoptosis, the programmed cell death pathway. The most significantly decreased transcript within this group was that derived from the gene encoding the cerebellar-degeneration-related 2 protein (*CDR2*). CDR2 is believed to down-regulate c-Myc, a nuclear transcription factor regulating cell growth and cell cycle progression, by binding and sequestering it in neuronal cytoplasm (Okano *et al.*, 1999). Down regulation of CDR2 in the brain leads to excess c-Myc in neurons, which is proposed to induce inappropriate cell signalling and p53-mediated apoptosis. The c-Myc gene has previously been linked to apoptosis in the developing retina (Linden *et al.*, 1999) and the observed down regulation of CDR2 in degenerating retinas suggests a possible mechanism of apoptotic death of primary and secondary retinal neurons.

The protein A20, which showed decreased expression in the *Rho*$^{-/-}$ mouse, is a dual inhibitor of nuclear factor-kappa B (NF-kappaB) and tumour necrosis factor (TNF)-mediated programmed cell death (Beyaert *et al.*, 2000). Overexpression of A20 has been shown in a number of recent studies to protect selected cell types against apoptosis (Grey *et al.*, 2003; Longo *et al.*, 2003). The reduction in transcript levels of the anti-apoptotic protein A20, may be a direct reflection of the absence of photoreceptor cells and/or of transcriptional change occurring in second order retinal neurons. The transcription factor MEF2C has also been associated with apoptotic pathways. Myocyte enhancer factor-2 (MEF2) transcription factors are expressed at high levels in neurons and are activated by mitogen-activated protein (MAP) kinases, a pathway which exerts anti-apoptotic effects on neurons during differentiation (Okamoto *et al.*, 2000). Paradoxically, during apoptosis resulting from exposure to stress, it has been shown that MEF2 proteins are cleaved by caspases, which causes the formation of dominant interfering forms of MEF2 proteins that have the ability to induce neuronal apoptosis in cell culture systems (Okamoto *et al.*, 2002). MEF2C has also been shown

recently to be involved in the transactivation of the neural retina leucine zipper (NRL) transcription factor, which is involved in the transcriptional control of rod-specific genes during development and differentiation, and has been implicated in RP when mutated (Akimoto *et al.,* 2003; Bessant *et al.,* 1999). MEF2C may therefore have an important role to play in controlling the development and survival of retinal neuronal cells.

The importance of phosphorylation and dephosphorylation in intracellular signalling pathways has long been recognized, and although attention has focused mainly on kinases, recent studies have also highlighted the importance of serine/threonine protein phosphatases in many processes, including apoptosis (Klumpp & Krieglstein, 2002). A number of these intracellular signalling components, including *Rck* for protein kinase, serum glucocorticoid regulated kinase (*Sgk*) and protein phosphatase 2A (*PP2A*), show considerable down-regulation in $Rho^{-/-}$ retinas according to microarray analysis. The male germ cell associated serine/threonine kinase *Rck,* is related to those involved in cell cycle regulation and transcripts have been found in photoreceptor cells, which suggests a possible role in signalling pathways in the retina (Bladt & Birchmeier, 1993). Serum glucocorticoid regulated kinase (SGK) is a component of the phosphoinositide 3 (PI 3)-kinase signaling pathway, and regulation is accomplished by several pathways including growth-factor and stress-mediated signalling (Park *et al.,* 1999; Shelly & Herrera, 2002). Induction of enzymatically active SGK has been shown to function as a key cell survival component in response to different environmental stress stimuli (Leong *et al.,* 2003). Protein phosphatase 2A is also involved in the regulation as well as in the cellular response of apoptosis (Van Hoof & Goris, 2003). The interaction between these and other genes in the retina has not been established, but they may have an important function in essential signalling pathways of the photoreceptor cells.

Other groups of genes, such as those involved with DNA processing, and several plasma membrane associated ion channels and receptors, also showed significantly decreased expression in $Rho^{-/-}$ retinas. The voltage-gated potassium channel (delayed rectifier) protein and member of the *Shab*-related sub-family of ion channels is reduced an average of 18.25-fold. Potassium channels are known to be present in the retina and reduced expression is a likely reflection of the combined loss of photoreceptors and degeneration of second-order retinal neurons (Pinto & Klumpp, 1998). Calcium influxes are known to regulate multiple events in photoreceptor cells

including phototransduction and synaptic transmission. The transient receptor protein (TRP) Ca^{2+} channel has been shown to be responsible for light-induced cation conductance in photoreceptor cells in drosophila, and transcripts of this gene are reduced in the *Rho*$^{-/-}$ retinas (Minke, 2001). Another calcium channel gene referred to as the L-type calcium channel beta 2a subunit, has also been down-regulated. A similar L-type calcium-channel gene has previously been shown to be mutated in incomplete X-linked congenital stationary night blindness (Strom *et al.,* 1998).

3.3.6 General features of up-regulated genes

A striking feature of the transcripts that show elevation in expression in *Rho*$^{-/-}$ retinas is the large number present that encode proteins involved in the maintenance of the extracellular matrix (ECM) and of the cytoskeleton. Of the 30 most significantly up-regulated genes that have been identified in this study, almost 50% were found to be associated with the ECM or the cytoskeleton. Up-regulation of genes encoding such proteins may represent an attempt by retinal glial cells (Muller cells) to strengthen the interphotoreceptor matrix, possibly in an attempt to slow down the degenerative process. Up-regulated transcripts include laminin, fibulin, entactin, procollagen type 1 alpha 2 chain and procollagen C-proteinase enhancer protein. All of these transcripts encode glycoproteins that are involved in ECM structure and maintenance. Fibulin binds laminin and entactin among other ECM components (Tran *et al.,* 1997), while entactin binds collagen type IV and laminin (Chung *et al.*, 1993). Basement membranes consist of highly specialized extracellular matrices that are known to contain laminins, entactin, type IV collagen and proteoglycans, with each of these groups growing in complexity as new proteins are discovered. Together they are involved in cell adhesion, differentiation, migration and signalling. The proteoglycan testican is up-regulated in the *Rho*$^{-/-}$ retina. Testican is expressed during neuromuscular junction formation and is thought to be part of the specialized ECM of the brain (Marr *et al.,* 2000). Cathepsin S, also significantly up-regulated, is involved in cleavage of elastin, another component of the ECM, and it is present in the RPE where it may play a role in the proteolytic processing of photoreceptor outer segments (Rakoczy *et al.,* 1998).

CD44 is a cell surface/adhesion molecule which is specifically localized to the Muller cell microvilli that appose the interphotoreceptor matrix (Chaitin *et al.,* 1998). It has been found that inherited retinal degeneration exhibited by the *rds* mouse, leads to an up-regulation of expression of CD44 in the retina (Krishnamoorthy *et al.,* 2000) and this study now shows CD44 to be up-regulated in the rhodopsin knockout mouse. Up-regulation of this and other cell adhesion components may again represent an attempt at stabilising the degenerating retina. Cytoskeletal proteins up-regulated in the $Rho^{-/-}$ retina include a protein with homology to myosin light chain 2, peripherin (distinct from peripherin-RDS), and a protein homologous to the actin-binding protein, filamin A. Myosin light chain 2 is an important protein in the regulation of myosin ATPase activity in muscle. Peripherin is a type III intermediate filament protein that has a role in stabilising the cellular architecture of the cell, and is required for the proper development of a subset of sensory neurons (Lariviere *et al.,* 2002). Actin-binding proteins such as filamin are responsible for the organisation of actin microfilaments in the cytoskeleton, and link actin filaments to glycoproteins in the plasma membrane (van der Flier & Sonnenberg, 2001). A member of the stress response heat shock proteins, Hsp27, is also up-regulated and modulation of the expression of this protein is believed to cause reorganization of the actin cytoskeleton (Wieske *et al.,* 2001). It has also been suggested that Hsp27 may play a role in the retinal pigment epithelium injury response such as seen in age-related macular degeneration (Strunnikova *et al.,* 2001).

3.4 DISCUSSION

This study is the first report of a large-scale comparative analysis of global gene expression between the retinas of wild type mice and mice lacking functional rod and cone photoreceptors, brought about by lack of the major constitutive protein of these cells, rhodopsin. While the amount of data generated is large, definite trends in the patterns of gene expression may be observed between wild-type and *Rho*$^{-/-}$ mice. A list of genes are presented which show differential expression, a number of which have been shown to map to within retinal degeneration loci, and therefore may be regarded as candidate genes involved in retinal disease. One of these genes, *IMPDHI*, maps to the RP10 locus. The screening of *IMPDH1* and identification of a pathogenic mutation is described in detail in Chapter 4. The identification of disease-causing mutations within the IMPDH1 gene directly validates the candidate gene hypothesis proposed in this study. Two additional genes, *CDR2* and *MEF2C* have also subsequently been screened in DNA from individuals suffering from degenerative retinal diseases, but pathogenic mutations were not identified in the individuals tested. Further screening for detection of deletions and analysis of promoter regions is required to completely exclude these two genes for disease involvement in these individuals.

Many of the genes identified as being most significantly down-regulated in *Rho*$^{-/-}$ retinas when compared to wild-type, encoded known photoreceptor-specific genes, most of which are involved in visual transduction pathways. This provided direct evidence that the microarray analysis was successful in the prediction of photoreceptor-specific or enriched transcripts. It is worthy of note that several of those genes showing down regulation in *Rho*$^{-/-}$ retinas encode proteins with established anti-apoptotic function, including the transcription factor A20 and cerebellar degeneration–related protein 2 (CDR2). Data accrued largely from studies of animal models of RP indicate that a "final common pathway" of photoreceptor cell death is apoptosis, although the molecular mechanisms linking the presence of primary mutations to the initiation of that process remain obscure at the present time. Down-regulation, within photoreceptor cells carrying primary mutations, or in other retinal neurons, of transcripts encoding proteins which have been implicated in apoptotic mechanisms in other cell systems, may contribute to pathological disease mechanisms.

Approximately half of those transcripts showing elevations in levels of expression in *Rho*$^{-/-}$ retinas when compared to wild type encode proteins of the cytoskeleton or extracellular matrix (ECM). Up-regulation of genes encoding such proteins may represent an attempt by retinal glial cells (Muller cells) to strengthen the interphotoreceptor matrix in an attempt to slow down the degenerative process. Extensive remodelling of the retina is known to occur after rod and cone cell death and resembles the responses of many CNS assemblies to deafferentation or trauma (Marc *et al.*, 2003). Retinal remodelling is predicted to involve additional neuronal cell death, neuronal and glial cell migration, elaboration of new neurites and synapses, the rewiring of retinal circuits and extensive growth of glial cells (Marc *et al.*, 2003; Jones *et al.*, 2003). Proteins showing elevated transcript levels which may have a role in these processes include laminin, fibulin, entactin, procollagen type 1 alpha 2 chain, procollagen C-proteinase enhancer protein, testican, cathepsin S, a protein with homology to myosin light chain 2, peripherin (distinct from peripherin-RDS), a protein with homology to the actin binding protein filamin and CD44.

Proteins that function as structural cytoskeletal, extracellular matrix or cell adhesion proteins have previously been implicated in hereditary neuroretinal degenerations. These include a number of Usher syndrome genes such as myosin 7A, usherin, cadherin 23 and procadherin 15, as described previously in Chapter 2. Mutations in the extracellular matrix gene, tissue inhibitor of metalloproteinases-3 (*TIMP3)* results in Sorsby's fundus dystrophy (Weber *et al.*, 1994) and interestingly the protein has been found to accumulate in retinas with RP not caused by *TIMP3* mutations (Fariss *et al.*, 1998). A mutation in the EGF-containing fibulin-like extracellular matrix protein 1 (*EFEMPI*) which, as the name suggests, is very closely related to fibulin, has also been linked to Doyne honeycomb retinal dystrophy (Stone *et al.*, 1999a). In light of these observations the expression of three of these genes for which mouse sequence was available, *TIMP3*, *CDH23* and *EFEMP1*, was investigated by quantitative RT-PCR by Dr. Avril Kennan, as only one of which, TIMP3 was represented on the microarray genechip. All three genes were found to be up-regulated in the *Rho*$^{-/-}$ retina. *TIMP3* was up-regulated by an average of 180% on the chip and 260% by quantitative RT-PCR and *CDH23* and *EFEMPI* were up-regulated by 300% and 310% respectively as measured by quantitative RT-PCR (Kennan *et al.*, 2002). This observation lends further weight to the potential candidacy of differentially expressed ECM or cytoskeletal genes in retinal degenerative diseases.

It has been shown previously that inherited retinal degeneration exhibited by the *rds* mouse, leads to an up-regulation of expression of CD44 in the retina (Krishnamoorthy *et al.,* 2000). The current study now shows CD44 to be up-regulated in the rhodopsin knockout mouse. Transcripts derived from the genes encoding amyloid precursor protein (*APP*) and Beta-2-microglobulin (*B2M*) also show increased expression in $Rho^{-/-}$ retinas. Increased expression of these genes has been implicated in the death of neuronal cells in Alzheimer disease, and amyloidosis respectively, both of which are characterised by deposition of fibrillar amyloid proteins (Hendriks *et al.,* 1996; Gorevic *et al.,* 1986). Amyloid beta deposits have also recently been found in drusen, the hallmark extracellular deposit in age-related macular dystrophy retinas (Johnson *et al.*, 2002; Dentchev *et al.,* 2003). Whether amyloid deposition in drusen contributes to, or results from, retinal degeneration processes is unknown.

3.5 CONCLUSION

In conclusion, while immense progress has been made in the identification of genes involved in retinal degenerations, genes at a substantial number of retinopathy loci remain to be characterised in hereditary forms of disease. The microarray analysis described in this study demonstrates the value of studies of global transcriptional profiles of degenerating retinal tissues in identifying disease causing genes, as validated by the identification of *IMPDH1*. A number of additional transcripts that showed significant changes in transcript level between wild-type and $Rho^{-/-}$ retinas have been shown to map to human retinopathy loci and may, rationally, represent candidates for hereditary and multifactorial forms of retinal disease.

The global response of the retina to degeneration of its photoreceptors is, as yet, not well understood. The study reported here, takes a first step towards an elucidation of the complex changes that occur in the retina during degeneration of neuronal cells, by providing a snapshot of the genes that are expressed at the end of this process, and therefore may have identified several key genes that underlie this response.

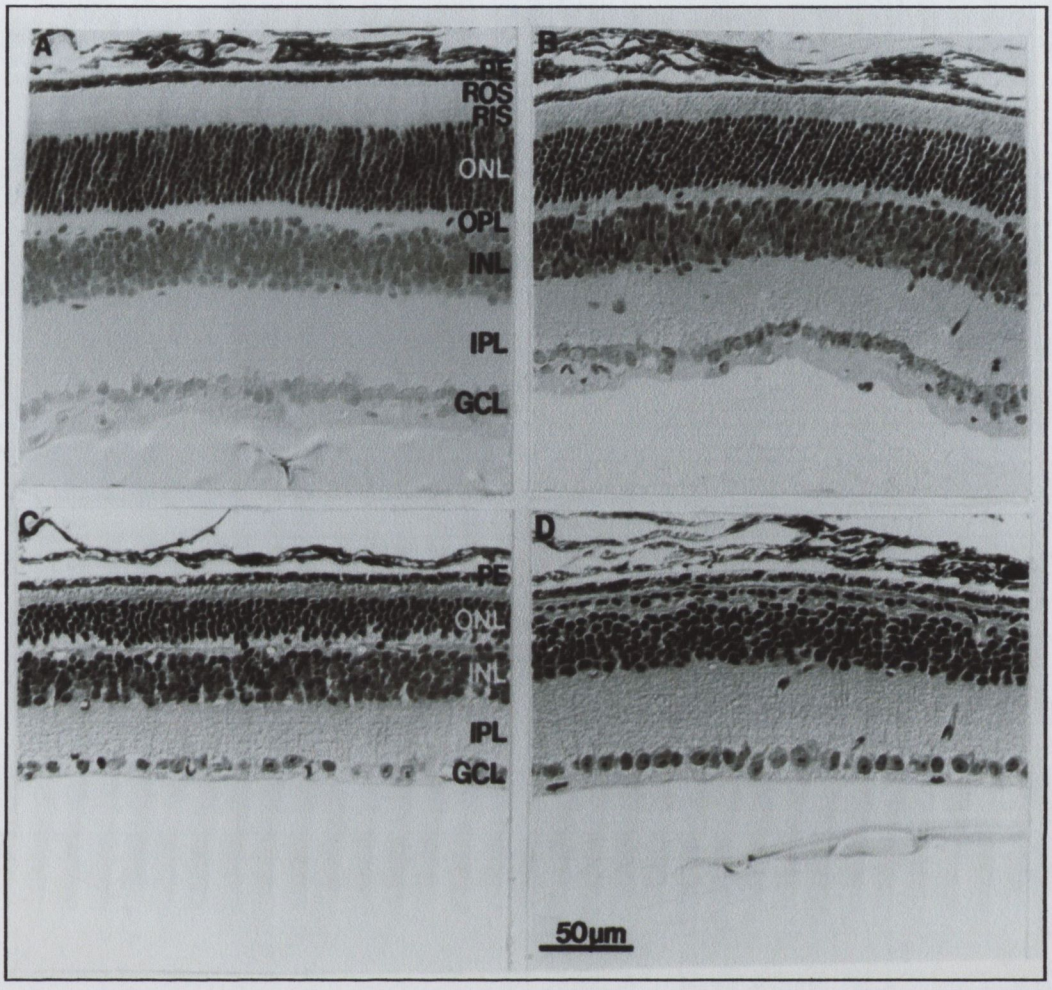

Figure 3.1. Retinal histology of wild-type (Wt) and *Rho*$^{-/-}$ mice.

Retinal sections are stained with hematoxylin and eosin. (**A**) Wt retina showing normal retinal histology, and *Rho*$^{-/-}$ retinal sections taken at (**B**) 24, (**C**) 48 and (**D**) 90 days are shown. The ONL of the *Rho*$^{-/-}$ retina is reduced to half the cell thickness at 48 days, and by 90 days the ONL is reduced to a single cell thickness and photoreceptor degeneration is essentially complete. (Taken from Humphries *et al.*, 1997).

PE, pigmented epithelium; ROS, rod outer segment; RIS, rod inner segment; ONL, outer nuclear layer; OPL, outer plexiform layer; INL, inner nuclear layer; IPL, inner plexiform layer; GCL, ganglion cell layer.

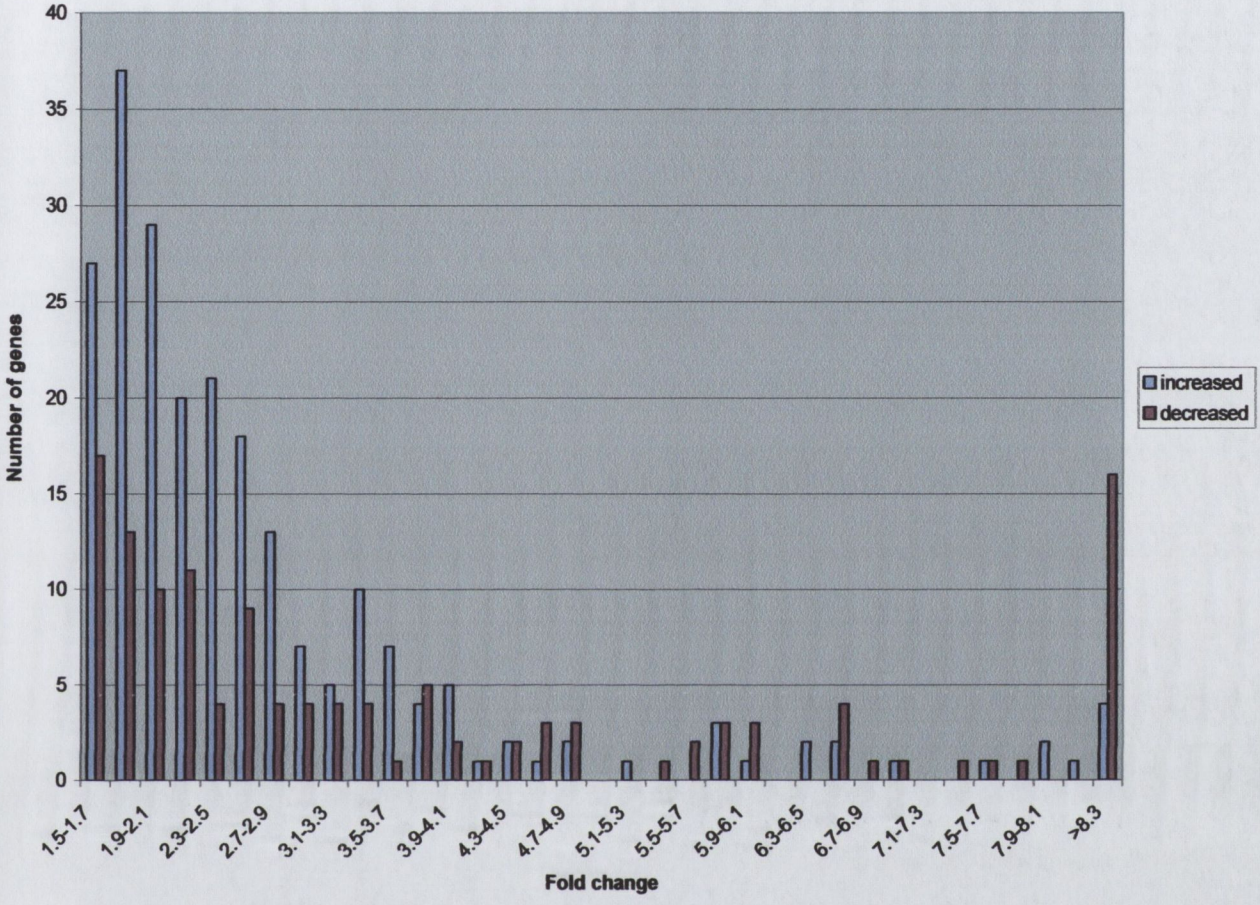

Figure 3.2. Comparison between the number and extent of genes up-regulated from wild-type to *Rho*$^{-/-}$ retina and those down-regulated. The 228 transcripts showing an average increase of >1.5-fold, and the 131 transcripts showing an average decrease of >1.5-fold in *Rho*$^{-/-}$ retinas, are classed into categories of fold-change. This illustrates the greater number of moderately increased genes and dramatically decreased genes. (Analysis carried out by Dr. David Simpson)

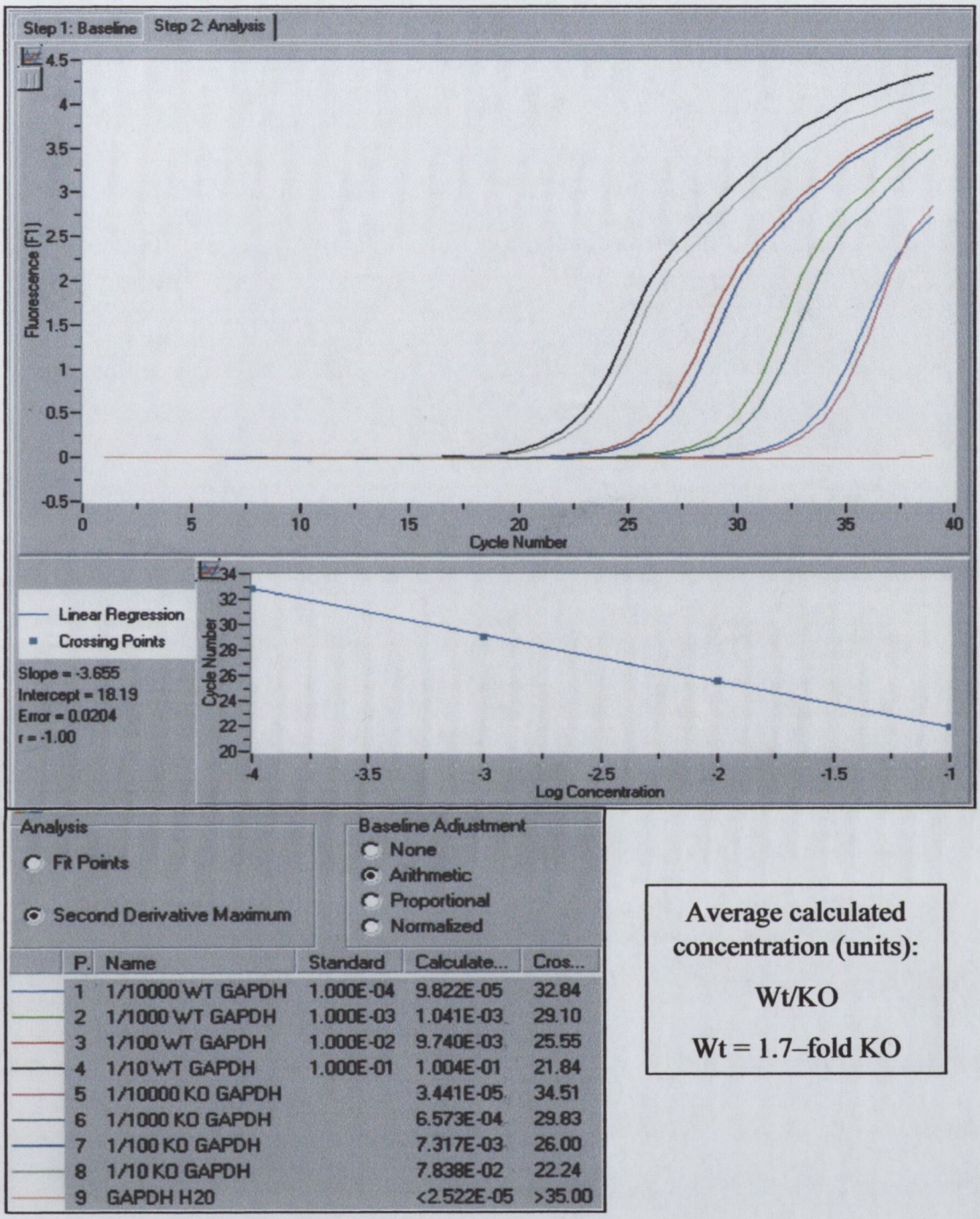

Average calculated concentration (units):

Wt/KO

Wt = 1.7–fold KO

Figure 3.3. Quantitative PCR analysis comparing the change in expression of a house-keeping gene GAPDH, between Wild-type (Wt) and *Rho*$^{-/-}$ (KO) mouse retinal cDNA at 4 months. The two cDNA samples were serially diluted from 1/10 to 1/10,000, and the calculated concentrations were compared between Wt and *Rho*$^{-/-}$ samples at each dilution. GAPDH transcripts were shown to be an average of 1.7-fold more concentrated in Wt cDNA than *Rho*$^{-/-}$ cDNA.

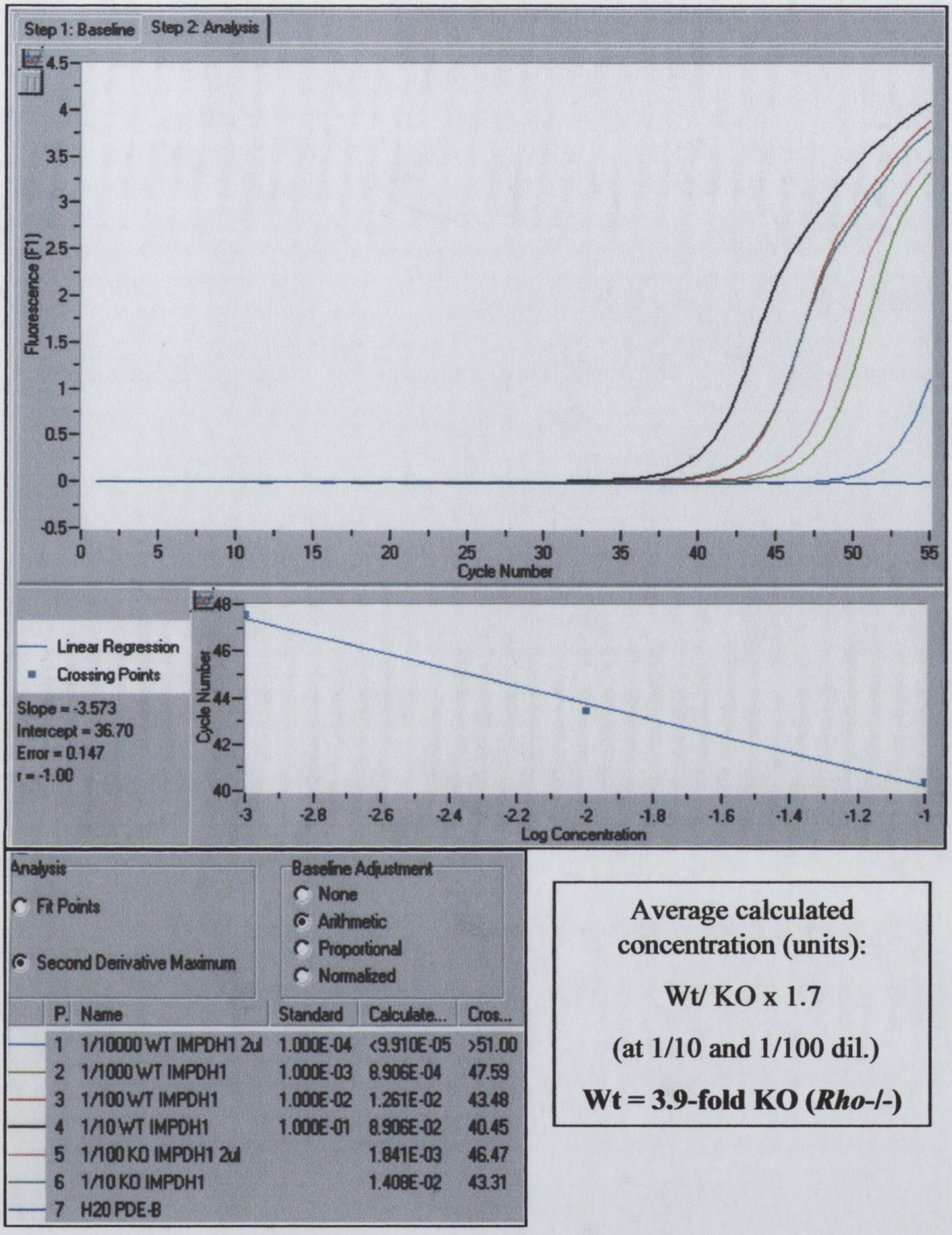

Average calculated concentration (units):

Wt/ KO x 1.7

(at 1/10 and 1/100 dil.)

Wt = 3.9-fold KO (*Rho*-/-)

Figure 3.4. Quantitative PCR analysis comparing the change in expression of the *IMPDH1* gene between Wild-type (Wt) and *Rho*$^{-/-}$ (KO) mouse retinal cDNA at 4 months. The Wt cDNA sample was serially diluted 1/10 to 1/10,000, which were used to generate a standard curve. 1/10 and 1/100 dilutions of *Rho*$^{-/-}$ cDNA were made and the relative concentration of the gene of interest in these samples obtained by comparison to the standard curve. The *Rho*$^{-/-}$ concentration value was multiplied by a factor of 1.7 to normalise cDNA concentrations (calculated following analysis of the GAPDH house-keeping gene). IMPDH transcripts showed an average 3.9-fold decrease in expression in *Rho*$^{-/-}$ cDNA when compared to Wt cDNA.

CHAPTER 4

THE STORY OF RP10;

Candidate gene screening and identification of disease-causing mutation within the IMPDH1 gene

4.1 INTRODUCTION

4.1.1 Introduction

A previous genetic linkage study undertaken by members of this group, resulted in the mapping of an autosomal dominant RP (adRP) locus in a large Spanish family denoted FA-84, to the long arm of chromosome 7, which was referred to as the RP10 locus (Jordan *et al.,* 1993). A major research effort has concentrated on the identification of the disease-associated gene that maps to the RP10 locus in the years since then. Prior to the present study, attempts were made to reduce the size of the disease interval and to prioritise candidate genes for further study. A number of candidate genes were screened previously for disease-causing mutations, but all were subsequently excluded as potential candidates. Therefore, the main aim of this study was to persist with approaches to identify the adRP gene on 7q.

A clinical description of RP is presented, along with an overview of the enormous clinical, genetic and allelic heterogeneity exhibited in this disease. An outline of the research carried out prior to this study on the RP10 interval is given, which includes the linkage mapping of the RP10 locus and a description of some positional candidate cloning approaches used in the identification of RP10 candidate genes. An introduction to the human genome and bioinformatics-based resources that are now available for use in gene identification studies is also presented. The selection and screening of a number of new candidate RP10 genes is described, with the reasons for their adoption as potential candidates detailed. A disease-causing mutation was finally identified in the inosine monophosphate dehydrogenase 1 (IMPDH1) gene which was found to segregate in all affected members of family FA-84.

4.1.2 Clinical features of retinitis pigmentosa

A brief description of the clinical features of RP has been provided in Chapter 1. Here, a more detailed picture of the disease is presented, with particular emphasis on diagnosis and genetic etiologies. Retinitis pigmentosa is the name commonly given to a

group of hereditary diseases characterised by night blindness, progressive visual field loss, pigmentary deposits and abnormal or non-recordable electroretinogram (ERG) (Heckenlively, 1988). The combined incidence worldwide has been estimated as being between 1 in 3000 and 1 in 5000 (Phelan & Bok, 2000; Rivolta *et al.,* 2002). Clinical features of RP vary considerably between individual patients, but there are many characteristic clinical findings that can be described in a general sense. Early clinical features are characterised by night blindness, or nyctalopia, owing to progressive degeneration of rod photoreceptor cells, which is usually experienced in the first or second decade of a patient's life (Weleber, 1989). Other early clinical features are the loss of mid-peripheral visual fields and a generalised diffuse depigmentation of the RPE. Retinal vessels appear relatively normal at this stage, but the ERG is usually abnormal (Heckenlively, 1988). As the degeneration progresses, visual fields are gradually reduced both centrally and peripherally, and retinal vessels begin to show thinning. The most marked changes are seen in the RPE, with most patients displaying pigment dispersion, followed by the adherence of pigment to smaller arteriolear vessels, creating the characteristic "bone spicule" pattern of retinal pigmentation (Heckenlively 1988). With disease progression, cone photoreceptor cells also become affected, precipitating more extensive degradation, with day vision and central visual acuity becoming compromised (Phelan & Bok, 2000). In later stages of the disease, retinal blood vessels become attenuated, the RPE becomes thinner with increased pigmentary deposits on the retinal surface, and the optic nerve head appears pale, often with a "waxy pallor" (Humphries *et al.,* 1992; Heckenlively, 1988). These morphological features of the degenerating retina can be usually be visualised by fundus examination (Fig. 4.1). Patients develop tunnel vision as visual fields constrict, which can eventually lead to complete blindness.

A number of atypical forms of RP also exist including retinitis *punctata albescens,* which is recessively inherited, and is characterised by numerous white spots on the retinal surface, and retinitis *sine pigmento* in which no pigmentary changes are observed (Heckenlively, 1988).

4.1.3 Diagnosis of retinitis pigmentosa

The diagnosis of RP is based initially on clinical examination, a history of night blindness, visual field loss and pigmentary retinopathy. A tool central to the diagnosis and classification of RP is the electroretinogram (ERG), which represents the global responses of the retina to a visual stimulus. The ERG shows accumulated responses from each layer of the retina relative to the signal processing mechanisms occuring within the tissue, and is usually recorded from the corneal surface by a contact lens electrode (Heckenlively, 1988). The ERG response, as recorded in a clinical setting, is biphasic, with the first negative downward peak called an a-wave and the next positive upward peak called the b-wave (Fig.4.2). The a-wave represents repolarisation of photoreceptor cells, while the b-wave is derived from cells in the bipolar region of the middle retina (Heckenlively, 1988). Photoreceptor cells are either dark-adapted, and given a dim flash of light (scotopic ERG), which measures the rod-mediated response, or can be adapted to a specific level of light and then stimulated with a brief flash of bright light (photopic ERG), which measures the cone response. Both the rod and cone systems can be stimulated by using a bright flash of light in the dark-adapted state. Rod-mediated ERGs have virtually no a-wave, while the b-wave amplitude is considerably larger than that seen in the cone-mediated ERG (Fig. 4.2) (Heckenlively, 1988). In the maximal bright flash, dark-adapted ERG, both a- and b- waves are larger than either the scotopic or photopic ERGs. This test can be useful when single-flash ERGs are very low, or non-recordable. ERG abnormalities can usually be detected even in presymptomatic cases of RP. In typical RP, the rods are more affected than cones and as a result the scotopic ERG is reduced in amplitude but may be normal or delayed in timing (Fig. 4.2B). Cone responses may also be affected, wave forms being abnormal in amplitude or timing, or both. In cone-rod dystrophies, the scotopic b-wave amplitude is larger than the photopic b-wave amplitude and both are abnormal (Heckenlively, 1988). In advanced cases of RP, all responses are extinguished (Fig. 4.2C).

A second diagnostic test is visual field testing which measures degree of visual field loss in RP patients. This usually begins with a slight loss of vision in the superior peripheral field and scotomous areas (obscuration of parts of visual field) in the midequatorial field (Heckenlively, 1988). The scotomous areas become confluent as disease progresses, eventually leaving a central island of visual field (Fig. 4.3). Best

corrected visual acuity tests are generally also carried out, as well as fundus photography, which documents retinal morphology (Fig. 4.1).

4.1.4 Genetics of retinitis pigmentosa

RP exhibits extreme genetic, allelic and clinical heterogeneity. Most forms are monogenic and can exhibit autosomal dominant (adRP), autosomal recessive (arRP), X-linked (xlRP) or mitochondrial inheritance patterns (Rivolta *et al.,* 2002). There have also been a number of more complex inheritance patterns described, such as digenic diallelic inheritance, which is seen in families where affected individuals are double heterozygotes for mutations in both the RDS and ROM1 genes (Kajiwara *et al.,* 1994). A form of digenic triallelic inheritance has been described in patients with RP, who suffer from a syndromic variant called Bardet-Biele syndrome (BBS). Mutations have been identified that affect both alleles at one BBS locus and one allele at a second BBS locus (Katsanis *et al.*, 2001; Rivolta *et al.,* 2002). An additional inheritance sub-type is dominant RP with reduced penetrance, which is often found in families in which the disease gene was originally linked to the RP11 locus, later found to be caused by mutations in the gene encoding the splicing factor, *PRPF31* (Vithana *et al.,* 2001). It has recently been suggested that partial penetrance in RP11 could be due to the coinheritance of a PRPF31 gene defect, and a wild-type allele that exhibits reduced expression (Vithana *et al.,* 2003). To further complicate matters, the existence of genetic modifier genes associated with RP has been suggested, which are genes that segregate with the disease gene, and can affect disease severity, age of onset or rate of disease progression (Rivolta *et al.,* 2002). The involvement of a genetic modifier effect has been suggested in association with the retinitis pigmentosa 1(RP1) gene, because of the variability in severity of visual field loss detected both within and among families segregating the same disease mutation (Jacobson *et al.,* 2000).

The number of genes identified as being mutated in RP patients has risen dramatically in the last number of years. The number of RP loci that have been mapped has now reached 38, but many more additional loci have also been identified for allied diseases and syndromic forms. A list of all known RP loci and cloned genes can be found in the RetNet database (http://www.sph.uth.tmc.edu/Retnet/), a copy of which has been included in Appendix C of this thesis. In general, RP genes are known or are

expected to be expressed in the photoreceptor cells of the retina or in the RPE (Phelan & Bok, 2000). In the case of 30 of the RP loci, the precise gene has been identified which includes twelve adRP genes, sixteen arRP genes and two xlRP genes. There is huge functional diversity amongst the genes that have been associated with RP to date. Many genes have been identified that are involved with the visual transduction cascade such as rhodopsin and cGMP-phosphodiestrerase (PDE) subunits, or that function as photoreceptor structural proteins, such as peripherin-RDS and retinal outer segment membrane protein 1 (ROM1). Additional functional groups include transcription factors, pre-RNA splicing factors and cytoskeletal proteins to name but a few. It is also important to note that a number of known RP genes have been found to be mutated in more than one clinical disease or syndrome. A full discussion on mitochondrially-inherited and syndromic RP which includes Usher syndrome and BBS, has been presented in Chapters 1 and 2.

4.1.5 Autosomal dominant retinitis pigmentosa

Autosomal dominant RP is thought to account for up to 20-25% of all RP cases (Saleem & Walter, 2002). The first adRP gene was localised in 1989 to chromosome 3q in a large Irish family, and was found to be tightly linked to the gene encoding the rod visual pigment, rhodopsin (McWilliam *et al.,* 1989; Farrar *et al.,* 1990). A Pro23His substitution in rhodopsin was the first sequence alteration to be associated with RP, and has subsequently been identified in 10% of adRP US Caucasian patients (Dryja *et al.,* 1990; Sohocki *et al.,* 2001). Rhodopsin has been found to account for over 70% of the total rod outer segment protein, and is essential for the initiation of the phototransduction cascade as described in Chapter 1 (Molday, 1998). Mutations in this gene account for 30 to 40% of autosomal dominant RP and up to 150 distinct mutations have been identified to date, making it the most commonly-mutated gene in RP (Sohocki *et al.,* 2001). Rhodopsin mutations have also been associated with dominant congenital stationary night-blindness (CSNB) and recessive RP but to a much lesser extent (Garriga & Manyosa, 2002).

The second gene to be associated with adRP was peripherin-RDS, in which a number of pathogenic mutations have been described to date, accounting for up to 5% of adRP (Kajiwara *et al.,* 1991; Farrar *et al.,* 1991; Sohocki *et al.,* 2001). This gene has

been found to exhibit digenic inheritance with a second gene, ROM1, and it is likely that mutations in ROM1 alone can also cause dominant RP (Kajiwara *et al.,* 1994; Dryja *et al.,* 1997; Bascom *et al.,* 1995). The peripherin-RDS and ROM1 proteins form heterotetramers at the margins of the rod outer segment discs, which are critical for stable photoreceptor disc formation (Loewen *et al.,* 2001). RDS mutations have also been identified in patients with a wide phenotypic variety of inherited retinal dystrophies, including cone-rod dystrophy and several macular dystrophies (Keen & Inglehearn, 1996). There have been great advances, especially in the last few years, in the identification of novel dominant RP-associated genes. A photoreceptor-specific gene called RP1, which accounts for 5-10% of adRP has been characterised, and has been shown recently to be required for the correct orientation and higher order stacking of outer segment discs (Sullivan *et al.,* 1999; Pierce *et al.,* 1999; Liu *et al.,* 2003). An additional adRP gene with a structural function has been identified as *FSCN2*, a retinal-specific fascin gene which crosslinks and bundles f-actin (Wada *et al.,* 2001). Mutations in the photoreceptor-specific transcription factors cone-rod homeobox (CRX) and neural retina leucine zipper (NRL) have also been identified in dominant RP and other retinopathies (Bessant *et al.,* 1999; Sohocki *et al.,* 1998). CRX and NRL interact with each other to promote the transcription of rhodopsin and other retinal genes, and are especially important in photoreceptor cell development (Swaroop *et al.,* 1999; Mears *et al.,* 2001).

Up until quite recently, all characterised adRP genes exhibited retinal-specific expression patterns, so it was quite unexpected when a number of RP-associated genes were discovered that showed widespread expression patterns. Mutations in three genes PRPC8, PRP31 and HPRP3, all of which encode components of the pre-mRNA splicing complex, have been implicated in adRP (McKie *et al.,* 2001; Vithana *et al.,* 2001; Chakarova *et al.,* 2002). All three genes were cloned in quick succession, and though they are expressed in all tissues of the body, mutations only cause a pathology in photoreceptor neurons. They function as components of the splicosome complex, which is an RNA-protein complex involved in the removal of pre-mRNA introns, a prerequisite for the expression of most eukaryotic genes. The pathogenesis of mutations in splicing factor genes is thought to be associated with the huge demand for rhodopsin splicing that is required in the photoreceptor cells (Vithana *et al.,* 2001). An adRP gene which encodes a molecular target of the Pim-1 kinase oncogene has been identified as the disease–causing gene in RP9, which is also expressed in many tissues

of the body, but its function has not yet been established (Keen *et al.*, 2002). The current study describes the identification of a ubiquitiously-expressed adRP gene called IMPDH1. All adRP genes identified or predicted to date are listed in Table 4.1.

Table 4.1. Thirteen loci for autosomal dominant RP and functions of cloned genes. This table demonstrates the functional diversity that exists between genes that are associated with a single sub-type of RP. From the thirteen adRP loci originally mapped, twelve causative genes have so far been identified (http://www.sph.uth.tmc.edu/Retnet/).

Gene Name	Chromosomal Location	Gene Function
RHO (RP4)	3q21-q24	Initiates the visual transduction cascade
RDS (RP7)	6p21.2-cen	Rod disc structural glycoprotein
ROM1	11q12.3	Retinal outer segment outer membrane protein Rod disc structural glycoprotein
FSCN2	17q25	Photoreceptor-specific paralog of fascin which crosslinks and bundles f-actin
CRX	19q13.3	Cone-rod photoreceptor homeobox transcription factor
NRL (RP27)	14q11.2	Retinal transcription factor which interacts with CRX and promotes transcription of rhodopsin and other retinal genes
RP1	8q11-13	Photoreceptor-specific protein, involved in outer segment disc stacking
PRPC8 (RP13)	17p13.3	Protein precursor mRNA processing protein C8
PRPF31 (RP11)	19q13.4	Component of the mRNA splicing complex
HPRP3 (RP18)	1q13-q23	Component of the mRNA splicing complex
IMPDH1 (RP10)	**7q31.2**	**Guanine nucleotide biosynthesis (Gene identified in this study, see results section).**
RP9	7p15.1-13	Pim-1 kinase protein target of unknown function, widespread expression.
RP17	17q22	Gene not identified

4.1.6 Autosomal recessive retinitis pigmentosa

Autosomal recessive RP is thought to account for 5-20% of RP where the inheritance pattern is known, and the majority of sporadic RP cases (Saleem & Walter, 2002). There have been 21 autosomal recessive RP loci mapped, and of these 17 genes have so far been identified, all of which are detailed in the Retnet database (http://www.sph.uth.tmc.edu/Retnet/). A number of these genes are also often associated with dominant RP, Usher syndrome, Leber's congenital amaurosis (LCA) or other retinal degenerative diseases.

Many arRP genes encode components of the visual transduction cascade and the visual cycle, both of which have been described in detail in Chapter 1. Visual transduction is the mechanism by which light absorption is translated into a neuronal signal. Mutations have been identified in the α- and β-subunits of rod cGMP-phosphodiesterase (PDE), the α- subunit of the cone cGMP-gated cation channel, the β-subunit of the rod cGMP-gated channel and arrestin. The retinoid or visual cycle is the series of biochemical steps that takes place in the RPE and photoreceptors, through which the chromophore of rhodopsin, 11-*cis* retinal, is provided and recycled. Genes in the retinoid cycle that have been associated with recessive RP include *LRAT, RGR, RPE65, RLBP1* and *ABCR,* many of which are preferentially expressed in the RPE cells. These genes either encode components of the visual cycle, or are involved in transport of retinal cycle proteins. *LRAT* catalyzes the first step in the visual cycle transforming vitamin A (retinol) into 11-*cis*-retinal (Thompson *et al.,* 2001). *RPE65* is involved in the metabolism of all *trans*-retinyl esters to 11-cis retinal, while *RGR* binds all *trans*-retinal, which is converted into *cis* retinal by light, the inverse reaction to that occurring within rhodopsin (Redmond *et al.,* 1998; Morimura *et al.,* 1999b). Mutations within the cellular retinaldehyde-binding protein gene (*RLBP1*), which is an intracellular carrier of 11-*cis* retinol, have been found to cause recessive RP and retinitis punctata albescens (Maw *et al.,* 1997; Morimura *et al.,* 1999a). The *ABCR* gene encodes rim protein (RmP), which is an ATP-binding transporter protein of the rod outer segment disc membranes, and is often associated with Stargardt disease, cone-rod dystrophy, recessive macular dystrophy as well as recessive RP (Sun *et al.,* 2000). A number of functions have been proposed for the protein product of ABCR, one of which involves the transport of all-*trans*-retinal or retinylidene-phosphatidylethanolamine across photoreceptor disc membranes (Ahn *et al.,* 2003).

Mutations within these retinoid cycle genes disrupt the cycling of retinal between the photoreceptors and the RPE, resulting in dysfunction of photoreceptor cells.

An arRP gene called *MERTK* has been shown to be involved in the phagocytosis of outer segment disc membranes, and likely functions directly in the RPE phagocytic process as a signaling molecule triggering outer segment ingestion (Gal *et al.,* 2000; Feng *et al.,* 2002). Additional arRP genes whose function in the retina and role in disease is less clear include *CRB1* and *TULP1*. CRB1 has been shown in a mouse model carrying a mutation within the *Crb1* gene, to be essential for external limiting membrane integrity and photoreceptor morphogenesis in the retina (den Hollander *et al.,* 1999a; Mehalow *et al.,* 2003), while TULP1 is proposed to be involved in transporting rhodopsin but may also function as a transcription factor (Hagstrom *et al.,* 2001). There also remains a number of additional arRP genes that have not yet been identified.

4.1.7 X-linked retinitis pigmentosa

X-Linked RP is generally considered the most severe form of RP. There have been five different loci identified on the X-chromosome, with two disease-causing genes cloned to date. The most commonly mutated X-linked RP gene is the retinitis pigmentosa GTPase regulator (RPGR) gene, which has been associated with a number of hereditary retinal degenerations and is thought to be involved in 70% of xlRP cases and an estimated 11% of all RP patients (Meindl *et al.,* 1996; Vervoort *et al.,* 2000). The function of RPGR is not yet fully understood, and while it is widely expressed, it exhibits retina-specific alternate splicing (Hong *et al.,* 2002). RPGR co-localises with a photoreceptor-specific RPGR-interacting protein (RPGRIP) in the photoreceptor connecting cilia, the thin bridges linking the cell body and the light-sensing outer segments, where it is thought that RPGR depends on RPGRIP for subcellular localization and normal function (Hong *et al.,* 2001; Zhao *et al.,* 2003). Null mutations in RPGRIP have also been found to lead to the retinal dystrophy, Leber congenital amaurosis (Dryja *et al.,* 2001). It is predicted that RPGR and RPGRIP may participate in protein trafficking through the connecting cilia and/or disk morphogenesis (Zhao *et al.,* 2003). The second most common X-linked RP gene to be identified is denoted RP2, which is mutated in 10-20% of X-linked RP patients in Europe and North

America (Hardcastle *et al.,* 1999; Mears *et al.,* 1999). This was the first of all the RP loci to be identified, but the disease gene was not cloned until 1998 (Bhattacharya *et al.,* 1984; Schwahn *et al.,* 1998). RP2 encodes a novel protein with similarity to human cofactor C, a protein involved in β-tubulin folding (Bartolini *et al.,* 2002). It localises to the plasma membrane of cells throughout the retina and may have a role in cell signalling (Chapple *et al.,* 2003). Three additional RP genes have been mapped to the X-chromosome, but have not yet been cloned.

4.1.8 A locus for autosomal dominant RP on chromosome 7q31 (RP10)

A major linkage study performed in this laboratory, resulted in the mapping of an autosomal dominant RP (adRP) gene to the long arm of chromosome 7, referred to as the RP10 locus (Jordan *et al.,* 1993). The investigation involved a genome wide search of DNA from members of a large Spanish family, FA84, segregating classic adRP (see pedigree Figure 4.4). The mean age of onset of RP in this family was 12.9 years (range 5-28 years). All affected individuals show severe constriction of the visual fields, and evidence of severe vitreous disturbance. A number of individuals have developed posterior capsular lens opacities of sufficient severity to warrant cataract extraction. All affected individuals exhibit fundus changes characteristic of RP including optic disc pallor, retinal vascular attenuation and bone spicule pigmentary deposits in the retinal mid-periphery. Affected individuals also demonstrate extinguished rod and cone ERG responses (Jordan *et al.,* 1993). It may be a common feature of RP10 patients, that a similar rate in the reduction of rod and cone ERGs is observed, rather than the more typical initial reduction in rod ERG amplitudes (Bowne *et al.,* 2002).

In the original 1993 study, thirty-six members of the family were originally typed for microsatellite markers from chromosome 7, and linkage analysis was carried out on the results (a background on linkage analysis has been presented in Chapter 1). The adRP gene was demonstrated to be most closely linked to microsatellite markers D7S480, D7S466 and D7S514, with a maximum LOD score of 7.51 at marker D7S480 (Jordan *et al.,* 1993). This placed the disease locus at 7q31-35. A second unrelated American family called UTAD045 segregating RP was linked to the same RP10 region shortly afterwards, showing a maximum LOD score of 5.26 at D7S514 (McGuire *et al.,* 1995). Data from both families was combined and the disease locus was found to lie

between the markers D7S530 and D7S686, spanning a 5cM interval (Fig. 4.5)(McGuire *et al.,* 1996a). These flanking markers were adopted because affected members of a branch of family UTAD-045 were recombinant at marker D7S530, thereby setting it as the telomeric disease boundary, and haplotype analysis revealed that an FA-84 individual did not appear to carry the disease haplotype at and proximal to the marker D7S686 (McGuire *et al.,* 1996b). Two additional adRP families, which are of British and Spanish origin were also reported to show linkage to the same markers on chromosome 7q31 (Mohamed *et al.,* 1996; Millan *et al.,* 1995).

Over a number of years, attempts were made in a collaboration with Dr. Steve Daiger and colleagues, University of Texas, Houston, USA, to narrow the disease interval, and combine the linkage data in all available RP10 families. The D7S686 marker was re-typed in the family FA-84 following a re-evaluation of the flanking markers by Dr. Avril Kennan, Trinity College Dublin (Kennan, 1999). There were a number of reasons for carrying out this analysis, including the acquisition of eight new family DNAs and the clinical reassessment of some of the younger family members. The new linkage and haplotype analysis led to the interval being extended slightly to the marker D7S2471, which is 0.59 cM proximal to D7S686 according to the Marshfield Genetic Linkage map (Kennan, 1999). This was probably caused by a haplotyping error in the previous analysis. Further analysis of the D7S530 flanking marker was also carried out using new polymorphic markers for fine haplotype analysis in both RP10 families, FA-84 and the American family UTAD045 by Dr. Sara Bowne, University of Texas, Houston (Bowne *et al.,* 2000a). The distance between D7S530 and D7S461, the closest non-recombinant marker, was estimated to be about 1 cM. A number of short tandem repeat markers were identified in the genomic sequence between these two markers, which led to movement of the telomeric boundary of the critical region from D7S530 to a region located between D7S461 and 60,000bp distal (Bowne *et al.* 2000a) (Fig. 4.5). This reduced the interval to a 4cM region located on chromosome 7q31 between D7S2471 and 60,000bp telomeric of D7S461 which corresponds to approximately 3.5 Mb of DNA. At the time of analysis the complete sequencing of the human genome was nearing completion, but a number of gaps remained in the sequence, which are regions of the genome that are particularly difficult to sequence, and as a result the arrangement of some genomic clones was subject to slight change.

4.1.9 Identification of candidate RP10 genes

When a linkage is initially established between a disease gene and a particular region of a chromosome, an investigation of the known genes that map to the region is undertaken. As a result of the completion and release of the human genome draft sequence, and the large number of additional genetic and web-based resources that are available, physical mapping of disease intervals has become considerably less labour intensive in recent times. The generation of genomic contigs and clones across an interval has largely become redundant, as their assembly and content is now freely available through accessing human genome databases such as the UCSC Human Genome Browser (http://genome.ucsc.edu/), the Ensembl Genome Browser (www.ensembl.org) and the NCBI Map Viewer database (http://www.ncbi.nlm.nih.gov/mapview/). Resources such as these allow the researcher to view the location of all known and mapped genes, as well as predicted novel genes, throughout the sequence of the human genome. Any gene that maps to within the flanking markers of a disease interval, may be considered a candidate disease gene, but a method of prioritising genes is often required before mutational screening is carried out. The decision on whether a particular gene is to be screened is generally based on its pattern of expression and/or function.

A number of candidate genes have already been investigated that map to within the RP10 disease interval on 7q31.3. Since the RP10 disease locus was mapped in 1993, a variety of different techniques have been employed in an effort to isolate the causative gene. It was anticipated that the disease-causing gene would show increased levels of expression in the retinal rod photoreceptors, and while it was thought likely that expression would be photoreceptor-specific, it was also possible that the gene would show expression in other tissues also. Most of the adRP-causing mutations that had been identified up to that point had been found in genes whose expression is limited to the photoreceptor cells such as rhodopsin, peripherin or CRX. A number of genes that map to within the RP10 interval were screened previously by Dr. Avril Kennan and Dr. Sara Bowne. These include glutamate receptor 8 (GRM8), diacylglycerol kinase iota (DGKι), ADP ribosylation factor 5 (ARF5) and retinally-expressed ESTs corresponding to the human homolog of the *Drosophila rdgA* gene and a ubinuclein-like gene, but all were excluded as candidates (Kennan, 1999, Bowne *et al.*, 2000b,

Bowne *et al.*, 2002). Some of the approaches used in the effort to identify the RP10 gene involved the use of human genome databases, the rhodopsin knockout mouse and expressed sequence tag (EST) analysis. Whilst these approaches towards the prioritisation of candidate genes were reasonably effective, the extreme genetic and functional diversity exhibited amongst RP-associated genes essentially meant that almost any gene in the RP10 region could be regarded as a candidate.

4.1.9.1 Human genome resources

In the last few years, internet-based bioinformatics resources have become an essential tool in the identification of candidate disease-causing genes. At the time this research on candidate gene identification for RP10 was undertaken, the human genome sequence and assembly was nearing completion, and databases were constantly updated with known and predicted genes. A working draft of the human genome was available for the RP10 region on chromosome 7q31, and it provided a comprehensive map of all the known and predicted genes at that time (Fig. 4.6)(http://genome.ucsc.edu/ ; www.ensembl.org). A number of additional internet-based resources were also routinely used such as the BLAST database (http://www.ncbi.nlm.nih.gov/BLAST/), which is a sequence homology search tool that provides a powerful way to compare novel sequences with previously characterised genes, and the Clustalw database (http://www.ebi.ac.uk/clustalw/) which carries out multiple sequence alignments. Gene prediction programs such as *Genscan* are routinely used to identify potential coding sequence in the emerging human genome raw sequence. These programs look for features such as ATG start sites, open reading frames, splice sites and termination codons. BLAST analysis and expressed sequence tag (EST) data, which is discussed in greater detail below, can be combined with the results to give an indication of the pattern of expression of a predicted gene. A gene is awarded 'confirmed' status in Human Genome Databases when it is shown to have significant similarity to a known sequence (DNA or protein) in a database. There is an issue with spurious prediction, because it still must be proven that the 'confirmed' gene is actually translated into protein, so a characterisation of proteins and their function is still required in many cases. An annotated collection of all publically available DNA sequences is available in the NIH genetic sequence database, Genbank (http://www.ncbi.nlm.nih.gov/Genbank/). The NCBI Locuslink database provides a single query interface to curated sequence and descriptive information about genetic

loci (http://www.ncbi.nlm.nih.gov/LocusLink/index.html). The Locuslink database is an example of another valuable database used extensively in this study, because it provides information on official nomenclature for a particular gene, sequence accession numbers, phenotypes, EC numbers, OMIM entries, homology, map locations, and links to related web sites.

Approximately half of the human genome sequence was in a highly accurate 'finished' state with the other half being referred to as 'draft' quality during the period this study was undertaken. The gene map of the RP10 region according to the human genome browser from the October 2001 release is shown in Figure 4.6, which was the most up-to date map that was available at that time. The latest release of the human genome sequence produced by the International Human Genome Sequencing Consortium was released in July 2003 (Fig. 4.7). This sequence now covers about 99 percent of the gene-containing regions in the genome, and has been sequenced to an accuracy of 99.99 percent (http://genome.ucsc.edu/cgi-bin/hgGateway). It is obvious that a number of additional genes have been confirmed in the intervening period, and all sequence gaps have been filled in the most recent version of the RP10 region. A view of the RP10 locus using the Ensembl Genome Browser is shown in Figure 4.8. These human genome browsers were used extensively in the search for the RP10 gene because they often contain different types of information about a particular gene. The *Ensembl* browser was used mainly for the prediction of novel genes with supporting evidence, while the UCSC browser was used extensively for marker and genomic clone analysis. Both databases provide an extremely valuable, and user-friendly resource for researchers working in the field of human genetics.

4.1.9.2 Rhodopsin knockout mouse

The generation of a mouse with a targeted disruption of the rhodopsin gene ($Rho^{-/-}$) has been described previously in Chapter 3. By three months of age the outer nuclear layer of the retinas in these mice is reduced to single cell thickness, and the degeneration of the photoreceptor cell layer is essentially complete (Humphries *et al.*, 1997). Therefore, no expression of rhodopsin, or any other photoreceptor-specific gene should be detectable in these animals after 3 months of age. The $Rho^{-/-}$ mouse model was used in this study because it enabled a comparison to be made between the expression of candidate genes in a wild-type mouse retina with a mouse retina where the photoreceptor cells are absent, thereby identifying potential photoreceptor-specific or

enriched transcripts. Since mouse eye tissue is more readily obtainable than human eye tissue, and exon sequences are usually well conserved between orthologous human and mouse genes, the isolation of the mouse homolog of a gene can be very useful in expression studies. A region of the mouse genome on chromosome 6 has been identified that exhibits synteny with human chromosome 7q, which means that this particular region of chromosome 6 contains many mouse homologues of the human genes found on chromosome 7q31. The human mouse homology map at the NCBI website provides details of those genes which are present in both species (http://www.ncbi.nlm.nih.gov/Homology/).

As discussed in detail in the Chapter 3, comparative microarray analysis can provide valuable clues into the expression of genes in the photoreceptor cells, and a large microarray analysis has been undertaken comparing the transcriptional profiles of wild-type and *Rho*$^{-/-}$ mouse retinas. This study predicted a number of differentially expressed genes, or genes that appeared to be expressed at higher levels in photoreceptor cells. We suggest that such transcripts could be regarded as possible candidate genes associated with retinal degenerations.

4.1.9.3 Expressed sequence tags (EST's)

For many years, it was generally believed that the RP10 disease gene probably encoded a novel, unknown transcript because there were no genes considered likely candidates mapping to the region on chromosome 7q31. Expressed sequence tags (ESTs) have provided a valuable resource in the search for disease genes, because their analysis helps to identify previously uncharacterised genes, their chromosomal location and tissue expression patterns. ESTs are single pass DNA fragments, typically 300-400 nucleotides in length, sequenced from the 3' or 5' end of cDNA molecules (Fannon, 1996). As discussed briefly in Chapter 3, a database of EST sequences derived from a comprehensive set of human tissues and cell lines is available on the NCBI website. This database is referred to as the UniGene collection, and contains gene-based clusters of sequences that include all ESTs from a particular gene (http://www.ncbi.nlm.nih.gov/UniGene/). One important use of the UniGene clusters is to identify novel, nonredundant mapping candidates for generating a transcript map that identifies all coding sequences in the genome. As well as containing sequences that represent a unique gene, each Unigene cluster also provides related information such as the tissue types in which the expression of a gene has detected and map location

(Boguski & Schuler, 1995). A second EST submission database exists which is based at the Institute of Genomic Research (TIGR). These EST sequence clusters are also used in the generation of microarrays for global gene expression studies. In order to identify additional novel candidate genes for inherited retinal disorders, novel EST clusters expressed in the retina have been identified from the TIGR Human Gene Index Database and mapped to specific sites (Malone *et al.,* 1999; Sohocki *et al.,* 1999). A number of EST clusters were originally identified that mapped to RP10 disease locus, and were previously analysed for expression in the retina using *in situ* hybridisation studies (Kennan, 1999). Many of the gene entries that were originally EST clusters in the Unigene database, are also listed in the Locuslink database which has been described previously.

4.1.10 Methods used in screening candidate RP10 genes

In the event of an interesting candidate gene being identified in the RP10 region, based on its function and/or expression, it was necessary to screen it for potential disease-causing mutations. If possible, an investigation into whether a candidate gene was actually expressed in the retina was carried out using both database searching and laboratory techniques. Upon confirmation of retinal expression, a candidate gene was screened for potential mutations using automated sequencing and/or an automated DHPLC instrument, the WAVE® Nucleic Acid Fragment Analysis System.

The WAVE® system provides a rapid, automated scanning method for mutations even when the nature and location of the mutation is unknown (Taylor *et al.,* 2000). Mutations are visualised as a characteristic pattern of peaks corresponding to the mixture of heteroduplexes and homoduplexes formed when wild-type and mutant DNAs are hybridised. Analysis is performed by denaturing high performance liquid chromatography (DHPLC) of PCR amplification products. DHPLC conditions are established by generating melting curves of the complete coding sequence of a target gene using 'WAVEmaker' software (Transgenomic). The optimum temperature for separation of fragments, as predicted by WAVEmaker software, is the temperature at which 75% of the fragment is helical. The patented separation column, the DNASep® cartridge matrix, is hydrophobic, and will adsorb DNA molecules only in the presence of the ion-pairing reagent triethylammonium acetate (TEAA). DNA fragments are

released from the matrix by gradually increasing the concentration of acetonitrile (ACN) in an elution buffer gradient. This unique chemistry allows for the detection of mutations due to the fact that if a mutation is present in a sequence, this causes the formation of heteroduplexes. Heteroduplexes are resolved ahead of homoduplexes on the column because they cause a slight change in the Tm of the sequence, resulting in an altered chromatogram. The detection efficiency of the WAVE system has been reported as being between 93-100%, and it is generally regarded as an efficient and sensitive detection method (Benit *et al.,* 2001; Liu et al, 1998). Increasingly, the use of proof-reading DNA polymerase is recommended, and has been shown to produce more accurate results (Liu *et al.,* 2002).

4.1.11 The aim of the study

The aim of this study was to isolate the disease-causing gene in the RP10 form of retinitis pigmentosa, which was originally linked to chromosome 7q31 in a large family, FA-84. Different approaches and techniques were used to select candidate genes in the RP10 region. The emerging human genome sequence was an essential tool in the initial identification of likely candidate RP10 genes, which were then screened and subsequently excluded if no disease-causing mutations were detected. A microarray analysis experiment described in Chapter 3, which compared the expression of transcripts between wild-type and *Rho*$^{-/-}$ mouse retinas, was instrumental in the adoption of IMPDH1 as a candidate gene. Expression of this gene was down-regulated in the *Rho*$^{-/-}$ retina, which provided a clue that it may be highly expressed in the photoreceptor cells of the retina. Subsequent screening of the *IMPDH1* gene in family FA-84 revealed a pathogenic mutation in the coding sequence of affected individuals.

4.2 MATERIALS AND METHODS

The protocols for PCR, PCR product purification and automated sequencing have been described previously in Chapter 2.

4.2.1 PCR for DHPLC analysis

In most instances, PCRs for DHPLC analysis were carried out as described previously. For some PCR reactions there was evidence of mis-primed products that caused undesired extra peaks in the resulting chromatogram, so for these reactions a proof-reading *Pfu* polymerase (Promega) was used. PCRs were performed according to the manufacturers' instructions, by combining 5 µl *Pfu* DNA polymerase 10X buffer, 100 µM dNTP mix, 25 pmol of each primer and 0.5-1µg DNA template. The *Pfu* polymerase, 1.25-3 U was added on ice just prior to loading the tubes into a thermal cycler that had been pre-heated to 95°C. The samples were initially denatured at 95°C for 1-2 minutes, followed by 25 cycles of denaturation at 95°C for 1 min, annealing at 55-65°C for 30 secs and extension at 72°C for 2-4 minutes. A final extension step of 5 minutes at 72°C was carried out.

For DHPLC analysis, the DNA polymerase in PCR products was inactivated by adding 2µl of a stop buffer (Appendix A.1). A heteroduplex step was carried out by heating samples to 95°C for 4 minutes, then cooling slowly to 25°C over a 45 minute period. The optimal melting temperatures for DHPLC analysis of PCR products were calculated using the WAVEmaker utility software (Transgenomic Inc.), which calculates the temperatures for analysis based on the nucleotide sequence of the wild-type DNA. The standard buffers used on the WAVE machine were Buffer A (0.1M TEAA) and Buffer B (0.1M TEAA, 25% acetonitrile), and the separation gradient used was the recommended 2% increase in Buffer B per minute.

4.2.2 Extraction of RNA from mouse retinas

All glassware was treated with RNAse Away (Molecular Bioproducts) and baked for 3 hours at 180°C prior to RNA work. Water was treated with diethylpyrocarbonate

(DEPC) to remove all traces of RNAses. Fresh mouse retinas were removed by Dr. Paul Kenna from a wild-type 129 four month old mouse, a one month old *Rho*$^{-/-}$ mouse and a four month *Rho*$^{-/-}$ mouse on a 129 background. The retinas were placed immediately into 175 µl RNA lysis buffer (4M guanidine thiocyanate, 1% β-mercaptoethanol) and extracted using the SV Total RNA Isolation System (Promega). The extraction procedure was carried out according to manufacturers' instructions. Briefly, samples were homogenized in lysis buffer, SV RNA Dilution buffer was added and tubes were centrifuged at 13,200 rpm for 10 minutes. The lysate was removed and placed in a fresh tube with 200 µl of ethanol. This mixture was placed into the spin column assembly provided and the column was centrifuged for 1 minute. The column was washed with SV RNA wash solution, followed by DNAse treatment and finally two more wash steps. The RNA was eluted by adding 100µl nuclease free water to the spin column, and collecting the eluted fraction in a fresh tube after spinning. RNA samples were subsequently stored at –80°C.

4.2.3 Reverse-Transcriptase PCR (RT-PCR)

RNA extracted from mouse retinas and also from Y79 Retinoblastoma cells (provided by Dr. Sophia Millington-Ward) was converted into cDNA using the enzyme reverse transcriptase. 2 µg of an RNA sample was added to 4 µl of 5x RT buffer (Boehringer), 100 µM each dNTP, 1 µl of10 µM random primers $Pd(N)_6$ (Boehringer) and 24U of RNAse inhibitor (Promega) in a final volume of 19 µl made up with DEPC-H_2O. The mixture was heated to 65°C for 5 minutes, followed by 10 minutes at 25°C. 1 µl (200U) of MMLV reverse transcriptase enzyme (Boehringer) was added and tubes were incubated at 37°C for 50 minutes. Samples were heated to 94°C for 5 minutes for termination of the reaction. For PCR reactions on cDNA samples, 1-2 µl cDNA was added per 25 µl PCR reaction, and PCRs were carried out as described previously.

4.3 RESULTS

4.3.1 Identification of candidate RP10 genes

A major linkage study previously carried out on a large adRP family, FA-84, resulted in the identification of a disease locus on chromosome 7q, subsequently referred to as RP10 (Jordan *et al.,* 1993). The aim of the present study was to identify the pathogenic mutation responsible for this form of RP. Initial identification of candidate genes mainly involved the use of emerging sequence information from the human genome project, which was first released in draft form in February 2001 and has resulted in many new genes being identified and mapped (Lander *et al.,* 2001). An inventory of genes that map in the interval was retrieved from the Ensembl Genome Browser database (www.ensembl.org/). Extensive database analysis was undertaken to identify homologous sequences, evidence of expression in different tissues and functional information about potential candidate genes. During the period of this analysis, there were at least 20 known or 'confirmed ' genes within the RP10 interval, and up to 40 additional predicted genes that were at that point unconfirmed (Fig. 4.6). Much progress has been made in the confirmation of genes since that time, and it appears that the number of predicted transcripts may have been over-estimated, since many were actually merged to form one large gene. This has resulted in a significantly reduced number of predicted genes that are currently mapped to within the interval (Fig. 4.7 & 4.8). The region now contains up to 25 known genes, with additional novel genes still predicted by *Ensembl* (www.ensembl.org) (Fig. 4.8).

The complete assembly of the RP10 region was incomplete in October 2001, and while many genomic clones were mapped correctly, the region clearly still contained some draft clones and a number of gaps in the sequence (caused by regions not amenable to sequencing). This made it difficult at times to accurately ascertain whether a particular gene lay inside or outside the RP10 flanking markers, because the exact sequence order of genes was occasionally altered. The selection of a likely candidate gene from the *Ensembl* database, was based on it's chromosomal location, predicted function (if available), comparison with other known RP disease genes and expression patterns of any homologous ESTs. A system was developed for preliminary

expression analysis of a candidate disease-causing gene, prior to complete sequencing of the gene in family FA-84, which can be expensive and labour-intensive if the gene involved is large. It was assumed that the disease-causing gene should show substantial levels of expression in photoreceptor cells if it is to cause degeneration of these cells only. Hence, a method was developed to determine whether a candidate gene of interest was photoreceptor-specific or enriched in photoreceptor cells, using the *Rho*$^{-/-}$ mouse model.

4.3.2 Analysis of candidate gene expression in the retina

A method was designed to determine whether a candidate gene of interest was expressed in the photoreceptor cells of the retina using the *Rho*$^{-/-}$ mouse model, which has been described in detail in Chapter 3. The *Rho*$^{-/-}$ mouse does not elaborate rod outer segments and loses its photoreceptor cell layer over 3 months (Humphries *et al.,* 1997). It was anticipated therefore that photoreceptor-specific or enriched transcripts would be expressed in wild-type (Wt) mouse retinas, but would not be expressed in *Rho*$^{-/-}$ retinas at three or more months. The majority of genes implicated in adRP at that time including rhodopsin, peripherin-RDS and cGMP-phosphodiesterase (PDE) were expressed exclusively in the photoreceptor cell layer of the retina. Hence it was suspected that the RP10 gene located on chromosome 7q31 would also be photoreceptor-specific, or at least expressed more abundantly in the photoreceptor cell layer. For this experiment, retinas were taken by Dr. Paul Kenna from the eyes of a four-month old wild-type 129 mouse, a one-month old *Rho*$^{-/-}$ 129 and a four-month old *Rho*$^{-/-}$ 129 mouse. RNA was extracted from each of these retinas, and was converted to cDNA using reverse transcriptase.

The homologous mouse sequence of a human retinally-expressed control or candidate gene was retrieved by accessing the previously described *Locuslink* or *Unigene* databases, or could also be identified by database homology searching of the mouse genome using BLAST analysis. If this sequence was obtained, both human and mouse coding sequences for genes of interest were aligned using a sequence alignment program (http://www.ebi.ac.uk/clustalw/) and primers were chosen in regions of complete homology. In order to ensure the amplification of expressed transcripts only, and not genomic DNA sequence, primers were designed to span an intron by

determining the exon-intron structure of each gene. By choosing primers that amplified both human and mouse sequences, the primers could also be used to amplify human retinal cDNA from Y79 cells, which was made from RNA extracted from a retinoblastoma cell library by Dr. Sophia Millington-Ward, and also a human retinal cDNA library which was obtained from Dr. Steve Daiger and colleagues.

The expression of a number of known photoreceptor-specific genes was initially investigated, in order to test the gene expression profile of RNA extracted from Wt and *Rho*$^{-/-}$ retinas. Primers spanning exon-intron boundaries were designed for amplification of the photoreceptor-specific genes rhodopsin, peripherin-RDS and PDE6A, and for amplification of beta 2 microglobulin (B2MG) for use as a 'house-keeping' gene, that was expected to show expression in all samples (all primer sequences and product sizes are listed in Appendix B.3). All four sets of primers successfully amplified their target sequences in Wt mouse retinal cDNA samples as expected, with the rhodopsin primers producing the strongest amplication product (Fig. 4.9). Weak PCR products were produced using the rhodopsin and PDE6A primers to amplify one-month old *Rho*$^{-/-}$ cDNA. There is believed to be a redundant rhodopsin transcript produced in the *Rho*$^{-/-}$ retina in the first month or two which may explain this weak amplification product. There was no amplification of rhodopsin or PDE6A in 4-month old *Rho*$^{-/-}$ animals, while the peripherin-RDS transcript was either absent or greatly reduced. The housekeeping gene B2MG was amplified in all three cDNA samples tested (Fig. 4.9). This experiment was designed in order to prioritise candidate genes for RP10 on the basis of their expression in the retina. It greatly depended on the availability of homologous mouse sequence for a candidate gene of interest. If the mouse sequence was not available, primers for amplification of human sequence only were designed and PCRs were carried out to test for expression of a candidate gene in either Y79 cDNA or a human retinal cDNA library. If evidence of retinal-expression was proven, the strongest candidate genes were then screened.

4.3.3 Screening candidate RP10 genes

Initial screening of candidate genes was carried out on an automated DHPLC instrument, the WAVE® Nucleic Acid Fragment Analysis System, and subsequently

automated sequence analysis was carried out if any variations were detected. The exon/intron structure and genomic sequence surrounding coding regions of a candidate gene were usually identified through accessing the UCSC Human Genome Browser database. Alternatively, the sequence was entered into the BLAST homology searching database, which generally locates the coding sequence surrounded by genomic sequence in the corresponding human genomic clone or contig. Primers were designed at least 50 base pairs away from the exon splice sites to ensure sequence analysis of the complete coding sequence (primer sequences available in Appendix B.4). It is generally recommended that PCR product size is kept under 600 bp for accurate DHPLC analysis, so this was adhered to in all cases. PCR amplification of exonic gene sequences from affected and unaffected individuals in family FA-84 was usually carried out using Taq DNA Polymerase, but it was found that it was often necessary to use proof-reading (*Pfu*) Taq for optimum resolution of fragments off the DHPLC column. The exact sequence of each PCR product to be analysed was input into 'WAVEmaker' software which calculates the melting temperature of a particular DNA sequence, and the optimum temperature at which it should be analysed. The temperatures chosen for each PCR product analysed using this system are summarised in Table 4.2.

As described previously, candidate genes were chosen for in-depth analysis on the basis of their expression and/or function. A number of genes have been screened previously including GRM8 and DGKι but no disease-causing mutation was detected in these genes, which resulted in their exclusion (Kennan, 1999). In this study, mutational screening analysis was undertaken on five separate genes that map to within the RP10 interval. These include a gene containing a GRIP-domain (called FLJ22035 or GCC1 in *Ensembl*), a cyclophilin-like gene, a zinc-finger gene (NCBI accession number AF218032) the gene for blue cone opsin (OPN1SW) and the *IMPDH1* gene. In all cases three affected and three unaffected individual's DNA from family FA-84 were examined. The location of the candidate genes screened in a map of the RP10 genomic region on chromosome 7q31-32 can be viewed in Figures 4.6-4.8.

4.3.4 GRIP-domain gene

A gene containing a GRIP-domain was one of the novel genes in the 7q disease interval predicted by the Ensembl Genome Browser. It was initially adopted as an RP10 candidate because it was classed as a member of the myosin heavy-chain protein family by the *Ensembl* database, a family that has 361 members. It showed 23% homology to the muscle myosin heavy chain protein, and was considered a possible candidate because mutations in one member of this family, myosin-7A, have previously been shown to cause Usher syndrome (Weil *et al.,* 1995). Little information was available about this novel gene other than it contains a GRIP domain, which is a golgi-targeting domain found in several coiled-coil proteins (Munro *et al.,* 1999).

The GRIP-domain gene as originally predicted by *Ensembl* (ENST00000223049) consisted of 2 exons separated by an intron of approximately 800 bp, and had a coding region of 2328 bp in length. It showed 100% homology to one human cDNA in the Genbank database with the accession number AK025688. An alignment carried out between the Ensembl-predicted GRIP-domain gene and AK025688 showed that the predicted GRIP-domain gene contained about 1000bp more coding sequence than the AK025688 cDNA. A homology search was carried out by entering the entire predicted GRIP-domain gene, into the BLASTn program against the non-redundant (nr) database. Results showed that in addition to the cDNA AK025688, it also showed strong homology (88%) to a mouse cDNA, AK016531 (Figure 4.10).

No other human or mouse cDNA was retrieved that spanned the entire length of the predicted GRIP-domain gene. A BLASTn search was subsequently carried out by entering the mouse AK016531 cDNA sequence and searching on this occasion against the high throughput genome sequence. The mouse cDNA was found to map to the region on mouse chromosome 6 that is known to be syntenic to human chromosome 7q31. The mouse gene AK016531 also consisted of two exons of similar structure to the predicted human gene. These results strongly suggested that AK016531 was, in fact, the mouse homolog of the predicted human GRIP-domain gene.

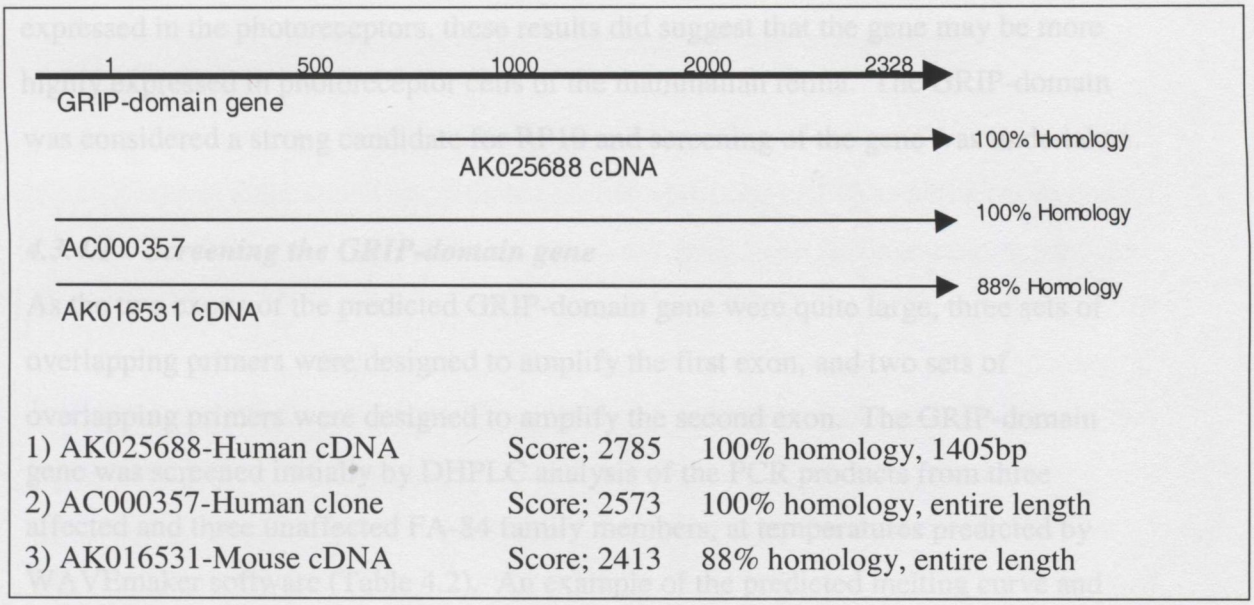

1) AK025688-Human cDNA	Score; 2785	100% homology, 1405bp
2) AC000357-Human clone	Score; 2573	100% homology, entire length
3) AK016531-Mouse cDNA	Score; 2413	88% homology, entire length

Figure 4.10. Summary of results obtained following BLAST homology analysis of the Ensembl-predicted GRIP-domain gene.

An experiment was then carried out to determine whether the GRIP-domain gene was actually expressed in the retina, and also if the full-length predicted GRIP-domain transcript was expressed, as opposed to the shorter AK025688 cDNA transcript found in the Genbank database. Primers were designed to amplify the longer *Ensembl*-predicted GRIP-domain transcript in both human and mouse cDNA (Appendix B.3). Following PCR amplification, the full-length predicted GRIP-domain gene was indeed found to show a high level of expression in a human retinal cDNA library, resulting in the expected amplification product size of 603bp (Fig. 4.11). Amplification of a number of other genes that are known to be highly expressed in the retina, including rhodopsin, PDE and RDS-peripherin, was carried out as a positive control. The resulting amplification product for the GRIP-domain gene was similar in intensity to that obtained for rhodopsin, indicating that this gene may be highly expressed in the human retina (Fig. 4.11).

The mouse GRIP-domain gene (AK016531) was amplified in Wt and *Rho*$^{-/-}$ retinal cDNA to investigate whether it was photoreceptor specific. Initial results indicated that the GRIP-domain gene was more highly expressed in the Wt mouse retina when compared to the *Rho*$^{-/-}$ retina at four months (Fig. 4.12). While further analysis revealed that the AK016531 transcript did not appear to be exclusively

expressed in the photoreceptors, these results did suggest that the gene may be more highly expressed in photoreceptor cells of the mammalian retina. The GRIP-domain was considered a strong candidate for RP10 and screening of the gene was undertaken.

4.3.4.1 Screening the GRIP-domain gene

As the two exons of the predicted GRIP-domain gene were quite large, three sets of overlapping primers were designed to amplify the first exon, and two sets of overlapping primers were designed to amplify the second exon. The GRIP-domain gene was screened initially by DHPLC analysis of the PCR products from three affected and three unaffected FA-84 family members, at temperatures predicted by WAVEmaker software (Table 4.2). An example of the predicted melting curve and suggested temperatures for DHPLC analysis of exon 1, PCR product 2, are shown in Figure 4.13. A change in the chromatogram pattern of peaks was revealed between affected and unaffected individuals when the PCR products from exon 1-2 were run at 64°C and 66°C (Fig. 4.14).

Exon 1 was sequenced and this revealed a G→A change in two affected individuals, which was not present in two unaffected individuals (Fig. 4.15). However, this base pair substitution was subsequently revealed to be a polymorphic non disease-causing variant, because it did not alter the amino acid sequence. The variant caused a CCG→CCA transition at codon position 625, both of which code for the amino acid glycine. Sequence analysis of the remaining coding regions of the gene was then undertaken, but did not reveal any further sequence variations. The GRIP-domain gene was therefore excluded as a candidate disease-causing gene for RP10.

A more recent database search has revealed that since this study, the full-length GRIP-domain gene has now been confirmed to have a coding region of 2328 bp, producing a protein product of 775 aa. The resulting protein product has been named golgi colied-coil (GCC1), and it is thought it may play a role in the organization of trans-Golgi network subcompartment involved with membrane transport (Kjer-Nielsen *et al.,* 1999). The mouse homologous gene has also been confirmed as AK016531. This shows the original genes predicted by Ensembl were accurate and reliable, even when there was little evidence available confirming the existence of a predicted gene. Results from this study have shown that the full-length sequence of the GRIP-domain gene is expressed in the retina, though its exact function is as yet unknown.

4.3.5 Cyclophilin-like gene

A cyclophilin-like gene (ENSG00000071293) was predicted in the RP10 interval, again by the *Ensembl* database. The predicted protein consisted of 136 aa and 2 exons and showed 70% homology to a human cyclophilin A gene. The first exon of the predicted gene also showed 64.5% identity to a bovine cDNA -BTRSC (Bos taurus retina-specific cyclophilin) mRNA, complete cds, which suggested that it may represent the human equivalent of a bovine retina-specific cyclophilin. It has previously been suggested that mutations in the gene encoding the human homolog(s) of the bovine retinal cyclophilins, could lead to specific degeneration of cone photoreceptor cells because they are thought to be involved in transporting opsins (Ferreira *et al.,* 1995). There was no strong homology detected with any other human or mouse cDNA or EST sequence.

There are many human cyclophilin genes (or cyclophilin-like genes) listed in the Genbank database (http://www.ncbi.nlm.nih.gov/Genbank/), but none that map to chromosome 7q. There have also been previous reports of the identification of the human cyclophilin gene along with 7 other cyclophilin-like genes, which are believed to be processed pseudogenes (Willenbrink *et al.* 1995; Haendler & Hofer, 1990). The 408bp *Ensembl*-predicted gene was compared to the sequence of the active human cyclophilin A gene (Genbank accession number NM_021130) which has five exons. This revealed that all five exons of the predicted gene were homologous to cyclophilin A, but appeared to be strung together in the *Ensembl*-predicted gene (as in cDNA). This indicated that the gene identified by *Ensembl* was possibly a pseudogene which had been reverse transcribed from a cyclophilin mRNA, and subsequently inserted into this position in the genome. An alignment was carried out between the seven cyclophilin pseudogene sequences available in Genbank and the candidate cyclophilin-like gene, but none of the known pseudogenes showed 100% homology to this candidate, or were of a similar length. It has been observed previously that reverse transcribed and re-inserted sequences can occasionally give rise to functional, processed genes and there are at least 8 such human genes that appear to have originated in this manner (Lander *et al.,* 2001). Despite this observation, it was decided that the gene would be screened using DHPLC analysis, its small size making this a relatively easy task. A single PCR fragment, encompassing both exons was screened in family members but no sequences changes were detected in affected individuals.

4.3.6 Zinc-finger gene

A gene containing a zinc-finger domain (NCBI accession number AF218032, also called Q9HBNO/LOC168850), was also predicted by *Ensembl* to map within the RP10 interval. It consists of four exons and is located on the genomic clone AC000127. The function of this candidate gene is unknown but zinc finger domains are usually found in nucleic acid binding proteins (Klug & Rhodes, 1987). Hence it was predicted that this protein may function as a transcription factor. It was chosen as a candidate gene because it shows 100% homology to a retinal EST (Genbank accession No. AA047055) thereby providing evidence for retinal expression. Primers were designed in intronic sequence to amplify the four coding exons for screening. PCRs were carried out using DNA from three affected and three unaffected individuals from family FA-84. PCR products were subsequently screened using DHPLC analysis. No difference was detected between the pattern of peaks obtained from affected and unaffected individuals in any of the 4 exons, therefore the zinc-finger gene was excluded as the RP10 gene. The same gene was also screened in DNA from an American RP10 family, UTAD-045, by Dr Steve Daiger and colleagues (personal communication), but again no disease-causing mutation was identified.

4.3.7 Blue cone opsin gene (OPN1SW)

The blue cone opsin gene encodes a transmembrane protein related to rhodopsin, which consists of 5 exons coding for 348 amino acids. Rhodopsin is found in rod cells and mediates scotopic vision while red green and blue opsins are found in cone cells and mediate photopic vision (Reviewed in Watson & Arkinstall, 1994). This gene had been screened in family FA-84 previously in our lab some years ago but it was decided to rescreen it using DHPLC analysis as it had not previously been screened in this manner. It is known to exhibit high levels of expression within the retina and maps to the RP10 region. Several mutations in the blue cone opsin gene have previously been identified in patients with tritanopia colour blindness, but had not previously been demonstrated in retinal degenerative diseases (Weitz *et al.*, 1992). Primers were designed to amplify all 5 exons of the blue cone pigment gene and resulting PCR products using family FA-84 DNA were analysed using DHPLC. No difference was detected between affected

and unaffected individuals, and therefore this gene was also excluded as an RP10 candidate.

4.3.8 Inosine monophosphate dehydrogenase, type 1 (*IMPDH1*) gene

The *IMPDH1* gene was identified as a candidate RP10 gene following comparative microarray analysis of wild-type and *Rho*$^{-/-}$ mouse retinas, as described in detail in Chapter 3. It was mapped within the RP10 candidate region on chromosome 7q31 a number of years ago (Gu *et al.*, 1994). Attempts were made previously to amplify the *IMPDH1* transcript from a retinal cDNA library, but it failed to amplify, and therefore prior to the microarray analysis results, it was not thought of as a likely candidate gene (McGuire, 1996b). The *IMPDH1* gene showed an average reduction in expression of –5.77-fold in the *Rho*$^{-/-}$ retina when compared to Wt according to microarray data. This down-regulation of expression was confirmed by quantitative PCR analysis as detailed in Chapter 3 (Table 3.1 and Fig. 3.4). While it is known that *IMPDH1* is expressed in many tissues of the body, this result nevertheless suggested that it may, within the retina, be preferentially expressed in photoreceptor cells as opposed to secondary retinal neurons. Thus, screening of the IMPDH1 gene in FA-84 individuals was undertaken.

4.3.8.1 Screening IMPDH1 in family FA-84

The *IMPDH1* gene consists of 17 exons, the first three of which are thought to be non-coding. The fourteen coding exons of *IMPDH1* span approximately 18kb of genomic sequence and encode a protein subunit of 514 amino acid residues (Fig. 4.16). Primers were designed in the genomic intronic sequence to amplify the 14 coding exons of *IMPDH1* (Appendix B.4). PCRs were carried out using DNA from three affected and three unaffected individuals from family FA84, and PCR products were subjected to DHPLC analysis. The resulting chromatogram patterns were inconclusive for some of the exons analysed (see DHPLC analysis below), and to ensure the entire gene was completely screened, all exons of *IMPDH1* were then screened in the family using automated sequence analysis. This revealed a CGC→CCC change within exon 7 of the gene (Fig. 4.17). The mutation was shown to segregate in all affected members of the family FA-84 by automated sequencing. The mutation was not detected in sequence

analysis of 100 chromosomes from non-related individuals of European origin, or in 50 Spanish chromosomes of unaffected, and married-in, members of family FA-84. The observed G to C base change is predicted to bring about an arginine to proline substitution at codon 224 of the IMPDH1 protein. It is of note that an arginine residue at codon 224 of the IMPDH1 protein is conserved in all four eukaryotic species for which sequence is available, human, mouse, drosophila and chinese hamster, suggesting that this amino acid is important in retaining the functionality of the IMPDH1 protein (Fig. 4.18). A second mutation which causes an Asp226Asn substitution in the protein sequence was identified in the American RP10 family, UTAD-045 (Bowne *et al.*, 2002). This amino acid is also very highly conserved amongst species. These data therefore provide strong evidence that mutations within the *IMPDH1* gene cause retinal degeneration in the RP10 form of retinitis pigmentosa.

4.3.8.2 DHPLC analysis of IMPDH1 exon 7

As mentioned previously, the PCR products of exon 7 of the *IMPDH1* gene were initially screened using DHPLC analysis. PCR products were run at the temperatures predicted by WAVEmaker software (Fig. 4.19), but resulted in a very similar chromatogram patterns being obtained for both affected and unaffected individuals following DHPLC analysis (Fig. 4.20A). While two different chromatogram patterns were originally detected following analysis at 64°C only, they did not appear to co-segregate with affected or unaffected individuals from family FA-84. Sequence analysis subsequently revealed a polymorphic C/G variant 60 base pairs upstream from the pathogenic G to C mutation in the exonic sequence (Fig. 4.21). This variant lies in the third "wobble" base of a glycine amino acid, and was detected in both affected and unaffected individuals at high frequency. It was discovered that the three affected individuals originally chosen for DHPLC analysis were homozygous for the consensus G at this position, while two of the unaffected individuals chosen were heterozygous for the C/G variant.

The PCR reactions were repeated using DNA from family FA-84, primers specific for amplification of *IMPDH1* exon 7 and *Pfu* Taq polymerase. The individuals carefully chosen for DHPLC analysis on this occasion included two affected and two unaffected individuals, with one of each displaying heterozygosity for the polymorphic G/C variant. On this occasion, four different chromatogram patterns were detected, but only a slight alteration was detected between the pattern obtained for an affected

individual segregating the Arg224 mutation only, and that for an unaffected individual segregating the C/G variant polymorphism only (Fig. 4.20B). For future screening of IMPDH1 exon 7 in RP individuals using DHPLC analysis, the presence of this polymorphic variant 60 bp upstream from a possible pathogenic mutation could make results very difficult to interpret. For this reason, automated sequence analysis of this particular gene in a screen of RP patients may prove to be considerably more reliable.

Table 4.2. RP10 candidate genes screened using DHPLC. The number of exons examined, size of PCR products and separation temperatures chosen are shown. (All primer sequences are listed in Appendix B.4).

Gene Name	Exon Number	PCR Product Size (bp)	DHPLC Analysis temperatures (°C)
GRIP-Domain gene	1.1	553	59, 61, 63
	1.2	621	60, 62, 64, 66
	1.3	569	58, 60, 62
	2.1	647	55, 59, 61, 63
	2.2	704	59, 61, 63
Cyclophilin-like gene	1	542	56, 58, 63
AF218032	2	331	56, 61, 63
	3	253	53, 57, 56
	4	450	52, 54, 56
	5.2	530	55, 57
	5.3	630	55, 57, 59
Blue Cone Pigment	1	513	58, 60, 62
(OPN1SW)	2	311	60, 63
	3	305	62, 64
	4	381	58, 60, 62, 64
	5	293	57, 59, 61
IMPDH1	1	434	nd
	2	205	62, 64
	3 + 4	464	63, 65
	5 + 6	596	60, 62, 64
	7	348	60, 62, 64
	8 + 9	577	61, 63, 65
	10 + 11	596	63, 65
	12 + 13	491	63, 65
	14	223	62, 64, 66

4.4 DISCUSSION

A locus for an autosomal dominant form of RP, RP10, was originally established in 1993 on chromosome 7q31, in a large Spanish family referred to as FA-84. Since then, a number of different approaches have been used in attempts to identify the disease-associated gene. The current study involved detailed analysis of the RP10 disease interval using a number of bioinformatic-based resources and molecular biological techniques, which led to the screening of a number of potential candidate genes. In total the screening and exclusion of four separate genes for disease-causing mutations was undertaken, prior to the analysis of *IMPDH1*. The *IMPDH1* gene was screened following a comparative microarray analysis of wild-type and *Rho*$^{-/-}$ mouse retinas. Results from this study showed that there was a 6-fold higher level of *IMPDH1* transcript in wild-type retinas when compared to *Rho*$^{-/-}$ retinas, in which the photoreceptor cell layer is completely absent. This suggested that *IMPDH1* was expressed at higher levels in the photoreceptor cell layer of the retina and so screening of this gene in family FA-84 was undertaken.

A pathogenic mutation was identified that brings about an Arg224Pro substitution in exon 7 of the *IMPDH1* gene, and was shown to segregate in affected family members of FA-84 only. This mutation was not detected in 75 control individuals and the sequence was conserved amongst species. A second mutation at position Asn226 in the sequence was also identified in a second American RP10 family, UTAD-045, providing strong evidence that mutations within the *IMPDH1* gene cause the RP10 form of retinitis pigmentosa (Bowne et al., 2002). Mutations within the IMPDH1 gene are predicted to account for up to 5% of all autosomal dominant RP (Daiger *et al.*, 2003).

The IMPDH1 protein consists of 514 amino acid residues, with the active IMPDH1 enzyme consisting of a homotetramer of these subunits (E.C Number 1.1.1.205) (Carr *et al.*, 1993). IMPDH1 catalyses the conversion of inosine monophosphate (IMP) to xanthosine monophosphate (XMP) with the concomitant reduction of NAD to NADH, which is the rate limiting step in guanine nucleotide biosynthesis. XMP is subsequently converted to GMP which gives rise to one of the building blocks of DNA (dGTP), a molecule that also plays an essential role in

intracellular signalling pathways. *IMPDH1* is the first gene that functions in the guanine nucleotide biosynthesis pathway to be associated with retinal disease.

A number of genes which show widespread expression patterns have been iimplicated in RP in recent years, including the three pre-mRNA splicing factor genes, which also cause autosomal dominant RP when mutated. The disease mechanisms that cause degeneration of photoreceptor cells in these forms of RP have not yet been established. Three major RNA transcripts for *IMPDH1*, which are differentially expressed from three alternative promoters have been identified, suggesting that *IMPDH1* expression may be regulated in a complex cell type-specific manner (Gu *et al.*, 1997; Zimmerman *et al.*, 1996). The mutation identified within IMPDH1 in this study results in the synthesis of a protein that produces clinically recognisable disease only in retinal tissues. Photoreceptor cells are amongst the most physiologically active of any cell type in the human body and guanine nucleotides are fundamentally important in signal transduction mechanisms (La Cour, 2002). Microarray analysis has previously revealed that *IMPDH1* is expressed at a higher level in photoreceptors than other retinal cell types in the mouse. This higher level of expression, together with the high GTP usage of photoreceptors, may go towards explaining the tissue specific nature of this disease. However, as this gene is expressed in many cell types of the body, this alone may not fully explain the absence of symptoms from other tissues. Alternative transcript processing is unlikely to be a contributing factor since analysis of ESTs derived from *IMPDH1* indicates that exon 7 of the gene is expressed in many tissues including heart, brain, skin and kidney (http://www4.ncbi.nlm.nih.gov/UniGene/).

A complete study of IMPDH1 function and structure is presented in Chapter 5. Included is a functional analysis of mutant IMPDH1 protein and a discussion on possible disease mechanisms brought about by mutations within the *IMPDH1* gene in retinitis pigmentosa patients.

4.5 CONCLUSION

This study has resulted in the identification of a mutation within the *IMPDH1* gene on chromosome 7q, that causes the degeneration of photoreceptor neurons in the RP10 form of retinitis pigmentosa. The *IMPDH1* gene is the first member of the guanine nucleotide biosynthesis pathway to be associated with retinal disease. *IMPDH1* can be included in a group of recently-identified genes, that show widespread expression in many tissues of the body, but cause disease only in retinal tissues when mutated. Future research will focus on the elucidation of the pathways of degeneration brought about by mutations in such genes.

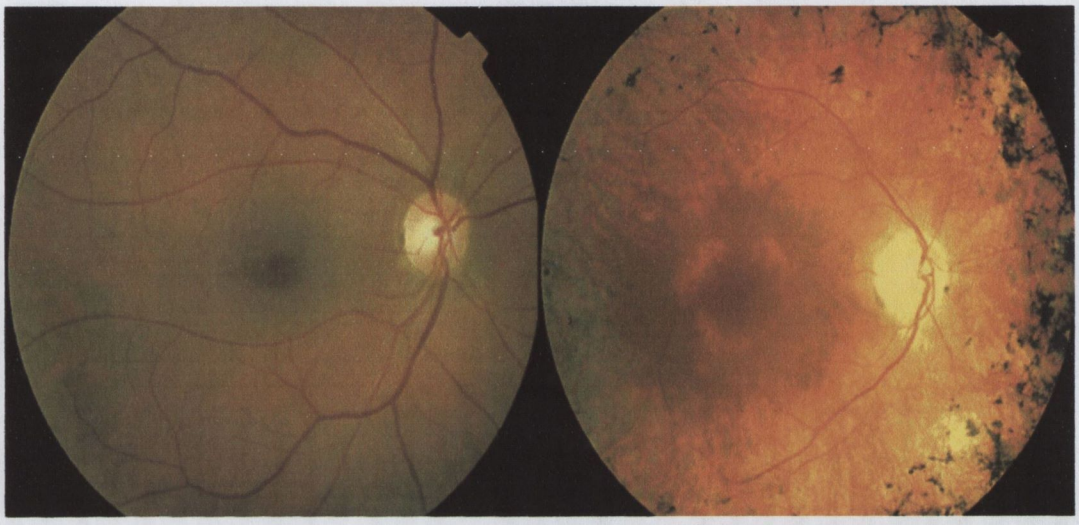

Figure 4.1. Fundus photography of a normal (left) and RP retina (right).

Features typical of RP, such as marked pigment epithelial thinning, optic disc pallor, retinal vascular attenuation and the classical 'bone spicule' intraretinal pigmentary deposits are clearly evident in the RP retina.

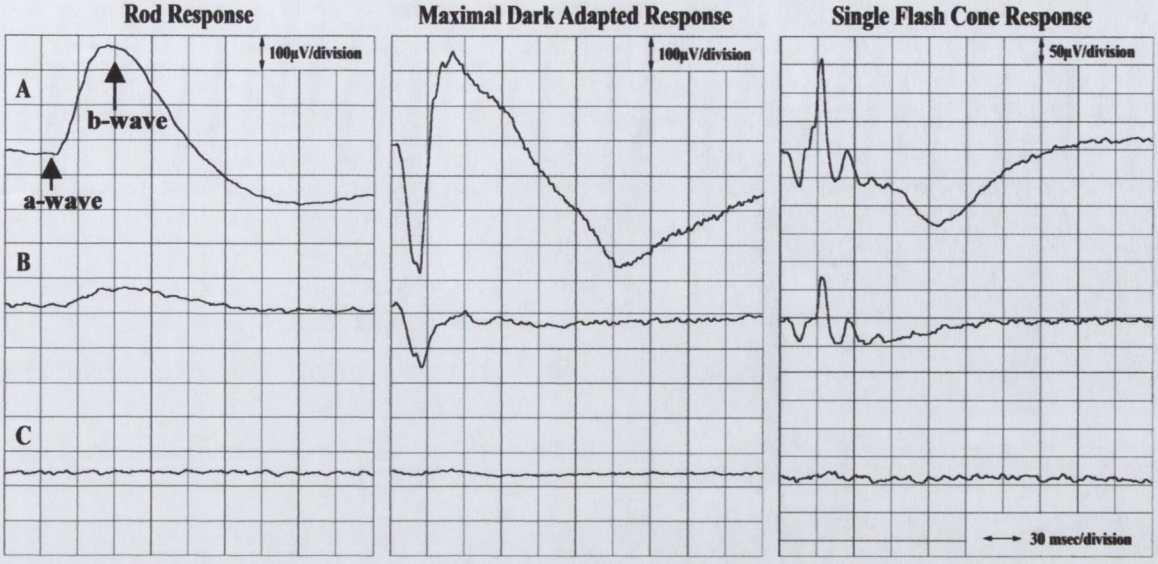

Figure 4.2. ERG analysis of normal and RP retinas.

Rod-isolated (scotopic), combined rod and cone responses to the maximal intensity flash in the dark-adapted state and single flash light-adapted cone (photopic) ERG responses are shown in; (**A**) a normal individual, (**B**) a patient with moderately advance RP and (**C**) a patient with advanced RP. The a-wave and b-waves are shown.

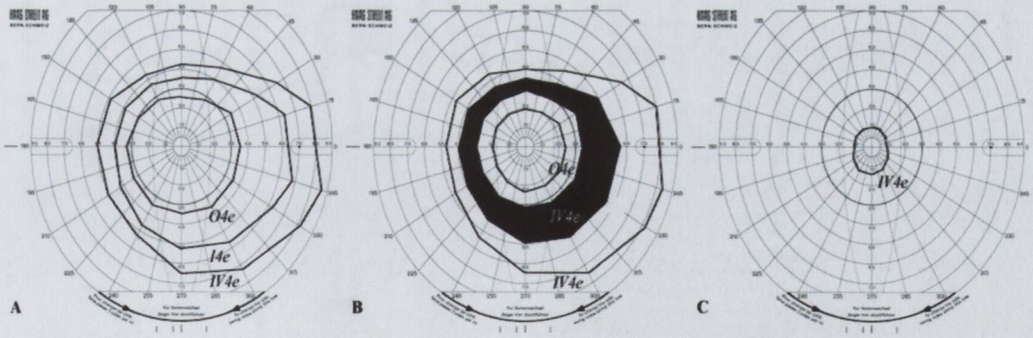

Figure 4.3. Visual field testing in normal and RP patients.

Visual field testing showing three field measurements in (**A**) a normal individual, (**B**) a patient with moderately advanced RP showing a mid-peripheral ring scotoma (black area) and narrowing of visual field and (**C**) a patient with advanced RP, showing constricted visual fields and resulting tunnel vision.

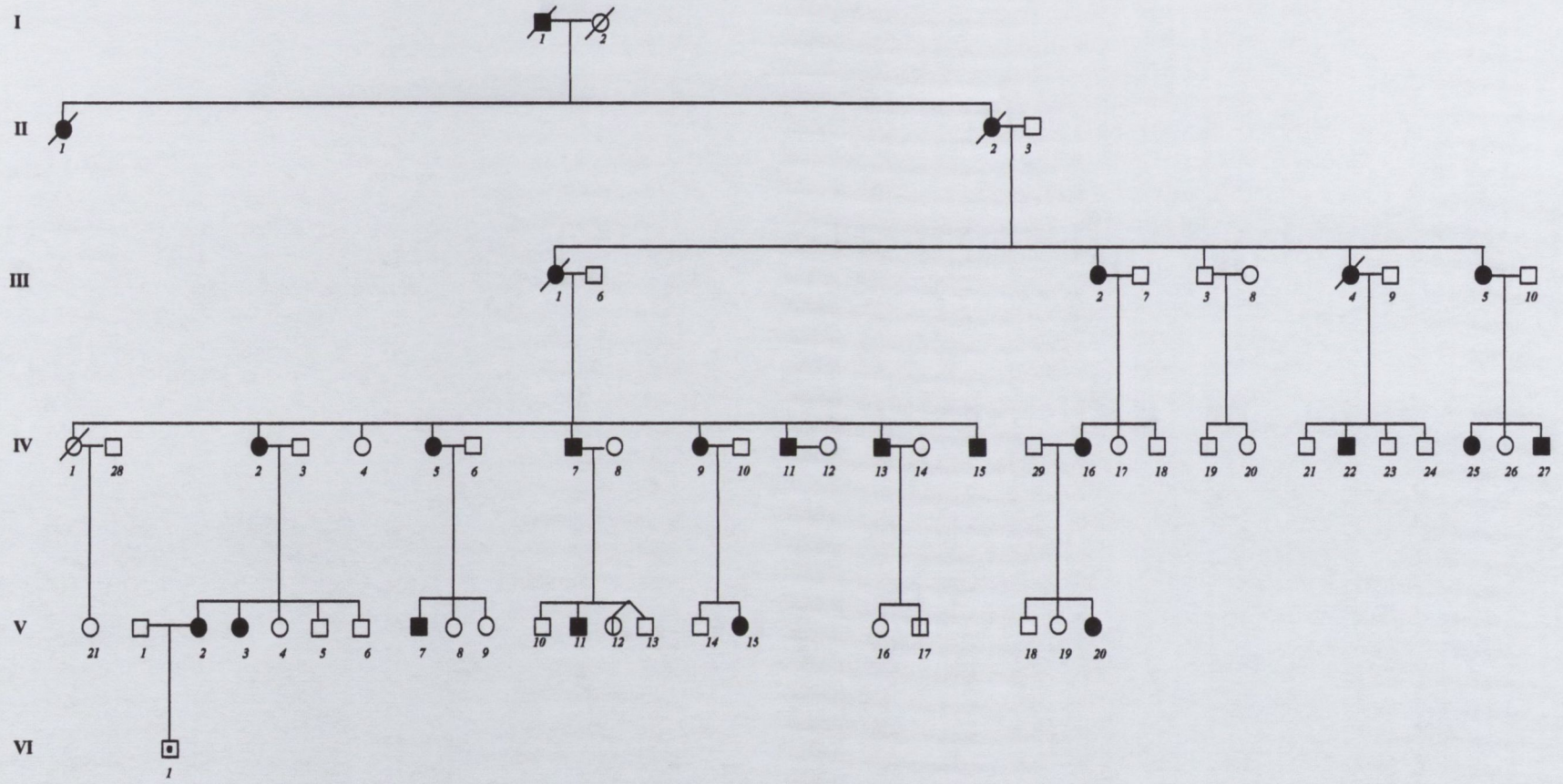

Figure 4.4. Pedigree for the adRP family FA-84. The original RP10 linkage was established in this large Spanish kindred. Individuals whose diagnosis status is uncertain are denoted by a vertical line in the middle of a square or circle.

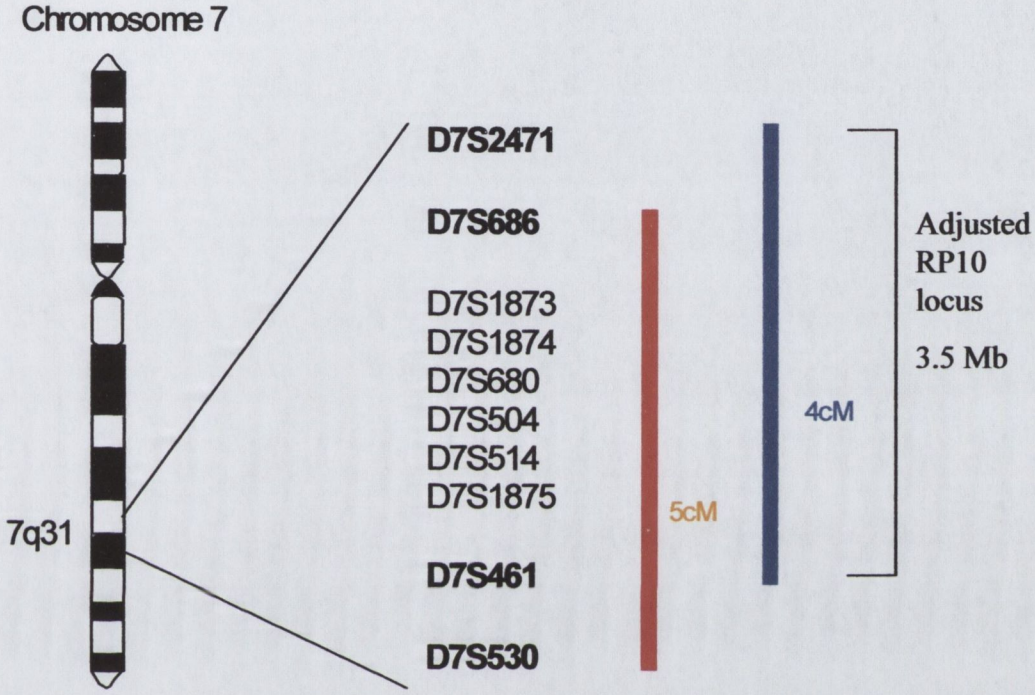

Figure 4.5. Schematic illustration of the RP10 region on chromosome 7q31 before (red) and after (blue) re-typing of markers and haplotype analysis. The order of a number of microsatellite markers in the region is shown. The adjusted region was estimated to span 3.5 million bases of DNA sequence.

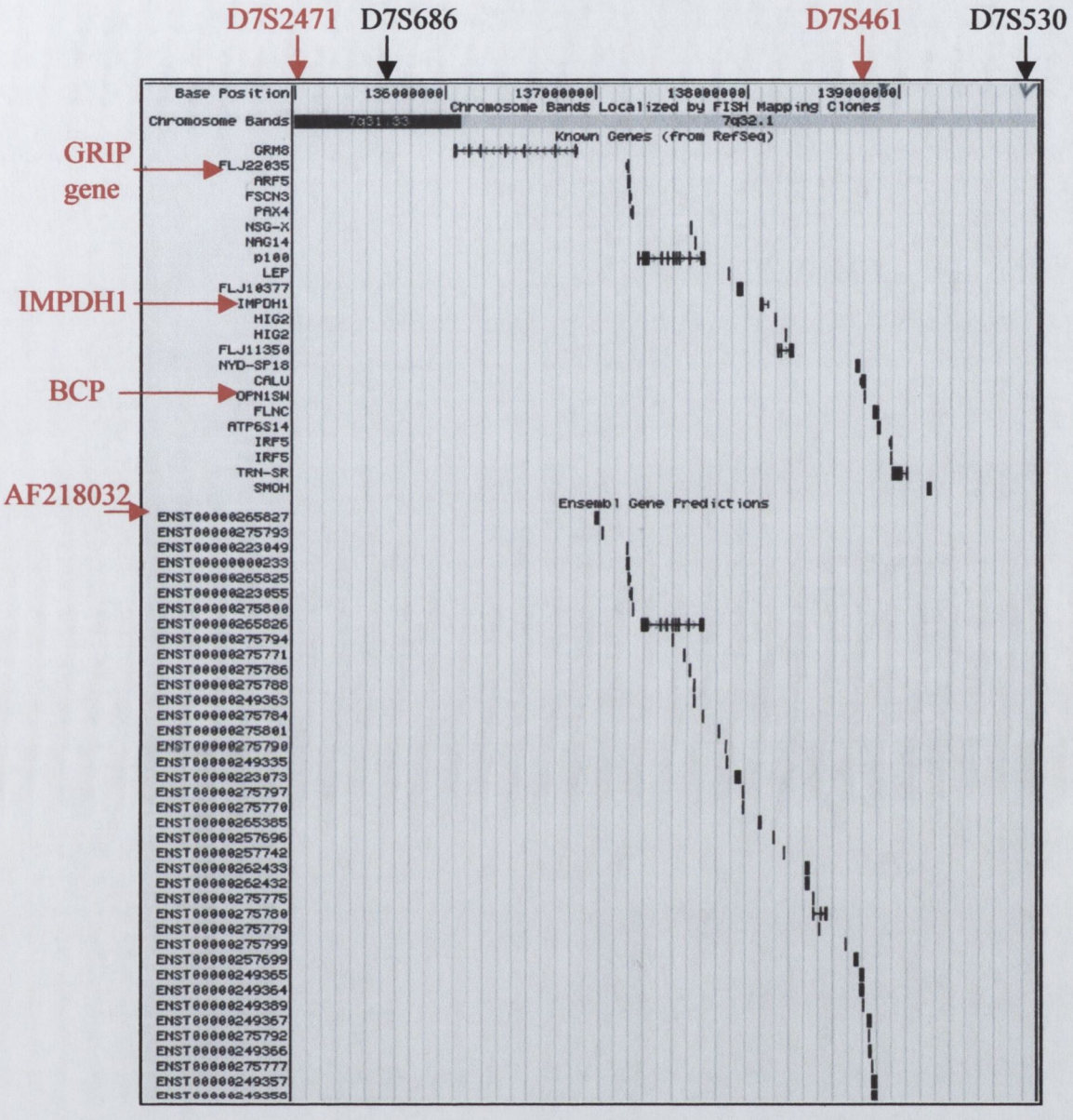

Figure 4.6. The RP10 locus on chromosome 7q31-32 as viewed using the UCSC Human Genome Browser (http://genome.ucsc.edu), October 2001 release. All the known genes and a number of the *Ensembl* predicted genes which mapped to the the RP10 region are shown in the genome map. The location of the significant flanking microsatellite markers are shown along the top of the genome map. The location of genes screened in this study are shown, and include a GRIP-domain gene (FLJ22835), IMPDH1, blue cone pigment (OPN1SW) and the predicted zinc-finger gene AF218032. Genes screened in previous studies include GRM8 and ARF5.

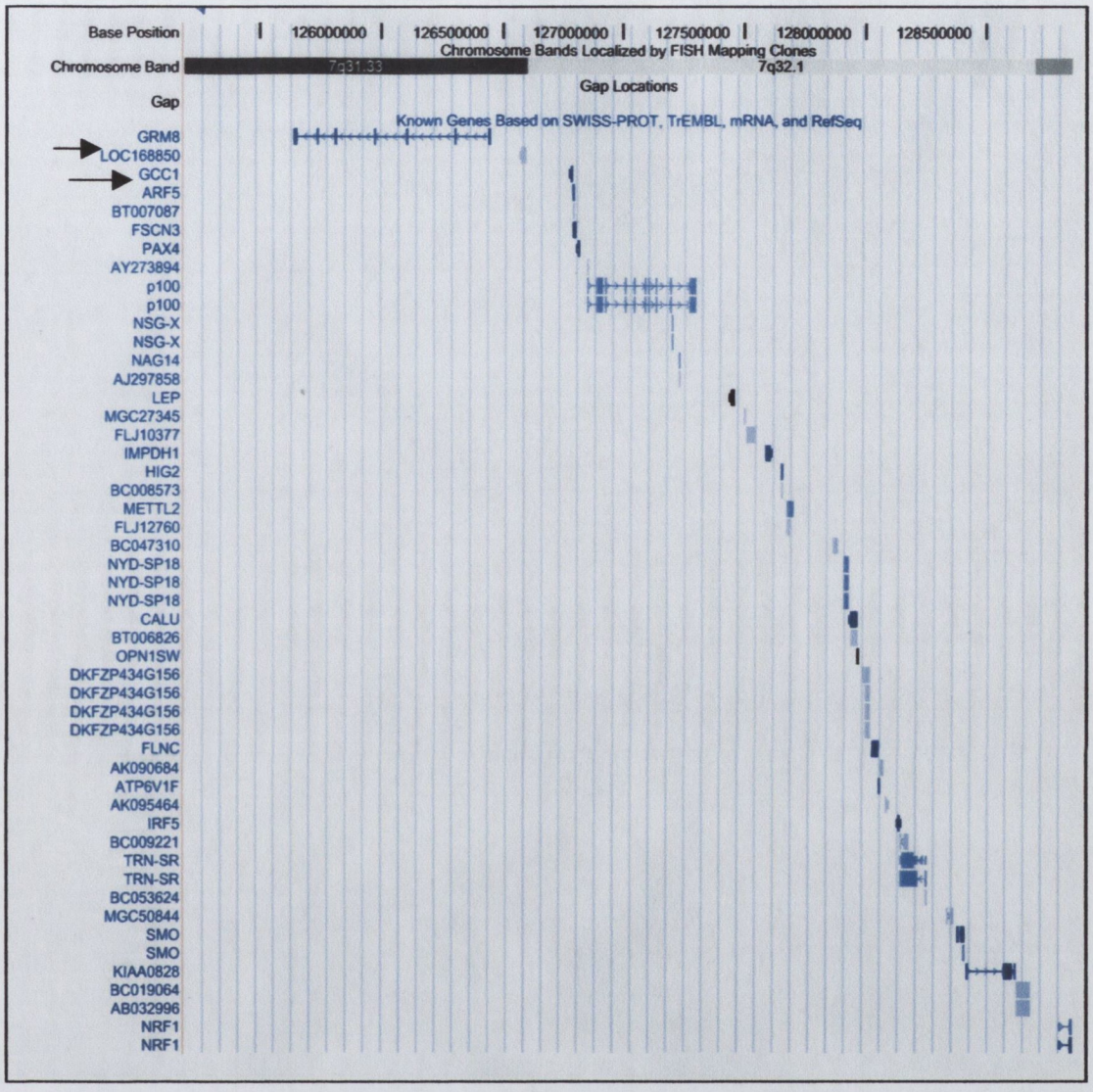

Figure 4.7. The RP10 region as viewed using the Human Genome Browser July 2003 release (http://genome.ucsc.edu/cgi-bin/hgGateway), showing all the known genes in the region. A number of previously predicted genes have been 'confirmed' in the past two years and there are no longer any gaps in this region of the genome sequence. The location of genes screened which were previously predicted but have now been confirmed are shown by the arrows. They correspond to the GRIP-domain gene (GCC1) and Zinc-finger domain gene (AF218032), now called LOC168850, which is still classed as a hypothetical protein according to this database.

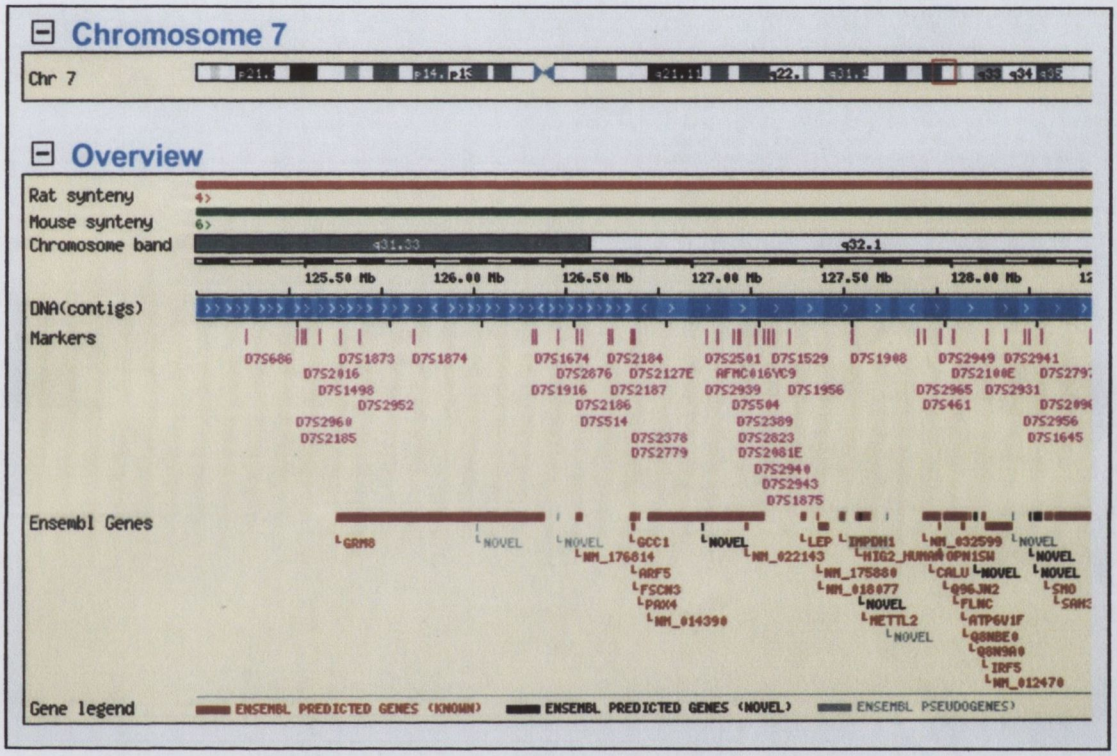

Figure 4.8. A view of the RP10 locus using the Ensembl Genome Browser as accessed in October 2003 (www.ensembl.org). The chromosomal location of a number of markers, including the RP10 flanking markers D7S686 and D7S461 are shown. Confirmed genes are denoted in red, and predicted or novel genes in black.

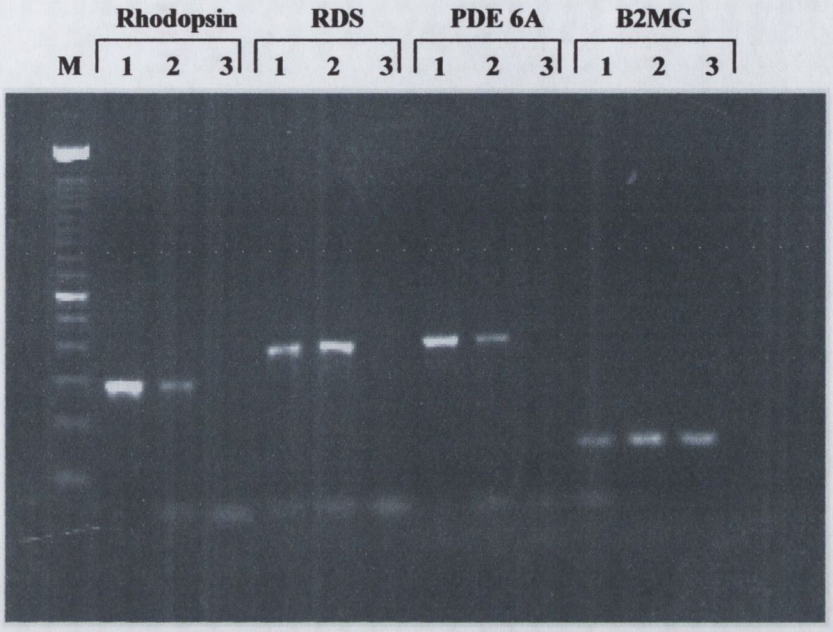

Figure 4.9. RT-PCR on RNA extracted from Wild-type (WT) and *Rho*$^{-/-}$ mouse retinas. Primers used were specific for amplification of the photoreceptor-specific transcripts rhodopsin, peripherin-RDS and phosphodiesterase (PDE6A). A fourth set of primers was used to amplify a house-keeping gene beta2-microglobulin (B2MG). Lane M, 100bp DNA ladder; lane 1, RNA from a 4-month old WT retina; lane 2, RNA from a 1-month old *Rho*$^{-/-}$ retina; lane 3, RNA from a 4-month old *Rho*$^{-/-}$ retina. There was no detection of rhodopsin, rds-peripherin or PDE transcripts in the 4-month old *Rho-/-* retinas. A redundent rhodopsin transcript is sometimes detected in one-mpnth old *Rho*$^{-/-}$ retinal RNA, even though this mouse does not have any functional rhodopsin.

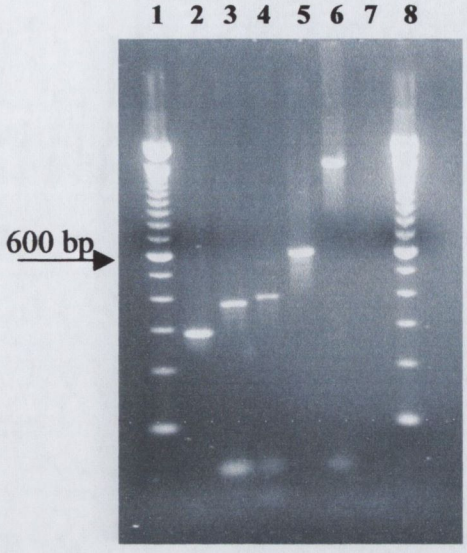

Figure 4.11. PCR analysis of a human retinal cDNA library to detect expression of a candidate GRIP-domain gene. Lanes 1& 8, 2kb marker; lanes 2-5, amplification of human retinal cDNA library with primers specific for amplification of; lane 2, rhodopsin; lane 3, RDS-peripherin; lane 4, PDE6A; lane 5, GRIP-domain candidate gene cDNA; lane 6, human DNA amplified with GRIP-domain candidate gene cDNA primers; lane 7, negative control.

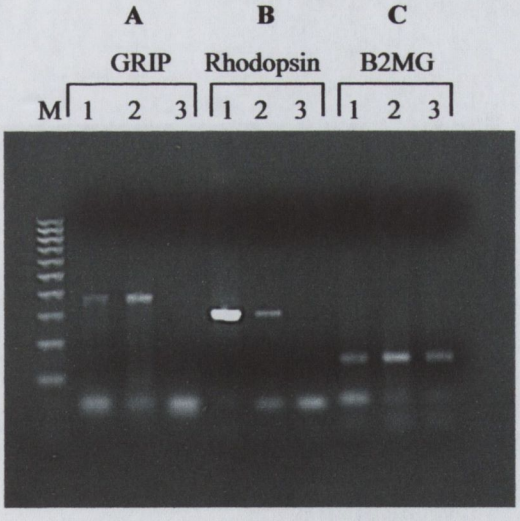

Figure 4.12. RT-PCR analysis on RNA extracted from wild-type (WT) and *Rho*$^{-/-}$ mouse retinas. Primer sequences were specific for amplification of (**A**) the mouse homolog of a GRIP-domain gene, (**B**) rhodopsin and (**C**) B2MG. Lane M, 100bp marker; lane 1, RNA from a 4-month old WT retina; lane 2, RNA from a 1-month old *Rho*$^{-/-}$ retina; lane 3, RNA from a 4-month old *Rho*$^{-/-}$ retina.

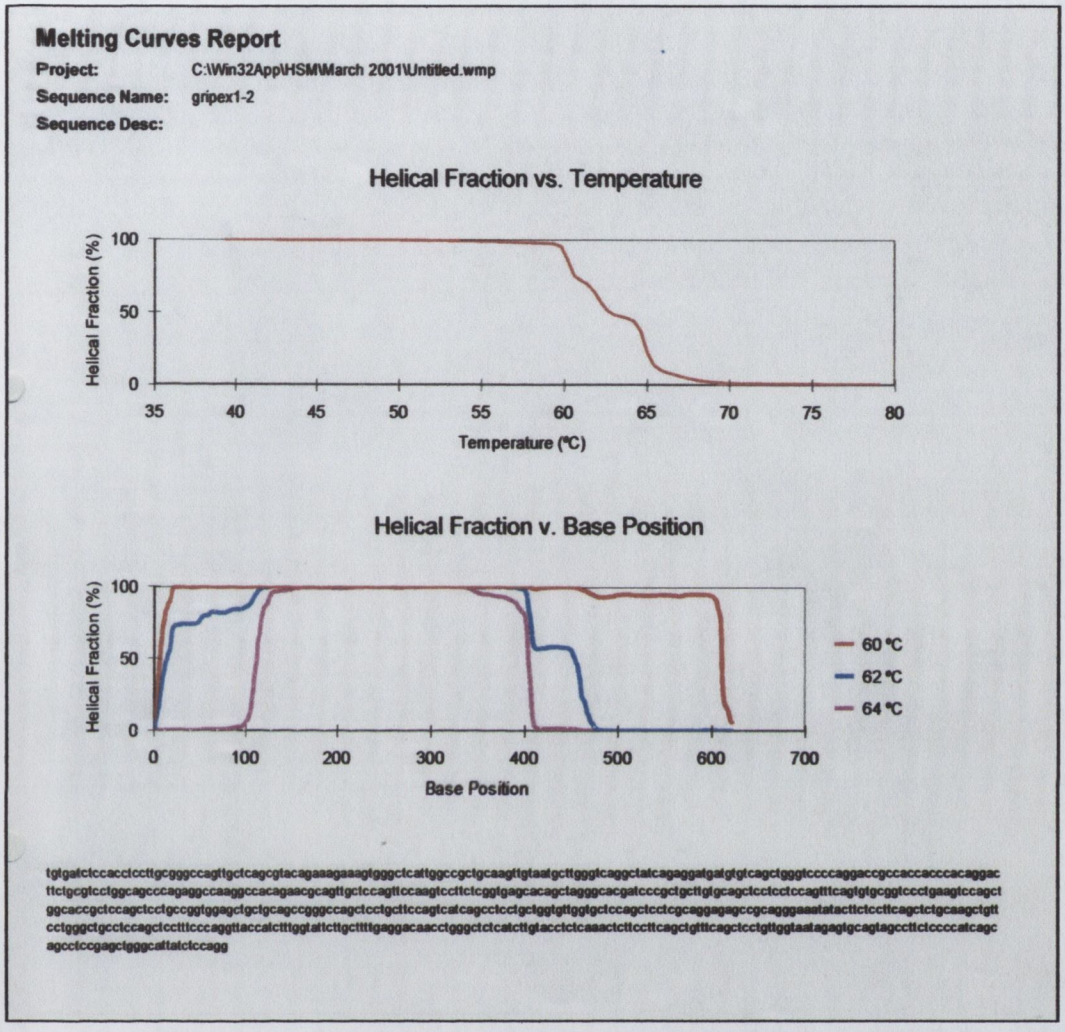

Figure 4.13. Melting curve report for the GRIP-domain gene exon 1-2. The DNA sequence was analysed using WAVEmaker software, and separation temperature predictions were based on the specific DNA sequence shown. Separation temperatures chosen for analysis were 60, 62, 64 and 66 °C. (Melting curve for analysis at 66°C which detects sequence from 150-350 bp not shown).

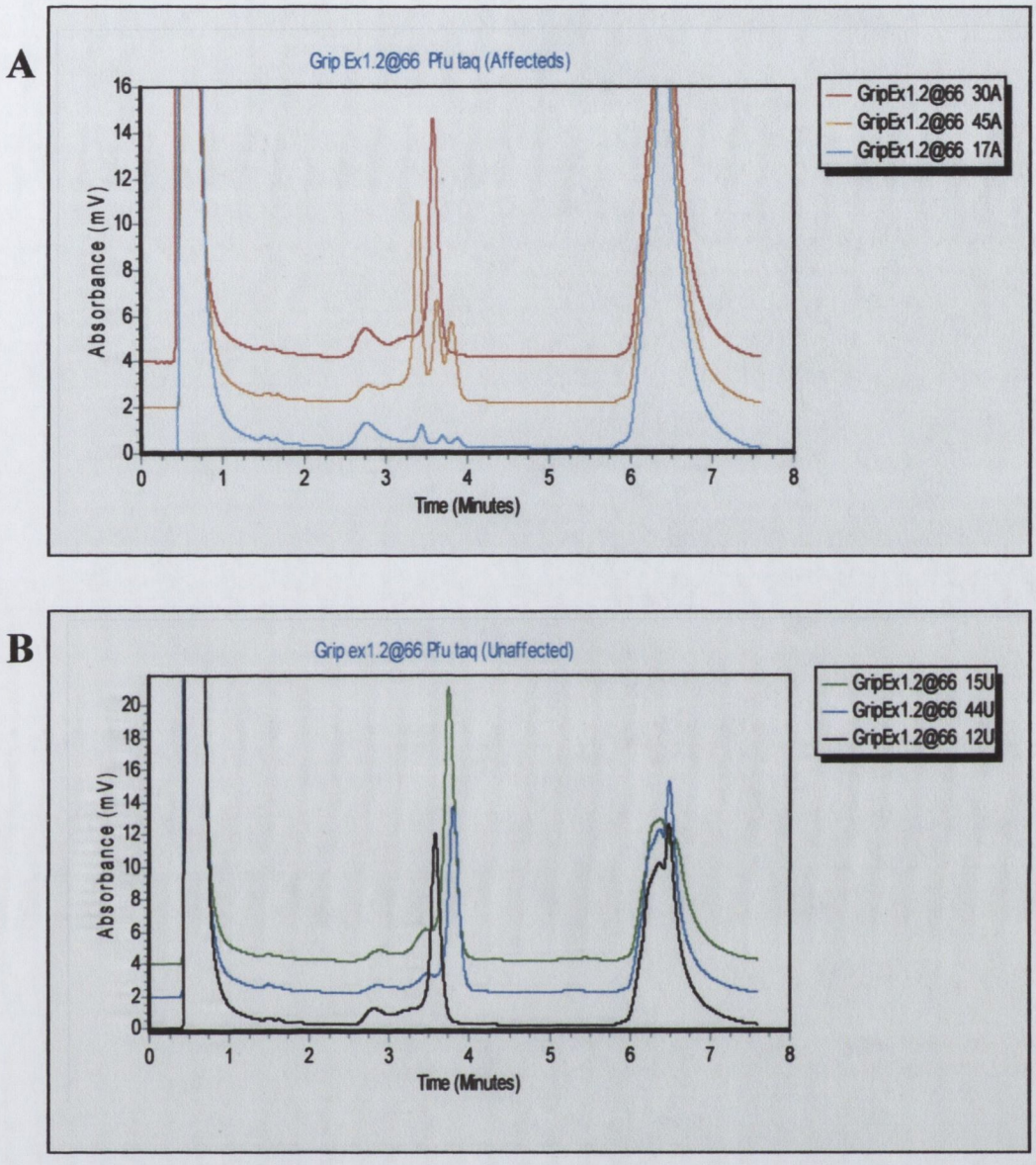

Figure 4.14. DHPLC analysis of exon 1-2 of a candidate GRIP-domain gene.

The chromatograms obtained following DHPLC analysis of exon 1-2 of the GRIP-domain gene are shown, which were analysed at 66°C. Chromatograms shown are from **(A)** 3 affected members and **(B)** 3 unaffected members of family FA-84.

Three different chromatogram patterns were detected using this method. Affected individuals 45A and 17A displayed identical chromatograms as did unaffected individuals 15U and 44U. All PCR products were subsequently analysed using automated sequencing.

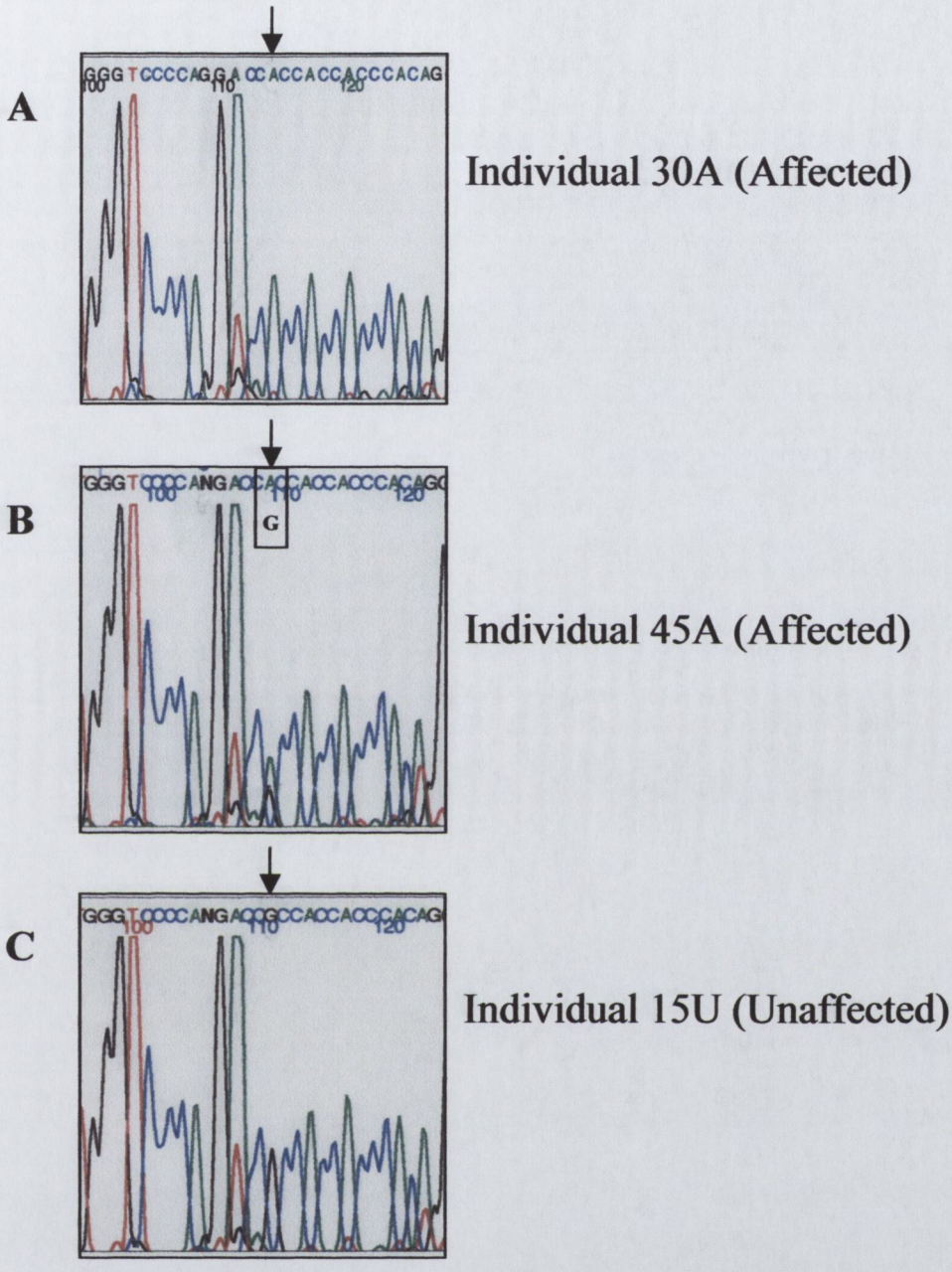

Figure 4.15. Automated sequence analysis of exon 1-2 of the GRIP-domain gene in DNA from members of family FA-84. **(A)** Affected individual 30A possesses an A variant, **(B)** affected individual 45A is heterozygous for A/G at this position and **(C)** the unaffected individual 15U possesses the consensus G nucleotide. This base pair substitution does not result in an amino acid substitution however, so was not found to represent the disease-causing mutation in this family.

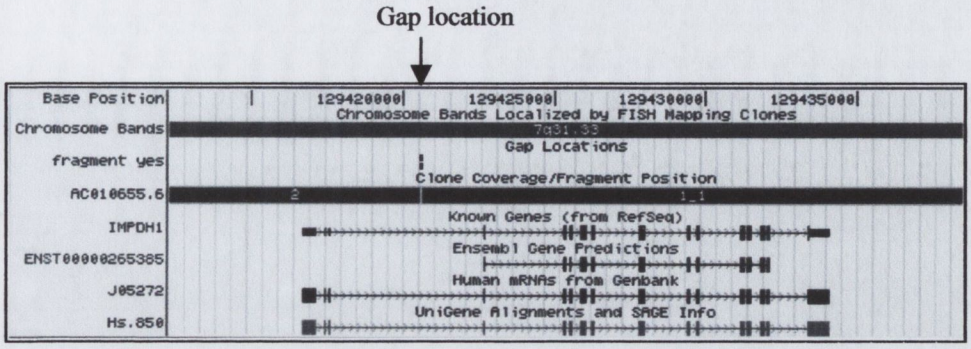

Figure 4.16. Schematic representation of the *IMPDH1* gene exon structure adapted from the Human Genome Browser September 2001 release (www.genome.ucsc.edu). The gene consists of seventeen exons, the first three of which are non-coding. The first coding exon is not represented because of a gap in the original sequence of clone AC010655, but this clone has since been sequenced in full.

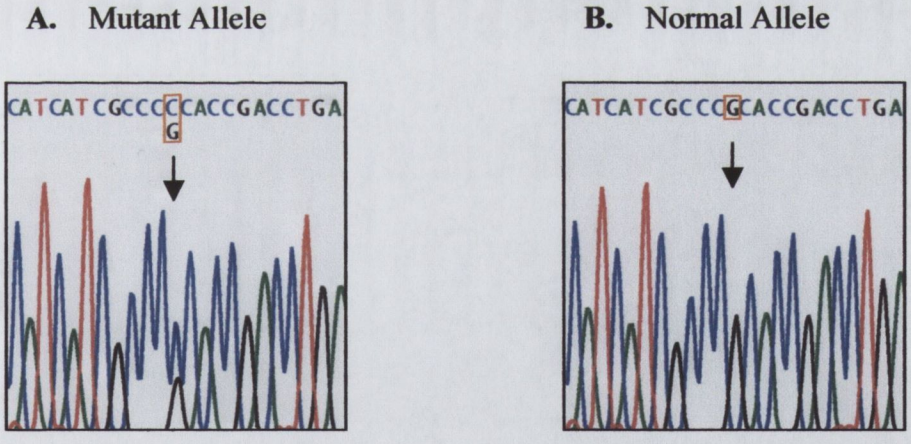

Figure 4.17. Automated sequence analysis of exon 7 of the *IMPDH1* gene.

(A) Affected member of family FA-84 showing a heterozygous C to G nucleotide substitution at Arg224. **(B)** Unaffected member of family FA-84 showing the consensus G nucleotide.

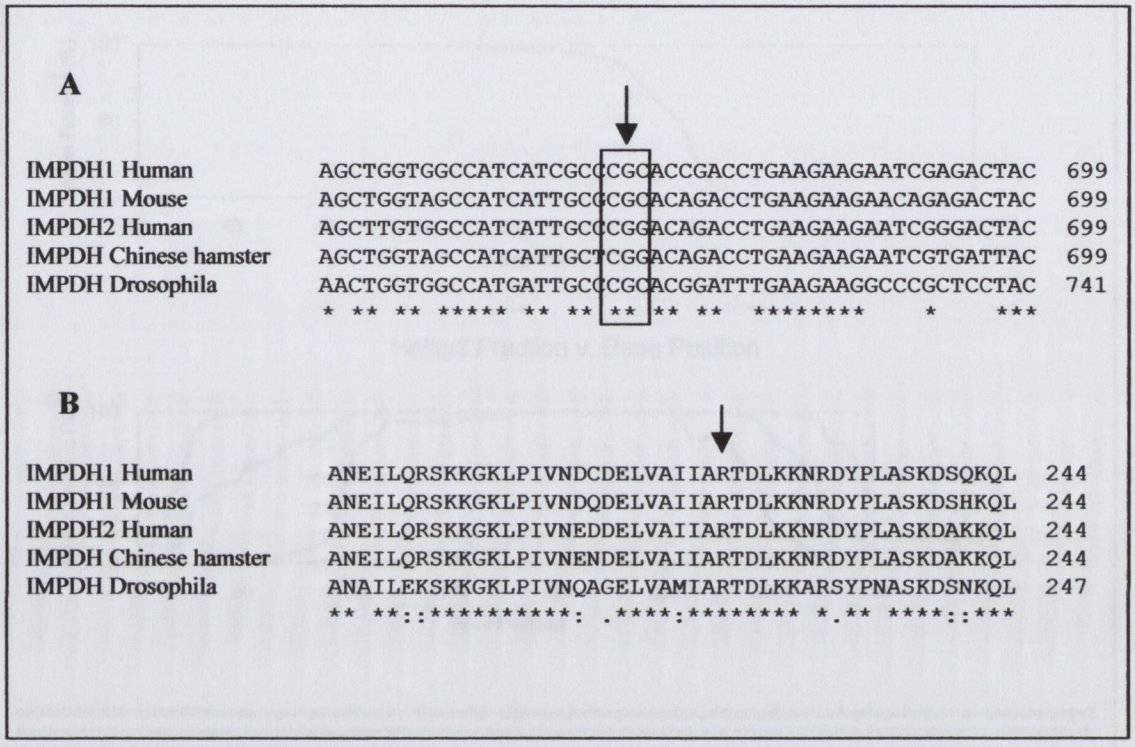

Figure 4.18. Clustalw alignment showing partial (**A**) nucleotide and (**B**) protein sequences of IMPDH from different species. The Arg224 codon (R) is conserved in all aligned sequences as indicated by the arrows.

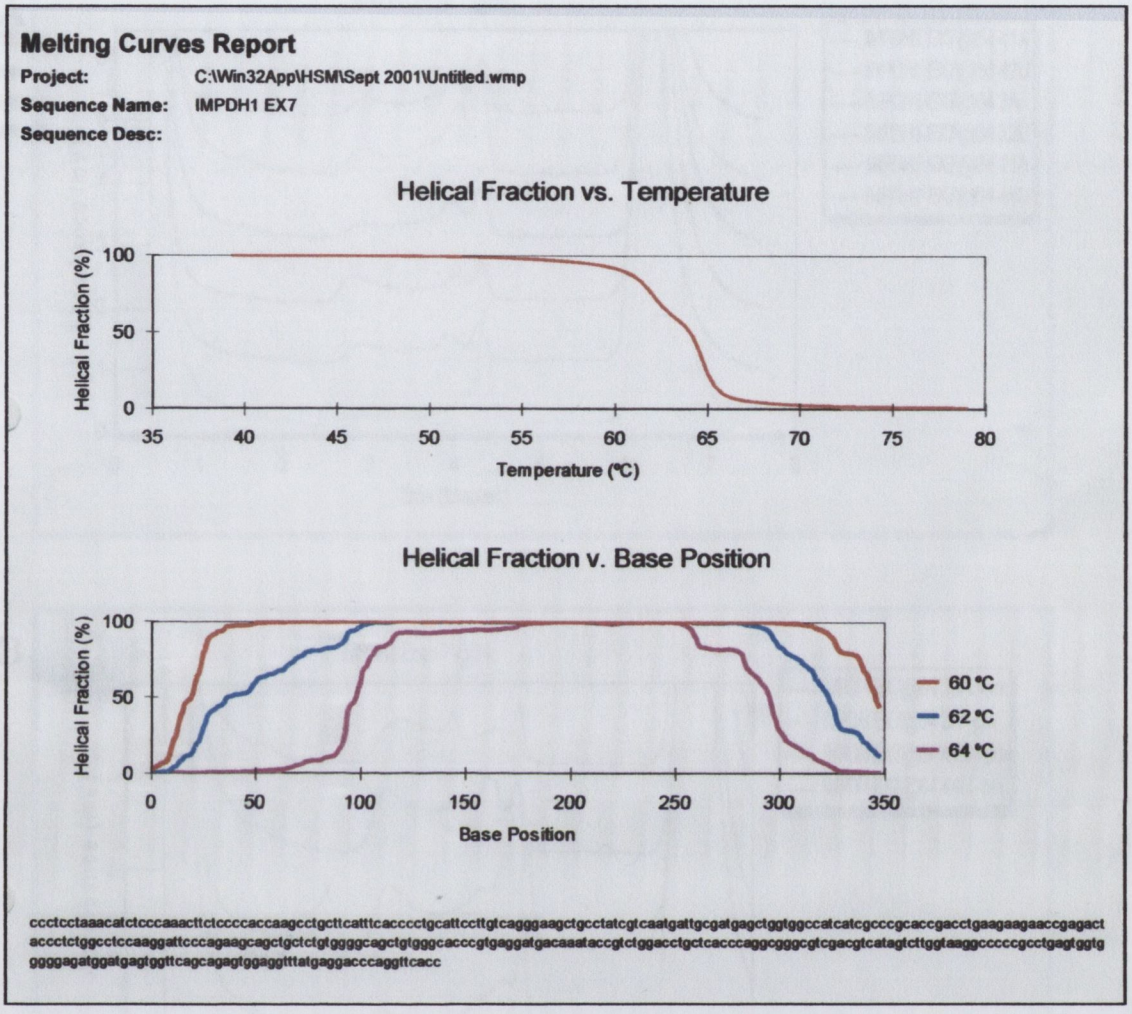

Figure 4.19. Melting curve predicted by WAVEmaker software for IMPDH1 exon 7 sequence. The CGC to CCC pathogenic mutation detected resides at position 120 in the sequence shown, while a polymorphic G/C variant is found at position 181. PCR products were analysed at 60, 62 and 64 degrees celsius.

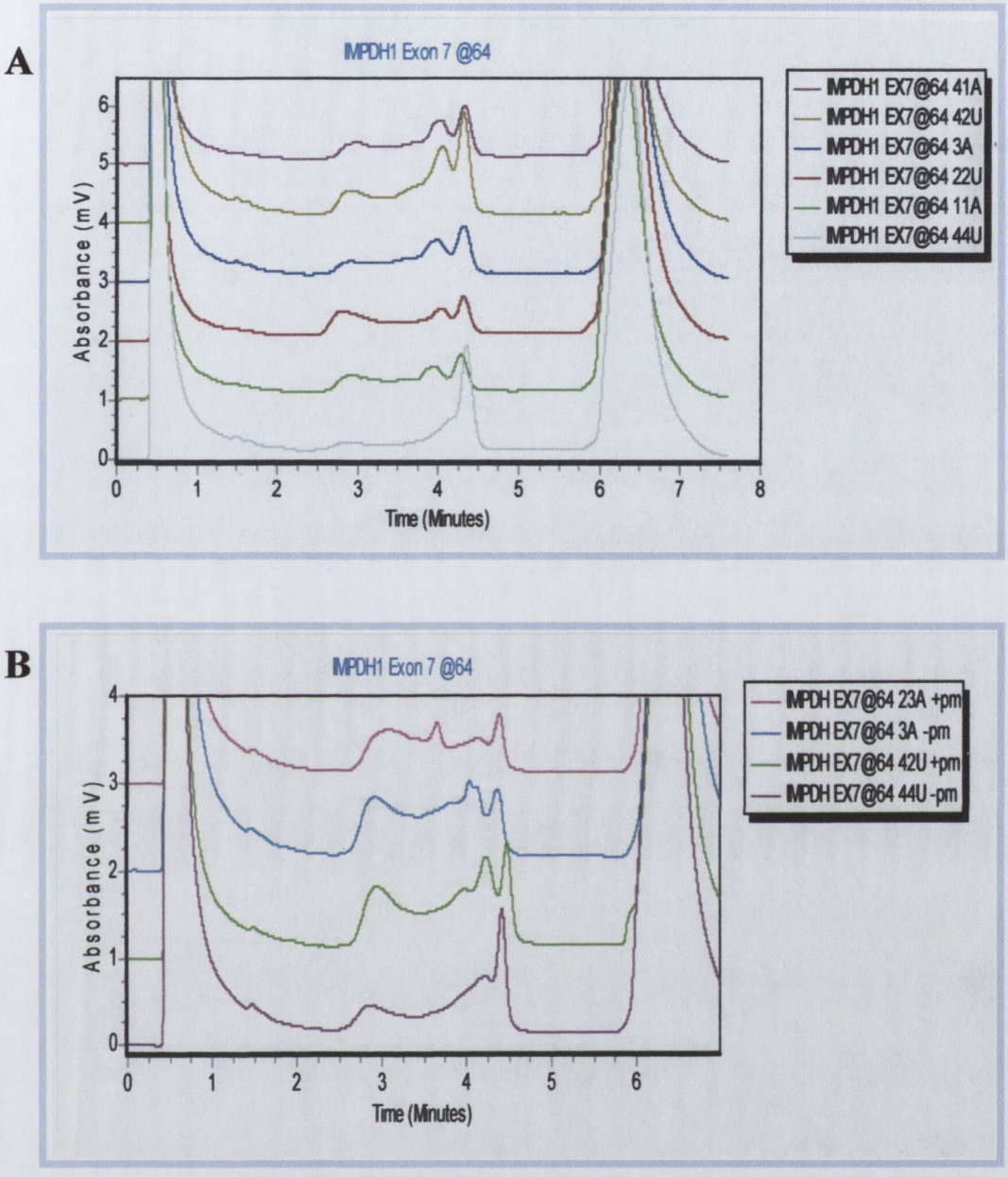

Figure 4.20. DHPLC analysis of IMPDH1 exon 7 PCR products from Family FA-84.

(**A**) Initial DHPLC analysis in affected (41A, 3A and 11A) and unaffected (42U, 22U and 44U) individuals. A pathogenic CGC to CCC mutation at Arg224 was subsequently identified in affected individuals. (**B**) Repeat of DHPLC analysis in DNA from; individual 23A who harbours the pathogenic mutation and is heterozygous for a C/G polymorphic variant 60 bp upsteam in the coding sequence, individual 3A harbours the pathogenic mutation only, individual 42U does not harbour the mutation but is heterozygous for the C/G polymorphic variant, and individual 44U harbours neither the mutation nor the heterozygous polymorphic variant.

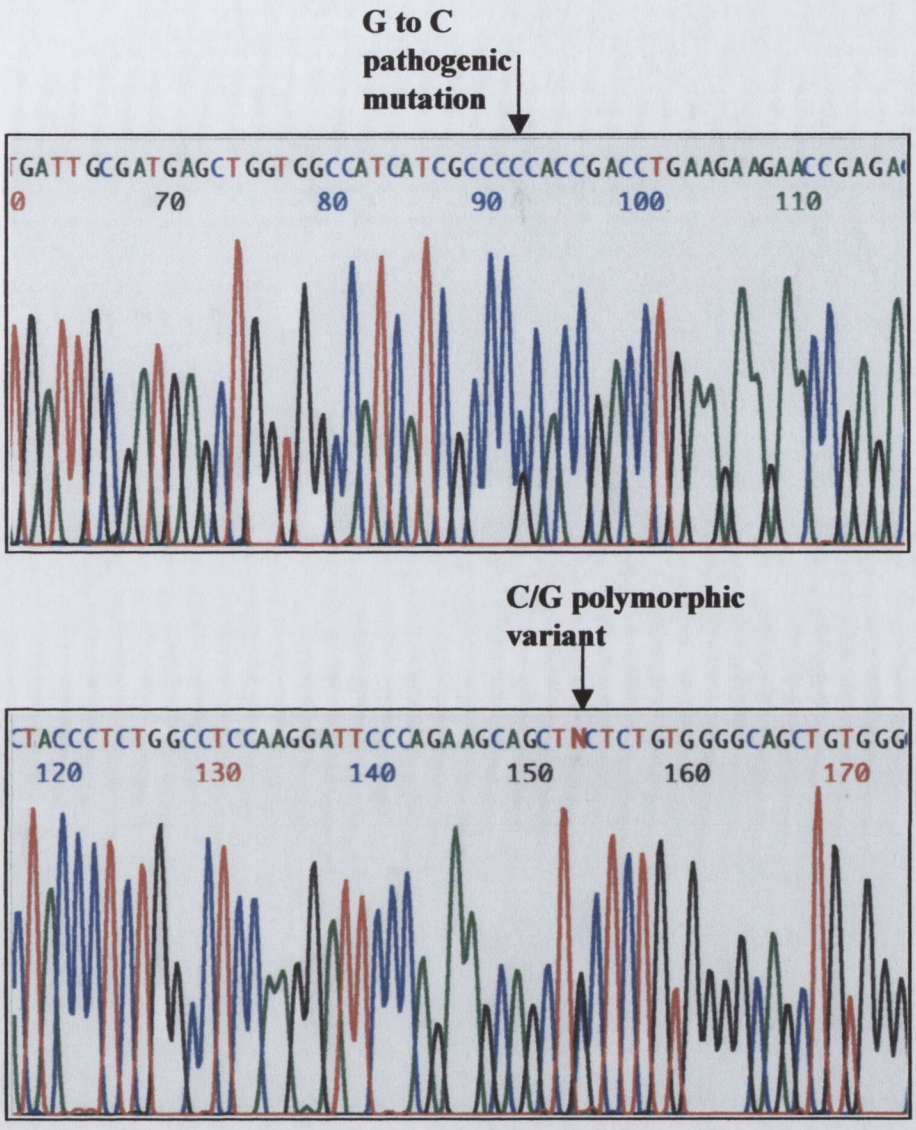

Figure 4.21. Automated sequence analysis of IMPDH1 exon 7 from an affected FA-84 family member (Individual 23A, Fig. 4.20). The pathogenic G to C mutation at codon 224 is shown. This individual is also heterozygous for a G/C polymorphic variant 60 base pairs upstream.

CHAPTER 5

MOLECULAR MECHANISMS IN IMPDH1-BASED RETINITIS PIGMENTOSA

5.1 INTRODUCTION

5.1.1 Introduction

The previous chapter has described the discovery of a novel autosomal dominant RP gene, *IMPDH1*, in a large Spanish kindred. Mutations within *IMPDH1* cause the RP10 form of retinitis pigmentosa, which is a devastating, early onset, degenerative retinopathy. The disease mechanism caused by *IMPDH1* mutations was completely unknown, because it was the first gene in the guanine nucleotide biosynthesis pathway to be implicated in retinal disease. While it not difficult to imagine why mutations in photoreceptor-specific genes such as rhodopsin or peripherin-rds cause disease in the retina specifically, it is considerably harder to predict why a defect in a widely-expressed gene such as a splicing factor gene or *IMPDH1* causes the death of photoreceptor cells only. A number of possible avenues of investigation can be explored, and often involve the use of cell-culture systems and model organisms. The generation of gene-targeted or transgenic mice is an especially valuable tool in an investigation into the role of a novel gene or protein within the retina.

The possible disease mechanisms initially proposed for this form of RP included perturbation of enzymatic activity, aberrant protein folding or interference to normal interactions with another unidentified protein. The main aim of this study was to determine whether pathogenic mutations in *IMPDH1* have an effect on enzyme activity and/or protein solubility or folding. A background in the pathogenic mutations identified to date within the *IMPDH1* gene is provided, along with functional and structural features of the native IMPDH1 protein. Results from studies on wild-type and mutant IMPDH1 enzyme activity, and expression of protein in bacterial and mammalian cells are detailed, along with observations on retinal function and histology in the *Impdh1*$^{-/-}$ mouse. The detection of a difference in solubility between wild-type and mutant IMPDH1 proteins is described, which suggests abnormal protein folding and aggregate formation are a feature of mutant proteins. Finally, a disease mechanism for this form of RP is proposed with a discussion on possible therapies that could be employed for attenuation of disease symptoms.

5.1.2 IMPDH1 mutations identified in retinitis pigmentosa

Three different mutations have to date been shown to segregate with disease phenotype in large RP10 families. Extensive genetic linkage and candidate gene studies have been carried out at this laboratory in a large Spanish family segregating adRP, with a mean age of onset of 13 years and exhibiting classic RP symptoms (Jordan et al, 1997). These studies resulted in the identification of a disease-causing mutation at position Arg224Pro in the protein sequence (Kennan *et al.*, 2002). A second mutation at Asp226Asn was identified in a large unrelated American family UTAD045, with later-onset RP, and also in four additional smaller adRP families (Bowne *et al.*, 2002). It was found that even within the same families, patients of comparable age had markedly different clinical severity (Bowne *et al.*, 2003). A third substitution at Arg231Pro has recently been identified in 17 members of a large adRP family, with many family members displaying very early onset of disease symptoms (Grover *et al.*, 2003). Additional screening of adRP patient isolates has also identified further IMPDH1 mutations which are summarised in Table 5.1.

Table 5.1. Spectrum of IMPDH1 substitutions identified in RP patients.

IMPDH1 mutation	Number of individuals or families	Location of mutation in protein	Reference
Arg224Pro	1 family	CBS2 Domain	Kennan *et al.*, 2002
Asp226Asn	5 families	CBS2 domain	Bowne *et al.*, 2002 Bowne *et al.*, 2003
Asp226Asn	6/190 individuals	CBS2 Domain	Wada *et al*, 2003
Arg231Pro	1 family	CBS2 domain	Grover *et al.*, 2003
Val268Ile	1 individual	?	Bowne *et al*, 2002
Thr116Met	1 individual	CBS1 domain	Bowne *et al.*, 2003
Gly324Asp	2 families [a]	Active site	Bowne *et al.*, 2003
His372Pro	1 individual	?	Bowne *et al.*, 2003

[a]One family member diagnosed with macular degeneration

The most prevalent mutation identified to date appears to be the Asp226Asn substitution, which has been identified in 5 separate RP10 families, and also in 6 out of 190 unrelated RP patients in a screen of RP isolates in the USA (Bowne *et al.,* 2002; Bowne *et al.,* 2003; Wada *et al.,* 2003). One report has estimated that this substitution accounts for up to 2% of RP cases worldwide (Wada *et al.,* 2003). There have not been any confirmed reports of IMPDH1 involvement in recessive RP or in association with any other forms of retinal disease or syndrome to date. It is of interest however that one member of a family segregating a Gly324Asp substitution was diagnosed with macular degeneration, because this suggests that IMPDH1 mutations may be involved in other, less severe retinal diseases, depending on the location of the mutation in the protein sequence. Information about severity of symptoms in other members of this family is not however available at this time.

5.1.3 IMPDH sequence conservation across species

The sequence for at least 35 different *IMPDH* genes across different species has been determined and there is extensive information available about functional domains and protein structure. A number of IMPDH sequences have been aligned in Figure 5.1, ranging from human and mouse IMPDH1 to *C. elegans* and bacterial IMPDH sequences. All adRP mutations identified to date lie in evolutionarily conserved amino acid sites (Fig. 5.1). The Asp226Asn and Gly324Asp mutations occur at sites that are conserved in all IMPDH sequences examined, while codons Arg224, Arg231 and His372 show fairly high degrees of conservation, at least amongst eukaryotic species. The Thr116Met and Val268Ile substitutions appear to reside at slightly less conserved sites, but the significance of this is unknown at present since the mutations have only been identified in a single patient, and their association with disease has yet to be fully established.

5.1.4 Function of IMPDH

The IMPDH1 enzyme (EC 1.1.1.205) functions as a tetramer composed of four identical subunits of 55kDa each. IMPDH1 catalyses the conversion of inosine

monophosphate (IMP) to xanthosine monophosphate (XMP) with the concomitant reduction of NAD^+ to NADH. This is the rate limiting step in the *de novo* guanine nucleotide biosynthesis pathway (Fig. 5.2). The functionally related enzyme, IMPDH2, also performs an identical enzymatic role, with the two proteins sharing 84% identity at the amino acid level (Natsumeda *et al.,* 1990). Guanine nucleotides may also be synthesized in the so-called salvage pathway by the enzyme hypoxanthine phosphoribosyl transferase (HPRT) (Fig. 5.2). Both IMPDH isoforms exhibit widespread expression patterns, but their regulation and levels of expression differ considerably. *IMPDH2* appears to exhibit inducible expression, and levels of expression are increased in proliferating and malignant cells (Nagai *et al.,* 1991; Nagai *et al.*, 1992; Carr *et al.,* 1993). The *IMPDH1* gene is believed to be constitutively expressed at relatively low levels, but there is variability of expression in different tissues (Nagai *et al.*, 1992; Senda *et al.,* 1994). Expression of IMPDH1 has recently been shown to be tissue-specific, with high levels of expression for example in the lung, thymus and brain, but no detectable expression in liver or testis (Gu *et al.,* 2003b). It has also been found that the induction of both type 1 and type 2 IMPDH contribute significantly to the T cell proliferative response (Dayton *et al.,* 1994).

Extensive studies have been carried out on the characterisation, mechanism, biological functions and inhibition of the IMPDH enzyme, especially on type 2, because of its role as a target for immunosuppressive, antitumour and anti-viral therapies (reviewed by Sintchak & Nimmesgern, 2000; Yalowitz & Jayeram, 2000). The role of IMPDH in maintaining GTP levels in the cell is thought to be essential for normal cell proliferation and function. Inhibition of cellular IMPDH brings about depletion of guanine nucleotides which causes an abrupt cessation of DNA synthesis and halts cell cycle progression, a signal for inhibition of growth as well as cellular apoptosis (Catapano *et al.,* 1995; Yalowitz & Jayeram, 2000; Gu *et al.,* 2003a). The majority of studies to date have focused on the role of IMPDH type 2 in apoptosis because of its elevated expression levels in malignant cells, and a number of IMPDH2-specific inhibitors exist for this reason (Barnes *et al.,* 2000). Whether or not the IMPDH type 1 isoform is also involved in a similar manner remains to be determined. *IMPDH1* is the first gene in the guanine nucleotide biosynthesis pathway to be associated with retinal disease.

5.1.5 IMPDH protein structure

The crystal structures for IMPDH from at least four different species have been characterised including those from human (type 2) (Colby *et al.,* 1999; Nimmesgern *et al.,* 1999), golden hamster (Sintchak *et al.,* 1996), Streptococcus pyogenes (Zhang *et al.,* 1999) and Trichomonas foetus (Whitby *et al.,* 1997). All structures demonstrate the same tetrameric organisation. The crystal structure of human IMPDH type 2 is the closest structure available for comparison to IMPDH type 1. The catalytic sites and structure of the two IMPDH isoforms would be expected to be very similar since they catalyse an identical enzymatic reaction. Each monomer of IMPDH2 consists of two domains; a major catalytic domain and a smaller flanking domain (Figure 5.3). The 394-residue catalytic domain of IMPDH forms an eight-stranded parallel α/β barrel core (Colby *et al.,* 1999). The active site is bounded by one face of the barrel, as well as an 18-residue "loop" (residues 325-342) and 54-residue "flap" (residues 398-451) inserted on the barrel face (Colby *et al.,* 1999) (Figure 5.3).

A smaller 120-residue flanking domain (residues 113-232) lies adjacent to the catalytic domain, inserted between the α2 helix and β3 sheet of the barrel (Colby *et al.,* 1999) (Figure. 5.3). Two cystathionine β-synthase (CBS) domains lie in this smaller subdomain, and form a dimer structure. The function of the CBS domains is unknown, and though they are not thought to be required for activity they may act as a regulatory region (Nimmesgern *et al.,* 1999; Sintchak & Nimmesgern, 2000). The core domain of IMPDH encompassing residues 1-108 and 244-514 has been expressed in *E. coli* without the subdomain, and it was found that it still formed a tetrameric structure and also retained its enzyme activity (Nimmesgern *et al.,* 1999). The subdomain (residues 99-244) of human IMPDH2 protein was also expressed alone as a His-tagged fusion protein, where it was found that the subdomain migrated as a monomer or dimer on a gel filtration column, and lacked enzymatic activity (Nimmesgern *et al.,* 1999). The second CBS domain is located between residues 177-232. Three established amino acid substitutions identified in RP10 families to date lie within this particular domain; Arg224Pro, Asp226Asn and Arg231Pro, suggesting it may be a 'hotspot ' for pathogenic mutations (Kennan *et al.,* 2002; Bowne *et al.,* 2002; Grover *et al.,* 2003).

5.1.6 IMPDH enzyme activity

Many detailed reports have been published previously on IMPDH enzyme activity function, and methods of measuring activity levels have been well-established. The activity of a particular enzyme may be measured by determining the rate of product formation during enzyme-catalysed reaction. Spectrophotometric assays are probably the most widely used procedures, and are particularly convenient when the reaction catalysed involves an absorbance change (Tipton, 2002). The reaction catalysed by IMPDH results in the production of NADH from one of it's substrates NAD^+, which causes an absorbance increase when measured at 340 nm. This increase in absorbance can be measured directly using a spectrophotometer in a continuous assay. Measurements can then be used to calculate specific activity (μmol/min /mg enzyme or U/mg), K_m values, which is the substrate concentration at which the reaction rate is half maximal and k_{cat} values, which is the amount of moles of substrate converted to product per second by one mole of enzyme. Studies comparing the specific activity of IMPDH1 and IMPDH2 have reported that they are enzymatically very similar. Values for k_{cat}, K_M and specific activities previously reported for IMPDH in a number of independent studies, are summarised in Table 5.2. The exact values and constants obtained for enzyme activity measurements can vary slightly between experiments, and depend on assay conditions used, purity of enzyme and measurement technique employed.

Table 5.2. Previously reported enzyme activity measurements for IMPDH.

IMPDH1 k_{cat} **(sec^{-1})**	**IMPDH2** k_{cat} **(sec^{-1})**	**K_m NAD (μM) IMPDH**		**K_m IMP (μM) IMPDH**		**Reference**
		1	**2**	**1**	**2**	
1.5	1.3	46	32	18	9.3	Carr *et al.*, 1993
1.8 S.A =1.5 U/mg	1.4 S.A=1.3 U/mg	42	32	14	9	Hager *et al.*,1995
—	1.5		35		19	Futer *et al.*, 2002

S.A.= Specific Activity
Vmax = Rate at which the enzyme is fully saturated with substrate.
K_m = Substrate concentration at which the reaction rate is half maximal.
K_{cat} = Moles of substrate converted to product per second by one mole of enzyme.

5.1.7 *Impdh1*$^{-/-}$ knockout mouse model

The function of IMPDH type 1 and type 2 *in vivo* has been investigated by the targeted deletion of these two genes in mice by Dr. Beverly Mitchell and colleagues at the University of North Carolina at Chapel Hill, USA. In mice, loss of both alleles of the *Impdh type 2* gene results in very early embryonic lethality (Gu *et al.,* 2000). A mouse deficient in the *Impdh type 1* gene has recently been generated using standard gene targeting techniques (Gu *et al.,* 2003b). In contrast to the *Impdh2* knockout it was found that Impdh type I enzymatic activity is not essential for normal mouse development or fertility. It was also demonstrated that there was no compensatory increase observed in either Impdh2 or Hprt in response to the loss of Impdh1 at the mRNA or protein level. This mouse was kindly made available to the Ocular genetics unit by Dr. Mitchell, to investigate whether loss of the *Impdh1* gene has any effect on mouse retinal function and histology. The human and mouse IMPDH1 proteins are very similar, sharing 98% identity at the amino acid level, so any effects due to the absence of this gene in the mouse should be very similar to those that would be expected in humans.

5.1.8 Molecular methods for analysis of protein function and properties

In this study, a functional and structural analysis of the IMPDH1 protein was undertaken, and involved the use of two different protein expression systems, bacterial and mammalian. For both expression systems, a number of different vector designs are now commercially available, which can incorporate a range of detection or fluorescent tags, different promoter regions and methods of selection. A bacterial expression system was chosen for the functional analysis of the IMPDH1 protein, because high levels of recombinant protein can be produced using this powerful technique. This method often results in such high expression levels that, after only a few hours, the target protein may constitute the majority of the cellular protein.

Mammalian expression systems enable post-translation modifications such as glycosylation to be introduced into a recombinant protein, which are essential features in protein production and folding in eukaryotes, and can often greatly influence the properties of a protein. In this study the IMPDH1 gene was cloned under the control of

the human cytomagalovirus immediate-early (CMV) promoter, which provides high level expression in a wide range of mammalian cells.

5.1.9 The aim of the study

The aim of this study was to evaluate the effects of two established adRP mutations, Arg224Pro and Asp226Asn, on the properties and activity of the IMPDH1 enzyme, with a view to establishing the disease mechanism that causes degeneration of photoreceptor cells in the RP10 form of retinitis pigmentosa. The enzyme activity measurements were carried out on recombinant protein expressed in a bacterial system, while solubility studies were undertaken on protein expressed in mammalian cells.

5.2 MATERIALS AND METHODS

Unless otherwise stated, reagents were purchased from Sigma-Aldrich, Ireland, Ltd. All solution components can be found in Appendix A: Stock solutions, and all primers sequences are listed in Appendix B:primers. Unless otherwise stated, enzymes and enzyme buffers were purchased from New England Biolabs (NEB), UK, and restriction digests were carried out according to manufacturers instructions.

5.2.1 Preparation of Competent Cells

XL1-Blue *E. coli* cells (Stratagene) were used for bacterial transformations and amplification of plasmid DNA unless otherwise stated. A single colony of XL1-Blue was used to inoculate 1ml of LB culture medium (Appendix A.3), and was grown overnight with shaking at 37°C. This culture was used to inoculate 30mls LB in a 250 ml flask. Cells were grown for approximately 3 hrs until an OD_{600} of 0.6 was reached, cells were placed on ice for 5 minutes and then spun at 3,000 rpm for 10 minutes. Supernatant was discarded and cells were resuspended in 30 mls cold 100 mM $MgCl_2$. Cells were spun again and supernatant discarded. Cells were then resuspended in 15 mls cold 100mM $CaCl_2$, and placed on ice for 20 minutes. Cells were spun again for 10 minutes, supernatant discarded and finally cells were resuspended in 1.5 mls cold 100mM $CaCl_2$. Competent cells were stored on ice for 1-24 hours, or frozen at –80°C in 15% glycerol stocks.

5.2.2 Transformation of XL-1 Blue cells

Competent cells were kept on ice, or thawed slowly on ice before use. Approximately 100 ng of plasmid or 5-10 µl ligation product was used to transform 200 µl competent cells. DNA was diluted in 100 µl 100 mM $CaCl_2$ on ice and then added to competent cells in sterile tubes and incubated on ice for 30 minutes. Tubes were incubated at 42°C to heat-shock cells for 2 minutes and afterwards immediately placed on ice. Following

the addition of 2.7 mls LB, cells were incubated at 37°C for one hour with gentle shaking. Aliquots of 50-250 µl cells were spread on LB agar (Appendix A.3) containing ampicillin for selection of transformants harbouring the desired plasmid. Plates were grown overnight at 37°C and colony PCR's were carried out to confirm presence of IMPDH1 insert using primers specific for vector of interest and IMPDH1 cDNA sequence. The protocol for PCR has been described in detail previously in Chapter 2.

5.2.3 Plasmid DNA Isolation

5.2.3.1. Boiling minipreps

A single colony was picked and grown overnight in 10 mls LB + Ampicillin at 37^0C. Cells were spun at 3000 rpm for 10 minutes and resuspended in 60 µl TT buffer (Appendix A.3). 20 µl of lysozyme (40 mg/ml) was added and cells were left for 10 minutes on ice. 550 µl M-STET Buffer (Appendix A.3) was added and the cells were held at room temp for 10 minutes. Samples were boiled for 1.5 minutes and then spun at 13200 rpm for 30 minutes. The pellet was removed with a toothpick, 1 µl RNAse was added and tubes were incubated at 37°C for 15 minutes. A 0.6 volume of isopropanol was added, tubes were mixed and incubated at room temp for 15 minutes. Samples were then spun for 10 minutes, isopropanol was poured off and pellet was washed with 80 % ethanol. Final DNA pellet was dissolved in 50 - 100 µl H_2O or TE buffer.

5.2.3.2. Maxipreps

Bacterial cultures were grown in 150-250 ml LB medium containing ampicillin for 12-16 hrs. Ultra pure plasmid was isolated using the HiSpeed Plasmid Maxi Kit (Qiagen) according to manufacturers instructions. Final concentration of pure plasmid was calculated by measuring the OD at 260 nm in a spectrophotometer. (O.D. unit of 1 represents a DNA concentration of 50 µg/ml.)

5.2.4 Construction of pET15b-IMPDH1 vector

The wild-type IMPDH1 cDNA in a pGEM vector was received from Dr Beverly Mitchell, University of North Carolina at Chapel Hill, USA. Primers referred to as IMPDH1-Xho1 F and IMPDH1-Xho1 R (Appendix B.6) were designed to introduce *Xho1* sites at either end of the IMPDH1 cDNA sequence and the 1.5kb IMPDH1 cDNA was amplified by PCR with *Pfu* DNA polymerase (Stratagene). IMPDH1 cDNA inserts (PCR products) were cut with *Xho1* restriction enzyme and agarose gel purified using the Qiaquick Gel extraction kit (Qiagen), according to manufacturers instructions. The pET-15b vector incorporates a His-tag at the N-terminus of the protein sequence and the protocol was designed so that the IMPDH1 protein sequence was in frame with the His-tag ATG start site (Fig. 5.4). The pET-15b vector (Novagen) was cut with *Xho1* and gel purified. A ligation reaction was carried out using a 1:10 ratio of vector to insert and T4 DNA Ligase (Roche) at 18°C overnight. XL1 blue cells were transformed with ligation reactions as described previously. Colony PCRs were carried out for confirmation of sequence insertion using PET-15b T7F2 and IMPDH1 cDNA ex3R primers (Appendix B.6). Miniprep and maxiprep reactions were carried for isolation of plasmid DNA. Treatment with *Xho1* restriction enzyme followed by agarose gel analysis, and automated sequencing was used to verify the presence and correct orientation of the IMPDH1 insert.

5.2.5 Site-directed mutagenesis

The single point mutations CGC to CCC (Arg224Pro) and GAC to AAC (Asp226Asn) were introduced by amplification of the pET15b-IMPDH1 vector using the forward and reverse primers IMPDH1-Arg224 and IMPDH1-Asp226 (Appendix B.5) and the Quikchange XL site-directed mutagenesis kit (Stratagene). This protocol was followed according to manufacturers instructions. Briefly, the PCR reactions were carried out with Pfu DNA polymerase (Stratagene) and amplification products were digested with Dpn-1 which degrades parental DNA, leaving only newly-amplified mutant sequence. XL-10 Gold cells were transformed with amplified DNA and plated. Single colonies were picked and the mini-prep procedure was carried out. All plasmid inserts were sequenced completely to verify the presence of mutations and to ensure that there was

no additional nucleotide alterations introduced during amplification. (The IMPDH1 cDNA sequence was compared to sequence accession number XM_004627).

5.2.6 Expression of wild type and mutant His-tagged IMPDH1 in *E.coli*

pET15b-IMPDH1 plasmids constructs were transformed into *E. coli* BL-21 (DE3) for protein expression. Strains were stored in 15% glycerol in cryovials at –80°C. Cells were scraped from frozen stocks and grown in starter cultures of 5 mls LB containing ampicillin overnight. The entire culture was transferred into 50-200 ml LB containing ampicillin in flasks, then grown at 37°C to an O.D. of 1.0 at which stage a 1 ml pre-induction total cell protein (TCP) sample was taken for analysis. Induction was carried out with a final concentration of 400 μM IPTG at 37°C or 25°C for 3-5 hours. A 1 ml post-induction TCP sample was removed for SDS-polyacrylamide gel electrophoresis (SDS-PAGE) analysis. Cell cultures were spun down and the pellet was stored at –20°C overnight. The cell pellet from 50mls culture volume was resuspended in 4 mls Ni-NTA bind buffer (Appendix A.4) (Novagen) with the addition of NaCl to 0.25M, treated with lysozyme to a final concentration of 1 mg/ml and 1 μl benzonase (Novagen) and incubated on ice for 10 minutes. Resuspended cells were sonicated on ice at the high setting for at least 20 bursts or until cell lysate became clear. Sonicated lysate was then spun at 13,200 rpm for 15 minutes to separate soluble and insoluble fractions and supernatant was retained. Pellets were resuspended in 1% SDS or 8% urea for SDS-PAGE analysis. TCP samples were spun down for 1 minute and resuspended in 100 μl PBS buffer. 20 μl SDS-PAGE loading dye was added and samples were passed through a 27 G needle several times to reduce viscosity.

5.2.7 Purification of His-tagged IMPDH1

Soluble cell lysate (4 mls) containing His-tagged IMPDH1 was added to 1ml washed Ni-NTA His-bind resin (Novagen) and His-tagged protein was isolated by batch purification under native conditions according to manufacturers instructions. Briefly, soluble lysate was incubated with His-bind resin for 1 hour at 4°C with gentle shaking

to allow the His-tagged protein to bind to the resin. The lysate Ni-NTA mixture was loaded into a column and beads were washed twice with 4ml Ni-NTA Wash buffer (Appendix A.4). Protein was eluted with 4 x 0.5 ml Ni-NTA Elution buffer (Appendix A.4) and all fractions were collected for SDS-PAGE analysis.

5.2.8 Protein quantification

Protein concentration was determined using the Bio-Rad protein assay adapted to a 96-well Microplate reader format. Bovine IgG standards (Biorad) were made up to 0.1-0.5 mg/ml concentrations. 10 µl of each standard or protein sample was added per well in a 96-well plate, with 200 µl of dye reagent (diluted 1:4 with water). Samples were incubated at room temperature for 5 minutes and the absorbance was measured at 595 nm using an Anthos Labtec 2010 Microplate reader.

5.2.9 SDS-PAGE analysis and Coomassie blue staining

Proteins samples were prepared for electrophoresis by adding 5x SDS-loading buffer (Appendix A.5) and heating to 95°C for 6 minutes. A broad range protein molecular weight marker was used to size proteins (NEB). Standard SDS-polyacrylamide gel electrophoresis (SDS-PAGE) was carried out as detailed by Maniatis *et al.,* 1992. Samples were loaded onto 10% SDS-polyacrylamide gels with a 5% stacking gel (Appendix A.5). Gels were run in SDS-PAGE running buffer at 80-100 V for 1-2 hrs. Gels were immersed in Coomassie Blue dye reagent (Appendix A.5) for staining, heated for one minute in the microwave and incubated with gentle rocking for one hour. Gels were destained by incubating in Destain solution (Appendix A.5), and solution was changed several times until protein bands were resolved.

5.2.10 Enzyme activity assay of recombinant IMPDH1 proteins

A standard method for enzyme activity assays can be found in John *et al.,* 2002. The standard enzyme assay buffer contained 0.1 M Tris, 0.1 M KCL, 3 mM EDTA, 2 mM

DTT pH 8.0, and the substrates 400 μM IMP and 400 μM NAD. The substrates IMP and NAD were added immediately before starting activity measurements and buffer was pre-incubated at 37°C. A blank reading was obtained by measuring the absorbance of buffer alone, and setting the absorbance to zero. Purified enzyme was diluted in reaction buffer (minus substrates) for a short period before measurement of reaction rates since potassium ions, which are present in assay buffer, are a necessary co-factor for IMPDH enzyme activity. The reaction was started by addition of 5-25 µg purified recombinant IMPDH1 to buffer in 1 cm cuvettes and mixing. The initial rate of activity was measured at 37°C in a temperature-controlled Cary 50 UV-Vis spectrophotometer by monitoring the absorbance increase at 340 nm over 1 min due to the formation of NADH. Cary WinUV software was used to measure reaction rates or slope of the resulting straight line as reaction proceeded. For Km[NAD] measurements the reaction buffer contained NAD concentrations of 2.5-400 µM.

5.2.11 Construction of mammalian expression vectors

The wild-type and mutant IMPDH1 cDNA sequences were sub-cloned from the pET15b vector by cutting with *Xho1* restriction enzyme followed by gel extraction of 1.5kb inserts. Inserts were blunt-ended by filling 5'-overhangs with Klenow (Roche). The pcDNA/His C vector (Fig. 5.13) was cut with *Acc65I* and also filled with Klenow. DNA/enzyme solutions were washed with equal volumes of phenol, phenol/chloroform and chloroform. Samples were vortexed thoroughly between each wash, spun in a centrifuge and the top layer was transferred to a fresh eppendorph tube. Finally DNA was pelleted by adding twice the volume of 100% cold ethanol and 3M Sodium Acetate (2.5%). Samples were placed at –20°C for 30 minutes, spun at top speed for 15 minutes and pellets were washed with 70% ethanol. The final pellet was resuspended in H_2O or TE buffer (Appendix A.3). The ligation reaction was carried out as described previously. Insertion of IMPDH1 cDNA sequence into the vector was confirmed by colony PCR's using pcDNA3.1/His F and IMPDH1 cDNA exon 3R or exon 12F and pcDNA/His R primers (Appendix B.6), and automated sequencing. Positive colonies were grown in 150 ml culture volumes and maxi-preps were carried out to isolate pure plasmid.

5.2.12 Mammalian cell culture techniques

All tissue culture reagents were purchased from Gibco-BRL, UK, unless stated otherwise. All cell cultures experiments were carried out in a laminar flow hood under sterile conditions.

Human embryonic kidney 293 (HEK 293T) adherent cells (ATCC number CRL-1573) were cultured in Dulbecco's Modified Eagle Medium (DMEM) supplemented with 10% fetal bovine serum, 2 mM L-Glutamine and 1 mM Sodium Pyruvate. Cells were grown at 37°C and in an atmosphere of 5% CO_2. Medium was changed every 2-3 days. When 90-100% confluency was reached, cells were passaged by washing with PBS (Appendix A.6) to remove all traces of medium, 2 mls of Trypsin-EDTA (Gibco-BRL) was added to cell monolayer and plates were incubated at 37°C for four minutes. Trypsin was then deactivated by addition of 8 mls complete medium and the cell suspension was spun at 1000 rpm for 4 minutes. Supernatant was removed and the cell pellet was resuspended in 10 mls complete medium. Cells were counted with the aid of a haemocytometer and seeded at a density of 1-3 x 10^6 per 100 mm plate, with the addition of 12 mls fresh medium. For cryopreservation, approximately 1 x 10^7 cells were resuspended in Fetal bovine serum containing 8.5% DMSO. 1 ml of cells were placed in cryovials, frozen slowly to –80°C and later transferred to liquid nitrogen storage.

5.2.13 Transient transfection of mammalian cells

Cells were seeded at a density of 1 x 10^6 cells per 10 cm dish overnight with DMEM+ medium containing 25 mM Hepes. 20 µg of each vector DNA was diluted to 200 µl with H_20 and 50 µl 2.5 M calcium chloride was added. 200 µl of 2x HBS (Appendix A.6) buffer was added to individual wells of a 24-well plate per transfection. DNA/$CaCl_2$ mixture was added dropwise to buffer in 24-well plate. Complexes were left to form for 20-30 minutes. The 500 ml precipitates were then added to cell monolayers in a 10 cm plate. Medium was changed after 6-18 hours and cells were incubated for 48 hours to allow expression of plasmid.

5.2.14 β-Galactosidase assay for assessment of transfection efficiency

As a positive transfection control, cells were transfected with the pcDNA/His/LacZ vector. Cells were washed in PBS, and fixed by addition of 4 mls PF Fixative (Appendix A.6) per 10 cm plate, and left at room temperature for 5 minutes. The fixative was removed and 4mls of PBS was added, and cells were left for 5 minutes at room temperature. PBS was removed and 4 mls of β-Gal staining buffer with freshly added X-Gal (Appendix A.6) was added and the plate was incubated at 37°C for 10 to 60 minutes or until a blue colour developed in positive cells.

5.2.15 Isolation of cellular compartment protein fractions

Cells were harvested by trypsinisation 48 hours after transfection, washed twice with PBS and centrifuged gently to pellet. A protein isolation protocol for extraction of cell fractions was adapted from Deery *et al.,* 2002. The cell pellet from one dish of cells was resuspended in 1 ml Protein Extraction Buffer A (Appendix A.6). The cells were incubated on ice for 10 minutes then re-pelleted by spinning for 10 minutes in a microfuge at 2000 rpm at 4°C. The cells were then resuspended in 300 µl buffer A, and for each prep a 100 µl sample was removed for whole cell protein analysis. NaCl was added to this aliquot to a conc of 1 M to lyse all membranes. To the remaining 200 µl of cell suspension detergent Nonidet P-40 was added to a concentration of 0.2%, the mixture was incubated on ice for 10 minutes and the suspension was spun at 3500 rpm for 10 minutes at 4°C. The supernatant which contains the soluble cytosolic proteins was removed. The pellet containing nuclei and insoluble components was resuspended in 200 µl Protein Extraction Buffer B (Appendix A.6) and NaCl was added to a final concentration of 1 M. After 45 minute incubation at 4°C, nuclear lysis occurs and viscosity was reduced by shearing DNA and passing 10 times through a 25 gauge needle. The suspension was then spun at 13000 rpm for 40 minutes at 4°C. The supernatant containing soluble nuclear proteins was preserved. The final pellet was resuspended in 100 µl of 1% SDS to denature and solubilise remaining proteins. Protein concentrations were then measured using BioRad Protein assay kit with IgG as standard as described previously.

5.2.16 Western Blot analysis of protein extracts

Aliquots containing equal amounts of total protein (30 μg) were loaded onto 10% SDS-PAGE gels in duplicate and run as described previously. One gel was stained with Coomassie blue and the proteins on the second gel were transferred by electroblotting onto nitrocellulose membrane (Schleicher and Schuell) in Transfer Blotting Buffer (Appendix A.7) for 2 hours at 160 mA. Blots were rinsed in TBS buffer (Appendix A.7) and blocked with 1% casein in TBS (Novagen) for one hour at room temperature. Blots were probed with an Anti His-tag monoclonal antibody (Novagen 200 ng/ml) diluted in blocking solution and incubated with gentle shaking overnight at 4°C. After rinsing the blot twice for 10 minutes in TBS-TT buffer (Appendix A.7), the blot was probed with a horseradish peroxidase-conjugated anti-mouse IgG secondary antibody (Sigma) diluted in blocking solution for one hour at room temperature. Blots were then washed 4 times for 10 minutes in TBS-TT buffer. Detection of signal was carried out using SuperSignal West Pico Chemiluminescent Substrate (Pierce) according to manufacturers instructions. Blots were exposed to X-ray film under safelight illumination for 1-10 minutes.

5.3 RESULTS

5.3.1 Expression of wild-type and mutant IMPDH1 proteins in *E.coli*

The aim of this study was to evaluate the effects of the two adRP mutations originally identified in large RP10 families, Arg224Pro and Asp226Asn, on the properties and activity of the IMPDH1 enzyme. The *IMPDH1* cDNA sequence was sub-cloned in-frame into a pET-15b vector (Novagen) which is under the control of the T7 promoter, and incorporates a His-tag at the N-terminus of the translated protein (Fig. 5.4). Expression is achieved by IPTG induction of a chromosomally integrated cassette in *E. coli* cells, in which the T7 RNA polymerase is expressed from the *lacUV5* promoter. Two amino acid substitutions, Arg224Pro and Asp226Asn, were introduced into the native *IMPDH1* cDNA sequence by site-directed mutagenesis and sequence alterations were confirmed by automated sequencing (Fig. 5.5). The three pET-15b-IMPDH1 vectors containing wild-type, Arg224Pro and Asp226Asn IMPDH1 sequences, were transformed into *E.coli* BL21(DE3) cells. Induction of protein expression in *E. coli* was carried out initially at 37°C for 3 hours. Soluble and insoluble cellular fractions were isolated and analysed by SDS-PAGE with Coomassie blue staining. There was an obvious induction band visible at 55 kDa, indicating over-expression of the desired IMPDH1 protein in the post-induction total cell protein fraction (Fig. 5.6). In many cases, recombinant proteins expressed in *E.coli,* especially at high levels, can aggregate and form insoluble inclusion bodies. Over-expression of the IMPDH1 protein tended to result in inclusion body formation, with about half of the wild-type IMPDH1 protein localising to the insoluble fraction (Fig. 5.7). The IMPDH1 protein containing the Arg224Pro mutation, however, appeared to exhibit significantly decreased solubility when compared to the wild-type. Following SDS-PAGE analysis, none of this mutant protein was found to be present in the soluble fraction, even though the level of expression in the total cell extract was similar (Figure 5.7). The experiment was repeated several times and this insolubility was always evident. Induction of protein expression was then carried out at 25°C because a lower induction temperature favours slower protein folding, which usually improves solubility and helps prevents inclusion-body formation. At this temperature a proportion of the mutant Arg224Pro IMPDH1

protein was found to be present in the soluble cell lysate, but perhaps not as high a quantity as was detected for the soluble wild-type protein. The second Asp226Asn mutant protein was not observed to exhibit a similar decrease in solubility at either temperature (Fig. 5.7).

Wild-type and mutant IMPDH1 proteins were purified from soluble cell lysates using Ni-NTA resin which selectively binds His-tagged protein. The Ni-NTA elution buffer contains imidazole which competes with His-tagged proteins for nickel ions attached to the resin in the purification column, and causes the His-tagged protein to become displaced. The step-wise washes and fractions that were eluted off the Ni-NTA His-bind column are shown in Figure 5.8. Soluble cell lysates prior to His-tag purification and post-purification wild-type and mutant IMPDH1 proteins are shown in Figure 5.9 and 5.10. The resulting protein fractions were of sufficient purity (estimated 80-90%) as determined by Coomassie blue staining of SDS-gels, to enable enzyme activity studies to be undertaken. Purified IMPDH1 protein fractions were quantified using the Biorad Bradford assay.

5.3.2 IMPDH1 enzyme activity assay

Initial rates of enzyme activity were determined by measuring the absorbance increase at 340 nm caused by the reduction of NAD^+ to NADH, after addition of purified IMPDH1 enzyme. Increasing quantities of diluted enzyme ranging from 5-25 μg were added to assay buffer, and the increase in absorbance detected was recorded over 1 minute. Cary UVwin software was used to calculate the rate of reaction (slope of line). For Km [NAD] measurements, concentration of NAD in assay buffer ranged from 2.5 to 400 μM. Graphs showing quantity of enzyme added, versus reaction rates were drawn using Graphpad Prism software (Fig. 5.11). Specific activities were calculated by dividing reaction rate by quantity (in mg) of IMPDH1 protein added. For Km [NAD] measurements, concentration of NAD in assay buffer ranged from 2.5 to 400 μM with the concentration of IMP kept at 400μM. Reaction rates obtained were plotted versus concentration of NAD and K_m values were calculated using Graphpad Prism software (Fig. 5.12). Specific enzyme activities, K_m [NAD] and K_{cat} values were calculated for wild-type (WT), Arg224Pro and Asp226Asn IMPDH1 enzymes and are summarised in Table 5.3. No significant difference in specific enzyme activity was

detectable between the wild-type and mutant IMPDH1 proteins. Enzyme activities were measured on soluble proteins only and all three enzymes showed similar levels of activity for up to seven days.

Table 5.3. Specific enzyme activities and kinetic constants calculated for IMPDH1 wild-type and mutant enzymes.

IMPDH1 Enzyme	Specific Activity $\mu mol\ min^{-1}mg^{-1}$	K_m [NAD] μM	K_{cat} sec^{-1}
Wild-type	1.22	20	1.7
Arg224Pro Mutant	1.30	14	1.58
Asp226Asn Mutant	1.28	12	1.6

There were slight differences detected in specific activity and K_m values between WT and mutant IMPDH1 enzymes, and slightly lower Kcat values for the mutant enzymes were calculated. This is more likely due to difficulties encountered with quantification as a consequence of mutant proteins coming out of solution, or to differences in levels of purity obtained between different protein fractions, than a real difference in the kinetic behaviour of the mutant enzymes. Calculated activities were comparable to previously published reports of IMPDH1 specific enzyme activity levels (Table 5.2). A dramatic reduction in enzyme activity would be expected if the disease-causing effects of the mutations were primarily attributable to diminished activity under physiological conditions.

Values for K_m [IMP], the second enzyme substrate, were not calculated for this study because very low concentrations were recorded in previously reported studies, which would make it very difficult to accurately measure K_m values (Table 5.2). Reaction rates at concentrations of 10 μM IMP were recorded and there was no substantial decrease in rate detected at this concentration for either of the mutant enzymes (data not shown). A more sensitive detection method such as fluorimetry could be employed to accurately calculate the K_m for IMP values. Due to time

limitations these measurements were not carried out in this study but it is very unlikely that an alteration in the K_m for IMP would be detected, since the specific activities of the mutant IMPDH1 proteins appear to be so similar to wild-type, and the mutations under investigation are not thought to lie in close proximity to the IMP catalytic binding site.

5.3.3 Analysis of wild-type and mutant IMPDH1 in mammalian cells

Mutant IMPDH1 proteins were found to exhibit decreased solubility in comparison to wild-type when expressed at a temperature of 37°C in bacterial cells. To investigate this observation further, the behaviour of these proteins in mammalian cells was explored. The pcDNA3.1/His vector (Invitrogen) is a CMV–promoter driven vector that incorporates a His-tag at the N-terminus of the resulting protein, for protein detection and purification purposes (Fig. 5.13). Mammalian expression constructs were generated by cloning the IMPDH1 wild-type, Arg224Pro or Asp226Asn mutant cDNA sequences in-frame into the pcDNA3.1/His C vector. Automated sequence analysis confirmed the correct insertion of the IMPDH1 cDNA (Fig. 5.14). Human embryonic kidney (HEK) 293T cells were transfected with a mammalian expression construct pcDNA3.1/His/LacZ as a positive control, pcDNA3.1/His without any insert as a negative control or vector containing IMPDH1 wild-type, Arg224Pro or Asp226Asn mutant cDNA sequences. Cells were transfected using the calcium phosphate method and harvested 48 hours post-transfection. The positive control cells which expressed the LacZ gene, were stained for β-galactosidase to determine the transfection efficiency (percentage of cells that express the desired plasmid). Transfection efficiency was estimated by counting the number of blue cells after staining and was estimated at between 70-80% (Fig. 5.15). This is generally accepted to be a good level of efficiency. The cells transfected with vector containing IMPDH1 inserts and vector alone were separated into total cell protein, soluble cytosolic, nuclear and insoluble pelleted fractions, which were subsequently analysed by SDS PAGE electrophoresis (Fig. 5.16a) and western blotting (Fig. 5.16b). Specific monoclonal antibodies for the His-tag sequence are commercially available and were used for the detection of tagged IMPDH1 protein in this study. Due to the similarity in sequence between IMPDH type

1 and 2 isoforms, an antibody was not available that was specific for detection of IMPDH type 1 protein.

Wild-type and mutant IMPDH1 proteins were expressed at similarly high levels in whole cell extracts with a band clearly visible at 55 kDa (Fig. 5.16a and Fig. 5.16b). No protein band of this size was evident in cells transfected with a construct that did not contain an *IMPDH1* cDNA insert. Following analysis of cellular fractions obtained after further purification steps, wild-type IMPDH1 protein was shown to localise to the soluble cytosolic fraction, while no mutant protein was detectable in this fraction. Both mutant proteins exhibited considerably decreased solubility and as a result almost all of the mutant protein localised to the final pellet, which was re-suspendable in strong denaturant. It is likely that such mutant IMPDH1 proteins are mis-folded, resulting in the formation of insoluble aggregates within the cell cytosol.

5.3.4 Computer modelling studies on IMPDH1

To further investigate the existence of possible tertiary structural perturbation in mutant IMPDH1, a series of molecular modelling computational simulations for the Arg224Pro mutation were undertaken in a collaboration with Dr. David Lloyd and Dr. Ian Alberts, De Novo Pharmaceuticals, Cambridge, UK. Proline residues located within α-helices have a tendency to distort the standard helical arrangement by causing the structure to kink about the position of the proline residue (Barlow & Thornton, 1988; Chang *et al.,* 1999). This distortion is primarily a consequence of the enhanced flexibility introduced by the proline ring, which leads to additional steric constraints with nearby backbone atoms as well as the removal of favourable intra-helix hydrogen-bonding interactions (Cordes *et al.,* 2002). To test the hypothesis that a mutation from Arg to Pro could result in a mutant protein with perturbed structure, correlating to impaired *in vitro* and *in vivo* function, structural homology models were constructed by Dr. Lloyd from both Arg-wild-type and Pro-mutant IMPDH1 sequences, building from available crystal structures of human (Colby *et al.,* 1999) and non-human (*Cricetulus griseus*)(Sintchak *et al.,* 1996) IMPDH which exhibited high homology to our sequence of interest. The resultant wild-type and mutant structures were subjected to an extensive computational molecular dynamics simulation by Dr. Alberts, to challenge and refine the models.

No significant deviation in structure was observed for the wild-type protein post-dynamics (not shown), but significant structural perturbation was noted in the mutant structure around the area of point mutation (Arg224 to Pro224) by the end of the simulation run. Figure 5.17 (a) and (b) illustrate the end-point results from molecular dynamics simulation on mutant (pink) and wild-type (blue) IMPDH1 homology models. The Arg to Pro mutation in the 'bud' or flanking region is highlighted in green in both models. The perturbation of predicted tertiary structure is clearly visible as the mutated protein loses cohesion of structure in the 'bud' domain, distant from the principal catalytic domain. Such structural perturbation would undoubtedly disrupt the formation of the biological homotetramer subunit and correlates to the observed physical and functional data for the mutant protein.

5.3.5 *Impdh* expression in the mouse retina

In situ hybridisation studies carried out by Dr. Avril Kennan showed that *Impdh1* is preferentially and strongly expressed within photoreceptor cells in mouse retinas (Kennan *et al.*, 2003). In contrast there was very little expression of either *Impdh2* or *Hprt* in the photoreceptor cell layer. These results thus indicate that IMPDH1 is largely responsible for the production of guanine nucleotides within photoreceptors. In mice lacking the *Impdh1* gene it has been observed that there is no compensatory mechanism for regulation of expression of *Impdh2* and *Hprt* (Gu *et al.*, 2003b). It is likely therefore, that in the case of a defective or absent IMPDH1 protein in the retina, IMPDH2 and HPRT may not be able to substitute for the loss of IMPDH1 activity. This is particularly relevant given that the retina is one of the most energy-demanding tissues of the body and that photoreceptor cells have a high requirement for GTP within the visual transduction cycle (La Cour *et al.*, 2002).

Previously, microarray and real-time PCR analysis had also suggested that IMPDH1 was expressed preferentially in the photoreceptor cell layer of the retina. As discussed in Chapter 3, the IMPDH1 gene was found to be down-regulated 5.8-fold in a microarray analysis between Wild-type and $Rho^{-/-}$ mouse retinas, and down-regulated 4-fold according to quantitative PCR studies (Chapter 3, Fig. 3.4). Quantitative PCR analysis was also undertaken on IMPDH2 transcripts, which did not detect a difference in levels of expression between Wt and $Rho^{-/-}$ retinas.

5.3.6 Retinal structure and function in *Impdh1-/-* mice

A rational interpretation of the *in situ* data is that IMPDH1 is important to normal photoreceptor function. Hence, photoreceptor activity in the retinas of *Impdh1*$^{-/-}$ mice was evaluated by Dr. Paul Kenna using electro-retinography (ERG), and retinal sections were prepared for histology by Dr. Niamh McNally. The results of these studies are presented in order to provide a more complete picture of the molecular mechanisms in this form of RP. Rod-isolated responses (Fig. 5.18a), maximal, dark-adapted, combined rod and cone responses (Fig. 5.18b) and light-adapted cone responses to single flash (Fig 5.18c) were recorded at 6 weeks of age, 5 months, 8 months, 11 months and 13 months (Fig. 5.18). At 11 months of age all responses showed a significant reduction in a- and b-wave amplitudes and, in the case of the cone responses, significant delay in b-wave timing (Fig. 5.18c). Further deterioration was noted by 13 months. In the case of the maximal, dark-adapted, combined rod and cone responses, progressive reduction in wave amplitudes was noted from 5 months of age indicating disturbance of phototransduction. This may be explained by disturbance in cGMP-dependent cation channel function which requires a constant turnover of cGMP, which must be synthesized from GTP. A reduction in ERG amplitude brought about by membrane hyperpolarisation and closing of these channels, may be due to the disturbance in guanine biosynthesis consequent to lack of IMPDH1 activity.

It is notable that the electroretinographic disturbances observed in *Impdh1*$^{-/-}$ mice are much milder than those recorded in humans with dominant *IMPDH1* mutations, where generally all ERG responses are unrecordable by the third decade. The response in an affected 17-year old male from the RP10 family FA-84, segregating an Arg224Pro IMPDH1 mutation to the maximal intensity flash presented in the dark adapted state, which normally elicits a mixed rod/cone response, shows no recordable photoreceptor activity (Fig. 5.18d). It is also of interest to note that photoreceptor dysfunction in the *Impdh1*$^{-/-}$ mouse is not the result of degeneration of photoreceptor cells, since the outer nuclear layer thickness of the retinas in these mice is similar to wild type retinas up to 10 months of age, and even by 13 months of age there is only marginal loss of nuclei from the outer nuclear layer of the retina (data not shown) (Fig. 5.19 a-c). Preliminary evidence suggests some degree of disorganisation of photoreceptor outer segments in older animals. Thus, IMPDH1 does not appear to be essential for normal retinal development or early visual function. In the light of such

observations, it appears unlikely that the autosomal dominant segregation pattern which is characteristic of the RP10 form of retinitis pigmentosa is caused as a result of 'haploinsufficiency' for the normal *IMPDH1* gene product. Rather, disease pathology is probably caused by a dominant-negative phenotypic effect exerted by mutant protein.

5.4 DISCUSSION

The RP10 gene was initially localized on chromosome 7q as a result of a systematic genetic linkage study mounted on DNA from a large Spanish family (Jordan *et al.,* 1993). Mutations within the *IMPDH1* gene have been found to cause the RP10 form of autosomal dominant RP (Kennan *et al.,* 2002; Bowne *et al.,* 2002). This genetic sub-type of disease may account for up to 5% of autosomal dominant cases of RP, or 20,000-30,000 cases world-wide at the present time (Daiger *et al.,* 2003). Studies on two mutant IMPDH1 proteins show that there are no detectable differences in enzyme activity compared to wild-type, but that a substantial difference in solubility between wild-type and mutant proteins is observable in both bacterial and mammalian cells. These observations are supported by perturbations in protein structure predicted by computer modeling of mutant IMPDH1 structure.

In situ hybridisation studies clearly demonstrate high levels of *IMPDH1* expression within the photoreceptor cell layer of mouse retinas. The retina has the highest metabolic rate of any tissue of the body, photoreceptors having a particularly high requirement for GTP in visual transduction processes (La Cour, 2002). Therefore, depletion of the GTP pool over time is the most likely explanation for the reduction in ERG amplitudes seen in the retinas of older *Impdh1*$^{-/-}$ mice. These animals represent the first murine model of a retinopathy in which a targeted deletion of a dominant RP-associated gene does not result in physical degeneration of the photoreceptors, in contrast, for example, to animals carrying targeted disruptions of the *rhodopsin, rds-peripherin, Rp1* or *Crx* genes (Humphries *et al.,* 1997; Sanyal *et al.,* 1980; Gao *et al.,* 2002; Furukawa *et al.,* 1999). In each of these mouse models there is a marked reduction in ERG amplitude or completely diminished ERG response by two months of age, and significant or complete degeneration of the outer nuclear layer by three months. The *IMPDH1* gene, when absent, causes a very different and milder retinopathy to those described previously, displaying normal ERG amplitudes up to 6 months and little to no retinal degeneration up to 10 months of age.

In the light of such observations, it appears unlikely that the autosomal dominant segregation pattern which is characteristic of the RP10 form of retinitis pigmentosa is caused as a result of 'haploinsufficiency' for the normal *IMPDH1* gene

product. Rather, disease pathology, at least in the case of the two mutations investigated in this study, is probably caused by a dominant-negative phenotypic effect exerted by misfolded or aggregated mutant protein. It is possible that the mutations examined affect normal IMPDH1 tetramer formation, and mutant forms of protein may also interfere with wild-type tetramer formation, but even taking this into account, the lack of a rapid retinopathy in *Impdh1*$^{-/-}$ mice suggests that simply a lack of functional IMPDH1 is not the sole cause of degeneration in this form of RP.

Similar differences in solubility have been demonstrated previously in relation to RP-associated proteins as in the case of the splicing factor mutant PRPF31 (Deery *et al.,* 2002) as well as folding defects associated with rhodopsin mutations (Kaushel & Khorana, 1994; Liu *et al.*, 1996; Hwa *et al.,* 2001). Many studies have been carried out on the structural implications of mutations in rhodopsin, and aggresome formation in mammalian cells resulting from rhodopsin point mutations have recently been demonstrated (Saliba *et al.,* 2002; Illing *et al.,* 2002). Hence, in RP10, mutant IMPDH1 protein misfolding and subsequent aggregation appears to be a central event in the initiation of neuronal cell death, as it is in a range of other hereditary or multifactorial neurodegenerative diseases including Alzheimer disease, Parkinson disease and amylotrophic lateral sclerosis (ALS) (Bence *et al.*, 2001; Sherman & Goldberg, 2001).

Recent findings suggest that neurons are particularly susceptible to mis-folded proteins, that form aggregates which are then targeted for ubiquitin-dependent destruction by the proteosome (Kopito, 2000; Sherman & Goldberg, 2001; Berke & Paulson, 2003). The exact mechanism by which aggregation of mutant proteins causes cell death remains elusive, but protein aggregates have been shown to impair the functioning of the ubiquitin-proteosome system, which may cause cellular disregulation and subsequent cell death (Bence *et al.,* 2001; Bucciantini *et al.,* 2002). AdRP can now been linked to this broad class of diseases and displays many common features including defective protein folding and aggregation, ubiquitinylation of mutant protein and similar delayed onset patterns (Saliba *et al.,* 2002; Illing *et al.,* 2002). RP differs however, in that there are no overt inclusion bodies or aggresomes detected in the photoreceptors of RP retinas. While aggregates can be defined by poor solubility and non-native protein secondary structure, inclusion bodies are microscopically distinct regions into which aggregates can be sequestered, while a micro-tubule dependent inclusion body is termed an aggresome (Kopito, 2000). Aggresomes or inclusion bodies are pathogenic features of cellular degeneration in most neurodegenerative

diseases such as Lewy bodies in Parkinson's disease, and hyaline inclusion bodies in ALS (Kopito, 2000). It has been shown however, as in the case of ALS, that aggregates of superoxide dismutase (SOD) mutant protein are sufficient to cause the early cellular pathology of motor neuron cell death, with the formation of inclusion bodies occurring several months afterwards (Johnson *et al.,* 2000). Therefore it is thought that the formation of aggregates is sufficient to manifest disease symptoms and the onset of neurodegeneration, but the issue of whether aggregates or inclusion bodies are directly cytotoxic still remains under debate (Berke & Paulson, 2003). It has been suggested that the absence of inclusion body formation in adRP degenerating retinas may be explained by the lack of a microtubule mechanism to sequester aggregated proteins in aggresomes (a process that could perhaps facilitate their degradation), which could lower the threshold for aggregate toxicity. Alternatively, photoreceptor neurons may have an increased capacity to eliminate damaged cells, so they could be destroyed before or immediately after the formation of inclusion bodies or aggresomes (Illing *et al.,* 2002; Saliba *et al.,* 2002). It is not clear why the only neurons affected by mutant IMPDH1 proteins are the photoreceptors, but it is most likely due to the higher expression levels of *IMPDH1* in these cells.

In light of the mild retinal disease phenotype and preserved photoreceptor structure in *Impdh1*$^{-/-}$ animals, it may be of interest to examine whether active site or recessive mutations in IMPDH1 could contribute to milder, later-onset retinal diseases such as AMD. One mutation in the active site region of the IMPDH1 gene has been reported to date with one affected family member diagnosed as having AMD (Table 5.2). However, information on the severity of symptoms in additional family members is not available at present.

The observations reported here clearly suggest a novel approach to therapy for RP10 patients, which, in principle, could slow the progression of the disease substantially. While the *IMPDH1* gene was implicated in disease etiology only within the last two years, the number of mutations identified within the gene in patients with RP is already rising (Table 5.3). Hence suppression strategies targeting individual mutations are unlikely to be viable in economic terms. In relation to autosomal dominant disease, the RP10 form of retinal degeneration represents an attractive therapeutic target for two reasons. Firstly, only a single suppression step, involving simultaneous silencing of both normal and mutant alleles of the *IMPDH1* gene would, in principle, be sufficient to remove the major dominant negative pathological effect of

mutant IMPDH1 protein, leaving a situation in which photoreceptor neurons continue to survive and remain sufficiently functional such as to provide useful vision, possibly well into adult life. Secondly, while gene silencing using RNA interference is now an established technique in mammalian systems (McManus & Sharp, 2002), discrimination between normal and mutant transcripts at the level of single nucleotides has so far met with only partial success (Miller *et al.*, 2003). In the case of the therapeutic approach outlined here, such constraints do not apply, since there is not a requirement to target single base changes.

It is notable that the data obtained from this study also suggest that delivery to ocular tissues of XMP or GTP (using, for example the technique of iontophoresis) might provide sufficient supplementation of these compounds such as to fully restore function in remaining photoreceptors of RP10 patients. The availability of both small and large animal RP10 models would be of substantial value in future explorations of such therapeutic strategies.

5.5 CONCLUSION

The previous chapter has described the identification of a novel gene implicated in autosomal domainant RP called IMPDH1. This is the first gene in the guanine nucleotide biosynthesis pathway to be associated with retinal disease. Results from functional studies suggest that mutations do not affect the enzymatic activity of mutant IMPDH1 proteins, at least in the case of the two mutations investigated in this study. Rather, these mutations within IMPDH1 are predicted to cause a dominant-negative pathology, which is likely brought about through aberrant protein folding and the formation of insoluble aggregates within the cell cytosol. Results from the histological and functional analysis of the *Impdh1*$^{-/-}$ mouse retina show normal retinal function in these animals up to 8 months of age, which supports the proposed dominant negative phenotypic effect of mutant protein. These data go some way towards explaining the molecular pathology of RP caused by mutations within the IMPDH1 gene, but additional work will be required to investigate the exact mechanism of degeneration and possible biochemical and molecular pathways involved.

5.6 FUTURE WORK

The work described in this study on the molecular mechanisms of photoreceptor degeneration in RP10 has introduced many potential avenues for future investigation. The *Impdh1*$^{-/-}$ mouse model will likely feature in a number of studies. Future and current projects include the construction of a mutant IMPDH1 transgene for use in the generation of transgenic mice, in an attempt to mimic the human form of adRP caused by mutations within IMPDH1 in a mouse model. It is expected that these mice should exhibit a considerably more rapid retinopathy than the *Impdh1*$^{-/-}$ model. Mice expressing mutant IMPDH1 protein would be of enormous benefit in testing potential gene therapies, one of which may include RNA interference or ribozyme cleavage of mutant and wild-type transcript, with possible supplementation with XMP or GTP in the retina.

It would be of interest also to investigate further the behaviour of wild-type and mutant IMPDH1 proteins in cell culture systems. A demonstration of aggresome formation following transfection of mutant IMPDH1 protein into mammalian cells would lend further support to the conclusions drawn in this study. It may also be possible to detect interactions with other, as yet, unidentified proteins or apoptosis–related pathways that are activated upon synthesis of mutant IMPDH1 protein in a cell culture system. A screen of the IMPDH1 gene in an increased number of dominant RP patients may identify a greater number of pathogenic mutations. It is also possible that a screen of the gene in milder RP or AMD patients may reveal a greater involvement of IMPDH1 in different forms of retinal degenerative disease.

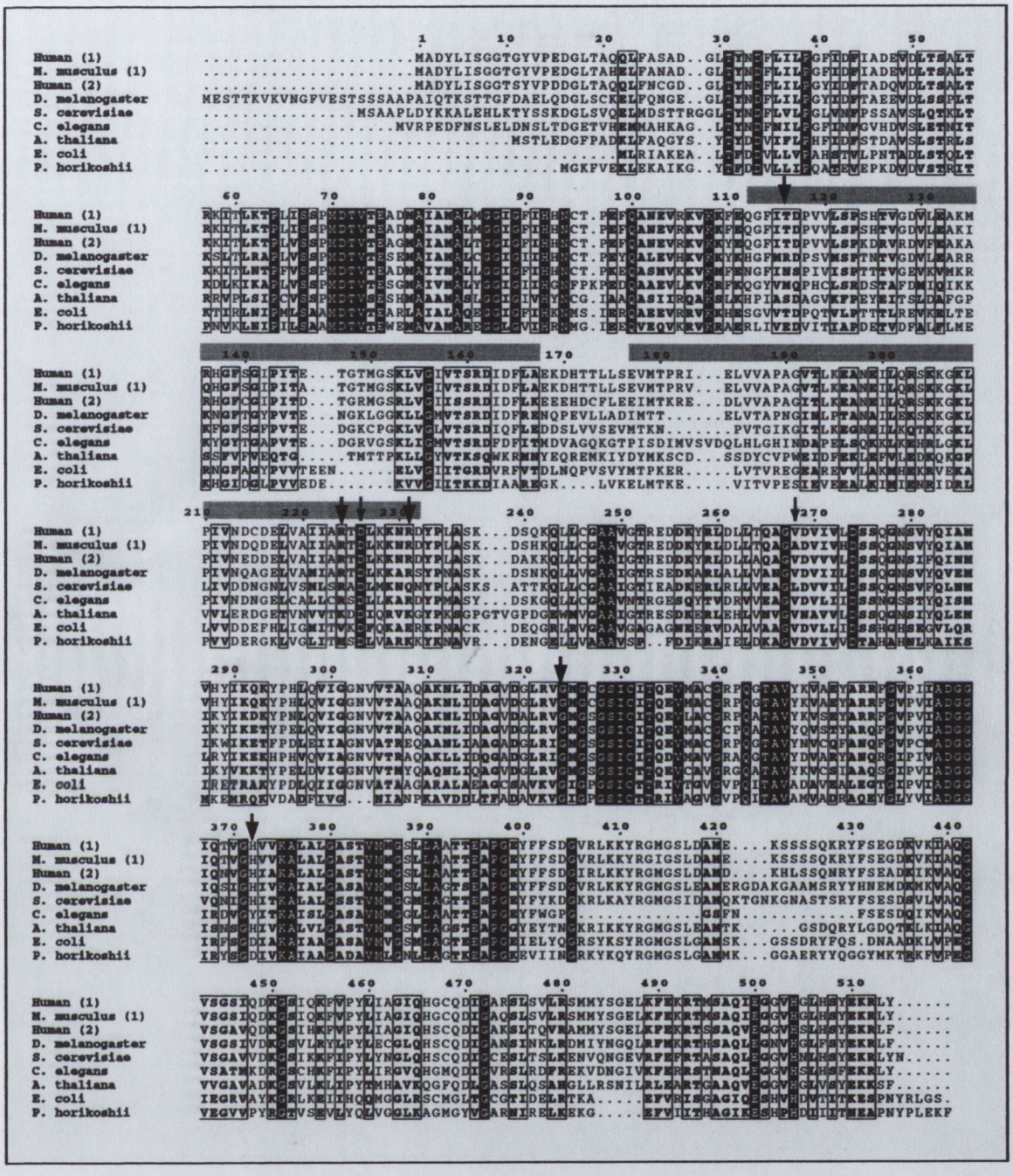

Figure 5.1. Alignment of IMPDH protein sequences from a range of organisms (adapted from Bowne *et al.*, 2002). Sequence numbering is based on human IMPDH1. Completely conserved residues are shown as white letters on a black background; highly conserved residues are boxed. Grey bars indicate the two CBS domains and arrows indicate location of mutations identified to date.

Swiss prot Accession Numbers: Human (1) (imd1_human,P20829), *Mus musculus* (1) (imd1_mouse, P50096), Human (2) (imd2_human, P12268), *Drosophila melanogaster* (imdh_drome, Q07152), *Saccharomyces cerevisiae* (imh1_yeast, P38697), *Caenorhabditis elegans* (PIR T3709), *Arabidopsis thaliana* (imh1_arath, P47996), *E.coli* (imdh_ecoli, P06981) and *Pyrococcus horikoshii* (impd_pyrho, O58045).

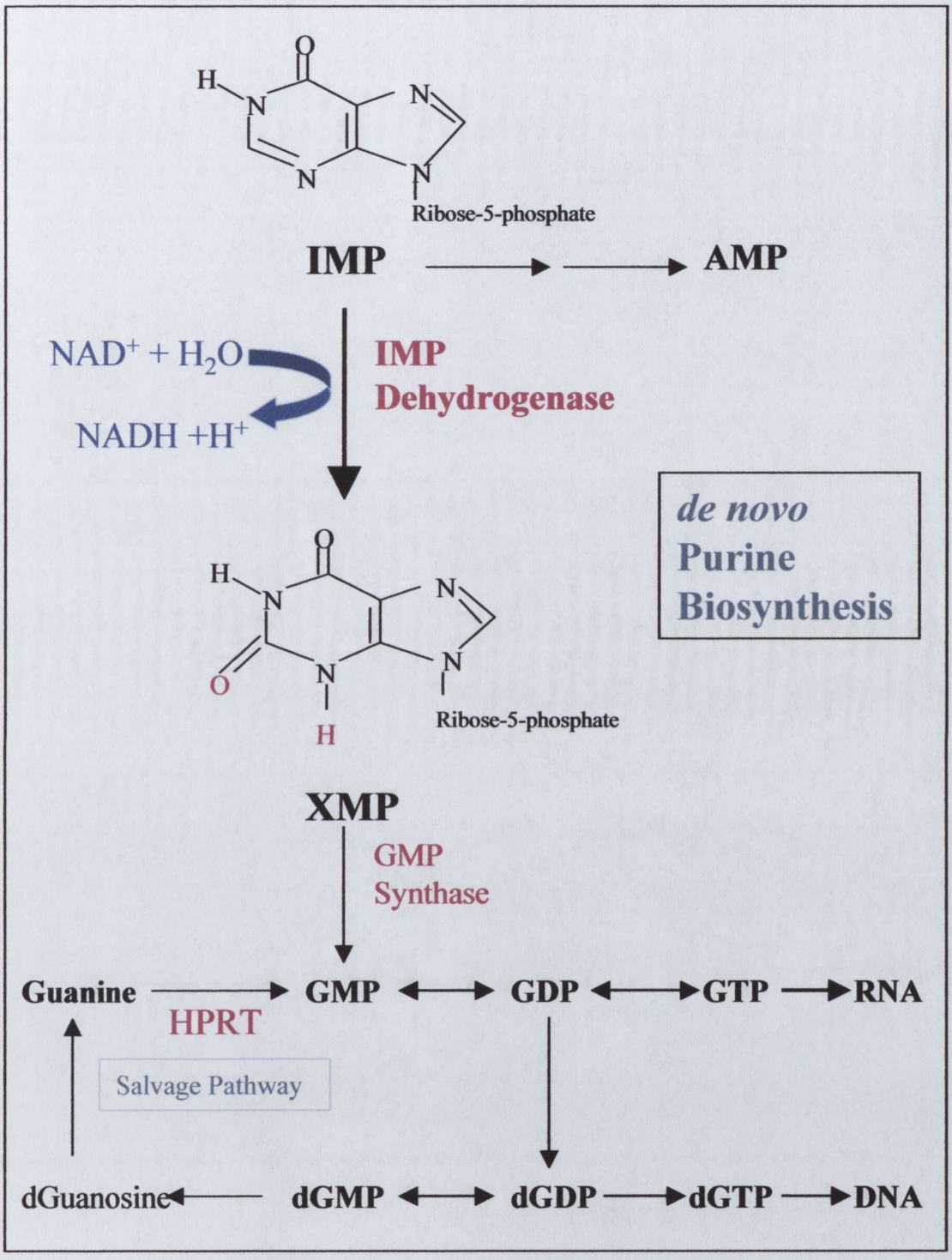

Figure 5.2. Schematic representation of the guanine nucleotide biosynthetic pathway. IMPDH catalyses the conversion of IMP to XMP with the concomitant reduction of NAD+ to NADH. The enzyme HPRT is involved in the salvage pathway.

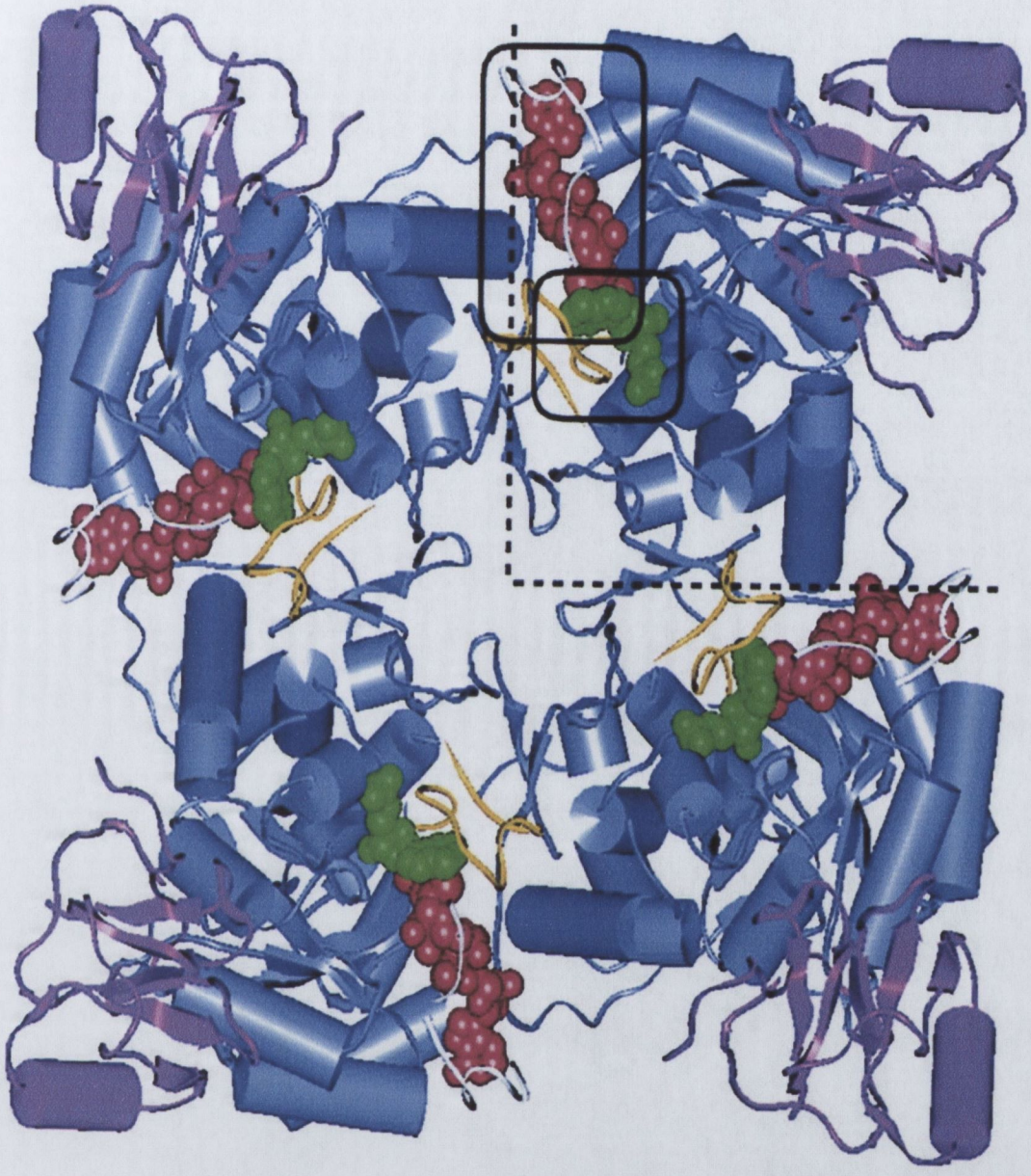

Figure 5.3. Structure of human Type II IMPDH tetramer with bound dinucleotide analogue SAD (circled, red) and substrate analogue 6-Cl-IMP (circled, green). The dinucleotide binds at the monomer-monomer interface (dotted lines). The following structures are illustrated: catalytic β-barrel domain (blue), flanking domain (magenta), active site loop (yellow) and active site flap fragments (white). (Figure taken from Colby *et al.,* 1999).

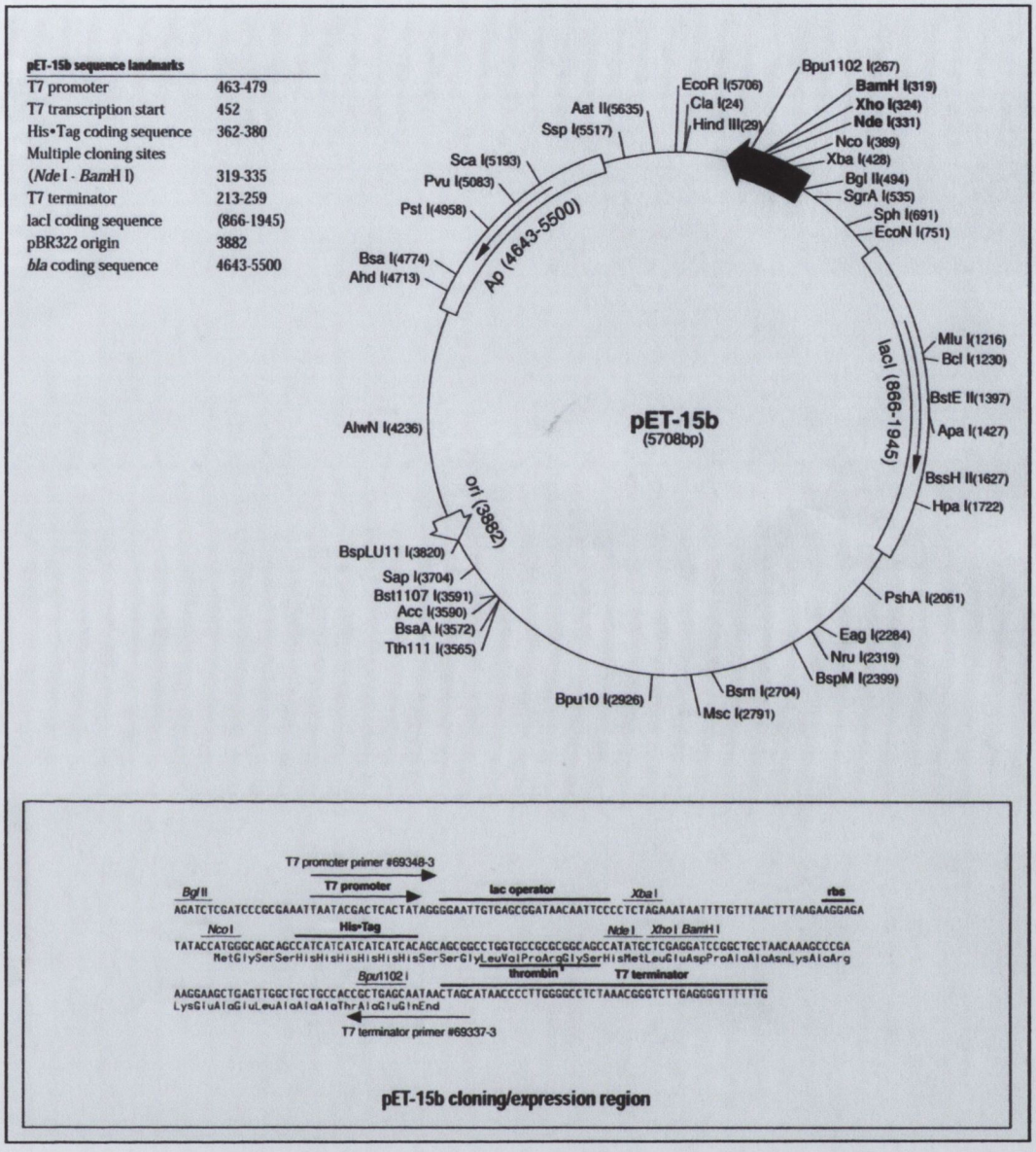

Figure 5.4. Diagramatic representation of the pET-15b bacterial expression vector which is under the control of the T7 promoter (Novagen). The IMPDH1 cDNA was cloned into the *Xho1* site, so that it was in-frame with the ATG start site and N-terminus His-tag following translation into protein.

(A) Wild-type IMPDH1

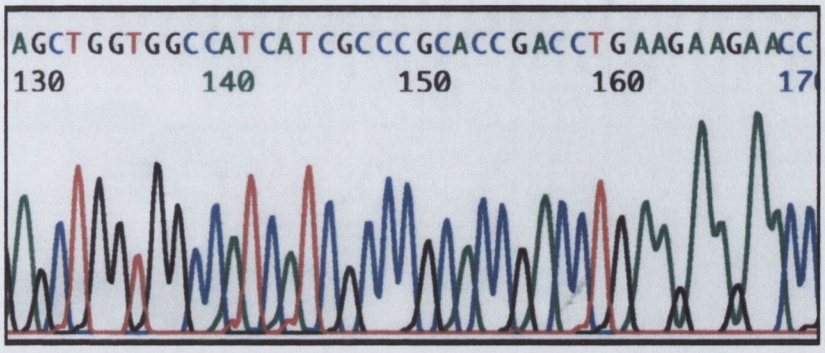

(B) Arg224Pro Mutant

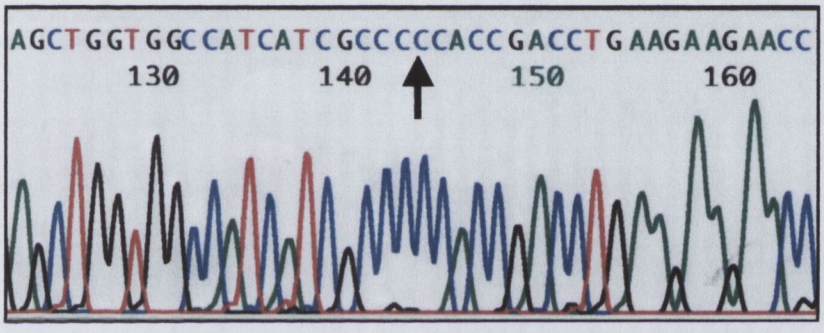

(C) Asp226Asn Mutant

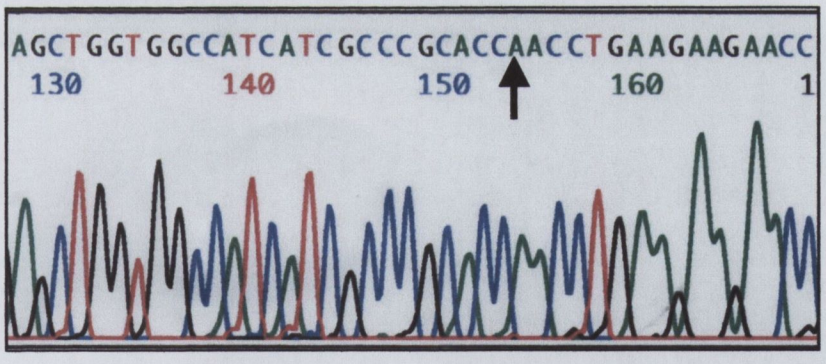

Figure 5.5. Automated sequencing of **(A)** Wild-type **(B)** Arg224Pro and **(C)** Asp226Asn IMPDH1 cDNA sequences in the pET-15b vector (Novagen). The two mutations shown in **(B)** and **(C)** were introduced by site-directed mutagenesis. Sequencing of all three pET-15b vectors was carried out using the IMPDH1 Ex 5F cDNA primer.

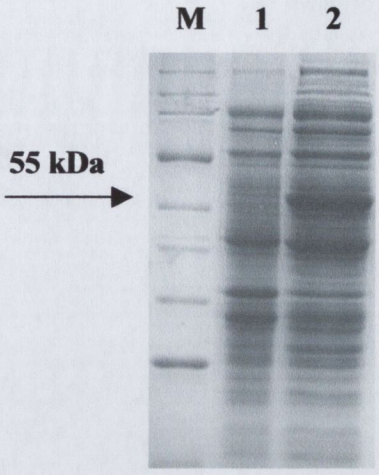

Figure 5.6. SDS-PAGE analysis with Coomassie blue staining of total cell protein (TCP) extracts from *E. coli* cells over-expressing IMPDH1 protein. Lanes; M, molecular weight marker; 1, Pre-induction TCP; 2, Post-induction TCP.

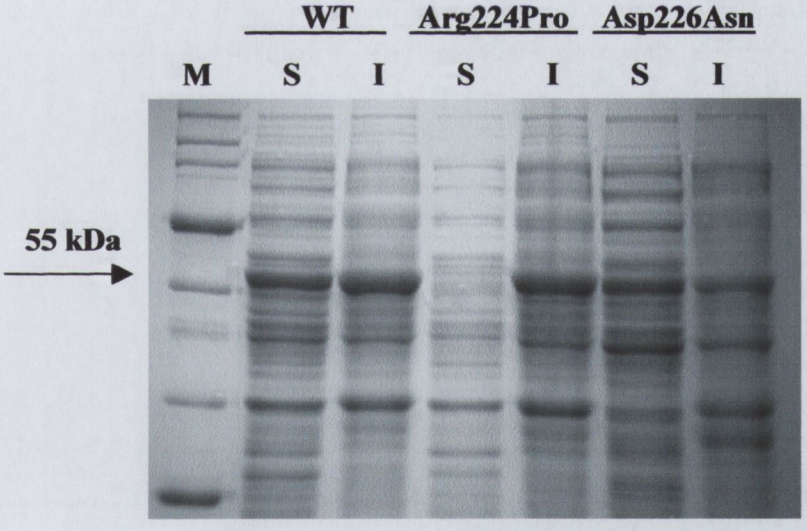

Figure 5.7. SDS-PAGE analysis of total cell lysates from E.coli expressing IMPDH1 proteins at 37°C with Coomassie Blue staining.

M, Marker ; S, Soluble fraction; I, Insoluble fraction; WT, wild-type IMPDH1; Arg224Pro & Asp226Asn, Mutant IMPDH1 proteins.

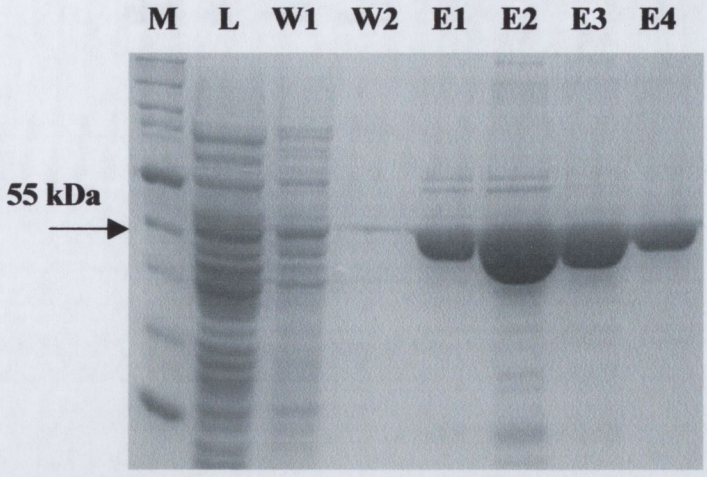

Figure 5.8. SDS-PAGE analysis of His-tag purified IMPDH1 protein (WT) extracts. Lanes: M, Marker; L, Soluble cell lysate; W1-W2, Column washes with Ni-NTA wash buffer; E1-E4, Stepwise elutions collected from His-tag purification resin following addition of Ni-NTA elute buffer.

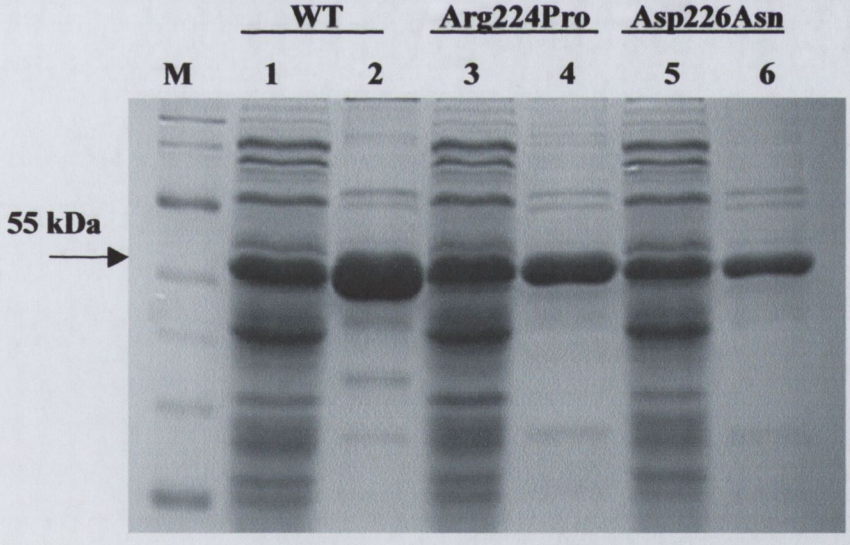

Figure 5.9. SDS-PAGE analysis of *E.coli* soluble cell lysates before and after His-tag purification.

Lanes: M, Molecular weight marker; 1,3, 5, Soluble cell lysates following induction with IPTG at 25°C for 5 hours; 2, 4, 6, His-tag purified IMPDH1 proteins.

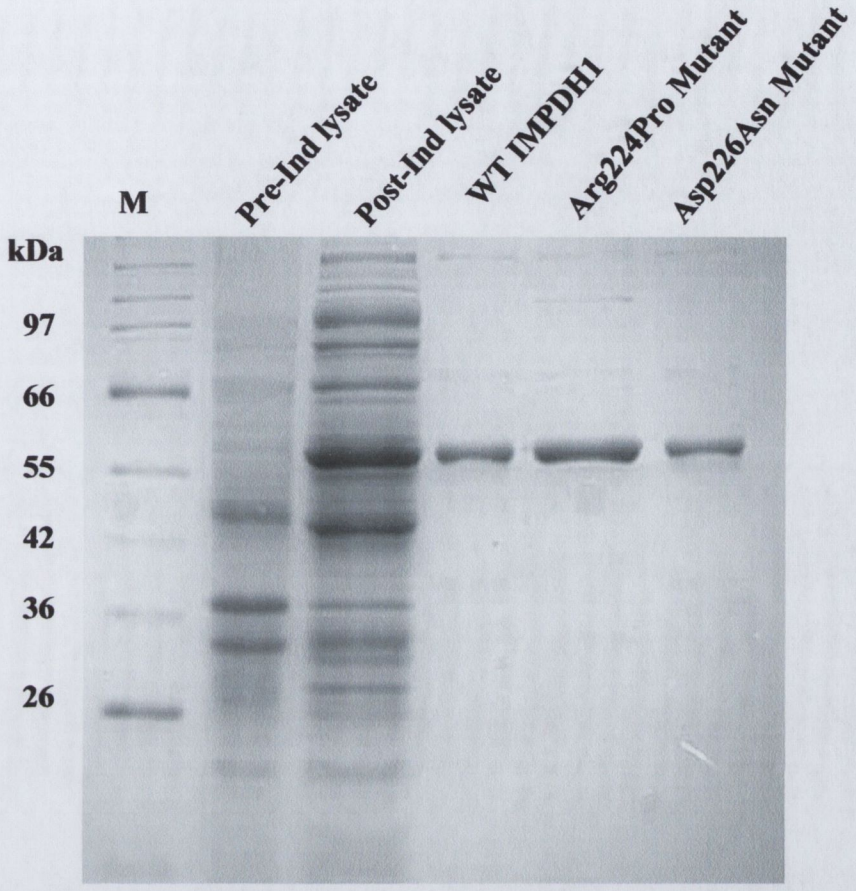

Figure 5.10. Expression and purification of IMPDH1 protein in *E.coli.*

SDS-PAGE analysis with Coomassie staining of total cell lysates and 15μg His-tag purified IMPDH1 proteins.

M, Molecular weight marker; Pre-induction total cell lysate; Post-induction wild-type (WT) soluble cell lysate; His-tag purified WT IMPDH1; Arg224Pro IMPDH1; Asp226Asn IMPDH1

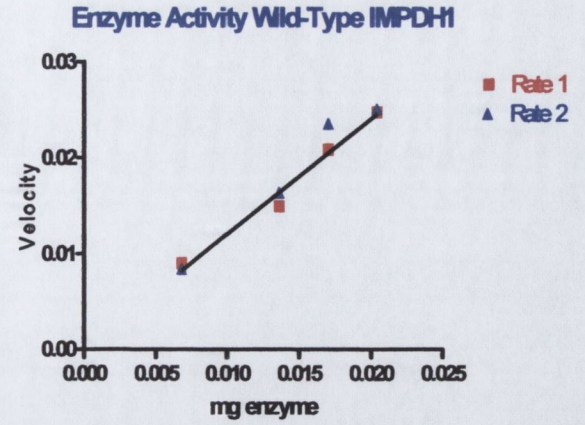

Specific Activity µmol /min/mg

1.22

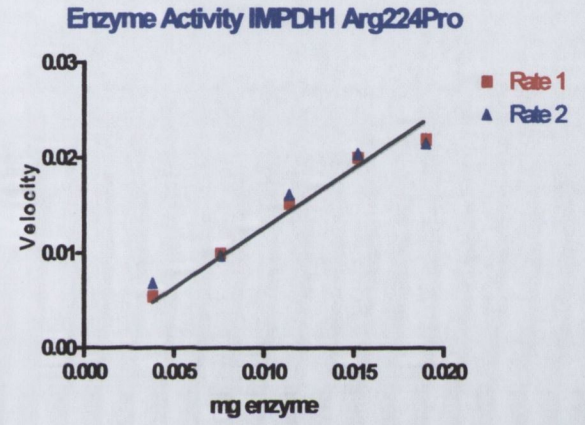

1.30

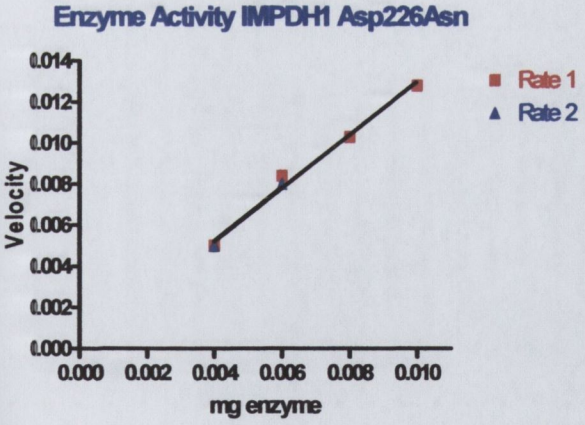

1.28

Figure 5.11. Graphs showing enzyme activity reaction rates of wild-type and mutant IMPDH1 proteins measured over 1 minute (and calculated using Cary WinUV software), versus quantity of enzyme added per reaction (mg). Repeat enzyme activity measurements were carried out for each quantity of enzyme added. Specific activity in µmol/min/mg or U/mg was calculated for each enzyme (Specific Activity = Velocity/mg enzyme).

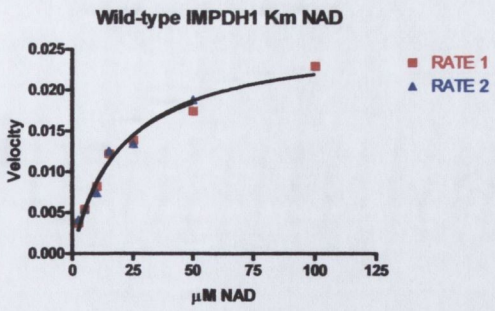

WT (2) 2.5-100 uM NAD	RATE 1	RATE 2
Michaelis-Menten		
Best-fit values		
VMAX	0.02643	0.02550
KM	20.67	19.23

Kcat =Vmax = µmol min^{-1}

[Et] µmol

WT IMPDH1

0.0136mg = 0.000245 µmol IMPDH1

Kcat = 0.025 = 102.04 min^{-1} = **1.7 sec^{-1}**

0.000245

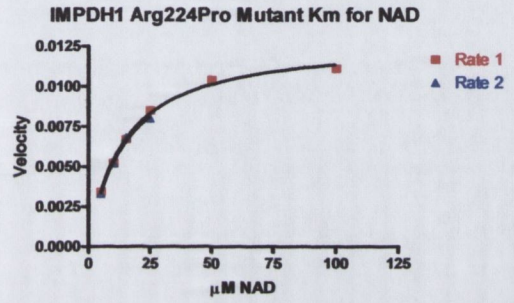

	Rate 1	Rate 2
Michaelis-Menten		
Best-fit values		
VMAX	0.01294	0.01253
KM	13.89	13.64

Arg224Pro IMPDH1

0.0076 mg = 0.000136 µmol IMPDH1

Kcat = 0.0129 = 92.8 min^{-1} = **1.58 sec^{-1}**

0.000136

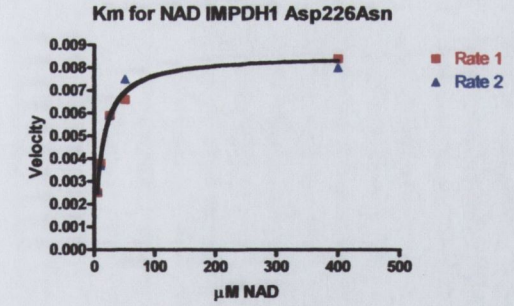

mut2 226 17-07-03	Rate 1	Rate 2
Michaelis-Menten		
Best-fit values		
VMAX	0.008557	0.008552
KM	12.36	11.38

Asp226Asn IMPDH1

0.005 mg = 0.0009 µmol IMPDH1

Kcat = 0.0086 = 95.55 min^{-1} = **1.6 sec^{-1}**

0 .000108

Figure 5.12. Graphs showing µM NAD in reaction buffer versus measured rate of reaction for calculation of Km [NAD] values. Two reaction rates were measured at each concentration of NAD. All graphs were drawn using Graphpad Prism software. Kcat or catalytic rate constant values were calculated for wild-type, Arg224Pro and Asp226Asn IMPDH1 enzymes. [Et] = Total enzyme concentration.

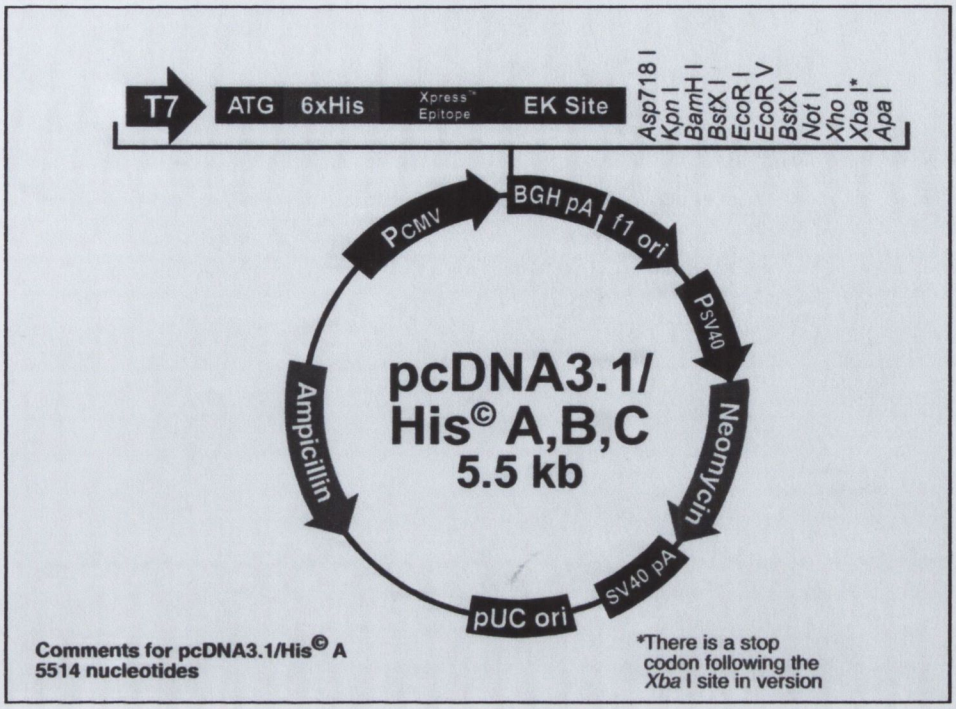

pcDNA3.1/His© C MCS

T7 promoter priming site

```
839  CACTGCTTAC TGGCTTATCG AAATTAATAC GACTCACTAT AGGGAGACCC AAGCTGGCTA
```

Hind III — Polyhistidine (6xHis) region

```
899  GCGTTTAAAC TTAAGCTTAC C ATG GGG GGT TCT CAT CAT CAT CAT CAT CAT
                             Met Gly Gly Ser His His His His His His

950  GGT ATG GCT AGC ATG ACT GGT GGA CAG CAA ATG GGT CGG GAT CTG TAC
     Gly Met Ala Ser Met Thr Gly Gly Gln Gln Met Gly Arg Asp Leu Tyr
```

Xpress™ Epitope — *Asp*718 I — *Kpn* I — *Bam*H I — *Bst*X I* — *Eco*R I

```
998  GAC GAT GAC GAT AAG GTA CCA GGA TCC AGT GTG GTG GAA TTC TGC AGA
     Asp Asp Asp Asp Lys Val Pro Gly Ser Ser Val Val Glu Phe Cys Arg
```

Enterokinase recognition sequence — EK cleavage site

*Eco*R V — *Bst*X I* — *Not* I — *Xho* I — *Xba* I — *Apa* I

```
1046 TAT CCA GCA CAG TGG CGG CCG CTC GAG TCT AGA GGG CCC GTT TAA
     Tyr Pro Ala Gln Trp Arg Pro Leu glu Ser Arg Gly Pro Val ***
```

BGH reverse priming site

```
1091 ACCCGCTGAT CAGCCTCGAC TGTGCCTTCT AGTTGCCAGC CATCTGTTGT TTGCCCCTCC
```

BGH poly (A) site

```
1151 CCCGTGCCTT CCTTGACCCT GGAAGGTGCC ACTCCCACTG TCCTTTCCTA ATAAAATGAG

1211 GAAATTGCAT
```

*Note that there are two *Bst*X I sites in the polylinker.

Figure 5.13. Diagrammatic representation of the pcDNA3.1/His C mammalian expression vector which is under the control of the CMV promoter (Invitrogen). IMPDH1 cDNA was cloned into the *Acc651 (Kpn1)* site so that it was in-frame with the ATG start site and His-tag following translation into protein.

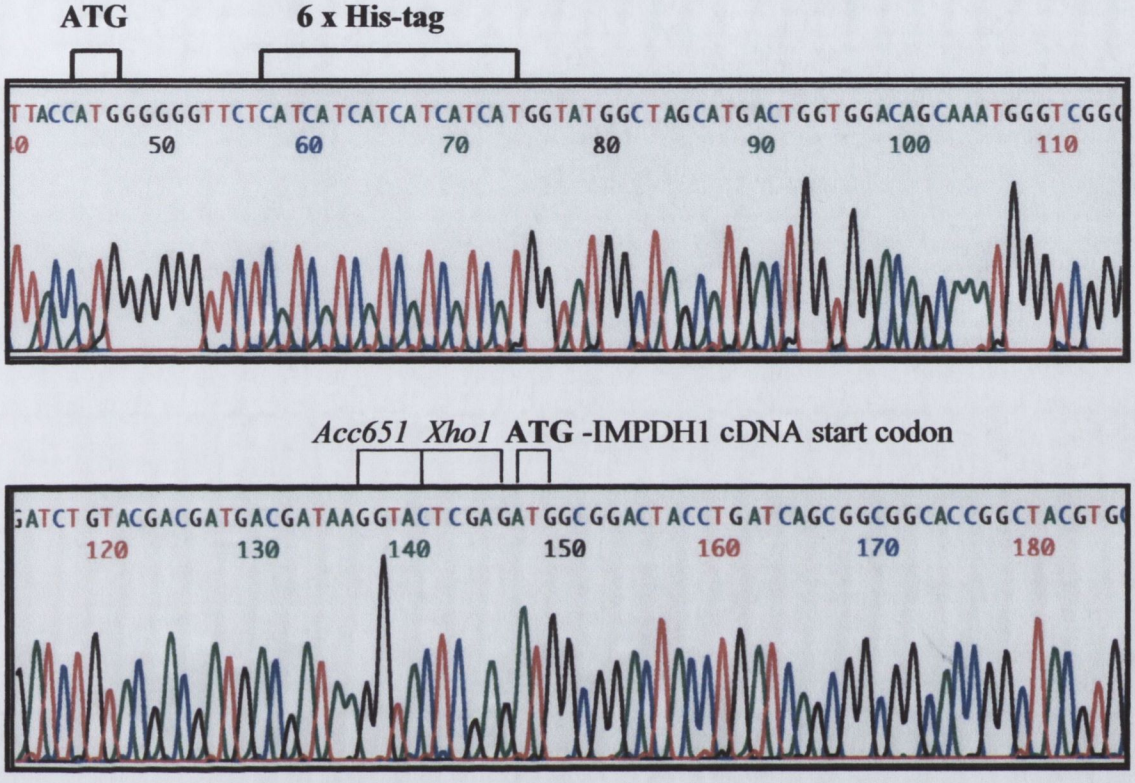

Figure 5.14. Automated sequence analysis of the pcDNA3.1/His C vector (Invitrogen) with insertion of IMPDH1 cDNA sequence into the blunted *Acc651* restriction site *(GGTACC)*. The ATG coding start site of the IMPDH1 sequence is cloned in-frame with the ATG translation start site and 6x His-tag sequence. The IMPDH1 sequence is flanked by a *Xho1 (CTCGAG)* restriction site.

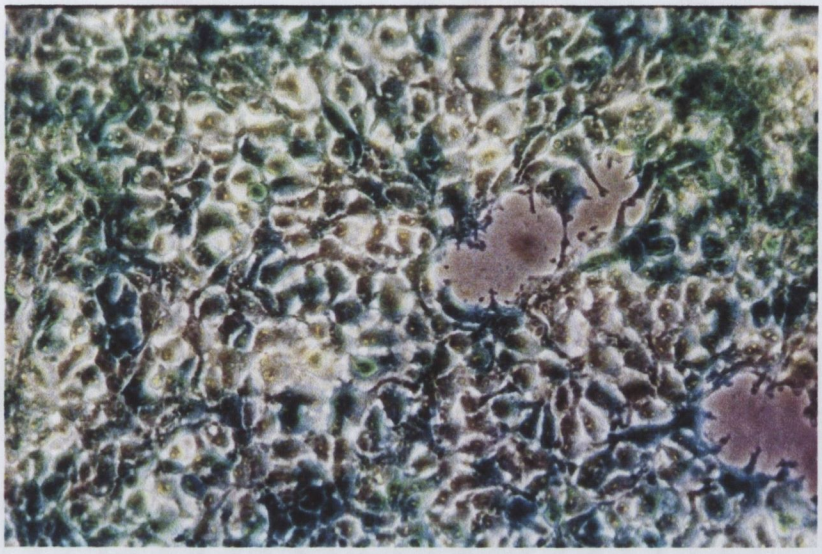

Figure 5.15. Positive transfection control in HEK293T mammalian cells. Cells were transfected with pcDNA3.1/His/LacZ vector and stained after 48 hours for β-galactosidase activity. Cells coloured blue indicates that cells are expressing desired plasmid. Transfection efficiency estimated at between 70-80%.

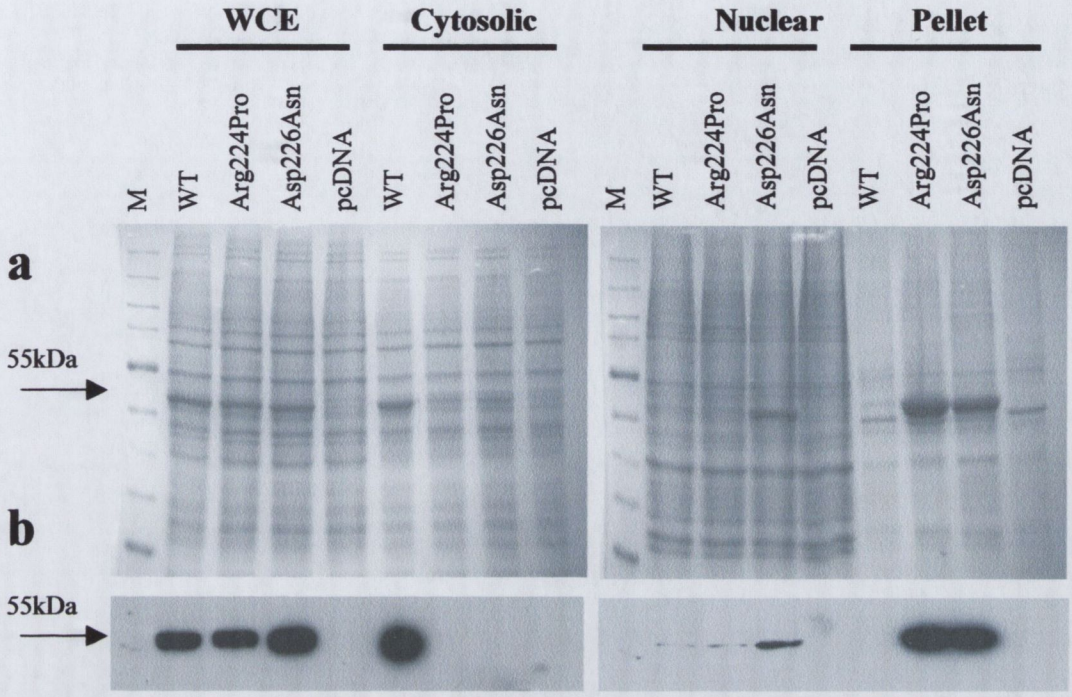

Figure 5.16. Analysis of wild-type and mutant IMPDH1 proteins expressed in HEK293T cells.

(**a**) SDS-PAGE with Coomassie Blue staining of protein extracts from cells transfected with pcDNA3.1/His constructs containing wild-type (WT), Arg224Pro and Asp226Asn mutant IMPDH1 sequences and pcDNA vector alone (negative control). Transfected cells were separated into whole cell extracts (WCE), soluble cytosolic fraction, nuclear fraction and final pelleted fraction (see materials and methods). M = Molecular mass marker.

(**b**) Western blotting of identical gel with protein transfer onto nitrocellulose membrane and probed with Anti-His antibody and HRP-conjugated secondary antibody. M = 50kDa His-tag protein positive control.

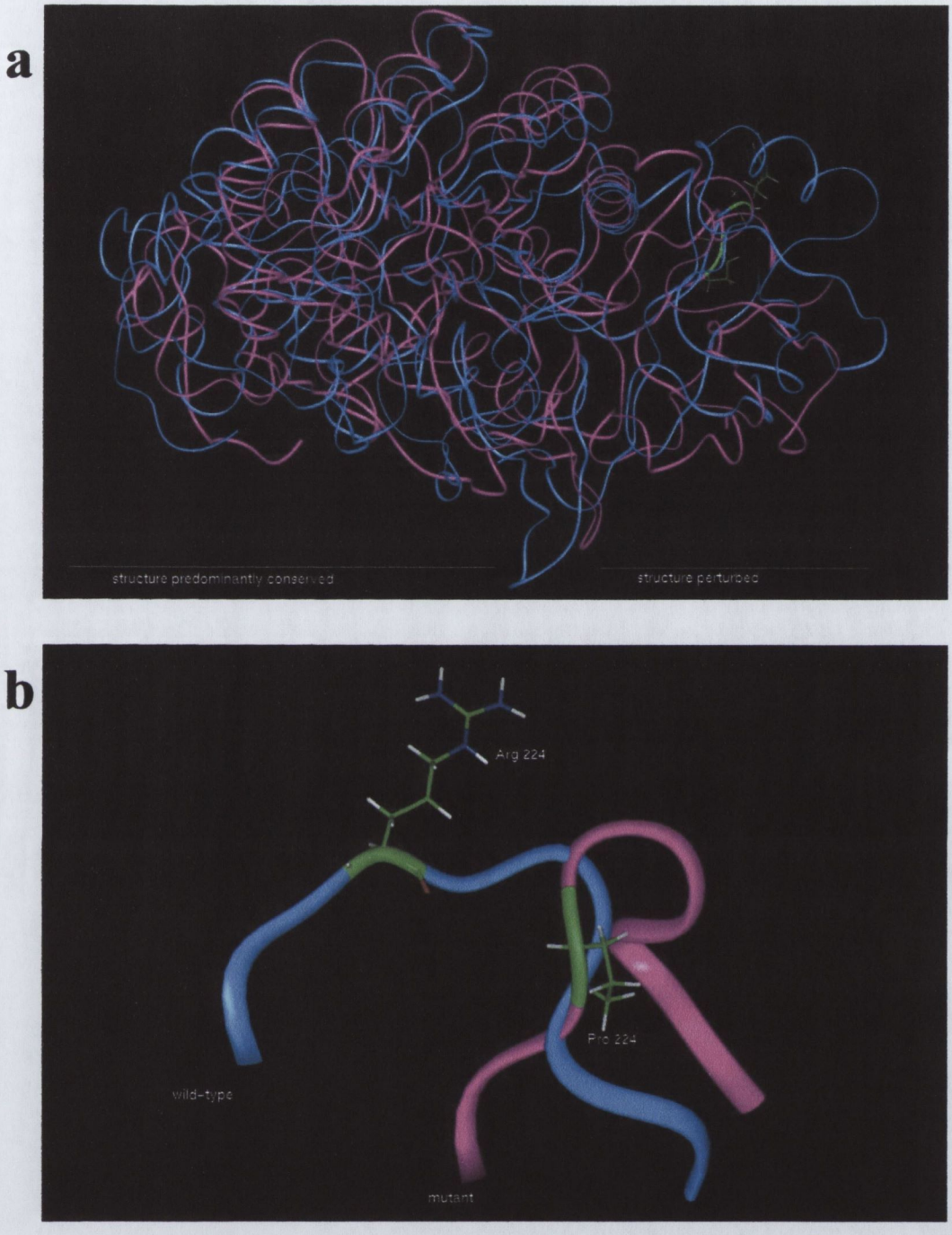

Figure 5.17. Computer molecular modelling studies of IMPDH1

(a) Endpoint comparison of molecular dynamics simulation run for wild-type (blue) and mutant (pink) homology models of human IMPDH1. **(b)** Model of mutant product (pink) exhibits significant predicted structural perturbation in region of Arg to Pro point mutation when compared to model of wild-type protein (blue). The Arg to Pro mutation in the 'bud' or flanking region is highlighted in green in both models. Protein homology figures supplied by Dr.. David Lloyd.

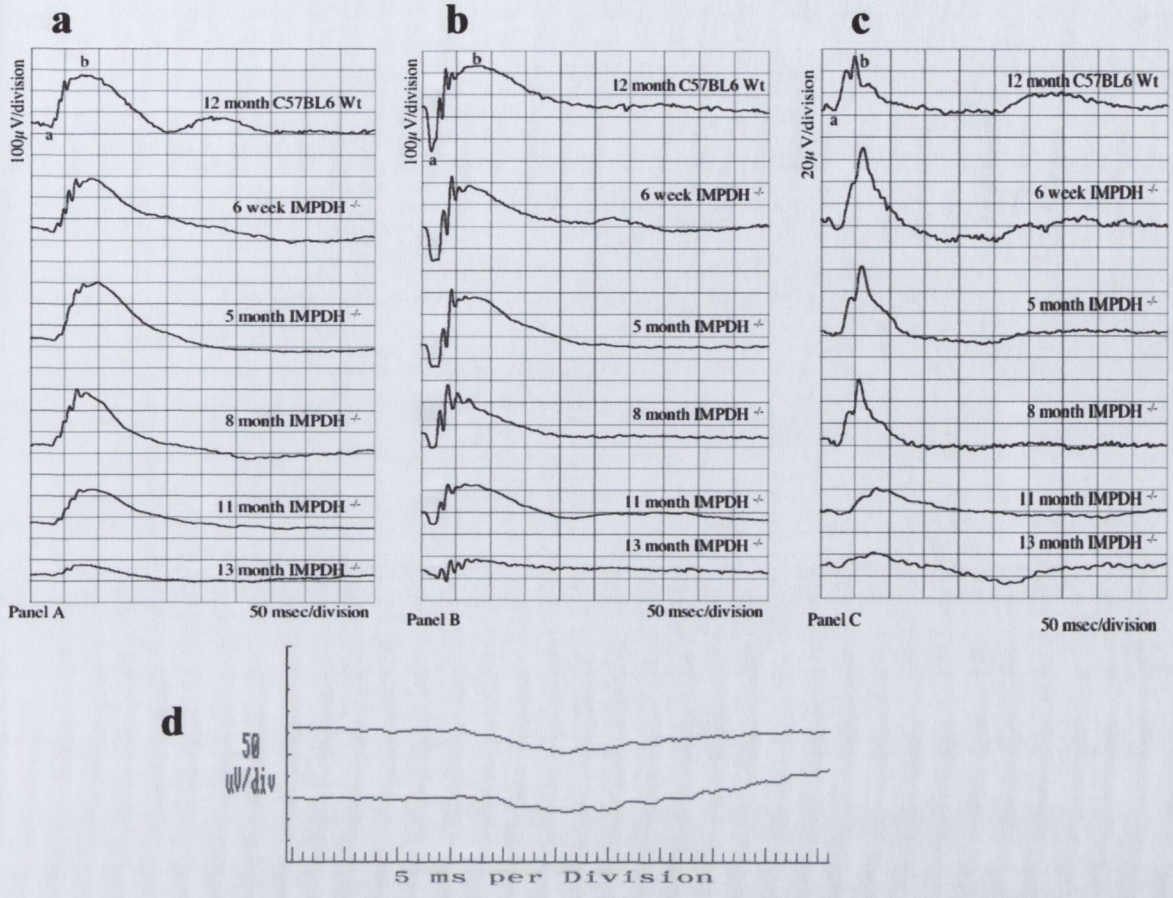

Figure 5.18. ERG analysis in *Impdh1*$^{-/-}$ mice.

(**a**) Rod-isolated responses, (**b**) maximal, dark-adapted, combined rod and cone responses and (**c**) light-adapted cone responses to single flash, were recorded in a 12-month C57 wild-type animal, and *Impdh1*$^{-/-}$ animals at 6 weeks of age, 5 months, 8 months, 11 months and 13 months. At 11 months of age all responses showed a significant reduction in a- and b- wave amplitudes and, in the case of the cone responses, significant delay in b wave timing. Further deterioration was noted by 13 months. In the case of the maximal, dark-adapted, combined rod and cone responses progressive reduction in a-wave amplitude was noted from 5 months of age indicating disturbance of phototransduction. (**d**) ERG analysis of combined rod and cone response in a 17-year old affected patient harbouring an Arg224Pro IMPDH1 mutation shows completely diminished responses.

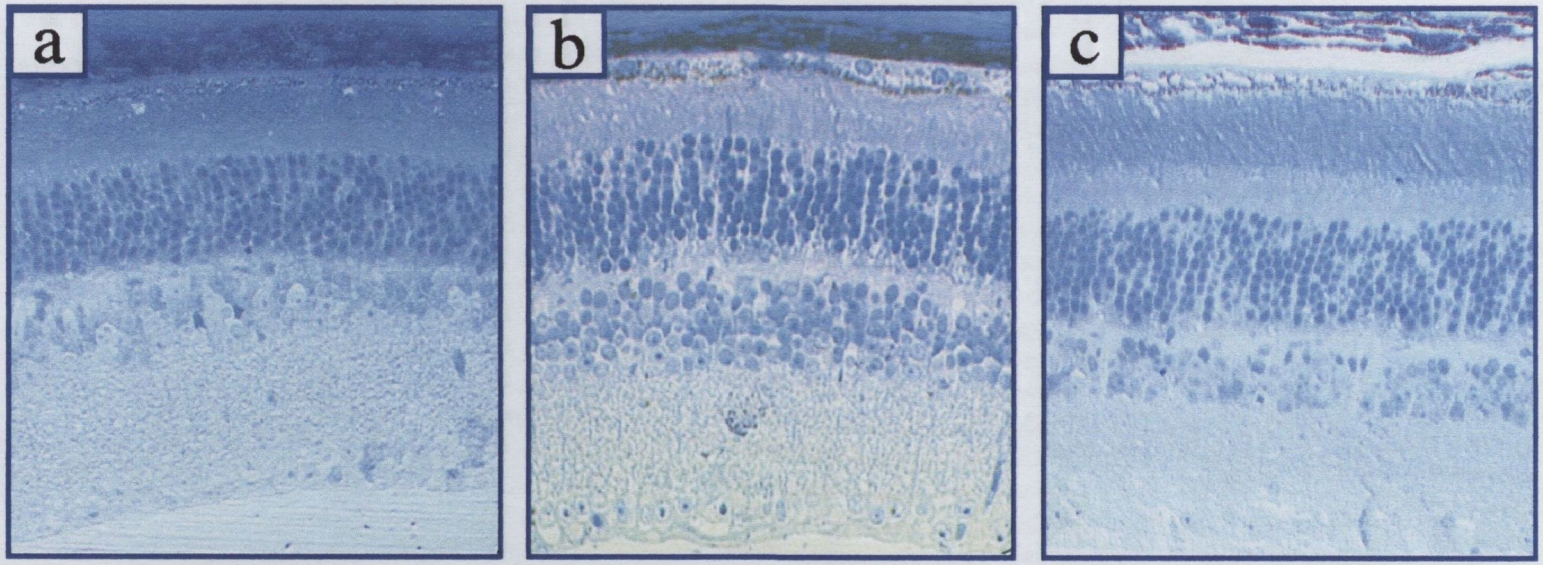

Figure 5.19. Light micrographs of retinal sections from *Impdh1*$^{-/-}$ mice.

Sections shown are (**a**) 6 month *Impdh1*$^{-/-}$, (**b**) 10 month *Impdh1*$^{-/-}$, (**c**) 10 month wild-type C57/BL6. The outer nuclear layer thickness of *Impdh1*$^{-/-}$ retina is virtually indistinguishable to that of wild-type up to 10 months of age.

REFERENCES

Abe, S., Katagiri, T., Saito-Hisaminato, A., Usami, S., Inoue, Y., Tsunoda, T. and Nakamura, Y. (2003) Identification of CRYM as a candidate responsible for nonsyndromic deafness, through cDNA microarray analysis of human cochlear and vestibular tissues. *Am J Hum Genet*, **72**, 73-82.

Acland, G.M., Aguirre, G.D., Ray, J., Zhang, Q., Aleman, T.S., Cideciyan, A.V., Pearce-Kelling, S.E., Anand, V., Zeng, Y., Maguire, A.M., Jacobson, S.G., Hauswirth, W.W. and Bennett, J. (2001) Gene therapy restores vision in a canine model of childhood blindness. *Nat Genet*, **28**, 92-95.

Adato, A., Vreugde, S., Joensuu, T., Avidan, N., Hamalainen, R., Belenkiy, O., Olender, T., Bonne-Tamir, B., Ben-Asher, E., Espinos, C., Millan, J.M., Lehesjoki, A.E., Flannery, J.G., Avraham, K.B., Pietrokovski, S., Sankila, E.M., Beckmann, J.S. and Lancet, D. (2002) USH3A transcripts encode clarin-1, a four-transmembrane-domain protein with a possible role in sensory synapses. *Eur J Hum Genet*, **10**, 339-350.

Ahmed, Z.M., Riazuddin, S., Bernstein, S.L., Ahmed, Z., Khan, S., Griffith, A.J., Morell, R.J., Friedman, T.B. and Wilcox, E.R. (2001) Mutations of the protocadherin gene PCDH15 cause Usher syndrome type 1F. *Am J Hum Genet*, **69**, 25-34.

Ahmed, Z.M., Riazuddin, S. and Wilcox, E.R. (2003) The molecular genetics of Usher syndrome. *Clin Genet*, **63**, 431-444.

Ahn, J., Beharry, S., Molday, L.L. and Molday, R.S. (2003) Functional interaction between the two halves of the photoreceptor-specific ATP binding cassette protein ABCR (ABCA4). Evidence for a non-exchangeable ADP in the first nucleotide binding domain. *J Biol Chem.* **10**,278.

Akimoto M., Khanna H., Filippova, E., Pei, G., Mears, A.J., Turner, D.L. and Swaroop A. (2003) Myocyte enhancer factor 2c and bHLH proteins regulate the expression of NRL, the bZIP transcription factor essential for rod differentiation. *Invest. Ophthalmol. Vis. Sci.* E. abstract **44**, 3537.

Alberts, B., Bray, D., Lewis, J., Raff, M., Roberts, K. and Watson, J.D. (1983) *Molecular Biology of the Cell*. Garland Publishing Inc., New York & London.

Alfinito, P.D. and Townes-Anderson, E. (2002) Activation of mislocalized opsin kills rod cells: a novel mechanism for rod cell death in retinal disease. *Proc Natl Acad Sci U S A*, **99**, 5655-5660.

Allikmets, R., Shroyer, N.F., Singh, N., Seddon, J.M., Lewis, R.A., Bernstein, P.S., Peiffer, A., Zabriskie, N.A., Li, Y., Hutchinson, A., Dean, M., Lupski, J.R. and Leppert, M. (1997a) Mutation of the Stargardt disease gene (ABCR) in age-related macular degeneration. *Science*, **277**, 1805-1807.

Allikmets, R., Singh, N., Sun, H., Shroyer, N.F., Hutchinson, A., Chidambaram, A., Gerrard, B., Baird, L., Stauffer, D., Peiffer, A., Rattner, A., Smallwood, P., Li, Y., Anderson, K.L., Lewis, R.A., Nathans, J., Leppert, M., Dean, M. and Lupski, J.R. (1997b) A photoreceptor cell-specific ATP-binding transporter gene (ABCR) is mutated in recessive Stargardt macular dystrophy. *Nat Genet*, **15**, 236-246.

Ansley, S.J., Badano, J.L., Blacque, O.E., Hill, J., Hoskins, B.E., Leitch, C.C., Kim, J.C., Ross, A.J., Eichers, E.R., Teslovich, T.M., Mah, A.K., Johnsen, R.C., Cavender, J.C., Lewis, R.A., Leroux, M.R., Beales, P.L. and Katsanis, N. (2003) Basal body dysfunction is a likely cause of pleiotropic Bardet-Biedl syndrome. *Nature*, **425**, 628-633.

Azarian, S.M. and Travis, G.H. (1997) The photoreceptor rim protein is an ABC transporter encoded by the gene for recessive Stargardt's disease (ABCR). *FEBS Lett*, **409**, 247-252.

Barlow, D.J. and Thornton, J.M. (1988) Helix geometry in proteins. *J Mol Biol*, **201**, 601-619.

Barnes, B.J., Eakin, A.E., Izydore, R.A. and Hall, I.H. (2000) Selective inhibition of human Molt-4 leukemia type II inosine 5'-monophosphate dehydrogenase by the 1,5-diazabicyclo[3.1.0]hexane-2,4-diones. *Biochemistry*, **39**, 13641-13650.

Bartolini, F., Bhamidipati, A., Thomas, S., Schwahn, U., Lewis, S.A. and Cowan, N.J. (2002) Functional overlap between retinitis pigmentosa 2 protein and the tubulin-specific chaperone cofactor C. *J Biol Chem*, **277**, 14629-14634.

Bascom, R.A., Liu, L., Heckenlively, J.R., Stone, E.M. and McInnes, R.R. (1995) Mutation analysis of the ROM1 gene in retinitis pigmentosa. *Hum Mol Genet*, **4**, 1895-1902.

Bech-Hansen, N.T., Naylor, M.J., Maybaum, T.A., Sparkes, R.L., Koop, B., Birch, D.G., Bergen, A.A., Prinsen, C.F., Polomeno, R.C., Gal, A., Drack, A.V., Musarella, M.A., Jacobson, S.G., Young, R.S. and Weleber, R.G. (2000) Mutations in NYX, encoding the leucine-rich proteoglycan nyctalopin, cause X-linked complete congenital stationary night blindness. *Nat Genet*, **26**, 319-323.

Bence, N.F., Sampat, R.M. and Kopito, R.R. (2001) Impairment of the ubiquitin-proteasome system by protein aggregation. *Science*, **292**, 1552-1555.

Benit, P., Bonnefont, J.P., Kara Mostefa, A., Francannet, C., Munnich, A. and Ray, P.F. (2001) Denaturing high-performance liquid chromatography (DHPLC)-based prenatal diagnosis for tuberous

sclerosis. *Prenat Diagn*, **21**, 279-283.

Bennett, J., Maguire, A.M., Cideciyan, A.V., Schnell, M., Glover, E., Anand, V., Aleman, T.S., Chirmule, N., Gupta, A.R., Huang, Y., Gao, G.P., Nyberg, W.C., Tazelaar, J., Hughes, J., Wilson, J.M. and Jacobson, S.G. (1999) Stable transgene expression in rod photoreceptors after recombinant adeno-associated virus-mediated gene transfer to monkey retina. *Proc Natl Acad Sci U S A*, **96**, 9920-9925.

Berke, S.J. and Paulson, H.L. (2003) Protein aggregation and the ubiquitin proteasome pathway: gaining the UPPer hand on neurodegeneration. *Curr Opin Genet Dev*, **13**, 253-261.

Berson, E.L., Rosner, B., Sandberg, M.A., Hayes, K.C., Nicholson, B.W., Weigel-DiFranco, C. and Willett, W. (1993) A randomized trial of vitamin A and vitamin E supplementation for retinitis pigmentosa. *Arch Ophthalmol*, **111**, 761-772.

Bessant, D.A., Ali, R.R. and Bhattacharya, S.S. (2001) Molecular genetics and prospects for therapy of the inherited retinal dystrophies. *Curr Opin Genet Dev*, **11**, 307-316.

Bessant, D.A., Payne, A.M., Mitton, K.P., Wang, Q.L., Swain, P.K., Plant, C., Bird, A.C., Zack, D.J., Swaroop, A. and Bhattacharya, S.S. (1999) A mutation in NRL is associated with autosomal dominant retinitis pigmentosa. *Nat Genet*, **21**, 355-356.

Beyaert, R., Heyninck, K. and Van Huffel, S. (2000) A20 and A20-binding proteins as cellular inhibitors of nuclear factor-kappa B-dependent gene expression and apoptosis. *Biochem Pharmacol*, **60**, 1143-1151.

Bhattacharya, G., Miller, C., Kimberling, W.J., Jablonski, M.M. and Cosgrove, D. (2002) Localization and expression of usherin: a novel basement membrane protein defective in people with Usher's syndrome type IIa. *Hear Res*, **163**, 1-11.

Bhattacharya, S.S., Wright, A.F., Clayton, J.F., Price, W.H., Phillips, C.I., McKeown, C.M., Jay, M., Bird, A.C., Pearson, P.L., Southern, E.M. and et al. (1984) Close genetic linkage between X-linked retinitis pigmentosa and a restriction fragment length polymorphism identified by recombinant DNA probe L1.28. *Nature*, **309**, 253-255.

Blackshaw, S., Fraioli, R.E., Furukawa, T. and Cepko, C.L. (2001) Comprehensive analysis of photoreceptor gene expression and the identification of candidate retinal disease genes. *Cell*, **107**, 579-589.

Bladt, F. and Birchmeier, C. (1993) Characterization and expression analysis of the murine rck gene: a protein kinase with a potential function in sensory cells. *Differentiation*, **53**, 115-122.

Boeda, B., El-Amraoui, A., Bahloul, A., Goodyear, R., Daviet, L., Blanchard, S., Perfettini, I., Fath, K.R., Shorte, S., Reiners, J., Houdusse, A., Legrain, P., Wolfrum, U., Richardson, G. and Petit, C. (2002) Myosin VIIa, harmonin and cadherin 23, three Usher I gene products that cooperate to shape the sensory hair cell bundle. *EMBO J*, **21**, 6689-6699.

Boguski, M.S. and Schuler, G.D. (1995) ESTablishing a human transcript map. *Nat Genet*, **10**, 369-371.

Bolz, H., von Brederlow, B., Ramirez, A., Bryda, E.C., Kutsche, K., Nothwang, H.G., Seeliger, M., del, C.S.C.M., Vila, M.C., Molina, O.P., Gal, A. and Kubisch, C. (2001) Mutation of CDH23, encoding a new member of the cadherin gene family, causes Usher syndrome type 1D. *Nat Genet*, **27**, 108-112.

Boughman, J.A., Vernon, M. and Shaver, K.A. (1983) Usher syndrome: definition and estimate of prevalence from two high-risk populations. *J Chronic Dis*, **36**, 595-603.

Bowes, C., Li, T., Danciger, M., Baxter, L.C., Applebury, M.L. and Farber, D.B. (1990) Retinal degeneration in the rd mouse is caused by a defect in the beta subunit of rod cGMP-phosphodiesterase. *Nature*, **347**, 677-680.

Bowne S.J., Tirpak D.L., Sullivan L.S., Kennan A., Humphries P. and Daiger S.P. (2000a) Searching for the RP10 gene: a model for positional candidate cloning in the post genome era. Poster Presentation Program Number 1392, American Society of Human Genetics Annual Meeting.

Bowne, S.J., Sullivan, L.S., Ding, L., Traer, E., Prescott, S.M., Birch, D.G., Kennan, A., Humphries, P. and Daiger, S.P. (2000b) Evaluation of human diacylglycerol kinase(iota), DGKI, a homolog of Drosophila rdgA, in inherited retinopathy mapping to 7q. *Mol Vis*, **6**, 6-9.

Bowne, S.J., Sullivan, L.S., Blanton, S.H., Cepko, C.L., Blackshaw, S., Birch, D.G., Hughbanks-Wheaton, D., Heckenlively, J.R. and Daiger, S.P. (2002) Mutations in the inosine monophosphate dehydrogenase 1 gene (IMPDH1) cause the RP10 form of autosomal dominant retinitis pigmentosa. *Hum Mol Genet*, **11**, 559-568.

Bowne S.J., Gire A., Sullivan L.S., Heckenlively J.R., Birch D.G., Hughbanks-Wheaton D., Lewis R.A. and Daiger S.P. (2003) Frequency and spectrum of IMPDH1 mutations associated with autosomal dominant retinitis pigmentosa. *Invest. Ophthalmol. Vis. Sci.* **44**, E-Abstract 2307.

Boylan, J.P. and Wright, A.F. (2000) Identification of a novel protein interacting with RPGR. *Hum Mol Genet*, **9**, 2085-2093.

Brown, M.D., Torroni, A., Shoffner, J.M. and Wallace, D.C. (1992) Mitochondrial tRNA(Thr) mutations and lethal infantile mitochondrial myopathy. *Am J Hum Genet*, **51**, 446-447.

Bucciantini, M., Giannoni, E., Chiti, F., Baroni, F., Formigli, L., Zurdo, J., Taddei, N., Ramponi, G., Dobson, C.M. and Stefani, M. (2002) Inherent toxicity of aggregates implies a common mechanism for protein misfolding diseases. *Nature*, **416**, 507-511.

Bykhovskaya, Y., Yang, H., Taylor, K., Hang, T., Tun, R.Y., Estivill, X., Casano, R.A., Majamaa, K., Shohat, M. and Fischel-Ghodsian, N. (2001) Modifier locus for mitochondrial DNA disease: linkage and linkage disequilibrium mapping of a nuclear modifier gene for maternally inherited deafness. *Genet Med*, **3**, 177-180.

Carr, S.F., Papp, E., Wu, J.C. and Natsumeda, Y. (1993) Characterization of human type I and type II IMP dehydrogenases. *J Biol Chem*, **268**, 27286-27290.

Catapano, C.V., Dayton, J.S., Mitchell, B.S. and Fernandes, D.J. (1995) GTP depletion induced by IMP dehydrogenase inhibitors blocks RNA-primed DNA synthesis. *Mol Pharmacol*, **47**, 948-955.

Chader, G.J. (2002) Animal models in research on retinal degenerations: past progress and future hope. *Vision Res*, **42**, 393-399.

Chaitin, M.H. and Brun-Zinkernagel, A.M. (1998) Immunolocalization of CD44 in the dystrophic rat retina. *Exp Eye Res*, **67**, 283-292.

Chakarova, C.F., Hims, M.M., Bolz, H., Abu-Safieh, L., Patel, R.J., Papaioannou, M.G., Inglehearn, C.F., Keen, T.J., Willis, C., Moore, A.T., Rosenberg, T., Webster, A.R., Bird, A.C., Gal, A., Hunt, D., Vithana, E.N. and Bhattacharya, S.S. (2002) Mutations in HPRP3, a third member of pre-mRNA splicing factor genes, implicated in autosomal dominant retinitis pigmentosa. *Hum Mol Genet*, **11**, 87-92.

Chang, D.K., Cheng, S.F., Trivedi, V.D. and Lin, K.L. (1999) Proline affects oligomerization of a coiled coil by inducing a kink in a long helix. *J Struct Biol*, **128**, 270-279.

Chapiro, E., Feldmann, D., Denoyelle, F., Sternberg, D., Jardel, C., Eliot, M.M., Bouccara, D., Weil, D., Garabedian, E.N., Couderc, R., Petit, C. and Marlin, S. (2002) Two large French pedigrees with non syndromic sensorineural deafness and the mitochondrial DNA T7511C mutation: evidence for a modulatory factor. *Eur J Hum Genet*, **10**, 851-856.

Chapple, J.P., Grayson, C., Hardcastle, A.J., Bailey, T.A., Matter, K., Adamson, P., Graham, C.H., Willison, K.R. and Cheetham, M.E. (2003) Organization on the plasma membrane of the retinitis pigmentosa protein RP2: investigation of association with detergent-resistant membranes and polarized sorting. *Biochem J*, **372**, 427-433.

Chapple, J.P., Grayson, C., Hardcastle, A.J., Saliba, R.S., van der Spuy, J. and Cheetham, M.E. (2001) Unfolding retinal dystrophies: a role for molecular chaperones? *Trends Mol Med*, **7**, 414-421.

Choi, S., Hao, W., Chen, C.K. and Simon, M.I. (2001) Gene expression profiles of light-induced apoptosis in arrestin/rhodopsin kinase-deficient mouse retinas. *Proc Natl Acad Sci U S A*, **98**, 13096-13101.

Chomczynski, P. and Sacchi, N. (1987) Single-step method of RNA isolation by acid guanidiniumthiocyanate-phenol-chloroform extraction. *Anal Biochem.*, **162**, 156-9.

Choo-Kang, A.T., Lynn, S., Taylor, G.A., Daly, M.E., Sihota, S.S., Wardell, T.M., Chinnery, P.F., Turnbull, D.M. and Walker, M. (2002) Defining the importance of mitochondrial gene defects in maternally inherited diabetes by sequencing the entire mitochondrial genome. *Diabetes*, **51**, 2317-2320.

Chow, A.Y., Chow, V.Y., Packo, K.H., Pollack, J.S., Peyman, G.A. and Schuchard, R. (2004) The artificial silicon retina microchip for the treatment of vision loss from retinitis pigmentosa. *Arch Ophthalmol*, **122**, 460-469.

Chowers, I., Gunatilaka, T.L., Farkas, R.H., Qian, J., Hackam, A.S., Duh, E., Kageyama, M., Wang, C., Vora, A., Campochiaro, P.A. and Zack, D.J. (2003) Identification of novel genes preferentially expressed in the retina using a custom human retina cDNA microarray. *Invest Ophthalmol Vis Sci*, **44**, 3732-3741.

Chung, A.E., Dong, L.J., Wu, C. and Durkin, M.E. (1993) Biological functions of entactin. *Kidney Int*, **43**, 13-19.

Clarke, G., Heon, E. and McInnes, R.R. (2000) Recent advances in the molecular basis of inherited photoreceptor degeneration. *Clin Genet*, **57**, 313-329.

Colby, T.D., Vanderveen, K., Strickler, M.D., Markham, G.D. and Goldstein, B.M. (1999) Crystal structure of human type II inosine monophosphate dehydrogenase: implications for ligand binding and drug design. *Proc Natl Acad Sci U S A*, **96**, 3531-3536.

Cordes, F.S., Bright, J.N. and Sansom, M.S. (2002) Proline-induced distortions of transmembrane helices. *J Mol Biol*, **323**, 951-960.

Cremers, F.P., van den Hurk, J.A. and den Hollander, A.I. (2002) Molecular genetics of Leber congenital amaurosis. *Hum Mol Genet*, **11**, 1169-1176.

Crimi, M., Galbiati, S., Perini, M.P., Bordoni, A., Malferrari, G., Sciacco, M., Biunno, I., Strazzer, S., Moggio, M., Bresolin, N. and Comi, G.P. (2003) A mitochondrial tRNA(His) gene mutation causing

pigmentary retinopathy and neurosensorial deafness. *Neurology*, **60**, 1200-1203.

Curcio, C.A., Sloan, K.R., Kalina, R.E. and Hendrickson, A.E. (1990) Human photoreceptor topography. *J Comp Neurol*, **292**, 497-523.

Cutler, D.J., Zwick, M.E., Carrasquillo, M.M., Yohn, C.T., Tobin, K.P., Kashuk, C., Mathews, D.J., Shah, N.A., Eichler, E.E., Warrington, J.A. and Chakravarti, A. (2001) High-throughput variation detection and genotyping using microarrays. *Genome Res*, **11**, 1913-1925.

Daiger, S.P. Sullivan, L.S., Bowne, S.J., Kennan, A., Humphries P., Birch, D.G., Heckenlively, J.R. and the RP1 consortium. (2003) Identification of the RP1 and RP10 (IMPDH1) genes causing autosomal dominant RP. In *Retinal Degenerations.* LaVail, M.M., Hollyfield, J.G. & Anderson, R.E. Eds. Kluwer Academic.

Dayton, J.S., Lindsten, T., Thompson, C.B. and Mitchell, B.S. (1994) Effects of human T lymphocyte activation on inosine monophosphate dehydrogenase expression. *J Immunol*, **152**, 984-991.

Deery, E.C., Vithana, E.N., Newbold, R.J., Gallon, V.A., Bhattacharya, S.S., Warren, M.J., Hunt, D.M. and Wilkie, S.E. (2002) Disease mechanism for retinitis pigmentosa (RP11) caused by mutations in the splicing factor gene PRPF31. *Hum Mol Genet*, **11**, 3209-3219.

den Hollander, A.I., ten Brink, J.B., de Kok, Y.J., van Soest, S., van den Born, L.I., van Driel, M.A., van de Pol, D.J., Payne, A.M., Bhattacharya, S.S., Kellner, U., Hoyng, C.B., Westerveld, A., Brunner, H.G., Bleeker-Wagemakers, E.M., Deutman, A.F., Heckenlively, J.R., Cremers, F.P. and Bergen, A.A. (1999a) Mutations in a human homologue of Drosophila crumbs cause retinitis pigmentosa (RP12). *Nat Genet*, **23**, 217-221.

den Hollander, A.I., van Driel, M.A., de Kok, Y.J., van de Pol, D.J., Hoyng, C.B., Brunner, H.G., Deutman, A.F. and Cremers, F.P. (1999b) Isolation and mapping of novel candidate genes for retinal disorders using suppression subtractive hybridization. *Genomics*, **58**, 240-249.

Dentchev, T., Milam, A.H., Lee, V.M., Trojanowski, J.Q. and Dunaief, J.L. (2003) Amyloid-beta is found in drusen from some age-related macular degeneration retinas, but not in drusen from normal retinas. *Mol Vis*, **9**, 184-190.

Diaz, E., Yang, Y.H., Ferreira, T., Loh, K.C., Okazaki, Y., Hayashizaki, Y., Tessier-Lavigne, M., Speed, T.P. and Ngai, J. (2003) Analysis of gene expression in the developing mouse retina. *Proc Natl Acad Sci U S A*, **100**, 5491-5496.

Djamgoz M.B.A., Archer S.N. and Vallerga S. (1995). *Neurobiology and clinical aspects of the outer*

retina. Chapman & Hall, London.

Dowling J.E. (1987) *The retina, an approachable part of the brain*. The Beknap Press of Harvard University Press, Cambridge, Massachusetts and London.

Dryja, T.P., Adams, S.M., Grimsby, J.L., McGee, T.L., Hong, D.H., Li, T., Andreasson, S. and Berson, E.L. (2001) Null RPGRIP1 alleles in patients with Leber congenital amaurosis. *Am J Hum Genet*, **68**, 1295-1298.

Dryja, T.P., Hahn, L.B., Kajiwara, K. and Berson, E.L. (1997) Dominant and digenic mutations in the peripherin/RDS and ROM1 genes in retinitis pigmentosa. *Invest Ophthalmol Vis Sci*, **38**, 1972-1982.

Dryja, T.P., McGee, T.L., Reichel, E., Hahn, L.B., Cowley, G.S., Yandell, D.W., Sandberg, M.A. and Berson, E.L. (1990) A point mutation of the rhodopsin gene in one form of retinitis pigmentosa. *Nature*, **343**, 364-366.

Edland, S.D., Tobe, V.O., Rieder, M.J., Bowen, J.D., McCormick, W., Teri, L., Schellenberg, G.D., Larson, E.B., Nickerson, D.A. and Kukull, W.A. (2002) Mitochondrial genetic variants and Alzheimer disease: a case-control study of the T4336C and G5460A variants. *Alzheimer Dis Assoc Disord*, **16**, 1-7.

Egensperger, R., Kosel, S., Schnopp, N.M., Mehraein, P. and Graeber, M.B. (1997) Association of the mitochondrial tRNA (A4336G) mutation with Alzheimer's and Parkinson's diseases. *Neuropathol Appl Neurobiol*, **23**, 315-321.

Eudy, J.D., Weston, M.D., Yao, S., Hoover, D.M., Rehm, H.L., Ma-Edmonds, M., Yan, D., Ahmad, I., Cheng, J.J., Ayuso, C., Cremers, C., Davenport, S., Moller, C., Talmadge, C.B., Beisel, K.W., Tamayo, M., Morton, C.C., Swaroop, A., Kimberling, W.J. and Sumegi, J. (1998) Mutation of a gene encoding a protein with extracellular matrix motifs in Usher syndrome type IIa. *Science*, **280**, 1753-1757.

Fannon, M.R. (1996) Gene expression in normal and disease states--identification of therapeutic targets. *Trends Biotechnol*, **14**, 294-298.

Fariss, R.N., Apte, S.S., Luthert, P.J., Bird, A.C. and Milam, A.H. (1998) Accumulation of tissue inhibitor of metalloproteinases-3 in human eyes with Sorsby's fundus dystrophy or retinitis pigmentosa. *Br J Ophthalmol*, **82**, 1329-1334.

Farrar, G.J., Kenna, P., Jordan, S.A., Kumar-Singh, R., Humphries, M.M., Sharp, E.M., Sheils, D.M. and Humphries, P. (1991) A three-base-pair deletion in the peripherin-RDS gene in one form of retinitis pigmentosa. *Nature*, **354**, 478-480.

Farrar, G.J., Kenna, P.F. and Humphries, P. (2002) On the genetics of retinitis pigmentosa and on mutation-independent approaches to therapeutic intervention. *Embo J*, **21**, 857-864.

Farrar, G.J., McWilliam, P., Bradley, D.G., Kenna, P., Lawler, M., Sharp, E.M., Humphries, M.M., Eiberg, H., Conneally, P.M., Trofatter, J.A. and et al. (1990) Autosomal dominant retinitis pigmentosa: linkage to rhodopsin and evidence for genetic heterogeneity. *Genomics*, **8**, 35-40.

Feng, W., Yasumura, D., Matthes, M.T., LaVail, M.M. and Vollrath, D. (2002) Mertk triggers uptake of photoreceptor outer segments during phagocytosis by cultured retinal pigment epithelial cells. *J Biol Chem*, **277**, 17016-17022.

Ferreira, P.A., Hom, J.T. and Pak, W.L. (1995) Retina-specifically expressed novel subtypes of bovine cyclophilin. *J Biol Chem*, **270**, 23179-23188.

Finckh, U., Xu, S., Kumaramanickavel, G., Schurmann, M., Mukkadan, J.K., Fernandez, S.T., John, S., Weber, J.L., Denton, M.J. and Gal, A. (1998) Homozygosity mapping of autosomal recessive retinitis pigmentosa locus (RP22) on chromosome 16p12.1-p12.3. *Genomics*, **48**, 341-345.

Finnila, S., Autere, J., Lehtovirta, M., Hartikainen, P., Mannermaa, A., Soininen, H. and Majamaa, K. (2001) Increased risk of sensorineural hearing loss and migraine in patients with a rare mitochondrial DNA variant 4336A>G in tRNAGln. *J Med Genet*, **38**, 400-405.

Flannery, J.G., Zolotukhin, S., Vaquero, M.I., LaVail, M.M., Muzyczka, N. and Hauswirth, W.W. (1997) Efficient photoreceptor-targeted gene expression in vivo by recombinant adeno-associated virus. *Proc Natl Acad Sci U S A*, **94**, 6916-6921.

Florentz, C. and Sissler, M. (2001) Disease-related versus polymorphic mutations in human mitochondrial tRNAs. Where is the difference? *EMBO Rep*, **2**, 481-486.

Furukawa, T., Morrow, E.M., Li, T., Davis, F.C. and Cepko, C.L. (1999) Retinopathy and attenuated circadian entrainment in Crx-deficient mice. *Nat Genet*, **23**, 466-470.

Futer, O., Sintchak, M.D., Caron, P.R., Nimmesgern, E., DeCenzo, M.T., Livingston, D.J. and Raybuck, S.A. (2002) A mutational analysis of the active site of human type II inosine 5'-monophosphate dehydrogenase. *Biochim Biophys Acta*, **1594**, 27-39.

Gal, A., Li, Y., Thompson, D.A., Weir, J., Orth, U., Jacobson, S.G., Apfelstedt-Sylla, E. and Vollrath, D. (2000) Mutations in MERTK, the human orthologue of the RCS rat retinal dystrophy gene, cause retinitis pigmentosa. *Nat Genet*, **26**, 270-271.

Gao, J., Cheon, K., Nusinowitz, S., Liu, Q., Bei, D., Atkins, K., Azimi, A., Daiger, S.P., Farber, D.B., Heckenlively, J.R., Pierce, E.A., Sullivan, L.S. and Zuo, J. (2002) Progressive photoreceptor degeneration, outer segment dysplasia, and rhodopsin mislocalization in mice with targeted disruption of the retinitis pigmentosa-1 (Rp1) gene. *Proc Natl Acad Sci U S A*, **99**, 5698-5703.

Garriga, P. and Manyosa, J. (2002) The eye photoreceptor protein rhodopsin. Structural implications for retinal disease. *FEBS Lett*, **528**, 17-22.

Gorevic, P.D., Munoz, P.C., Casey, T.T., DiRaimondo, C.R., Stone, W.J., Prelli, F.C., Rodrigues, M.M., Poulik, M.D. and Frangione, B. (1986) Polymerization of intact beta 2-microglobulin in tissue causes amyloidosis in patients on chronic hemodialysis. *Proc Natl Acad Sci U S A*, **83**, 7908-7912.

Grey, S.T., Longo, C., Shukri, T., Patel, V.I., Csizmadia, E., Daniel, S., Arvelo, M.B., Tchipashvili, V. and Ferran, C. (2003) Genetic engineering of a suboptimal islet graft with A20 preserves beta cell mass and function. *J Immunol*, **170**, 6250-6256.

Grover S., Fishman G.A. and Stone E.M. (2003) Clinical Features of a severe form of autosomal dominant RP in a large family with a novel IMPDH1 mutation (Arg231Pro). *Invest. Ophthalmol. Vis. Sci.* **44**, E-Abstract 540.

Gu, J.J., Gathy, K., Santiago, L., Chen, E., Huang, M., Graves, L.M. and Mitchell, B.S. (2003a) Induction of apoptosis in IL-3-dependent hematopoietic cell lines by guanine nucleotide depletion. *Blood*, **101**, 4958-4965.

Gu, J.J., Kaiser-Rogers, K., Rao, K. and Mitchell, B.S. (1994) Assignment of the human type I IMP dehydrogenase gene (IMPDH1) to chromosome 7q31.3-q32). *Genomics*, **24**, 179-181.

Gu, J.J., Spychala, J. and Mitchell, B.S. (1997) Regulation of the human inosine monophosphate dehydrogenase type I gene. Utilization of alternative promoters. *J Biol Chem*, **272**, 4458-4466.

Gu, J.J., Stegmann, S., Gathy, K., Murray, R., Laliberte, J., Ayscue, L. and Mitchell, B.S. (2000) Inhibition of T lymphocyte activation in mice heterozygous for loss of the IMPDH II gene. *J Clin Invest*, **106**, 599-606.

Gu, J.J., Tolin, A.K., Jain, J., Huang, H., Santiago, L. and Mitchell, B.S. (2003b) Targeted Disruption of the Inosine 5'-Monophosphate Dehydrogenase Type I Gene in Mice. *Mol Cell Biol*, **23**, 6702-6712.

Haendler, B. and Hofer, E. (1990) Characterization of the human cyclophilin gene and of related processed pseudogenes. *Eur J Biochem*, **190**, 477-482.

Hager, P.W., Collart, F.R., Huberman, E. and Mitchell, B.S. (1995) Recombinant human inosine monophosphate dehydrogenase type I and type II proteins. Purification and characterization of inhibitor binding. *Biochem Pharmacol*, **49**, 1323-1329.

Hagstrom, S.A., Adamian, M., Scimeca, M., Pawlyk, B.S., Yue, G. and Li, T. (2001) A role for the Tubby-like protein 1 in rhodopsin transport. *Invest Ophthalmol Vis Sci*, **42**, 1955-1962.

Haider, N.B., Jacobson, S.G., Cideciyan, A.V., Swiderski, R., Streb, L.M., Searby, C., Beck, G., Hockey, R., Hanna, D.B., Gorman, S., Duhl, D., Carmi, R., Bennett, J., Weleber, R.G., Fishman, G.A., Wright, A.F., Stone, E.M. and Sheffield, V.C. (2000) Mutation of a nuclear receptor gene, NR2E3, causes enhanced S cone syndrome, a disorder of retinal cell fate. *Nat Genet*, **24**, 127-131.

Haider, N.B., Naggert, J.K. and Nishina, P.M. (2001) Excess cone cell proliferation due to lack of a functional NR2E3 causes retinal dysplasia and degeneration in rd7/rd7 mice. *Hum Mol Genet*, **10**, 1619-1626.

Hardcastle, A.J., Thiselton, D.L., Van Maldergem, L., Saha, B.K., Jay, M., Plant, C., Taylor, R., Bird, A.C. and Bhattacharya, S. (1999) Mutations in the RP2 gene cause disease in 10% of families with familial X-linked retinitis pigmentosa assessed in this study. *Am J Hum Genet*, **64**, 1210-1215.

Heckenlively, J.R, (1988). *Retinitis Pigmentosa*. J.B. Lippincott Company, Philadelphia.

Hendriks, L., Jonghe, C., Cras, P., Martin, J.J. and Broeckhoven, C.V. (1996) Beta-amyloid precursor protein and early-onset Alzheimer's disease. *Ciba Found Symp*, **199**, 170-180.

Hobson, A.H., Donovan, M., Humphries, M.M., Tuohy, G., McNally, N., Carmody, R., Cotter, T., Farrar, G.J., Kenna, P.F. and Humphries, P. (2000) Apoptotic photoreceptor death in the rhodopsin knockout mouse in the presence and absence of c-fos. *Exp Eye Res*, **71**, 247-254.

Holt, I.J., Harding, A.E., Petty, R.K. and Morgan-Hughes, J.A. (1990) A new mitochondrial disease associated with mitochondrial DNA heteroplasmy. *Am J Hum Genet*, **46**, 428-433.

Hong, D.H. and Li, T. (2002) Complex expression pattern of RPGR reveals a role for purine-rich exonic splicing enhancers. *Invest Ophthalmol Vis Sci*, **43**, 3373-3382.

Hong, D.H., Yue, G., Adamian, M. and Li, T. (2001) Retinitis pigmentosa GTPase regulator (RPGRr)-interacting protein is stably associated with the photoreceptor ciliary axoneme and anchors RPGR to the connecting cilium. *J Biol Chem*, **276**, 12091-12099.

Hoque, M.O., Lee, C.C., Cairns, P., Schoenberg, M. and Sidransky, D. (2003) Genome-wide genetic

characterization of bladder cancer: a comparison of high-density single-nucleotide polymorphism arrays and PCR-based microsatellite analysis. *Cancer Res*, **63**, 2216-2222.

Humayun, M.S., Weiland, J.D., Fujii, G.Y., Greenberg, R., Williamson, R., Little, J., Mech, B., Cimmarusti, V., Van Boemel, G., Dagnelie, G. and de Juan, E. (2003) Visual perception in a blind subject with a chronic microelectronic retinal prosthesis. *Vision Res*, **43**, 2573-2581.

Humphries, M.M., Kiang, S., McNally, N., Donovan, M.A., Sieving, P.A., Bush, R.A., Machida, S., Cotter, T., Hobson, A., Farrar, J., Humphries, P. and Kenna, P. (2001) Comparative structural and functional analysis of photoreceptor neurons of Rho-/- mice reveal increased survival on C57BL/6J in comparison to 129Sv genetic background. *Vis Neurosci*, **18**, 437-443.

Humphries, M.M., Rancourt, D., Farrar, G.J., Kenna, P., Hazel, M., Bush, R.A., Sieving, P.A., Sheils, D.M., McNally, N., Creighton, P., Erven, A., Boros, A., Gulya, K., Capecchi, M.R. and Humphries, P. (1997) Retinopathy induced in mice by targeted disruption of the rhodopsin gene. *Nat Genet*, **15**, 216-219.

Humphries, P., Kenna, P. and Farrar, G.J. (1992) On the molecular genetics of retinitis pigmentosa. *Science*, **256**, 804-808.

Hutchin, T. and Cortopassi, G. (1995) A mitochondrial DNA clone is associated with increased risk for Alzheimer disease. *Proc Natl Acad Sci U S A*, **92**, 6892-6895.

Hutchin, T.P. and Cortopassi, G.A. (2000) Mitochondrial defects and hearing loss. *Cell Mol Life Sci*, **57**, 1927-1937.

Hutchin, T.P., Parker, M.J., Young, I.D., Davis, A.C., Pulleyn, L.J., Deeble, J., Lench, N.J., Markham, A.F. and Mueller, R.F. (2000) A novel mutation in the mitochondrial tRNA(Ser(UCN)) gene in a family with non-syndromic sensorineural hearing impairment. *J Med Genet*, **37**, 692-694.

Hwa, J., Klein-Seetharaman, J. and Khorana, H.G. (2001) Structure and function in rhodopsin: Mass spectrometric identification of the abnormal intradiscal disulfide bond in misfolded retinitis pigmentosa mutants. *Proc Natl Acad Sci U S A*, **98**, 4872-4876.

Illing, M.E., Rajan, R.S., Bence, N.F. and Kopito, R.R. (2002) A rhodopsin mutant linked to autosomal dominant retinitis pigmentosa is prone to aggregate and interacts with the ubiquitin proteasome system. *J Biol Chem*, **277**, 34150-34160.

Inana, G., Murakami, A., Sakuma.,H., Higashide, T., Yajima, T. and McLaren, M.J. (1997) Isolation of candidate genes for retinal degenerations. In *Degenerative Retinal Diseases.* LaVail, M.M. *et al.* Eds.

Plenum Press, New York, pp 205-226.

Jaakson, K., Zernant, J., Kulm, M., Hutchinson, A., Tonisson, N., Glavac, D., Ravnik-Glavac, M., Hawlina, M., Meltzer, M.R., Caruso, R.C., Testa, F., Maugeri, A., Hoyng, C.B., Gouras, P., Simonelli, F., Lewis, R.A., Lupski, J.R., Cremers, F.P. and Allikmets, R. (2003) Genotyping microarray (gene chip) for the ABCR (ABCA4) gene. *Hum Mutat*, **22**, 395-403.

Jacobson, S.G., Cideciyan, A.V., Iannaccone, A., Weleber, R.G., Fishman, G.A., Maguire, A.M., Affatigato, L.M., Bennett, J., Pierce, E.A., Danciger, M., Farber, D.B. and Stone, E.M. (2000) Disease expression of RP1 mutations causing autosomal dominant retinitis pigmentosa. *Invest Ophthalmol Vis Sci*, **41**, 1898-1908.

John, R.J. (2002) Photometric Assays. In: *Enzyme Assays: A Practical Approach, 2nd Edition.* Eisenthal R., Danson, M.J. Eds. Oxford University Press, pp 49-78.

Johnson, L.V., Leitner, W.P., Rivest, A.J., Staples, M.K., Radeke, M.J. and Anderson, D.H. (2002) The Alzheimer's A beta -peptide is deposited at sites of complement activation in pathologic deposits associated with aging and age-related macular degeneration. *Proc Natl Acad Sci U S A*, **99**, 11830-11835.

Johnson, S., Halford, S., Morris, A.G., Patel, R.J., Wilkie, S.E., Hardcastle, A.J., Moore, A.T., Zhang, K. and Hunt, D.M. (2003) Genomic organisation and alternative splicing of human RIM1, a gene implicated in autosomal dominant cone-rod dystrophy (CORD7)(small star, filled). *Genomics*, **81**, 304-314.

Johnston, J.A., Dalton, M.J., Gurney, M.E. and Kopito, R.R. (2000) Formation of high molecular weight complexes of mutant Cu, Zn-superoxide dismutase in a mouse model for familial amyotrophic lateral sclerosis. *Proc Natl Acad Sci U S A*, **97**, 12571-12576.

Jones, B.W., Watt, C.B., Frederick, J.M., Baehr, W., Chen, C.K., Levine, E.M., Milam, A.H., Lavail, M.M. and Marc, R.E. (2003) Retinal remodeling triggered by photoreceptor degenerations. *J Comp Neurol*, **464**, 1-16.

Jordan, S.A., Farrar, G.J., Kenna, P., Humphries, M.M., Sheils, D.M., Kumar-Singh, R., Sharp, E.M., Soriano, N., Ayuso, C., Benitez, J. and et al. (1993) Localization of an autosomal dominant retinitis pigmentosa gene to chromosome 7q. *Nat Genet*, **4**, 54-58.

Kajiwara, K., Berson, E.L. and Dryja, T.P. (1994) Digenic retinitis pigmentosa due to mutations at the unlinked peripherin/RDS and ROM1 loci. *Science*, **264**, 1604-1608.

Kajiwara, K., Hahn, L.B., Mukai, S., Travis, G.H., Berson, E.L. and Dryja, T.P. (1991) Mutations in the human retinal degeneration slow gene in autosomal dominant retinitis pigmentosa. *Nature*, **354**, 480-483.

Katsanis, N., Ansley, S.J., Badano, J.L., Eichers, E.R., Lewis, R.A., Hoskins, B.E., Scambler, P.J., Davidson, W.S., Beales, P.L. and Lupski, J.R. (2001) Triallelic inheritance in Bardet-Biedl syndrome, a Mendelian recessive disorder. *Science*, **293**, 2256-2259.

Kaushal, S. and Khorana, H.G. (1994) Structure and function in rhodopsin. 7. Point mutations associated with autosomal dominant retinitis pigmentosa. *Biochemistry*, **33**, 6121-6128.

Kawamura, S. (1995) Photransduction, excitation and adaptation. In: *Neurobiology and Clinical Aspects of the Outer Retina*. Djamgoz, M.B.A., Archer, S.N. and Vallerga, S. Eds. Chapman & Hall, London, pp. 105-131.

Keats, B.J. and Corey, D.P. (1999) The usher syndromes. *Am J Med Genet*, **89**, 158-166.

Keen, T.J., Hims, M.M., McKie, A.B., Moore, A.T., Doran, R.M., Mackey, D.A., Mansfield, D.C., Mueller, R.F., Bhattacharya, S.S., Bird, A.C., Markham, A.F. and Inglehearn, C.F. (2002) Mutations in a protein target of the Pim-1 kinase associated with the RP9 form of autosomal dominant retinitis pigmentosa. *Eur J Hum Genet*, **10**, 245-249.

Keen, T.J. and Inglehearn, C.F. (1996) Mutations and polymorphisms in the human peripherin-RDS gene and their involvement in inherited retinal degeneration. *Hum Mutat*, **8**, 297-303.

Kelsell, R.E., Gregory-Evans, K., Payne, A.M., Perrault, I., Kaplan, J., Yang, R.B., Garbers, D.L., Bird, A.C., Moore, A.T. and Hunt, D.M. (1998) Mutations in the retinal guanylate cyclase (RETGC-1) gene in dominant cone-rod dystrophy. *Hum Mol Genet*, **7**, 1179-1184.

Kenna, P., Mansergh, F., Millington-Ward, S., Erven, A., Kumar-Singh, R., Brennan, R., Farrar, G.J. and Humphries, P. (1997) Clinical and molecular genetic characterisation of a family segregating autosomal dominant retinitis pigmentosa and sensorineural deafness. *Br J Ophthalmol*, **81**, 207-213.

Kennan AM. (1999) *On the molecular genetics of retinal dystrophies and glaucoma*. PhD Thesis, Trinity College, Dublin.

Kennan, A., Aherne, A., Palfi, A., Humphries, M., McKee, A., Stitt, A., Simpson, D.A., Demtroder, K., Orntoft, T., Ayuso, C., Kenna, P.F., Farrar, G.J. and Humphries, P. (2002) Identification of an IMPDH1 mutation in autosomal dominant retinitis pigmentosa (RP10) revealed following comparative microarray analysis of transcripts derived from retinas of wild-type and Rho(-/-) mice. *Hum Mol Genet*, **11**, 547-557.

Kennan, A., Aherne, A., S.J., Daiger, S.P., Farrar, G.J., Kenna, P.F., and Humphries P. (2003) On the role of IMPDH1 in retinal degeneration. In *Retinal Degenerations*. LaVail, M.M., Hollyfield, J.G. &

Anderson, R.E. Eds. Kluwer Academic/Plenum publishers.

Kjer-Nielsen, L., Teasdale, R.D., van Vliet, C. and Gleeson, P.A. (1999) A novel Golgi-localisation domain shared by a class of coiled-coil peripheral membrane proteins. *Curr Biol*, **9**, 385-388.

Klug, A. and Rhodes, D. (1987) Zinc fingers: a novel protein fold for nucleic acid recognition. *Cold Spring Harb Symp Quant Biol*, **52**, 473-482.

Klumpp, S. and Krieglstein, J. (2002) Serine/threonine protein phosphatases in apoptosis. *Curr Opin Pharmacol*, **2**, 458-462.

Kobayashi, A., Higashide, T., Hamasaki, D., Kubota, S., Sakuma, H., An, W., Fujimaki, T., McLaren, M.J., Weleber, R.G. and Inana, G. (2000) HRG4 (UNC119) mutation found in cone-rod dystrophy causes retinal degeneration in a transgenic model. *Invest Ophthalmol Vis Sci*, **41**, 3268-3277.

Kopito, R.R. (2000) Aggresomes, inclusion bodies and protein aggregation. *Trends Cell Biol*, **10**, 524-530.

Krishnamoorthy, R., Agarwal, N. and Chaitin, M.H. (2000) Upregulation of CD44 expression in the retina during the rds degeneration. *Brain Res Mol Brain Res*, **77**, 125-130.

La Cour, M. (2002) The retinal pigment epithelium. In: *Adler's Physiology of the eye. 10th Ed.* Kaufman, P.L., Alm, A. Eds. Mosby, St. Louis, pp 348-357.

Lander, E.S. *et al.* (2001) Initial sequencing and analysis of the human genome. *Nature*, **409**, 860-921.

Lariviere, R.C., Nguyen, M.D., Ribeiro-da-Silva, A. and Julien, J.P. (2002) Reduced number of unmyelinated sensory axons in peripherin null mice. *J Neurochem*, **81**, 525-532.

Lauber, J., Marsac, C., Kadenbach, B. and Seibel, P. (1991) Mutations in mitochondrial tRNA genes: a frequent cause of neuromuscular diseases. *Nucleic Acids Res*, **19**, 1393-1397.

LaVail, M.M., Yasumura, D., Matthes, M.T., Drenser, K.A., Flannery, J.G., Lewin, A.S. and Hauswirth, W.W. (2000) Ribozyme rescue of photoreceptor cells in P23H transgenic rats: long-term survival and late-stage therapy. *Proc Natl Acad Sci U S A*, **97**, 11488-11493.

Leong, M.L., Maiyar, A.C., Kim, B., O'Keeffe, B.A. and Firestone, G.L. (2003) Expression of the serum- and glucocorticoid-inducible protein kinase, Sgk, is a cell survival response to multiple types of environmental stress stimuli in mammary epithelial cells. *J Biol Chem*, **278**, 5871-5882.

Linden, R., Rehen, S.K. and Chiarini, L.B. (1999) Apoptosis in developing retinal tissue. *Prog Retin Eye Res*, **18**, 133-165.

Lipshutz, R.J., Fodor, S.P., Gingeras, T.R. and Lockhart, D.J. (1999) High density synthetic oligonucleotide arrays. *Nat Genet*, **21**, 20-24.

Liu, M.R., Pan, K.F., Li, Z.F., Wang, Y., Deng, D.J., Zhang, L. and Lu, Y.Y. (2002) Rapid screening mitochondrial DNA mutation by using denaturing high-performance liquid chromatography. *World J Gastroenterol*, **8**, 426-430.

Liu, Q., Lyubarsky, A., Skalet, J.H., Pugh, E.N., Jr. and Pierce, E.A. (2003) RP1 Is Required for the Correct Stacking of Outer Segment Discs. *Invest Ophthalmol Vis Sci*, **44**, 4171-4183.

Liu, W., Smith, D.I., Rechtzigel, K.J., Thibodeau, S.N. and James, C.D. (1998) Denaturing high performance liquid chromatography (DHPLC) used in the detection of germline and somatic mutations. *Nucleic Acids Res*, **26**, 1396-1400.

Liu, X., Garriga, P. and Khorana, H.G. (1996) Structure and function in rhodopsin: correct folding and misfolding in two point mutants in the intradiscal domain of rhodopsin identified in retinitis pigmentosa. *Proc Natl Acad Sci U S A*, **93**, 4554-4559.

Liu, X., Vansant, G., Udovichenko, I.P., Wolfrum, U. and Williams, D.S. (1997a) Myosin VIIa, the product of the Usher 1B syndrome gene, is concentrated in the connecting cilia of photoreceptor cells. *Cell Motil Cytoskeleton*, **37**, 240-252.

Liu, X.Z., Walsh, J., Mburu, P., Kendrick-Jones, J., Cope, M.J., Steel, K.P. and Brown, S.D. (1997b) Mutations in the myosin VIIA gene cause non-syndromic recessive deafness. *Nat Genet*, **16**, 188-190.

Livesey, F.J., Furukawa, T., Steffen, M.A., Church, G.M. and Cepko, C.L. (2000) Microarray analysis of the transcriptional network controlled by the photoreceptor homeobox gene Crx. *Curr Biol*, **10**, 301-310.

Loewen, C.J., Moritz, O.L. and Molday, R.S. (2001) Molecular characterization of peripherin-2 and rom-1 mutants responsible for digenic retinitis pigmentosa. *J Biol Chem*, **276**, 22388-22396.

Longo, C.R., Arvelo, M.B., Patel, V.I., Daniel, S., Mahiou, J., Grey, S.T. and Ferran, C. (2003) A20 protects from CD40-CD40 ligand-mediated endothelial cell activation and apoptosis. *Circulation*, **108**, 1113-1118.

Lynn, S., Wardell, T., Johnson, M.A., Chinnery, P.F., Daly, M.E., Walker, M. and Turnbull, D.M. (1998) Mitochondrial diabetes: investigation and identification of a novel mutation. *Diabetes*, **47**, 1800-1802.

Malone, K., Sohocki, M.M., Sullivan, L.S. and Daiger, S.P. (1999) Identifying and mapping novel retinal-expressed ESTs from humans. *Mol Vis*, **5**, 5.

Maniatis T., Fritsh E.F. and Sambrook J. (1992) *Molecular Cloning: a laboratory manual.* Cold Spring Harbour laboratory New York.

Mansergh, F.C., Millington-Ward, S., Kennan, A., Kiang, A.S., Humphries, M., Farrar, G.J., Humphries, P. and Kenna, P.F. (1999) Retinitis pigmentosa and progressive sensorineural hearing loss caused by a C12258A mutation in the mitochondrial MTTS2 gene. *Am J Hum Genet*, **64**, 971-985.

Marc, R.E., Jones, B.W., Watt, C.B. and Strettoi, E. (2003) Neural remodeling in retinal degeneration. *Prog Retin Eye Res*, **22**, 607-655.

Marmorstein, L.Y., Munier, F.L., Arsenijevic, Y., Schorderet, D.F., McLaughlin, P.J., Chung, D., Traboulsi, E. and Marmorstein, A.D. (2002) Aberrant accumulation of EFEMP1 underlies drusen formation in Malattia Leventinese and age-related macular degeneration. *Proc Natl Acad Sci U S A*, **99**, 13067-13072.

Marr, H.S., Basalamah, M.A., Bouldin, T.W., Duncan, A.W. and Edgell, C.J. (2000) Distribution of testican expression in human brain. *Cell Tissue Res*, **302**, 139-144.

Maw, M.A., Kennedy, B., Knight, A., Bridges, R., Roth, K.E., Mani, E.J., Mukkadan, J.K., Nancarrow, D., Crabb, J.W. and Denton, M.J. (1997) Mutation of the gene encoding cellular retinaldehyde-binding protein in autosomal recessive retinitis pigmentosa. *Nat Genet*, **17**, 198-200.

Mayr-Wohlfart, U., Rodel, G. and Henneberg, A. (1997) Mitochondrial tRNA(Gln) and tRNA(Thr) gene variants in Parkinson's disease. *Eur J Med Res*, **2**, 111-113.

McGuire, R.E., Gannon, A.M., Sullivan, L.S., Rodriguez, J.A. and Daiger, S.P. (1995) Evidence for a major gene (RP10) for autosomal dominant retinitis pigmentosa on chromosome 7q: linkage mapping in a second, unrelated family. *Hum Genet*, **95**, 71-74.

McGuire, R.E., Jordan, S.A., Braden, V.V., Bouffard, G.G., Humphries, P., Green, E.D. and Daiger, S.P. (1996a) Mapping the RP10 locus for autosomal dominant retinitis pigmentosa on 7q: refined genetic positioning and localization within a well-defined YAC contig. *Genome Res*, **6**, 255-266.

McGuire RE. (1996b) The story of RP10: a positional cloning approach to the identification of an autosomal dominant Retinitis Pigmentosa gene. Ph.D thesis, University of Texas, Health Science Center, Houston.

McKie, A.B., McHale, J.C., Keen, T.J., Tarttelin, E.E., Goliath, R., van Lith-Verhoeven, J.J., Greenberg, J., Ramesar, R.S., Hoyng, C.B., Cremers, F.P., Mackey, D.A., Bhattacharya, S.S., Bird, A.C., Markham, A.F. and Inglehearn, C.F. (2001) Mutations in the pre-mRNA splicing factor gene PRPC8 in autosomal dominant retinitis pigmentosa (RP13). *Hum Mol Genet*, **10**, 1555-1562.

McManus, M.T. and Sharp, P.A. (2002) Gene silencing in mammals by small interfering RNAs. *Nat Rev Genet*, **3**, 737-747.

McWilliam, P., Farrar, G.J., Kenna, P., Bradley, D.G., Humphries, M.M., Sharp, E.M., McConnell, D.J., Lawler, M., Sheils, D., Ryan, C. and et al. (1989) Autosomal dominant retinitis pigmentosa (ADRP): localization of an ADRP gene to the long arm of chromosome 3. *Genomics*, **5**, 619-622.

Mears, A.J., Gieser, L., Yan, D., Chen, C., Fahrner, S., Hiriyanna, S., Fujita, R., Jacobson, S.G., Sieving, P.A. and Swaroop, A. (1999) Protein-truncation mutations in the RP2 gene in a North American cohort of families with X-linked retinitis pigmentosa. *Am J Hum Genet*, **64**, 897-900.

Mears, A.J., Kondo, M., Swain, P.K., Takada, Y., Bush, R.A., Saunders, T.L., Sieving, P.A. and Swaroop, A. (2001) Nrl is required for rod photoreceptor development. *Nat Genet*, **29**, 447-452.

Mehalow, A.K., Kameya, S., Smith, R.S., Hawes, N.L., Denegre, J.M., Young, J.A., Bechtold, L., Haider, N.B., Tepass, U., Heckenlively, J.R., Chang, B., Naggert, J.K. and Nishina, P.M. (2003) CRB1 is essential for external limiting membrane integrity and photoreceptor morphogenesis in the mammalian retina. *Hum Mol Genet*, **12**, 2179-2189.

Meindl, A., Dry, K., Herrmann, K., Manson, F., Ciccodicola, A., Edgar, A., Carvalho, M.R., Achatz, H., Hellebrand, H., Lennon, A., Migliaccio, C., Porter, K., Zrenner, E., Bird, A., Jay, M., Lorenz, B., Wittwer, B., D'Urso, M., Meitinger, T. and Wright, A. (1996) A gene (RPGR) with homology to the RCC1 guanine nucleotide exchange factor is mutated in X-linked retinitis pigmentosa (RP3). *Nat Genet*, **13**, 35-42.

Meltzer, P.S. (2001) Spotting the target: microarrays for disease gene discovery. *Curr Opin Genet Dev*, **11**, 258-263.

Michaelides, M., Hunt, D.M. and Moore, A.T. (2003) The genetics of inherited macular dystrophies. *J Med Genet*, **40**, 641-650.

Milam, A.H., Rose, L., Cideciyan, A.V., Barakat, M.R., Tang, W.X., Gupta, N., Aleman, T.S., Wright, A.F., Stone, E.M., Sheffield, V.C. and Jacobson, S.G. (2002) The nuclear receptor NR2E3 plays a role in human retinal photoreceptor differentiation and degeneration. *Proc Natl Acad Sci U S A*, **99**, 473-478.

Millan, J.M., Martinez, F., Vilela, C., Beneyto, M., Prieto, F. and Najera, C. (1995) An autosomal dominant retinitis pigmentosa family with close linkage to D7S480 on 7q. *Hum Genet*, **96**, 216-218.

Miller, V.M., Xia, H., Marrs, G.L., Gouvion, C.M., Lee, G., Davidson, B.L. and Paulson, H.L. (2003) Allele-specific silencing of dominant disease genes. *Proc Natl Acad Sci U S A*, **100**, 7195-7200.

Millington-Ward, S., O'Neill, B., Tuohy, G., Al-Jandal, N., Kiang, A.S., Kenna, P.F., Palfi, A., Hayden, P., Mansergh, F., Kennan, A., Humphries, P. and Farrar, G.J. (1997) Strategems in vitro for gene therapies directed to dominant mutations. *Hum Mol Genet*, **6**, 1415-1426.

Minke, B. (2001) The TRP channel and phospholipase C-mediated signaling. *Cell Mol Neurobiol*, **21**, 629-643.

Mohamed, Z., Bell, C., Hammer, H.M., Converse, C.A., Esakowitz, L. and Haites, N.E. (1996) Linkage of a medium sized Scottish autosomal dominant retinitis pigmentosa family to chromosome 7q. *J Med Genet*, **33**, 714-715.

Molday, R.S. (1998) Photoreceptor membrane proteins, phototransduction, and retinal degenerative diseases. The Friedenwald Lecture. *Invest Ophthalmol Vis Sci*, **39**, 2491-2513.

Morimura, H., Berson, E.L. and Dryja, T.P. (1999a) Recessive mutations in the RLBP1 gene encoding cellular retinaldehyde-binding protein in a form of retinitis punctata albescens. *Invest Ophthalmol Vis Sci*, **40**, 1000-1004.

Morimura, H., Fishman, G.A., Grover, S.A., Fulton, A.B., Berson, E.L. and Dryja, T.P. (1998) Mutations in the RPE65 gene in patients with autosomal recessive retinitis pigmentosa or leber congenital amaurosis. *Proc Natl Acad Sci U S A*, **95**, 3088-3093.

Morimura, H., Saindelle-Ribeaudeau, F., Berson, E.L. and Dryja, T.P. (1999b) Mutations in RGR, encoding a light-sensitive opsin homologue, in patients with retinitis pigmentosa. *Nat Genet*, **23**, 393-394.

Munro, S. and Nichols, B.J. (1999) The GRIP domain - a novel Golgi-targeting domain found in several coiled-coil proteins. *Curr Biol*, **9**, 377-380.

Nagai, M., Natsumeda, Y., Konno, Y., Hoffman, R., Irino, S. and Weber, G. (1991) Selective up-regulation of type II inosine 5'-monophosphate dehydrogenase messenger RNA expression in human leukemias. *Cancer Res*, **51**, 3886-3890.

Nagai, M., Natsumeda, Y. and Weber, G. (1992) Proliferation-linked regulation of type II IMP dehydrogenase gene in human normal lymphocytes and HL-60 leukemic cells. *Cancer Res*, **52**, 258-261.

Natsumeda, Y., Ohno, S., Kawasaki, H., Konno, Y., Weber, G. and Suzuki, K. (1990) Two distinct cDNAs for human IMP dehydrogenase. *J Biol Chem*, **265**, 5292-5295.

Newell F.W. (1982) *Opthalmology, Principles and Concepts, 5th Ed.* The C.V. Mosby Co., St. Louis.

Nimmesgern, E., Black, J., Futer, O., Fulghum, J.R., Chambers, S.P., Brummel, C.L., Raybuck, S.A. and Sintchak, M.D. (1999) Biochemical analysis of the modular enzyme inosine 5'-monophosphate dehydrogenase. *Protein Expr Purif*, **17**, 282-289.

Nussbaum, J.J., Pruett, R.C. and Delori, F.C. (1981) Historic perspectives. Macular yellow pigment. The first 200 years. *Retina*, **1**, 296-310.

Ogden, T.E. (1989) Topography of the retina. In: *Retina Volume 1.Basic science and inherited retinal disease.* Ryan, S.J. Ed. The C.V. Mosby Co., St. Louis, pp 32-37.

Okamoto, S., Krainc, D., Sherman, K. and Lipton, S.A. (2000) Antiapoptotic role of the p38 mitogen-activated protein kinase-myocyte enhancer factor 2 transcription factor pathway during neuronal differentiation. *Proc Natl Acad Sci U S A*, **97**, 7561-7566.

Okamoto, S., Li, Z., Ju, C., Scholzke, M.N., Mathews, E., Cui, J., Salvesen, G.S., Bossy-Wetzel, E. and Lipton, S.A. (2002) Dominant-interfering forms of MEF2 generated by caspase cleavage contribute to NMDA-induced neuronal apoptosis. *Proc Natl Acad Sci U S A*, **99**, 3974-3979.

Okano, H.J., Park, W.Y., Corradi, J.P. and Darnell, R.B. (1999) The cytoplasmic Purkinje onconeural antigen cdr2 down-regulates c-Myc function: implications for neuronal and tumor cell survival. *Genes Dev*, **13**, 2087-2097.

Olsson, J.E., Gordon, J.W., Pawlyk, B.S., Roof, D., Hayes, A., Molday, R.S., Mukai, S., Cowley, G.S., Berson, E.L. and Dryja, T.P. (1992) Transgenic mice with a rhodopsin mutation (Pro23His): a mouse model of autosomal dominant retinitis pigmentosa. *Neuron*, **9**, 815-830.

O'Neill, B., Millington-Ward, S., O'Reilly, M., Tuohy, G., Kiang, A.S., Kenna, P.F., Humphries, P. and Farrar, G.J. (2000) Ribozyme-based therapeutic approaches for autosomal dominant retinitis pigmentosa. *Invest Ophthalmol Vis Sci*, **41**, 2863-2869.

Park, J., Leong, M.L., Buse, P., Maiyar, A.C., Firestone, G.L. and Hemmings, B.A. (1999) Serum and glucocorticoid-inducible kinase (SGK) is a target of the PI 3-kinase-stimulated signaling pathway. *EMBO*

J, **18**, 3024-3033.

Petrukhin, K., Koisti, M.J., Bakall, B., Li, W., Xie, G., Marknell, T., Sandgren, O., Forsman, K., Holmgren, G., Andreasson, S., Vujic, M., Bergen, A.A., McGarty-Dugan, V., Figueroa, D., Austin, C.P., Metzker, M.L., Caskey, C.T. and Wadelius, C. (1998) Identification of the gene responsible for Best macular dystrophy. *Nat Genet*, **19**, 241-247.

Petters, R.M., Alexander, C.A., Wells, K.D., Collins, E.B., Sommer, J.R., Blanton, M.R., Rojas, G., Hao, Y., Flowers, W.L., Banin, E., Cideciyan, A.V., Jacobson, S.G. and Wong, F. (1997) Genetically engineered large animal model for studying cone photoreceptor survival and degeneration in retinitis pigmentosa. *Nat Biotechnol*, **15**, 965-970.

Phelan, J.K. and Bok, D. (2000) A brief review of retinitis pigmentosa and the identified retinitis pigmentosa genes. *Mol Vis*, **6**, 116-124.

Pieke-Dahl, S., Moller, C.G., Kelley, P.M., Astuto, L.M., Cremers, C.W., Gorin, M.B. and Kimberling, W.J. (2000) Genetic heterogeneity of Usher syndrome type II: localisation to chromosome 5q. *J Med Genet*, **37**, 256-262.

Pierce, E.A., Quinn, T., Meehan, T., McGee, T.L., Berson, E.L. and Dryja, T.P. (1999) Mutations in a gene encoding a new oxygen-regulated photoreceptor protein cause dominant retinitis pigmentosa. *Nat Genet*, **22**, 248-254.

Pinto, L.H. and Klumpp, D.J. (1998) Localization of potassium channels in the retina. *Prog Retin Eye Res*, **17**, 207-230.

Portera-Cailliau, C., Sung, C.H., Nathans, J. and Adler, R. (1994) Apoptotic photoreceptor cell death in mouse models of retinitis pigmentosa. *Proc Natl Acad Sci U S A*, **91**, 974-978.

Primdahl, H., Wikman, F.P., von der Maase, H., Zhou, X.G., Wolf, H. and Orntoft, T.F. (2002) Allelic imbalances in human bladder cancer: genome-wide detection with high-density single-nucleotide polymorphism arrays. *J Natl Cancer Inst*, **94**, 216-223.

Pusch, C.M., Zeitz, C., Brandau, O., Pesch, K., Achatz, H., Feil, S., Scharfe, C., Maurer, J., Jacobi, F.K., Pinckers, A., Andreasson, S., Hardcastle, A., Wissinger, B., Berger, W. and Meindl, A. (2000) The complete form of X-linked congenital stationary night blindness is caused by mutations in a gene encoding a leucine-rich repeat protein. *Nat Genet*, **26**, 324-327.

Rakoczy, P.E., Lai, M.C., Baines, M.G., Spilsbury, K. and Constable, I.J. (1998) Expression of cathepsin S antisense transcripts by adenovirus in retinal pigment epithelial cells. *Invest Ophthalmol Vis Sci*, **39**,

2095-2104.

Redmond, T.M., Yu, S., Lee, E., Bok, D., Hamasaki, D., Chen, N., Goletz, P., Ma, J.X., Crouch, R.K. and Pfeifer, K. (1998) Rpe65 is necessary for production of 11-cis-vitamin A in the retinal visual cycle. *Nat Genet*, **20**, 344-351.

Reid, F.M., Vernham, G.A. and Jacobs, H.T. (1994) A novel mitochondrial point mutation in a maternal pedigree with sensorineural deafness. *Hum Mutat*, **3**, 243-247.

Reme, C.E., Grimm, C., Hafezi, F., Wenzel, A. and Williams, T.P. (2000) Apoptosis in the Retina: The Silent Death of Vision. *News Physiol Sci*, **15**, 120-124.

Reuter, J.H. and Sanyal, S. (1984) Development and degeneration of retina in rds mutant mice: the electroretinogram. *Neurosci Lett*, **48**, 231-237.

Rivolta, C., Sharon, D., DeAngelis, M.M. and Dryja, T.P. (2002) Retinitis pigmentosa and allied diseases: numerous diseases, genes, and inheritance patterns. *Hum Mol Genet*, **11**, 1219-1227.

Rosenberg, T., Haim, M., Hauch, A.M. and Parving, A. (1997) The prevalence of Usher syndrome and other retinal dystrophy-hearing impairment associations. *Clin Genet*, **51**, 314-321.

Rozet, J.M., Perrault, I., Gerber, S., Hanein, S., Barbet, F., Ducroq, D., Souied, E., Munnich, A. and Kaplan, J. (2001) Complete abolition of the retinal-specific guanylyl cyclase (retGC-1) catalytic ability consistently leads to leber congenital amaurosis (LCA). *Invest Ophthalmol Vis Sci*, **42**, 1190-1192.

Saleem, R.A. and Walter, M.A. (2002) The complexities of ocular genetics. *Clin Genet*, **61**, 79-88.

Saliba, R.S., Munro, P.M., Luthert, P.J. and Cheetham, M.E. (2002) The cellular fate of mutant rhodopsin: quality control, degradation and aggresome formation. *J Cell Sci*, **115**, 2907-2918.

Sanyal, S., De Ruiter, A. and Hawkins, R.K. (1980) Development and degeneration of retina in rds mutant mice: light microscopy. *J Comp Neurol*, **194**, 193-207.

Schon, E.A. (2000) Mitochondrial genetics and disease. *Trends Biochem Sci*, **25**, 555-560.

Schultz, D.W., Klein, M.L., Humpert, A.J., Luzier, C.W., Persun, V., Schain, M., Mahan, A., Runckel, C., Cassera, M., Vittal, V., Doyle, T.M., Martin, T.M., Weleber, R.G., Francis, P.J. and Acott, T.S. (2003) Analysis of the ARMD1 locus: Evidence that a mutation in HEMICENTIN-1 is associated with age-related macular degeneration in a large family. *Hum Mol Genet*.

Schwahn, U., Lenzner, S., Dong, J., Feil, S., Hinzmann, B., van Duijnhoven, G., Kirschner, R., Hemberger, M., Bergen, A.A., Rosenberg, T., Pinckers, A.J., Fundele, R., Rosenthal, A., Cremers, F.P., Ropers, H.H. and Berger, W. (1998) Positional cloning of the gene for X-linked retinitis pigmentosa 2. *Nat Genet*, **19**, 327-332.

Senda, M. and Natsumeda, Y. (1994) Tissue-differential expression of two distinct genes for human IMP dehydrogenase (E.C.1.1.1.205). *Life Sci*, **54**, 1917-1926.

Sharon, D., Blackshaw, S., Cepko, C.L. and Dryja, T.P. (2002) Profile of the genes expressed in the human peripheral retina, macula, and retinal pigment epithelium determined through serial analysis of gene expression (SAGE). *Proc Natl Acad Sci U S A*, **99**, 315-320.

Shelly, C. and Herrera, R. (2002) Activation of SGK1 by HGF, Rac1 and integrin-mediated cell adhesion in MDCK cells: PI-3K-dependent and -independent pathways. *J Cell Sci*, **115**, 1985-1993.

Sherman, M.Y. and Goldberg, A.L. (2001) Cellular defenses against unfolded proteins: a cell biologist thinks about neurodegenerative diseases. *Neuron*, **29**, 15-32.

Shoffner, J.M., Brown, M.D., Torroni, A., Lott, M.T., Cabell, M.F., Mirra, S.S., Beal, M.F., Yang, C.C., Gearing, M., Salvo, R. and et al. (1993) Mitochondrial DNA variants observed in Alzheimer disease and Parkinson disease patients. *Genomics*, **17**, 171-184.

Shore, P. and Sharrocks, A.D. (1995) The MADS-box family of transcription factors. *Eur J Biochem*, **229**, 1-13.

Shroyer, N.F., Lewis, R.A., Yatsenko, A.N., Wensel, T.G. and Lupski, J.R. (2001) Cosegregation and functional analysis of mutant ABCR (ABCA4) alleles in families that manifest both Stargardt disease and age-related macular degeneration. *Hum Mol Genet*, **10**, 2671-2678.

Siemens, J., Kazmierczak, P., Reynolds, A., Sticker, M., Littlewood-Evans, A. and Muller, U. (2002) The Usher syndrome proteins cadherin 23 and harmonin form a complex by means of PDZ-domain interactions. *Proc Natl Acad Sci U S A*, **99**, 14946-14951.

Sies, H. and Stahl, W. (2003) Non-nutritive bioactive constituents of plants: lycopene, lutein and zeaxanthin. *Int J Vitam Nutr Res*, **73**, 95-100.

Simon, D.K., Mayeux, R., Marder, K., Kowall, N.W., Beal, M.F. and Johns, D.R. (2000) Mitochondrial DNA mutations in complex I and tRNA genes in Parkinson's disease. *Neurology*, **54**, 703-709.

Sinha, S., Sharma, A., Agarwal, N., Swaroop, A. and Yang-Feng, T.L. (2000) Expression profile and

chromosomal location of cDNA clones, identified from an enriched adult retina library. *Invest Ophthalmol Vis Sci*, **41**, 24-28.

Sintchak, M.D., Fleming, M.A., Futer, O., Raybuck, S.A., Chambers, S.P., Caron, P.R., Murcko, M.A. and Wilson, K.P. (1996) Structure and mechanism of inosine monophosphate dehydrogenase in complex with the immunosuppressant mycophenolic acid. *Cell*, **85**, 921-930.

Sintchak, M.D. and Nimmesgern, E. (2000) The structure of inosine 5'-monophosphate dehydrogenase and the design of novel inhibitors. *Immunopharmacology*, **47**, 163-184.

Smith, A.J., Schlichtenbrede, F.C., Tschernutter, M., Bainbridge, J.W., Thrasher, A.J. and Ali, R.R. (2003) AAV-Mediated gene transfer slows photoreceptor loss in the RCS rat model of retinitis pigmentosa. *Mol Ther*, **8**, 188-195.

Sohocki, M.M., Daiger, S.P., Bowne, S.J., Rodriquez, J.A., Northrup, H., Heckenlively, J.R., Birch, D.G., Mintz-Hittner, H., Ruiz, R.S., Lewis, R.A., Saperstein, D.A. and Sullivan, L.S. (2001) Prevalence of mutations causing retinitis pigmentosa and other inherited retinopathies. *Hum Mutat*, **17**, 42-51.

Sohocki, M.M., Malone, K.A., Sullivan, L.S. and Daiger, S.P. (1999) Localization of retina/pineal-expressed sequences: identification of novel candidate genes for inherited retinal disorders. *Genomics*, **58**, 29-33.

Sohocki, M.M., Sullivan, L.S., Mintz-Hittner, H.A., Birch, D., Heckenlively, J.R., Freund, C.L., McInnes, R.R. and Daiger, S.P. (1998) A range of clinical phenotypes associated with mutations in CRX, a photoreceptor transcription-factor gene. *Am J Hum Genet*, **63**, 1307-1315.

Sternberg, D., Chatzoglou, E., Laforet, P., Fayet, G., Jardel, C., Blondy, P., Fardeau, M., Amselem, S., Eymard, B. and Lombes, A. (2001) Mitochondrial DNA transfer RNA gene sequence variations in patients with mitochondrial disorders. *Brain*, **124**, 984-994.

Stoeckert, C.J., Jr., Causton, H.C. and Ball, C.A. (2002) Microarray databases: standards and ontologies. *Nat Genet*, **32 Suppl**, 469-473.

Stone, E.M., Lotery, A.J., Munier, F.L., Heon, E., Piguet, B., Guymer, R.H., Vandenburgh, K., Cousin, P., Nishimura, D., Swiderski, R.E., Silvestri, G., Mackey, D.A., Hageman, G.S., Bird, A.C., Sheffield, V.C. and Schorderet, D.F. (1999a) A single EFEMP1 mutation associated with both Malattia Leventinese and Doyne honeycomb retinal dystrophy. *Nat Genet*, **22**, 199-202.

Stone, J., Maslim, J., Valter-Kocsi, K., Mervin, K., Bowers, F., Chu, Y., Barnett, N., Provis, J., Lewis, G., Fisher, S.K., Bisti, S., Gargini, C., Cervetto, L., Merin, S. and Peer, J. (1999b) Mechanisms of

photoreceptor death and survival in mammalian retina. *Prog Retin Eye Res*, **18**, 689-735.

Strachan T., Read A.P. (1999) Genetic mapping of mendelian characters. In; *Human Molecular Genetics 2*. Bios Scientific, Oxford, pp 269-282.

Strom, T.M., Nyakatura, G., Apfelstedt-Sylla, E., Hellebrand, H., Lorenz, B., Weber, B.H., Wutz, K., Gutwillinger, N., Ruther, K., Drescher, B., Sauer, C., Zrenner, E., Meitinger, T., Rosenthal, A. and Meindl, A. (1998) An L-type calcium-channel gene mutated in incomplete X-linked congenital stationary night blindness. *Nat Genet*, **19**, 260-263.

Strunnikova, N., Baffi, J., Gonzalez, A., Silk, W., Cousins, S.W. and Csaky, K.G. (2001) Regulated heat shock protein 27 expression in human retinal pigment epithelium. *Invest Ophthalmol Vis Sci*, **42**, 2130-2138.

Stryer, L. (1995) Genes: Replication and Expression. In: *Biochemistry, Fourth Ed.* WH Freeman & Company, New York.

Sue, C.M., Tanji, K., Hadjigeorgiou, G., Andreu, A.L., Nishino, I., Krishna, S., Bruno, C., Hirano, M., Shanske, S., Bonilla, E., Fischel-Ghodsian, N., DiMauro, S. and Friedman, R. (1999) Maternally inherited hearing loss in a large kindred with a novel T7511C mutation in the mitochondrial DNA tRNA(Ser(UCN)) gene. *Neurology*, **52**, 1905-1908.

Sullivan, L.S., Heckenlively, J.R., Bowne, S.J., Zuo, J., Hide, W.A., Gal, A., Denton, M., Inglehearn, C.F., Blanton, S.H. and Daiger, S.P. (1999) Mutations in a novel retina-specific gene cause autosomal dominant retinitis pigmentosa. *Nat Genet*, **22**, 255-259.

Sun, H., Smallwood, P.M. and Nathans, J. (2000) Biochemical defects in ABCR protein variants associated with human retinopathies. *Nat Genet*, **26**, 242-246.

Sun, H., Tsunenari, T., Yau, K.W. and Nathans, J. (2002) The vitelliform macular dystrophy protein defines a new family of chloride channels. *Proc Natl Acad Sci U S A*, **99**, 4008-4013.

Swaroop, A., Wang, Q.L., Wu, W., Cook, J., Coats, C., Xu, S., Chen, S., Zack, D.J. and Sieving, P.A. (1999) Leber congenital amaurosis caused by a homozygous mutation (R90W) in the homeodomain of the retinal transcription factor CRX: direct evidence for the involvement of CRX in the development of photoreceptor function. *Hum Mol Genet*, **8**, 299-305.

Swaroop, A. and Zack, D.J. (2002) Transcriptome analysis of the retina. *Genome Biol*, **3**, Reviews 1022.

Tachibanaki, S., Tsushima, S. and Kawamura, S. (2001) Low amplification and fast visual pigment

phosphorylation as mechanisms characterizing cone photoresponses. *Proc Natl Acad Sci U S A*, **98**, 14044-14049.

Taylor P., Munson K. and Gjerde D. (2000) *Detection of mutations and polymorphisms on the WAVE nucleic acid fragment analysis system.* Transgenomic Inc., Application Note 101.

Thompson, D.A., Li, Y., McHenry, C.L., Carlson, T.J., Ding, X., Sieving, P.A., Apfelstedt-Sylla, E. and Gal, A. (2001) Mutations in the gene encoding lecithin retinol acyltransferase are associated with early-onset severe retinal dystrophy. *Nat Genet*, **28**, 123-124.

Thykjaer, T., Workman, C., Kruhoffer, M., Demtroder, K., Wolf, H., Andersen, L.D., Frederiksen, C.M., Knudsen, S. and Orntoft, T.F. (2001) Identification of gene expression patterns in superficial and invasive human bladder cancer. *Cancer Res*, **61**, 2492-2499.

Tipton K.F. (2002) Principles of Enzyme assays and kinetic studies. In: *Enzyme Assays: A Practical Approach, 2nd Edition.* Eisenthal R., Danson, M.J. Eds. Oxford University Press, pp 1-45.

Toda, K., Bush, R.A., Humphries, P. and Sieving, P.A. (1999) The electroretinogram of the rhodopsin knockout mouse. *Vis Neurosci*, **16**, 391-398.

Tran, H., VanDusen, W.J. and Argraves, W.S. (1997) The self-association and fibronectin-binding sites of fibulin-1 map to calcium-binding epidermal growth factor-like domains. *J Biol Chem*, **272**, 22600-22606.

Trudeau, M.C. and Zagotta, W.N. (2002) An intersubunit interaction regulates trafficking of rod cyclic nucleotide-gated channels and is disrupted in an inherited form of blindness. *Neuron*, **34**, 197-207.

van den Ouweland, J.M., Bruining, G.J., Lindhout, D., Wit, J.M., Veldhuyzen, B.F. and Maassen, J.A. (1992) Mutations in mitochondrial tRNA genes: non-linkage with syndromes of Wolfram and chronic progressive external ophthalmoplegia. *Nucleic Acids Res*, **20**, 679-682.

van der Flier, A. and Sonnenberg, A. (2001) Structural and functional aspects of filamins. *Biochim Biophys Acta*, **1538**, 99-117.

Van Hoof, C. and Goris, J. (2003) Phosphatases in apoptosis: to be or not to be, PP2A is in the heart of the question. *Biochim Biophys Acta*, **1640**, 97-104.

Velculescu, V.E., Zhang, L., Vogelstein, B. and Kinzler, K.W. (1995) Serial analysis of gene expression. *Science*, **270**, 484-487.

Verpy, E., Leibovici, M., Zwaenepoel, I., Liu, X.Z., Gal, A., Salem, N., Mansour, A., Blanchard, S., Kobayashi, I., Keats, B.J., Slim, R. and Petit, C. (2000) A defect in harmonin, a PDZ domain-containing protein expressed in the inner ear sensory hair cells, underlies Usher syndrome type 1C. *Nat Genet*, **26**, 51-55.

Vervoort, R., Lennon, A., Bird, A.C., Tulloch, B., Axton, R., Miano, M.G., Meindl, A., Meitinger, T., Ciccodicola, A. and Wright, A.F. (2000) Mutational hot spot within a new RPGR exon in X-linked retinitis pigmentosa. *Nat Genet*, **25**, 462-466.

Vithana, E.N., Abu-Safieh, L., Allen, M.J., Carey, A., Papaioannou, M., Chakarova, C., Al-Maghtheh, M., Ebenezer, N.D., Willis, C., Moore, A.T., Bird, A.C., Hunt, D.M. and Bhattacharya, S.S. (2001) A human homolog of yeast pre-mRNA splicing gene, PRP31, underlies autosomal dominant retinitis pigmentosa on chromosome 19q13.4 (RP11). *Mol Cell*, **8**, 375-381.

Vithana, E.N., Abu-Safieh, L., Pelosini, L., Winchester, E., Hornan, D., Bird, A.C., Hunt, D.M., Bustin, S.A. and Bhattacharya, S.S. (2003) Expression of PRPF31 mRNA in Patients with Autosomal Dominant Retinitis Pigmentosa: A Molecular Clue for Incomplete Penetrance? *Invest Ophthalmol Vis Sci*, **44**, 4204-4209.

Wada, Y., Abe, T., Takeshita, T., Sato, H., Yanashima, K. and Tamai, M. (2001) Mutation of human retinal fascin gene (FSCN2) causes autosomal dominant retinitis pigmentosa. *Invest Ophthalmol Vis Sci*, **42**, 2395-2400.

Wada Y, McGee TL, Stillberger MA, Sandberg MA, Berson EL, Dryja TP. (2003) Mutation survey of the IMPDH1 gene in patients with autosomal dominant retinitis pigmentosa and review of the clinical findings associated with IMPDH1 mutations. *Invest. Ophthalmol. Vis. Sci.* **44**, E-Abstract 2306.

Wallace, D.C. (1999) Mitochondrial diseases in man and mouse. *Science*, **283**, 1482-1488.

Wallace DC, Brown MD, and Lott MT. (1996). Mitochondrial Genetics. In: *Emery and Rimoin's Principles and Practice of Medical Genetics*. Rimoin DL, Connor JM, Pyeritz RE, Emery AEH, Eds. Churchill Livingstone, London. pp. 277-332.

Watson, S.J. and Akil, H. (1999) Gene chips and arrays revealed: a primer on their power and their uses. *Biol Psychiatry*, **45**, 533-543.

Watson S. and Arkinstall S. (1994) Opsins. In: *The G-protein Linked Receptor Factsbook*. Academic Press, London. pp. 214-222.

Weber, B.H., Vogt, G., Pruett, R.C., Stohr, H. and Felbor, U. (1994) Mutations in the tissue inhibitor of

metalloproteinases-3 (TIMP3) in patients with Sorsby's fundus dystrophy. *Nat Genet*, **8**, 352-356.

Weil, D., Blanchard, S., Kaplan, J., Guilford, P., Gibson, F., Walsh, J., Mburu, P., Varela, A., Levilliers, J., Weston, M.D. and et al. (1995) Defective myosin VIIA gene responsible for Usher syndrome type 1B. *Nature*, **374**, 60-61.

Weil, D., El-Amraoui, A., Masmoudi, S., Mustapha, M., Kikkawa, Y., Laine, S., Delmaghani, S., Adato, A., Nadifi, S., Zina, Z.B., Hamel, C., Gal, A., Ayadi, H., Yonekawa, H. and Petit, C. (2003) Usher syndrome type I G (USH1G) is caused by mutations in the gene encoding SANS, a protein that associates with the USH1C protein, harmonin. *Hum Mol Genet*, **12**, 463-471.

Weitz, C.J., Miyake, Y., Shinzato, K., Montag, E., Zrenner, E., Went, L.N. and Nathans, J. (1992) Human tritanopia associated with two amino acid substitutions in the blue-sensitive opsin. *Am J Hum Genet*, **50**, 498-507.

Weleber, R.G. (1989) Retinitis pigmentosa and allied disorders. In: *Retina. Volume 1 Basic science and inherited retinal disease.* Ryan S.J. & Ogden, T.E. Eds. The C.V. Mosby Company, Missouri, pp 299-420.

Whitby, F.G., Luecke, H., Kuhn, P., Somoza, J.R., Huete-Perez, J.A., Phillips, J.D., Hill, C.P., Fletterick, R.J. and Wang, C.C. (1997) Crystal structure of Tritrichomonas foetus inosine-5'-monophosphate dehydrogenase and the enzyme-product complex. *Biochemistry*, **36**, 10666-10674.

Wieske, M., Benndorf, R., Behlke, J., Dolling, R., Grelle, G., Bielka, H. and Lutsch, G. (2001) Defined sequence segments of the small heat shock proteins HSP25 and alphaB-crystallin inhibit actin polymerization. *Eur J Biochem*, **268**, 2083-2090.

Willenbrink, W., Halaschek, J., Schuffenhauer, S., Kunz, J. and Steinkasserer, A. (1995) Cyclophilin A, the major intracellular receptor for the immunosuppressant cyclosporin A, maps to chromosome 7p11.2-p13: four pseudogenes map to chromosomes 3, 10, 14, and 18. *Genomics*, **28**, 101-104.

Williams, D.S. (2002) Transport to the photoreceptor outer segment by myosin VIIa and kinesin II. *Vision Res*, **42**, 455-462.

Yalowitz, J.A. and Jayaram, H.N. (2000) Molecular targets of guanine nucleotides in differentiation, proliferation and apoptosis. *Anticancer Res*, **20**, 2329-2338.

Yamamoto, S., Sippel, K.C., Berson, E.L. and Dryja, T.P. (1997) Defects in the rhodopsin kinase gene in the Oguchi form of stationary night blindness. *Nat Genet*, **15**, 175-178.

Yoshida, S., Yashar, B.M., Hiriyanna, S. and Swaroop, A. (2002) Microarray analysis of gene expression in the aging human retina. *Invest Ophthalmol Vis Sci*, **43**, 2554-2560.

Yu, J., Farjo, R., MacNee, S.P., Baehr, W., Stambolian, D.E. and Swaroop, A. (2003) Annotation and analysis of 10,000 expressed sequence tags from developing mouse eye and adult retina. *Genome Biol*, **4**, R65.

Zhang, K., Kniazeva, M., Han, M., Li, W., Yu, Z., Yang, Z., Li, Y., Metzker, M.L., Allikmets, R., Zack, D.J., Kakuk, L.E., Lagali, P.S., Wong, P.W., MacDonald, I.M., Sieving, P.A., Figueroa, D.J., Austin, C.P., Gould, R.J., Ayyagari, R. and Petrukhin, K. (2001) A 5-bp deletion in ELOVL4 is associated with two related forms of autosomal dominant macular dystrophy. *Nat Genet*, **27**, 89-93.

Zhang, R., Evans, G., Rotella, F.J., Westbrook, E.M., Beno, D., Huberman, E., Joachimiak, A. and Collart, F.R. (1999) Characteristics and crystal structure of bacterial inosine-5'-monophosphate dehydrogenase. *Biochemistry*, **38**, 4691-4700.

Zhao, Y., Hong, D.H., Pawlyk, B., Yue, G., Adamian, M., Grynberg, M., Godzik, A. and Li, T. (2003) The retinitis pigmentosa GTPase regulator (RPGR)- interacting protein: subserving RPGR function and participating in disk morphogenesis. *Proc Natl Acad Sci U S A*, **100**, 3965-3970.

Zimmermann, A., Gu, J.J., Spychala, J. and Mitchell, B.S. (1996) Inosine monophosphate dehydrogenase expression: transcriptional regulation of the type I and type II genes. *Adv Enzyme Regul*, **36**, 75-84.

APPENDIX A: STOCK SOLUTIONS

A.1 PCR Solutions

10x PCR reaction buffer

100 mM Tris HCL pH 9.0

500 mM KCL

10-25 mM $MgCl_2$

0.1% gelatin

1% triton

Direct sequencing buffer

5 mM Tris pH 7.8

2.5 mM $MgCl_2$

3 mM DTT

DHPLC PCR Stop buffer

5mM EDTA

60mM NaCl

10mM Tris HCL, pH 8.0

A.2 Electrophoresis Solutions

50X TAE Buffer

Tris base	242g
Acetic acid	57g
EDTA	0.37g

Made up to 1L with dH_20

10X TBE Buffer

Tris base	108g
Boric acid	55g

0.5 M EDTA, pH 8.0	40 ml

Made up to 1L with dH_20.

8% non-denaturing polyacrylamide gel

20% denaturing acrylamide mix	31 ml
Urea solution (1M in 1xTBE)	44 ml
10% ammonium persulphate (APS)	600 µl
TEMED	75 µl

Agarose Gel Loading Dye

Bromophenol blue	13 mg
Xylene cyanol	13 mg
Glycerol	15 ml

made up to 50ml with dH_2O.

Direct sequencing formamide loading dye

Bromophenol blue	10 mg
Xylene cyanol	10 mg
0.5 M EDTA pH 8.0	0.2 ml

made up to 10 ml with formamide.

A.3 Culture media and plasmid purification

LB broth

Bactotryptone	10g
Yeast extract	5g
NaCl	10g

Made up to 1L with H_20 and autoclaved.

NZY+ Broth

NZ Amine (casein hydrolysate)	10g
NaCl	5g
Yeast extract	5g

Made up to 1L, autoclaved and added prior to use:

1M $MgCl_2$	12.5 ml
1M $MgSO_4$	12.5 ml
20% w/v Glucose	20 ml

Filter-sterilised

LB Agar

NaCl	10g
Tryptone	10g
Yeast extract	5g
Agar	20g

Made up to 1L with H_2O, autoclaved and poured into petri dishes.

TT Buffer

50 mM Tris pH 8.0

25% Sucrose

2 mM EDTA

M-STET Buffer

50mM Tris pH 8.0

50mM EDTA

5% Triton

5% Sucrose

TE Buffer

10 mM Tris-HCl (pH 7.5)

1 mM EDTA

IPTG (100 mM)

0.238g IPTG in 10 ml sterile H_20, filter-sterilised and stored at -20^0C.

Ampicillin

25 mg/ml in sterile H_20, stored at -20^0C. Used at 50 μg/ml.

A.4 His-tag purification buffers

Ni-NTA Bind Buffer (1x)

50 mM NaH_2PO_4, pH 8.0

300 mM NaCl

10mM imidazole

Ni-NTA Wash Buffer (1x)

50 mM NaH_2PO_4, pH 8.0

300 mM NaCl

20mM imidazole

Ni-NTA Elute Buffer (1x)

50 mM NaH_2PO_4, pH 8.0

300 mM NaCl

250mM imidazole

Enzyme Assay Buffer

0.1 M Tris

0.1 M KCL

3 mM EDTA

2 mM DTT pH 8.0

A.5 SDS polyacrylamide gel electrophoresis solutions

SDS-Loading Buffer (5x)

250mM Tris pH 6.8

500Mm DTT

10% SDS

0.5% Bromophenol Blue

50% Glycerol

5% β-Mercaptoethanol

SDS polyacrylamide gels

	10%	5%(mls)
30% Acrylamide	3.3	1.7
H_2O	4.0	6.8
1.5M Tris (pH 8.8)	1.3	
1.0M Tris (pH 6.8)		1.25
10% SDS	0.1	0.1
10% ammonium persulphate	0.1	0.1
TEMED	0.004	0.01

SDS-PAGE Running Buffer

25 mM Tris-Cl

250 mM Glycine (pH 8.3)

0.1% SDS

Coomassie Blue Stain

40% Methanol

7% Acetic Acid

0.25% Brilliant Blue

Destain Soln.

40% Methanol

7% Acetic Acid

A.6 Mammalian cell culture solutions

Phosphate-Buffered Sulphate (PBS) Buffer (10X)

100 mM sodium phosphate, 1.4 M NaCl containing:

$Na_2HPO_4.2H_2O$	7.12g
$NaH_2PO_4.H_2O$	1.38g
NaCl	40.95g

Made up to 500ml with H2O, pH 7.4.

2x HBS Buffer

280 mM NaCl

10 mM KCl

1.5 mM Na_2HPO_4

12 mM Dextrose

50 mM HEPES, pH 7.1

PF Fixative

PBS, pH 7.2 containing:

2% paraformaldehyde

0.2% gluteraldehyde

β-Gal Staining Buffer

PBS, pH 7.2 containing:

5 mM Potassium Ferricyanide

5 mM Potassium Ferrocyanide

2 mM $MgCl_2$

0.02% NP-40

0.01% SDS

1 mg/ml X-gal (added just before use)

Protein Extraction Buffer A

10 mM HEPES pH 7.9

1.5 mM MgCl2, 10 mM KCl

0.5 mM DTT

0.5 mM PMSF

0.25 mM benzamidine

Protein Extraction Buffer B

5 mM HEPES pH 7.9

1.5 mM MgCl2

0.2 mM EDTA

0.5 mM PMSF

0.25 mM benzamidine

A.7 Western Blotting solutions

Transfer Blotting Buffer

25 Mm Tris

150 mM Glycine

20% Methanol (pH 8.3)

TBS Buffer

10 mM Tris-Cl, pH 7.5

150 mM NaCl

TBS-TT Buffer

20 mM Tris-Cl, pH 7.5

500 mM NaCl

0.05% (v/v) Tween-20

0.2% (v/v) Triton X-100

Western Blot Blocking Solution

1% Alkali-soluble casein in TBS (Novagen)

APPENDIX B: PRIMER SEQUENCES

For all primer sequences; F denotes 5' to 3' sequence and R denotes 3' to 5' sequence direction.

B.1 Mitochondrial tRNA primers

Mt 501F:	CCATCCTACCCAGCACACACA
Mt 711R:	TAGAGGGTGAACTCACTGGA
Mt1531F:	CCCCTACGCATTTATATAGAGG
Mt1781R:	CATCTTTCCCTTGCGGTACT
Mt3151F:	ACTTCACAAAGCGCCTTCCC
Mt3356R:	CGGTAAGCATTAGGAATGCCA
Mt4189F:	CCACTCACCCTAGCATTACT
Mt4523R:	TGCGAGCTTAGCGCTGTGAT
Mt5451F:	ACACTCATCGCCCTTACCAC
Mt5772R:	CGAAGAAGCAGCTTCAAACC
Mt5701F:	AGGCACCCTAATCAACTGGC
Mt5942R:	GGTATAGTGTTCCAATGTCT
Mt7369F:	CCATAAACCTGGAGTGACTA
Mt7639R:	CATGAAAGGTGATAAGCTCT
Mt8207F:	CCCATCGTCCTAGAATTAAT
Mt8418R:	GATGAGGAATAGTGTAAGGA
Mt9917F:	CGCCGCCTGATACTGGCATT
Mt10150R:	ATGTAGCCGTTGAGTTGTGG
Mt10337F:	ATTAATCATCATCCTAGCCC
Mt10521R:	GAGCGATATACTAGTATTCC
Mt12067F:	CATGTTCATACACCTATCCCC
Mt12389R:	TAACGAGGGTGGTAAGGATG
Mt14611F:	GAGAAGGCTTAGAAGAAAACC
Mt14793R:	GGGGAGGTCGATGAATGAGT
Mt15806F:	GCATCCGTACTATACTTCAC
Mt16076R:	CGAAATACATAGCGGTTGTTG

B.2 Real-time quantitative PCR primers

GAPDH mouse F;	CCATGGAGAAGGCTGGGG
GAPDH mouse R;	CAAAGTTGTCATGGATGACC
IMPDH1 mouse cDNA Ex6 F;	GCAGGTGTGACGTTGAAAGA
IMPDH1 mouse cDNA Ex8 R;	CACCATGGCGATCTGATACA
Mouse B-PDE F;	CAACTGTAGAACACGCAGAAGC
Mouse B-PDE R;	GTTTAGATAGGCCCGGACAG
Mouse testican F;	CAACGCCAATTTCCTAGACA
Mouse testican R;	TGGTCGAAGGGCTTGTTG
Mouse CRABP F;	CCAAGACGGGGATCAGTTCT
Mouse CRABP R;	CGTGGGTAAACTCCTGCATT
Mouse Cathepsin S F;	CCAGCCATTCCTCCTTCTTC
Mouse Cathepsin S R;	GCCATCCGAATGTATCCTTG
Myosin LC2 F;	CTTTGCCTGCTTTGATGAGG
Myosin LC2 R;	GTGTTTGAGGATGCGAGTGA

B.3 Primer sequences for amplification of mouse or human cDNA (product size in base pairs)

Beta-2 Microglobulin human/mouse F;	TTCAGCAAGGACTGGTCTTTC
Beta-2 Microglobulin human R;	GCTGCTTACATGTCTCGATCC
Beta-2 Microglobulin mouse R;	CTTGATCACATGTCTCGATCC (129bp)
Rhodopsin human/mouse F;	TTCCTCACGCTCTAGTCAC
Rhodopsin human/mouse R;	TTCTCCCCGAAGCGGAAGTT (286bp)
RDS-peripherin human/mouse F;	CTGGCTGGGAAGATCTGCTA
RDS-peripherin human/mouse R;	CCATCCACGTTGCTCTTGAT (377bp)
PDE6A, rod, α-human/mouse F;	CCACTTCACCAAGAGAGATG
PDE6A, rod, α-human/mouse R;	TTCGGGATGACTTTGATGTC (398bp)

GRIP –domain gene

Human cDNA F;	TGAGATTGCTGACGGAGTTG	
Human cDNA R;	CTGCACCAGCTGAAGACTCA	(603bp)
Human/mouse cDNA F2;	TGTCTTGTTCTCCAGGTCCA	
Human/mouse cDNA R;	TTGAACTGCAGACCAAGCAG	(358bp)

B.4 Primer sequences used to screen candidate RP10 genes

Grip-domain gene

Exon 1.1 F;	AAGAGGCAGCAGAAACCAGA
Exon 1.1 R;	CAGAAGTCCTGTGGGTGGTG
Exon 1.2 F;	TGTGATCTCCACCTCCTTGC
Exon 1.2 R;	CTGGAGATAATGCCCAGCTC
Exon 1.3 F;	GACAACCTGGGCTCTCATCT
Exon 1.3 R;	CAAACCTGTGACCCTTTTGC
Exon 2.1 F;	GCTCTAACTAGCAAAGGAGGAAAA
Exon 2.1 R;	CTGCACCAGCTGAAGACTCA
Exon 2.2 F;	GCCTTGTTACTGGCATCCTC
Exon 2.2 R;	CGCTCGCTGTTTCTTTAAGC

Cyclophilin-like gene

Exon 1 F;	GTTGTTCACAGTTCACAATGG
Exon 1 R;	CACATGTGGAATAAACAGTG

Zinc-finger gene (AF218032)

Exon 2 F;	ATAACTGGCTTATGCTAGGG
Exon 2 R;	ACGTATCTGGAAAATGCAGC
Exon 3 F;	CTCTAGACCAAGTCAGTATT
Exon 3 R;	TGCGGGCACAAGTGTGATTA
Exon 5 F2;	TGGAAGGGGGTGAAGATTCT
Exon 5 R2;	CCGTCACATTCGAAAAGTAC
Exon 5 F3;	CTTACTGCGTCCTTTAGAGG

Exon 5 R3; ATTAGAGGGCTACAGCAGGC

Blue Cone Pigment (OPN1SW)

Exon 1 F; TCATTCACAGAGCCCAAGTG

Exon 1 R; TCTTTAGGAACCCCCTCCAG

Exon 2 F; CGATCTGTTTGCCACTCTGC

Exon 2 R; AAGCTCTCTTTCCACCCACA

Exon 3 F; GAACACAATCCAGGCATCTCA

Exon 3 R; GCACTCTTCCTTCTCATGTGG

Exon 4 F; AAGCATCCAGAGGGCCAGGA

Exon 4 R; TCCAGGGTGCTCTGAGTTAAA

Exon 5 F; TGCAAGGCTTTGGTGATACA

Exon 5 R; TTTGGTTTCTGACGGAGACA

IMPDH1 primers for exon screening

IMPDH1 Ex1 F; AGAGGAGGAAGGGGACAGG

IMPDH1 Ex 1 R; GTCAGCAGTAGCAGCAGCAG

IMPDH1 Ex 2 F; CTGCCTCCTCTGGCATGG

IMPDH1 Ex 2 R; CTGCCCCTGAGCAAGAAGT

IMPDH1 Ex 3+4 F; AGCTCAGTGAGTGAGTGTCCAG

IMPDH1 Ex 3+4 R; CAGGGAGTGTAGCAGTGCAG

IMPDH1 Ex 5+6 F; CTGCATCCTCTGTTCCCTGT

IMPDH1 Ex 5+6 R; GAAGGAACAACGGGACTGTG

IMPDH1 Ex 7 F; CCCTCCTAAACATCTCCCAAA

IMPDH1 Ex 7 R; GGTGAACCTGGGTCCTCATA

IMPDH1 Ex 8+9 F; CTCCCTCCTGCCTTGAGAAT

IMPDH1 Ex 8+9 R; AGGGCCTGGCAGAGAGAGTA

IMPDH1 Ex 10+11 F; GTGCACAGGAGGAAGAGCTG

IMPDH1 Ex 10+11 R; GCCTCAGTTTCCAGAACCAC

IMPDH1 Ex 12 F; GTATCCCGTTTTTGCCCTTA

IMPDH1 Ex 12 R; GGTAGGTGGAGCAGATCAGG

IMPDH1 Ex 13 F; GGCTCCTGCTTCCTTTCTCT

IMPDH1 Ex 13 R; TGGAACCTCAGCTTGACCTC

IMPDH1 Ex 14 F; GAAAGGGTTTTGGGAAGGAG

IMPDH1 Ex 14 R; CCTCTCTGCCTGGAAAGGA

B.5 IMPDH1 site-directed mutagenesis primers

Human IMPDH1 Arg224Pro mutant probe F; ccatcatcgccc**C**caccgacctgaagaa

Human IMPDH1 Arg224Pro mutant probe R; ttcttcaggtcggtg**G**gggcgatgatgg

Human IMPDH1 Asp226Asn mutant probe F; catcatcgcccgcacc**A**acctgaagaagaacc

Human IMPDH1 Arg226Asn mutant probe R; ggttcttcttcaggt**T**ggtgcgggcgatgatg

Mouse IMPDH1 Arg224Pro mutant probe F; gccatcattgcgc**C**cacagacctgaaga

Mouse IMPDH1 Arg224Pro mutant probe R; tcttcaggtctgtg**G**gcgcaatgatggc

B.6 IMPDH1 cDNA cloning and sequencing primers

IMPDH1-Xho1 F; ATATCTCGAGATGGCGGACTACCTGATCAG

IMPDH1-Xho1 R; AGAGCTCGAGTCAGTACAGCCGCTTTTCGT

IMPDH1 cDNA ex1 Hu F; CTACGTGCCCGAGGATGG

IMPDH1 cDNA ex3 Hu R; CGTCTTCAGCGTGATCTTCC

IMPDH1 cDNA ex2 Hu F; CCTGATTCTCCCAGGATTCA

IMPDH1 cDNA ex4 Hu/MoR; CTTCATTGGCCTGGAACTCT

IMPDH1 cDNA ex5 Hu/Mo F; CTTGCTGAGAAGGACCACAC

IMPDH1 cDNA ex 12 R; GGTAGGTGGAGCAGATCAGG

IMPDH1 cDNA ex 13F; GGCTCCTGCTTCCTTTCTCT

PET-15b Vector: T7 F2; GCGGATAACAATTCCCCTCT

IMPDH1 cDNA exon 3R; CGTCTTCAGCGTGATCTTCC

IMPDH1 cDNA exon 12 F; CTCATAGCAGGCATCCAACA

pET15b Vector T7 Terminator R; CCCCAAGGGGTTATGCTAGT

pcDNA3.1/His F; CCACTGCTTACTGGCTTATCG

pcDNA3.1/His R; GCGATGCAATTTCCTCATTT

APPENDIX C

Cloned and/or mapped genes causing retinal degenerations. Adapted from the Retnet database, accessed September 17th 2003 (http://www.sph.uth.tmc.edu/Retnet/disease.htm).

Chromosome 1				
Symbol; OMIM Number	**Location**	**Disease; Protein**	**Mapping Method; Comments**	**References**
LCA9	1p36	recessive Leber congenital amaurosis	linkage mapping; single consanguineous Pakistani family	Keen 03
RPE65, LCA2, RP20; 180069, 204100	1p31.2	recessive Leber congenital amaurosis; recessive RP; protein: retinal pigment epithelium-specific 65 kD protein [LocusLink]	cloned gene; accounts for 2% of recessive RP and 7 to 16% of LCA; same as *RPE65-/-* Swedish Briard-Beagle dog; protein is necessary for production of 11-*cis*-vitamin A; 9-*cis*-retinal restores visual function in mouse model; sucessful gene therapy in dog; in same pathway as LRAT	Acland 01; Aguirre 98; Gu 97; Lotery 00; Marlhens 97; Morimura 98; Redmond 98; Van Hooser 00; Veske 99
ABCA4, ABCR, RP19, STGD1; 248200, 601691, 601718	1p22.1	recessive Stargardt disease, juvenile and late onset; recessive MD; recessive RP; recessive fundus flavimaculatus; recessive cone-rod dystrophy; protein: ATP-binding cassette transporter - retinal [LocusLink]	linkage mapping, cloned gene; may be involved in age-related macular degeneration; same as ROS1.2 and rim protein, expressed in rod outer segment and foveal cones; ABCA4 mutation may increase severity of STGD3; flippase for all-*trans* retinal and N-retinylidene-PE	Allikmets 97; Allikmets 97a; Allikmets 00; Cremers 98; Gerber 95; Gerber 98; Kaplan 93; Lewis 99; Martínez-Mir 97; Martínez-Mir 98; Maugeri 00; Molday 00; Nasonkin 98; Rozet 98; Stone 98; Sun 97; Sun 99; Weng 99; Zhang 99
COL11A1, STL2; 120280, 154780, 604841	1p21.1	dominant Stickler syndrome, type II; dominant Marshall syndrome; protein: collagen, type XI, alpha 1 [LocusLink]	linkage mapping, cloned gene; mutations in COL11A1 cause a variety of symptoms including facial-skeletal abnormalities, sensorineural hearing loss, and multiple ocular disorders such as glaucoma, myopia and retinal detachment (Stickler syndrome); retinal findings are considered a consequence of vitreous abnormalities; see also COL2A1	Annunen 99; Richards 96
GNAT2, ACHM4; 139340	1p13.3	recessive achromatopsia; protein: guanine nucleotide binding protein (G protein) cone-specifc transducin alpha subunit [LocusLink]	cloned gene; total color blindness and other cone-related abnormalities (rod monochromacy); GNAT2 accounts for a minor fraction of achromatopsia cases whereas CNGA3 accounts for 20-30% and CNGB3 accounts for 40-50%	Aligianis 02; Kohl 02
CORD8;	1q12-q24	recessive cone-rod dystrophy	linkage mapping;	Khaliq 00

605549			consanguineous Pakistani family	
HPRP3, HPRP3P, RP18; 601414, 607301	1q21.2	dominant RP; protein: human homolog of yeast pre-mRNA splicing factor 3 [LocusLink]	linkage mapping, cloned gene; English and Danish families; early onset night blindness; recurrent Thr494Met mutation; protein is a highly-conserved, ubiquitously-expressed member of the U4/U6-U5 tri-snRNP particle complex which includes PRPF31 (RP11) and PRPF8 (RP13)	Chakarova 02; Heng 98; Xu 96a; Xu 98
ARMD1; 603075	1q25-q31	dominant MD, age-related	linkage mapping; possible model for acquired age-related macular degeneration; chromosomal region overlaps with an AMD susceptibility locus	Klein 98; Weeks 01
AXPC1	1q31-q32	recessive ataxia, posterior column with RP	linkage mapping	Higgins 99
CRB1, RP12; 600105, 604210, 268030	1q31.3	recessive RP with para-arteriolar preservation of the RPE (PPRPE); recessive RP; recessive Leber congenital amaurosis; protein: crumbs homolog 1 [LocusLink]	linkage mapping; homologous to *Drosophila* crumbs protein, possibly involved in cell-cell interactions and cell polarity; homozygous or compound heterozygous mutations in 10 unrelated patients; causes 9 to 13% of LCA; symptoms may include Coats-like exudative vasculopathy; mutations result in thick retina with abnormal lamination	den Hollander 99a; den Hollander 01; Heckenlively 82; Jacobson 03; Leutelt 95; Lotery 01; Lotery 01a; van Soest 94
USH2A; 276901	1q41	recessive Usher syndrome, type 2a; recessive RP; protein: usherin [LocusLink]	linkage mapping, cloned gene; usherin is a basement membrane protein, with laminin EGF and fibronectin type III domains, found in many tissues, including capillary and structural basement membranes in retina and inner ear; common 2299delG mutation with atypical phenotype; Cys759Phe mutation found in 4 to 5% of recessive RP without hearing loss	Bhattacharya 02; Eudy 98; Kimberling 90; Kimberling 95; Lewis 90; Liu 99; Rivolta 00; Saouda 98; Weston 00

Chromosome 2

Symbol; OMIM Number	Location	Disease; Protein	Mapping Method; Comments	References
RP28; 606068	2p16-p11	recessive RP	homozygosity mapping; consanguineous Indian family	Gu 99
EFEMP1, DHRD, MTLV, FBLN3; 126600, 601548	2p16.1	dominant radial, macular drusen; dominant Doyne honeycomb retinal degeneration (Malattia Leventinese); protein: EGF-containing fibrillin-like	linkage mapping, cloned gene; single mutation (Arg345Trp) found in all affected individuals to date; possible model for age-related macular	Edwards 98; Héon 96; Héon 96a; Kermani 99; Gregory 96; Marmorstein 02; Stone 99

		extracellular matrix protein 1 [LocusLink]	degeneration; normal protein is secreted from RPE whereas mutant protein is misfolded and partly retained in RPE; both proteins accumulate between the RPE and drusen, but not within drusen	
ALMS1, ALSS; 203800	2p13.1	recessive Alström syndrome; protein: ALMS1 protein [LocusLink]	homozygosity and linkage mapping, cloned gene; symptoms include RP (cone-rod dystrophy), cardiomyopathy, obesity and diabetes (similar to BBS); gene identified in balanced chromosomal translocation; widely expressed gene with product of unknown function	Collin 97; Collin 99; Hearn 02; Macari 98
CNGA3, ACHM2, CNCG3, RMCH2; 216900, 600053	2q11.2	recessive achromatopsia; protein: cone photoreceptor cGMP-gated cation channel alpha subunit [LocusLink]	homozygosity mapping, cloned gene; total color blindness and other cone-related abnormalities (rod monochromacy); CNGA3 accounts for 20-30% of achromatopsia cases whereas CNGB3 accounts for 40-50% and GNAT2 accounts for a minor fraction	Arbour 97; Kohl 98; Kohl 02; Wissinger 98; Wissinger 01
MERTK; 604705	2q13	recessive RP; protein: c-mer protooncogene receptor tyrosine kinase [LocusLink]	cloned gene; several affected familes; human ortholog of the mouse *Mertk* gene; causes defective phagocytosis of photoreceptor outer segments by the RPE and retinal degeneration in the *RCS* rat; successful gene therapy in rat; expressed in multiple tissues including RPE/sclera	D'Cruz 00; Gal 00; Vollrath 01
RP26	2q31-q33	recessive RP	linkage mapping; MPP4 is excluded	Bayés 98; Conte 02
BBS5; 603650	2q31	recessive Bardet-Biedl syndrome	linkage mapping	Beales 01; Young 99
SAG; 181031, 258100	2q37.1	recessive Oguchi disease; recessive RP; protein: arrestin (s-antigen) [LocusLink]	cloned gene; CSNB and fundus pallor in Japanese primarily; recessive RP in Japanese	Fuchs 95; Maw 95; Nakazawa 98; Wada 96

Chromosome 3

Symbol; OMIM Number	Location	Disease; Protein	Mapping Method; Comments	References
USH2B, DFNB6; 276905, 600971	3p24.2-p23	recessive Usher syndrome, type 2; recessive sensorineural deafness without RP	linkage mapping	Hmani 99; Pieke Dahl 93
GNAT1; 139330	3p21.31	dominant CSNB, Nougaret type; protein: rod transducin alpha subunit [LocusLink]	cloned gene; Gly38Asp mutation in a single large French family, may affect	Dryja 96; Maumenee-Hussels 96; Muradov 00

			taste perception, attenuates visual signaling	
SCA7, ADCA2, OPCA3; 164500	3p14.1	dominant spinocerebellar ataxia w/ MD or retinal degeneration; protein: SCA7 protein [LocusLink]	linkage mapping, cloned gene; Moroccan, Belgian, French, Swedish, American and African-American families; shows anticipation with expanding CAG repeat in coding sequence of protein with unknown function; regional retinal dysfunction, cone-rod type	Aleman 02; Benomar 95; David 97; Del Favero 98; Gouw 95; Holmberg 95
BBS3; 600151	3p13-p12	recessive Bardet-Biedl syndrome	homozygosity and linkage mapping; Canadian family; milder phenotype with normal IQ, reversible obesity and polydactyly of the feet only in most patients	Beales 97; Beales 01; Sheffield 94; Woods 99; Young 98
RHO, RP4; 180380	3q22.1	dominant RP; dominant CSNB; recessive RP; protein: rhodopsin [LocusLink]	linkage mapping, cloned gene; accounts for 30 to 40% of autosomal dominant RP; more than 100 distinct mutations but RhoPro23His causes 10% of adRP in US Caucasians; 'RP4' withdrawn; naturally occurring Thr4Arg mutation in English Mastiff dog	Dryja 90; Dryja 90a; Dryja 91; Dryja 93; Farrar 90a; Kijas 02; McWilliams 89; Nathans 84; Rosenfeld 92
RP5; 180102	same as RHO	not distinct from RHO/RP4	linkage mapping; mutation screening; mapping error; 'RP5' withdrawn	Farrar 92
USH3A, USH3; 276902	3q25.1	recessive Usher syndrome, type 3; protein: clarin-1 [LocusLink]	linkage mapping, cloned gene; clarin-1 is a novel, 4-transmembrane protein with a possible role in hair cell and photoreceptor synapses; accounts for 40% of Usher syndrome in Finland; possible digenic deafness with MYO7A	Adato 99; Adato 02; Joensuu 01; Sankila 95
OPA1; 165500, 605290	3q29	dominant optic atrophy, Kjer type; protein: OPA1 protein [LocusLink]	linkage mapping, cloned gene; gene is widely expressed and abundant in retina; protein is a dynamin-related GTPase which localizes to mitochondria; OPA1 mutations cause 30 to 50% of dominant optic atrophy; disease may be the consequence of haploinsufficiency with reduced penetrance; OPA1 alleles are also associated with normal tension glaucoma	Alexander 00; Aung 02; Bonneau 95; Brown 97a; Delettre 00; Eiberg 94; Johnston 97; Lunkes 95; Pesch 01; Seller 97; Toomes 01; Votruba 97; Votruba 98

Chromosome 4

Symbol; OMIM Number	Location	Disease; Protein	Mapping Method; Comments	References
STGD4; 603786	4p	dominant Stargardt-like macular dystrophy	linkage mapping; Caribbean family	Kniazeva 99
MCDR2	4p16.3-	dominant MD, bull's-eye	linkage mapping; single	Michaelides 03

	p15.2		British family; locus overlaps with STDG4	
PDE6B, CSNB3; 163500, 180072	4p16.3	recessive RP; dominant CSNB; protein: rod cGMP phosphodiesterase beta subunit [LocusLink]	linkage mapping, cloned gene; same as retinal degeneration in the *rd* mouse, *r* mouse and *rcd1* Irish Setter dog; accounts for 3 to 4% of recessive RP; photoreceptor rescue with calcium-channel blocker in mouse but not dog	Altherr 92; Bateman 92; Bayés 95; Bowes 90; Collins 92; Farber 92; Frasson 99; Gal 94; Gal 94a; McLaughlin 93; McLaughlin 95; Pearce-Kelling 01; Piriev 98; Pittler 91; Pittler 93; Suber 93; Valverde 95; Weber 91
WFS1, DFNA38; 222300, 598500	4p16.1	recessive Wolfram syndrome; dominant low frequency sensorineural hearing loss; protein: wolframin [LocusLink]	linkage mapping, cloned gene; symptoms of recessive disease include diabetes, optic atrophy and deafness; often associated with multiple mitochondrial deletions; symptoms of dominant disease include non-syndromic low frequency loss without profound deafness	Barrientos 96; Barrientos 96a; Bespalova 01; Collier 96; Inoue 98; Polymeropoulos 94; Strom 98a; Young 01
PROML1; 604365	4p15.32	recessive retinal degeneration; protein: prominin (mouse)-like 1 [LocusLink]	homozygosity mapping, cloned gene; Indian family; prominin is a 5-transmembrane glycoprotein associated with plasma membrane evaginations in rod outer segments	Maw 00
CNGA1, CNCG, CNCG1; 123825	4p12	recessive RP; protein: rod cGMP-gated channel alpha subunit [LocusLink]	cloned gene; nonsense, missense and deletion mutations in four RP families	Dhallan 92; Dryja 95; Griffin 93
WFS2; 604928	4q22-q24	recessive Wolfram syndrome; dominant	homozygosity mapping, linkage mapping; symptoms include diabetes, optic atrophy and deafness; three Jordanian families; WFS1 excluded	El-Shanti 00
MTP, ABL; 200100, 157147	4q23	recessive abetalipoproteinemia; protein: microsomal triglyceride transfer protein [LocusLink]	cloned gene; multiple lipid abnormalities including pigmentary retinal degeneration	Narcisi 95; Sharp 93; Shoulders 93
BBS7, BBS2L1; 607590	4q27	recessiveBardet Biedl syndrome; protein: BBS7 protein [LocusLink]	cloned gene; protein of unknown function with sequence similarity to BBS2	Badano 03
RP29	4q32-q34	recessive RP	linkage mapping; consanguineous Pakistani family	Hameed 01
LRAT; 604863	4q32.1	recessive RP, severe early-onset; protein: lecithin retinol acyltransferase [LocusLink]	cloned gene; gene is expressed in RPE; protein catalyzes first step in visual cycle transforming vitamin A into 11-*cis*-retinol; same pathway as RPE65	Ruiz 99; Ruiz 01; Thompson 01
BCD; 210370	4q35-qter	recessive Bietti crystalline corneoretinal dystrophy	linkage mapping; symptoms include RP and crystals in the retina, cornea and lymphocytes; more common in Asians	Jiao 00

Chromosome 5

Symbol; OMIM Number	Location	Disease; Protein	Mapping Method; Comments	References
MCDR3	5p15.33-p13.1	dominant MD	linkage mapping; single British family; clincally similar to North Carolina macular dystrophy, MCDR1	Michaelides 03a
WGN1, ERVR; 143200	5q13-q14	dominant Wagner disease and erosive vitreoretinopathy	linkage mapping; vitreoretinopathy alone (Brown 95) or with ocular abnormalities (Black 99a), may be allelic or distinct genes	Black 99a; Brown 95
USH2C; 605472	5q14-q21	recessive Usher syndrome, type 2	linkage mapping; five unrelated families, mild RP, possible dental abnormalities	Pieke-Dahl 00
PDE6A; 180071	5q33.1	recessive RP; protein: cGMP phosphodiesterase alpha subunit [LocusLink]	cloned gene; homozygote and compound heterozygote mutations; causes 3 to 4% of recessive RP in North America; same as *PRA* in Cardigan Welsh corgi dog	Dryja 99; Huang 95; Peterson-Jones 99; Pittler 90

Chromosome 6

Symbol; OMIM Number	Location	Disease; Protein	Mapping Method; Comments	References
TULP1, RP14; 600132, 602280	6p21.31	recessive RP; protein: tubby-like protein 1 [LocusLink]	linkage mapping, cloned gene; two Dominican families and others; protein localizes to developing and adult rods and cones; possibly involved in transport of rhodopsin from inner to outer segment; a similar gene in *tub* mouse causes obesity, deafness and retinal degeneration	Banerjee 98; Banerjee 98a; Gu 98; Hagstrom 98; Hagstrom 01; Knowles 94; Milam 00
RDS, RP7; 179605	6p21.2	dominant RP; dominant MD; digenic RP with ROM1; dominant adult vitelliform MD; protein: peripherin 2 [LocusLink]	linkage mapping, cloned gene; dominant mutations; also, compound heterozygotes with ROM1; accounts for 5% of dominant RP; same as *rds* mouse; 'RP7' withdrawn; photoreceptor rescue in mouse model	Ali 00; Arikawa 92; Connell 90; Connell 91; Dryja 97; Farrar 91; Felbor 97a; Jordan 92a; Kajiwara 91; Kajiwara 94; Travis 91; Travis 91a
GUCA1A, COD3, GCAP1; 602093, 600364	6p21.1	dominant cone dystrophy; dominant cone-rod dystrophy; protein: guanylate cyclase activating protein 1A [LocusLink]	linkage mapping, cloned gene; British family with constitutively active mutant; variable phenotype within families	Downes 01; Payne 97; Payne 98; Sokal 98
RP25; 602772	6cen-q15	recessive RP	homozygosity mapping, linkage mapping; Spanish and Pakistani families; accounts for 10 to 20% of recessive RP in Spain; mapped to region containing GABA receptors	Khaliq 99; Ruiz 98
LCA5;	6q11-q16	recessive Leber congenital	linkage mapping; American	Dharmaraj 00

604537		amaurosis	families of Old Order River Brethren descended from Swiss immigrants; may be allelic to other 6q retinopathies	
RIMS1, CORD7, RIM1; 603649, 606629	6q13	dominant cone-rod dystrophy; protein: regulating synaptic membrane exocytosis protein 1or rab3A-interacting molecule [LocusLink]	linkage mapping, cloned gene; expressed in brain and photoreceptors; protein localizes to ribbon synapses and interacts with RAB3A, a protein that regulates synaptic vesicle exocytosis	Johnson 03; Kelsell 98; Kniazeva 99a; Wang 97; Wang 00
MCDR1, PBCRA; 136550, 600790	6q14-q16.2	dominant MD, North Carolina type; dominant progressive bifocal chorioretinal atrophy	linkage mapping; North Carolina, German, Belizean and British families; MCDR1 is clinically distinct from PBCRA (same locus) but similar to MCDR3 (different locus)	Kelsell 95; Rabb 98; Sauer 97a; Small 92; Small 97; Small 99
ELOVL4, STGD3; 600110	6q14.1	dominant MD, Stargardt-like; protein: elongation of very long fatty acids protein [LocusLink]	linkage mapping, cloned gene; large North American family with 5 bp deletion; protein is a photoreceptor-specific component of the fatty acid elongation system, consistent with suggested modifying role of ABCA4; mapping overlaps with CORD7; MCRD1 excluded; includes STGD2	Edwards 01; Griesinger 00; Kniazeva 99a; Kniazeva 00; Stefko 00; Stone 94; Zhang 99; Zhang 01
RCD1; 180020	6q25-q26	dominant retinal-cone dystrophy 1	deletion mapping	OMIM 2001

Chromosome 7

Symbol; OMIM Number	Location	Disease; Protein	Mapping Method; Comments	References
CYMD; 153880	7p21-p15	dominant MD, cystoid	linkage mapping; distinct from RP9	Inglehearn 94a; Kremer 94
RP9, PAP1, PIM1K; 180104, 607331	7p14.3	dominant RP; protein: RP9 protein or PIM1-kinase associated protein 1 [LocusLink]	linkage mapping, cloned gene; mutations in this gene are the likely but not certain cause of RP9; widely-expressed gene; protein with unknown function	Inglehearn 93; Inglehearn 94b; Inglehearn 98; Keen 95; Keen 02; Kim 95
PEX1, IRD; 266510, 602136	7q21.2	recessive Refsum disease, infantile; protein: peroxisome biogenesis factor 1 [LocusLink]	cloned gene; symptoms include RP, retardation and hearing deficit	Portsteffen 97; Reuber 97
IMPDH1, RP10; 146690, 180105	7q32.1	dominant RP; protein: inosine monophosphate dehydrogenase 1 [LocusLink]	linkage mapping, cloned gene; Spanish, Scottish and American families; the gene is one of two ubiquitously-expressed isoforms of IMPDH in humans; IMPDH is a highly-conserved enzyme, found in bacteria and eukaryotes, which catalizes the rate-limiting step in guanine synthesis; a common mutation, Asp226Asn, is at a site conserved in all species	Bowne 02; Daiger 97; Jordan 93; Kennan 02; McGuire 95; McGuire 96; Millán 95; Mohamed 96

OPN1SW, BCP, CBT; 190900	7q32.1	dominant tritanopia; protein: blue cone opsin [LocusLink]	cloned gene; several mutations; progressive retinopathy not observed	Fitzgibbon 94; Nathans 86; Nathans 92; Nathans 93; Weitz 92; Weitz 92a

Chromosome 8

Symbol; OMIM Number	Location	Disease; Protein	Mapping Method; Comments	References
CORD9	8p11	recessive cone-rod dystrophy	linkage mapping; consanguineous Brazilian family; RP1 excluded	Danciger 01
RP1; 180100, 603937	8q12.1	dominant RP; protein: RP1 protein [LocusLink]	linkage mapping, cloned gene; causes 5 to 10% of adRP; large Kentucky family and others; highly variable expression; two common mutations, Arg677X and 2280del4; protein is photoreceptor-specific, with similarity to doublecortin, and localizes to connecting cilia	Blanton 91; Bowne 99; Daiger 97; Guillonneau 99; Jacobson 00; Liu 02; Pierce 99; Roderick 97; Sadler 93; Sullivan 99; Xu 96
TTPA; 600415	8q12.3	recessive RP and/or recessive or dominant ataxia; protein: alpha-tocopherol-transfer protein [LocusLink]	cloned gene; TPA mutations found in patients with vitamin E deficiency	Yokota 96
CNGB3, ACHM3; 262300, 605080	8q21.3	recessive achromatopsia Pingelapese; protein: cone cyclic nucleotide-gated cation channel beta 3 subunit [LocusLink]	linkage mapping; includes total color blindness, photophobia and nystagmus; European and American families, and 4-10% of Pingelapese on the Eastern Caroline Islands; protein generates cone electrical response; common 1148delC mutation; CNGB3 accounts for 40-50% of achromatopsia cases whereas CNGA3 accounts for 20-30% and GNAT2 accounts for a minor fraction; same as *cd* in Alaskan Malamute and German Pointer dogs	Kohl 00; Kohl 02; Milunsky 99; Sidjanin 02; Sundin 00; Winick 99
VMD1; 153840	not 8q24	dominant MD, atypical vitelliform	linkage exclusion; linked to GPT but later excluded	Daiger 97; Ferrell 83; Leach 96; Sohocki 97

Chromosome 9

Symbol; OMIM Number	Location	Disease; Protein	Mapping Method; Comments	References
RP21; 601850	not 9q34-qter	dominant RP with sensorineural deafness	linkage mapping; later mapped to MTTS2 in mitochondrion; 'RP21' withdrawn	Kenna 97; Mansergh 99

Chromosome 10

Symbol; OMIM Number	Location	Disease; Protein	Mapping Method; Comments	References
PHYH, PAHX, RDPA; 266500, 602026	10p13	recessive Refsum disease; protein: phytanoyl-CoA hydroxylase [LocusLink]	homozygosity mapping, cloned gene; symptoms include RP, peripheral neuropathy and cerebellar ataxia; same proteins with different names	Jansen 97; Jansen 97a; Mihalik 97; Nadal 95
RNANC; 221900	10q21	recessive nonsyndromal congenital retinal nonattachment	homozygosity mapping; 1% prevalence in isolated Iranian population	Ghiasvand 98; Ghiasvand 00
PCDH15, USH1F; 602083, 605514	10q21.1	recessive Usher syndrome, type 1f; protein: protocadherin 15 [LocusLink]	homozygosity mapping, cloned gene; mapping in inbred Hutterite family, mutations in Pakistani families; distinct from USH1D; same as mouse waltzer (*av*) with balance and hearing loss only	Ahmed 01; Alagramam 01; Alagramam 01a; Wayne 97
CDH23, DFNB12, USH1D; 601067	10q22.1	recessive Usher syndrome, type 1d; recessive deafness without RP; protein: cadherin-like gene 23 [LocusLink]	homozygosity mapping, cloned gene; CDH23 is expressed in retina and cochlea; cadherins are intercellular adhesion proteins; same as *v* waltzer deafness mouse; consanguineous Cuban, Indian, Pakistani and Turkish families; may cause 56% of Usher syndrome and 5% of recessive nonsyndromic deafness	Astuto 02; Bolz 01; Bork 01; Di Palma 01; Wayne 96
RGR; 600342	10q23.1	recessive RP; dominant choroidal sclerosis; protein: RPE-retinal G protein-coupled receptor [LocusLink]	cloned gene; protein is rhodopsin homolog found in RPE and Müller cells exclusively but, in inverse of rhodopsin, binds all-*trans* retinal which light converts to 11-*cis* retinal	Chen 96; Morimura 99a
RBP4; 180250	10q23.33	recessive RPE degeneration; protein: retinol-binding protein 4 [LocusLink]	cloned gene; RPE atrophy with night blindness and reduced visual acuity; carrier protein for serum retinol	Seeliger 99
PAX2, ONCR; 120330, 167409	10q24.31	dominant renal-coloboma syndrome; protein: paired homeotic gene 2 protein [LocusLink]	cloned gene; optic nerve colobomas with renal abnormalities; similar malformations in *Pax2(1Neu)* mouse mutation	Favor 96; Sanyanusin 95; Sanyanusin 95a
OAT; 258870	10q26.13	recessive gyrate atrophy; protein: ornithine aminotransferase [LocusLink]	cloned gene; many mutations reported	Valle 00

Chromosome 11

Symbol; OMIM Number	Location	Disease; Protein	Mapping Method; Comments	References
AA; 108985	11p15	dominant atrophia areata; dominant chorioretinal degeneration, helicoid	linkage mapping	Fossdal 95

USH1C, DFNB18; 276904, 605242	11p15.1	recessive Usher syndrome, Acadian; recessive deafness without RP; protein: harmonin [LocusLink]	linkage mapping; harmonin is a PDZ-containing protein expressed in inner ear sensory hair cells; contiguous gene syndrome includes deafness, hyperinsulinism and enteropathy; possibly same as *rd5* mouse; nonsyndromic deafness may involve alternately spliced isoforms unique to inner ear	Ahmed 02; Ayyagari 95; Bitner-Glindzicz 00; Heckenlively 95; Keats 94; Noun 93; Nouri 94; Ouyang 02; Smith 92; Verpy 00
EVR3; 605750	11p13-p12	dominant familial exudative vitreoretinopathy	linkage mapping; large Scottish family	Downey 01
ROM1; 180721	11q12.3	dominant RP; digenic RP with RDS; protein: retinal outer segment membrane protein 1 [LocusLink]	cloned gene; compound heterozygote with peripherin/RDS; dominant RP is rare and doubtful	Bascom 92; Bascom 92a; Bascom 93; Bascom 93a; Bascom 95; Dryja 97; Kajiwara 94; Martínez-Mir 97a; Nichols 94; Sakuma 95
VMD2; 153700	11q12.3	dominant MD, Best type; protein: bestrophin [LocusLink]	linkage mapping, cloned gene; retina-specific expression; protein localizes to the basolateral plasma membrane of the RPE and functions as a novel, transmembrane, oligmeric chloride channel; lipofuscin accumulation may be secondary to abnormal ion flux; 1 to 2% of AMD cases may have late-onset VMD2 mutations	Forsman 92; Graff 94; Lotery 00a; Petrukhin 98; Marmorstein 00; Marquardt 98; Nichols 94; Stone 92a; Sun 02; Wadeilus 93; Weber 93; Weber 94a; Weber 94c; Zhaung 93
FZD4, EVR1,FEVR; 133780, 604579	11q14.2	dominant familial exudative vitreoretinopathy; protein: frizzled-4 Wnt receptor homolog [LocusLink]	linkage mapping, cloned gene; Criswick-Schepens syndrome; distinct from VRNI; protein is a 7 transmembrane-spanning member of the Wnt (*Drosophila* wingless) receptor signaling pathway, possibly invloved in retinal angiogenesis	Li 92; Li 92a; Müller 94; Robitaille 02
BBS1; 209900, 209901	11q13	recessive Bardet-Biedl syndrome; protein: BBS1 protein [LocusLink]	linkage mapping, cloned gene; approximately 40% of BBS families; ubiquitously-expressed gene of unknown function but weak similarity to BBS2; common Met390Arg mutation; evidence does not support triallelic inheritance with BBS2, BBS4 or MKKS	Beales 97; Bruford 97; Cornier 95; Katsanis 99; Katsanis 01; Leppert 94; Mykytyn 02; Woods 99; Young 99a
VRNI; 193235	11q13	dominant neovascular inflammatory vitreoretinopathy	linkage mapping; distinct from EVR1	Stone 92
MYO7A, DFNB2, USH1B; 276903, 600060	11q13.5	recessive Usher syndrome, type 1; recessive congenital deafness without RP; recessive atypical Usher syndrome (USH3-like); protein: myosin VIIA [LocusLink]	linkage mapping, cloned gene; MY07A, an unconventional myosin, is a common component of cilia and microvilli; same as *sh1* shaker-1 mouse (but no RP) and *mariner* zebrafish; possible digenic deafness with USH3A	Adato 97; Adato 99; Bonné-Tamir 94; El-Amraoui 96; Ernest 00; Gibson 95; Kelley 97; Kimberling 92; Lévy 97; Liu 97; Liu 97a; Liu 97b; Liu 98; Smith 92; Weil 95; Weil 97; Weston 95; Weston 96; Wolfrum 98
C1QTNF5, CTRP5	11q23.3	dominant MD, late onset; protein: C1q and tumor necrosis-related protein 5 collagen [LocusLink]	linkage mapping, cloned gene; common mutation (Ser163Arg) found in 7 of 14 families with late-onset	Hayward 03

			retinal degeneration (L-ORD), a possible model for AMD; C1QTNF5 protein is a small collagen secreted by RPE, a possible constituent of Bruch's membrane	

Chromosome 12

Symbol; OMIM Number	Location	Disease; Protein	Mapping Method; Comments	References
COL2A1, AOM, STL1; 108300, 120140, 132450, 143200, 183900, 200610	12q13.11	dominant Stickler syndrome, type I; dominant Wagner syndrome; dominant epiphyseal dysplasia; protein: collagen, type II, alpha 1 [LocusLink]	linkage mapping, cloned gene; mutations in COL2A1 cause a variety of symptoms including facial-skeletal abnormalities, sensorineural hearing loss, and multiple ocular disorders such as glaucoma, myopia, retinal detachment and retinal degeneration (Stickler syndrome); symptoms vary considerable between individuals and may be limited to retinal or vitreoretinal findings alone, such as rhegmatogenous retinal detachment; see also COL11A1	Francomano 87; Go 03; Lee 89; Snead 99
RDH5, RDH1; 136880, 601617	12q13.2	recessive fundus albipunctatus; recessive cone dystrophy, late onset; protein: 11-*cis* retinol dehydrogenase 5 [LocusLink]	cloned gene; stationary night blindness with subretinal spots and delayed dark adaptation; protein is an RPE microsomal enzyme involved in converting 11-*cis* retinol to 11-*cis* retinal; extremely delayed rod and cone resensitization in null mutation	Cideciyan 00; Nakamura 00; Simon 96; Yamamoto 99

Chromosome 13

Symbol; OMIM Number	Location	Disease; Protein	Mapping Method; Comments	References
RB1; 180200	13q14.2	dominant germline or somatic retinoblastoma; benign retinoma; pinealoma; osteogenic sarcoma; protein: retinoblastoma protein 1 [LocusLink]	deletion mapping, cloned gene; requires 'second hit' loss of heterozygosity; 5 to 10% inherited, 20 to 30% new mutation, remainder sporadic; preferential loss of maternal chromosome; protein is cell-cycle regulatory element	Dryja 89; Francke 76; Friend 86; Knudson 71; Lee 87; Lohmann 96; Mancini 94; Sparkes 83; Toguchida 93
RHOK, RK; 180381	13q34	recessive CSNB, Oguchi type; protein: rhodopsin kinase [LocusLink]	cloned gene; several mutations in Japanese	Cideciyan 98; Khani 98; Maw 98; Yamamoto 97
STGD2; 153900	not 13q34	dominant MD, Stargardt type	linkage mapping; cloned gene; large American family, later remapped to ELOVL4 on 6q11	Zhang 94; Zhang 01

Chromosome 14

Symbol; OMIM Number	Location	Disease; Protein	Mapping Method; Comments	References
ACHM1, RMCH; 216900	14	recessive rod monochromacy or achromatopsia	uniparental isodisomy; total color blindness or 'day blindness'	Pentao 92
RP16	not 14	recessive RP	linkage mapping; withdrawn by senior author; 'RP16' withdrawn	Bruford 94
MCDR4	14q	dominant MD, North Carolina-like with progressive sensorineural hearing loss	linkage mapping; English family	Francis 03
NRL, RP27; 162080	14q11.2	dominant RP; protein: neural retina lucine zipper [LocusLink]	linkage mapping, cloned gene; NRL is a retinal transcription factor which interacts with CRX, promotes transcription of rhodopsin and other retinal genes, and is required for rod photoreceptor development	Bessant 99; Farjo 97; Mears 01; Rehemtulla 96; Swaroop 92; Yang-Feng 92
RPGRIP1, LCA6; 605446	14q11.2	recessive Leber congenital amaurosis; protein: RPGR-interacting protein 1 [LocusLink]	cloned gene; mutations in 6% of patients; RPGRIP1 protein interacts with RPGR, with species specific colocalization (rod and cone outer segments in humans, connecting cilia in mice)	Boylan 00; Dryja 01; Hong 01; Mavlyutov 02; Roepman 00
LCA3; 604232	14q24	recessive Leber congenital amaurosis	homozygosity mapping; consanguineous Saudi Arabian family	Stockton 98
USH1A, USH1; 276900	14q32	recessive Usher syndrome, French	linkage mapping	Kaplan 91; Larget-Piet 94
TTC8, BBS8; 209900, 608132	14q32.11	recessive Bardet-Biedl syndrome; protein: tetratricopeptide repeat domain 8 [LocusLink]	cloned gene; TTC8 protein includes a prokaryotic domain, *pilF*, involved in pilus formation, localizes to ciliated structures such as the connecting cilium in photoreceptors, and interacts with PCM1, a protein involved in ciliogenesis; thus BBS proteins play a role in basal body - ciliary function; multiple BBS8 families, one with random left-right body axis symmetry	Ansley 03

Chromosome 15

Symbol; OMIM Number	Location	Disease; Protein	Mapping Method; Comments	References
NR2E3, ESCS, PNR; 268100, 604485	15q23	recessive enhanced S-cone syndrome; recessive RP in Portuguese Crypto Jews; Goldmann-Favre syndrome; protein: nuclear receptor	cloned gene; symptoms include increased blue sensitivity, night blindness and retinal degeneration consistent with increased	Gerber 00; Haider 00; Haider 01; Kobayashi 99; Kaplan 99; Sharon 03

		subfamily 2 group E3 [LocusLink]	density/sensitivity of blue (S wavelength) cones, a novel gain-of-function disorder; may include clumped pigmentary retinal findings; protein is a ligand-dependent transcription factor; same as *rd7* mouse	
(MRST); 602685	15q24	recessive retardation, spasticity and retinal degeneration	linkage mapping; inbred Pakistani family	Mitchell 98
BBS4; 600374	15q24.1	recessive Bardet-Biedl syndrome; protein: BBS4 protein [LocusLink]	homozygosity and linkage mapping; approximately 3 to 6% of BBS families; protein similar to O-linked N-acetylglucosamine transferases involved in signal transduction in plants and animals; involved in triallelic inheritance: two BBS2 alleles and a third BBS1, BBS4 or MKKS allele	Beales 97; Bruford 97; Carmi 95; Katsanis 01; Katsanis 02; Mykytyn 01
RLBP1, CRALBP; 180090	15q26.1	recessive RP; recessive Bothnia dystrophy; recessive retinitis punctata albescens; recessive Newfoundland rod-cone dystrophy; protein: cellular retinaldehyde-binding protein [LocusLink]	cloned gene; consanguineous Indian family, Swedish families, Newfoundland isolate and others	Burstedt 99; Eichers 02; Maw 97; Morimura 99

Chromosome 16

Symbol; OMIM Number	Location	Disease; Protein	Mapping Method; Comments	References
ABCC6, ARA, MRP6, PXE; 177850, 264800, 603234	16p13.11	recessive pseudoxanthoma elasticum; pseudoxanthoma elasticum, dominant; protein: ATP-binding casette, subfamily C, member 6 [LocusLink]	linkage mapping, cloned gene; symptoms include progressive abnormalities in skin, retinal Bruch membrane and arteries leading to hemorrhage, calcification and vascular changes, with retinal angioid streaks; may be an extracellular transport protein; ABCC6 mutations in 60 to 80% of patients	Bergen 00; Le Saux 00; Le Saux 01; Ringpfeil 00; Struk 97; van Soest 97
RP22; 602594	16p12.3-p12.1	recessive RP	homozygosity mapping; Indian families	Finckh 98
CLN3, JNCL; 204200	16p11.2	recessive Batten disease (ceroid-lipofuscinosis, neuronal 3), juvenile; protein: Batten disease protein [LocusLink]	linkage mapping, cloned gene; symptoms include early-onset retinal pigmentary degeneration with later mental deterioration; protein is integral to Golgi membranes	Batten Disease 95; Eiberg 89; Gardiner 90; Kremmidiotis 99; Mitchison 95; Mitchison 95a; Mitchison 97; Munroe 97
BBS2; 209900	16q12.2	recessive Bardet-Biedl syndrome, type 2; protein: BBS2 protein [LocusLink]	linkage mapping, cloned gene; large Bedouin family and approximately 20% of BBS families; protein of unknown function with sequence similarity to BBS7; may require triallelic	Beales 97; Beales 01; Bruford 97; Katsanis 01; Kwitek-Black 93; Nishimura 01; Woods 99

			inheritance: two BBS2 alleles and a third BBS1, BBS4 or MKKS allele	
CNGB1, CNCG2, CNCG3L, GAR1, GARP; 600724	16q13	recessive RP; protein: rod cGMP-gated channel beta subunit [LocusLink]	homozygosity mapping, cloned gene; consanguineous French family; CNGB1 encodes a complex transcription unit with at least 6 non-overlapping transcripts, one of which is the disease gene in this case	Ardell 00; Bareil 01
CDH3, CDHP, PCAD; 114021, 601553	16q22.1	recessive MD, juvenile with hypotrichosis; protein: cadherin 3, type 1, placental [LocusLink]	homozygosity mapping, cloned gene; mutations found in two extended, unrelated, consanguineous Arab Israeli (Druze) families; invloves early hair loss followed by progressive macular degeneration culminating in blindness; cadherins are calcium-dependent cell-cell adhesion factors	Indelman 02; Sprecher 01

Chromosome 17

Symbol; OMIM Number	Location	Disease; Protein	Mapping Method; Comments	References
CACD; 215500	17p13	dominant central areolar choroidal dystrophy	linkage mapping	Hughes 98; Lotery 96
PRPF8, RP13, PRPC8; 600059	17p13.3	dominant RP; protein: human homolog of yeast pre-mRNA splicing factor C8 [LocusLink]	linkage mapping, cloned gene; South African and European families; protein is a highly-conserved, ubiquitously-expressed member of the U4/U6-U5 tri-snRNP particle complex which includes HPRP3 (RP18) and PRPF31 (RP11)	Goliath 95; Greenberg 94; Kojis 96; Inglehearn 98; McKie 01; Tarttelin 96
AIPL1, LCA4; 604392, 604393	17p13.2	recessive Leber congenital amaurosis; dominant cone-rod dystrophy; protein: arylhydrocarbon-interacting receptor protein-like 1 [LocusLink]	linkage mapping, cloned gene; locus distinct from CORD5 and RP13; accounts for 10% of recessive LCA; expression limited to photoreceptors and pineal gland; protein may be involved in nuclear transport or chaperone activity and localizes to rods only, from inner segments through outer plexiform layer	Hameed 00; Sohocki 99; Sohocki 00; van der Spuy 02
GUCY2D, CORD6, LCA1, RETGC, RETGC1; 204000, 600179, 601777	17p13.1	recessive Leber congenital amaurosis; dominant cone-rod dystrophy; protein: retinal-specific guanylate cyclase [LocusLink]	linkage mapping, cloned gene; North African families and several mutations; same as chicken *rd/rd*; causes approximately 6% of LCA and at least 7% of dominant COD or CORD	Camuzat 95; Camuzat 96; Kelsell 97; Kelsell 98a; Lotery 00; Payne 01; Perrault 96; Perrault 98; Semple-Rowland 98
CORD5, RCD2; 600977, 601251	same as GUCY2D	dominant cone-rod dystrophy, progressive;	linkage mapping, mutation screening; locus remapped	Balciuniene 95; Payne 99; Small 95; Small 96; Udar 03

		recessive cone-rod dystrophy	and dominant-acting mutations in GUCY2D detected; a family with recessive CORD maps to this region too - may or may not be allelic	
CORD4	17q	cone-rod dystrophy	association with neurofibromatosis; presumed dominant like NF	Klystra 93
UNC119, HGR4; 604011	17q11.2	dominant cone-rod dystrophy; protein: human homolog of *C. elegans* unc119 protein [LocusLink]	cloned gene; missense mutation in one family; UNC119 is a photoreceptor synaptic protein homologous to *C. elegans* neuroprotein unc119; protein localizes to rod and cone ribbon synapses	Kobayashi 00
PDE6G, PDEG; 180073	17q21.1/12p12.3	mouse recessive retinal degeneration; protein: cGMP phosphodiesterase gamma subunit [LocusLink]	cloned gene; targeted disruption transgene	Dollfus 93; Tsang 95
RP17; 600852	17q22	dominant RP	linkage mapping; South African and Dutch families; PDEG excluded; same location as dog *prcd* progressive rod-cone degeneration; FSCN2 excluded	Acland 98; Bardien 95; Bardien-Kruger 99; den Hollander 99; Inglehearn 98
SANS, USH1G; 606943	17q24-q25	recessive Usher syndrome; protein: human homolog of mouse scaffold protein containing ankyrin repeats and SAM domain [LocusLink]	linkage mapping, cloned gene; consanguineous Pakistani family from Jordan; linkage region overlaps isolated deafness loci DFNA20 and DFNA26; mutations in mouse *Sans* cause Jackson shaker (*js*) phenotype with deafness and vestibular dysfunction; SANS associates with the USH1C protein as part of hair cell bundles	Kikkawa 03; Mustapha 02; Weil 03
FSCN2; 607643	17q25	dominant RP; protein: retinal fascin homolog 2, actin bundling protein [LocusLink]	cloned gene; mutations in 3% of Japanese patients with dominant RP; protein is a photoreceptor-specific paralog of fascin which crosslinks and bundles f-actin; distinct from RP17	Bardien-Kruger 99; Tubb 00; Wada 01

Chromosome 18

Symbol; OMIM Number	Location	Disease; Protein	Mapping Method; Comments	References
OPA4; 605293	18q12.2-q12.3	dominant optic atrophy, Kjer type	linkage mapping; American family of German descent; previously linked to Kidd blood group	Kerrison 99; Kivlin 83
CORD1; 600624	18q21.1-q21.3	cone-rod dystrophy; de Grouchy syndrome	deletion mapping; isolated case; symptoms include COD, retardation and hearing impairment	Manhant 95; Warburg 91

Chromosome 19

Symbol; OMIM Number	Location	Disease; Protein	Mapping Method; Comments	References
CRX, CORD2; 120970, 602225	19q13.32	dominant cone-rod dystrophy; recessive, dominant and *de novo* Leber congenital amaurosis; dominant RP; protein: cone-rod otx-like photoreceptor homeobox transcription factor [LocusLink]	linkage mapping, cloned gene; meiotic drive suggested; CRX also activates pineal genes; interacts with NRL; *Crx*-deficient mice have diminished circadian entrainment; causes approximately 3% of LCA	Bellingham 97; Evans 94; Evans 95; Freund 97; Freund 98; Furukawa 99; Gregory 94; Li 98; Lotery 00; Sohocki 98; Swain 97; Swaroop 99
OPA3, MGA3; 258501	19q13.32	recessive optic atrophy with ataxia and 3-methylglutaconic aciduria; protein: OPA3 protein [LocusLink]	linkage mapping, cloned gene; Iraqi-Jewish families; protein may play a role in mitochondrial processes; ubiquitously expressed, prominently in skeletal muscle, kidney and brain	Anikster 01; Nystuen 98
PRPF31, RP11, PRP31; 600138, 606419	19q13.42	dominant RP; protein: human homolog of yeast pre-mRNA splicing factor 31 [LocusLink]	linkage mapping, cloned gene; high frequency in British Isles (21%); bimodal, highly variable expression, perhaps influenced by alleles in *trans*; protein is a highly-conserved, ubiquitously-expressed member of the U4/U6-U5 tri-snRNP particle complex which includes HPRP3 (RP18) and PRPF8 (RP13)	Al-Maghtheh 94; Al-Maghtheh 96; Inglehearn 98; McGee 97; Vithana 98; Vithana 01

Chromosome 20

Symbol; OMIM Number	Location	Disease; Protein	Mapping Method; Comments	References
JAG1, AGS; 118450, 601920	20p12.2	dominant Alagille syndrome; protein: Jagged protein 1 [LocusLink]	deletion mapping, cloned gene; multiple affected organs including chorioretinal atrophy and retinal pigment changes; Jagged is the ligand for Notch proteins, involved in cell-cell interactions	Hol 95; Li 97; Oda 97; Oda 97a; Schnittger 89
MKKS, BBS6; 236700, 604896, 605231	20p12.2	recessive Bardet-Biedl syndrome; protein: McKusick-Kaufman syndrome protein [LocusLink]	linkage mapping, cloned gene; MKKS mutations also cause McKusick-Kaufman syndrome with multiple congenital and developmental anomalies in Old Order Amish families; protein has sequence similarity to chaperonins; often involved in triallelic inheritance: two BBS2 alleles and a third BBS1, BBS4 or MKKS allele	Beales 01; Katsanis 00; Katsanis 01; Slavotinek 00; Stone 98a; Stone 00

Chromosome 21

Symbol; OMIM Number	Location	Disease; Protein	Mapping Method; Comments	References
USH1E; 602097	21q21	recessive Usher syndrome, type 1	linkage mapping	Chäib 97

Chromosome 22

Symbol; OMIM Number	Location	Disease; Protein	Mapping Method; Comments	References
TIMP3, SFD; 136900, 188826	22q12.3	dominant Sorsby's fundus dystrophy; protein: tissue inhibitor of metalloproteinases-3 [LocusLink]	linkage mapping, cloned gene; model for ARMD; common British mutation; vitamin A reverses night blindness	Felbor 95; Felbor 97; Jacobson 95; Peters 95; Stöhr 95; Weber 94; Weber 94b; Wijesuriya 96

X Chromosome

Symbol; OMIM Number	Location	Disease; Protein	Mapping Method; Comments	References
RP23; 300424, 607480	Xp22	X-linked RP	linkage mapping; distinct from RP2 and RP3	Hardcastle 00
RS1, XLRS1; 312700	Xp22.13	retinoschisis; protein: retinoschisin [LocusLink]	linkage mapping, cloned gene; retinoschisin contains a large discoidin domain; expression is limited to photoreceptors but protein is secreted into the inner retina	Bergen 93a; Grayson 00; Huopaniemi 97; Retinoschisis 98; Sauer 97; Sieving 90
(- - -)	Xp21-q21	RP with mental retardation	linkage mapping; may be contiguous gene syndrome including RP2	Aldred 94
RP6; 312612	Xp21.3-p21.2	X-linked RP	linkage mapping; distinct from RP2 and RP3	Breuer 00; Musarella 90; Ott 90
DMD; 310200	Xp21.2-p21.1	Oregon eye disease (probably); protein: dystrophin [LocusLink]	cloned gene; exons 20-28 involved in retinal disease	D'Souza 95; Pillers 93; Ray 92
AIED, OA2; 300600	Xp11.4-q21	Åland island eye disease	linkage mapping; CACNA1F mutations in ÅIED-like patients but not the original ÅIED family	Alitalo 91; Glass 93; Schwartz 91; Wutz 02
COD4	Xp11.4-q13.1	X-linked progressive cone-rod dystrophy	linkage mapping; large Finish family	Jalkanen 03
OPA2; 311050	Xp11.4-p11.2	X-linked optic atrophy	linkage mapping; large Dutch family	Assink 97
NYX, CSNB1; 300278, 310500	Xp11.4	X-linked CSNB; protein: nyctalopin [LocusLink]	linkage mapping, cloned gene; nyctalopin is an extracellular glycosylphosphatidyl (GPI)-anchored member of the small leucine-rich	Bech-Hansen 00; Bergen 95; Boycott 98; Gal 89; Musarella 89; Pusch 00

			proteoglycan (SLRP) protein family; expressed in several tissues but more abundant in retina and kidney; NYX mutations are found in a majority of X-linked complete-CSNB patients	
CSNB4; 300071	same as NYX	X-linked CSNB	linkage mapping, mutation screening; mutation found in NYX; 'CSNB4' also refers to rhodopsin	Hardcastle 97; Pusch 00
RPGR, RP3; 300389, 312610	Xp11.4	X-linked RP, recessive; X-linked RP, dominant; X-linked CSNB; X-linked cone dystrophy 1; X-linked atrophic MD, recessive; protein: retinitis pigmentosa GTPase regulator [LocusLink]	linkage mapping, cloned gene; mutations are found in 70% of RP3 cases, with dominant mutations in ORF15 (a mutational hot spot); ortholog may cause XLPRA in Siberian husky dog; exceptionally heterogeneous, retina-specific alternate splicing; protein is similar to RCC1, and binds PDE-delta and RPGRIP1 with species-specific colocalization (rod/cone outer segments in humans, connecting cilia in mice); rare association with hearing loss and recurrent infections	Andréasson 97; Ayyagari 02; Bader 03; Buraczynska 97; Fujita 97; Hermann 96; Kirschner 99; Linari 99; Mavlyutov 02; Meindl 96; Musarella 90; Ott 90; Roepman 96; Roepman 96a; Rozet 02; Vervoort 00; Zeiss 00; Zito 03
COD1; 304020	same as RPGR	X-linked cone dystrophy 1	linkage mapping, mutation screening; locus remapped and deletions in ORF15 of RPGR detected	Bartley 89; Bergen 93; Dash-Modi 96; Demirci 02; Hong 94; Meire 94; Seymour 98; Yang 02
RP15; 300029	same as RPGR	X-linked RP, dominant	linkage mapping, mutation screening; locus remapped and *de novo* insertion in ORF15 of RPGR detected; 'RP15' withdrawn	McGuire 95a; Mears 00
PRD; 312550	Xp11.3-p11.23	retinal dysplasia, primary	linkage mapping; linked to Norrie disease, may be same locus	Ravia 93
NDP, EVR2; 310600, 305390	Xp11.3	Norrie disease; familial exudative vitreoretinopathy; Coats disease; protein: Norrie disease protein [LocusLink]	linkage mapping, cloned gene; expressed in multiple tissues, function unknown; some mutations cause FEVR but evidence of genetic heterogeneity; associated with retinopathy of prematurity; somatic mutation causes Coats disease	Berger 92; Berger 92a; Black 99; Chen 92; Chen 93; Chen 93a; Fuchs 94; Fuchs 96; Fullwood 93; Gal 85; Isashiki 95; Meindl 92; Meindl 95; Rehm 97; Schuback 95; Shastry 95; Shastry 97; Shastry 97a; Shastry 97b; Strasberg 95
CACNA1F, CSNB2, CSNBX2; 300071, 300110	Xp11.23	X-linked CSNB, incomplete; ÅIED-like disease; protein: L-type voltage-gated calcium channel alpha-1 subunit [LocusLink]	linkage mapping, cloned gene; founder mutation in Mennonites; CACNA1F mutations are found in 60 to 90% of X-linked incomplete-CSNB patients; retina-specific expression with synaptic localization of protein; mutations in ÅIED-like patients but not the original ÅIED family; associated with optic atrophy in a Japanese family	Aldred 92; Bech-Hansen 92; Bech-Hansen 98; Berger 95; Boycott 01; Morgans 01; Nakamura 03; Strom 98; Wutz 02
RP2; 312600	Xp11.23	X-linked RP; protein: novel XRP2 protein similar to human cofactor C	linkage mapping, cloned gene; human cofactor C is involved in beta-tubulin	Bhattacharya 84; Hardcastle 99; Mears 99; Schwahn 98; Teague 94; Thiselton 96

		[LocusLink]	folding; accounts for 10% of XlRP in European and North American families	
PGK1; 311800	Xq21.1	RP with myopathy; protein: phosphoglycerate kinase [LocusLink]	cloned gene; one case only - RP is not usually found with PGK deficiency	Tonin 93
CHM; 303100	Xq21.2	choroideremia; protein: geranylgeranyl transferase Rab escort protein 1 [LocusLink]	linkage mapping, cloned gene; ubiquitously expressed protein (REP2 can substitute); attaches isoprenoids to Rab (e.g., Rab 27) proteins	Andres 93; Beaufrère 96; Cremers 90; Nussbaum 85; Seabra 93; van Bokhoven 94; van Bokhoven 94a; van den Hurk 92; van den Hurk 97
TIMM8A, DDP, DDP2, DFN1; 300356, 304700, 311150	Xq22.1	optic atrophy with deafness-dystonia syndrome; protein: inner mitochondrial membrane translocase 8 homolog A [LocusLink]	linkage mapping, cloned gene; symptoms include progressive optic nerve atrophy, nerve deafness and dementia; also known as Mohr-Tranebjaerg or Jensen syndrome; protein involved in transport of metabolites into mitochondria	Jin 96; Koehler 99; Tranebjaerg 95
RP24; 300155	Xq26-q27	X-linked RP	linkage mapping; single large family; RP2, RP3 and RP15 excluded	Gieser 98
COD2, XLPCD; 300085	Xq27	X-linked progressive cone dystrophy, 2	linkage mapping	Bergen 97
OPN1LW, GCP, CBD; 303800	Xq28	deuteranopia and rare macular dystrophy in blue cone monochromacy with loss of locus control element; protein: green cone opsin [LocusLink]	cloned gene; one to five copies 3' to red pigment gene or more complex organization	Ayyagari 99; Nathans 86; Nathans 92; Neitz 95; Winderickx 92
OPN1MW, RCP, CBP; 303900	Xq28	protanopia and rare macular dystrophy in blue cone monochromacy with loss of locus control element; protein: red cone opsin [LocusLink]	cloned gene; Ala180Ser polymorphism with spectral shift	Ayyagari 99; Nathans 86; Nathans 92

Mitochondrion

Symbol; OMIM Number	Location	Disease; Protein	Mapping Method; Comments	References
KSS; 530000	mitochondrion	Kearns-Sayre syndrome including retinal pigmentary degeneration; protein: several mitochondrial proteins	sequencing; multiple large deletions	OMIM 2001; Puddu 93; Wallace 99
LHON, MTND1, MTND4, MTND6; 535000, 516000, 516003, 516006	mitochondrion	Leber hereditary optic neuropathy; protein: complex I, III or IV proteins	sequencing; three mutations (MTND1-3460, MTND4-11778 and MTND6-14484) account for 95% of European cases and one (11778) for 80% of Japanese cases; penetrance influenced by mtDNA haplotype; uncertain role of rare variants; spontaneous recovery possible	Brown 92; Brown 97; Hofmann 97; Howell 97; Howell 98; Huoponen 93; Mashima 93; Nikoskelainen 96; OMIM 2001; Riordan-Eva 95; Torroni 97; Wallace 88
MTTL1, DMDF; 520000, 590050	mitochondrion	macular pattern dystrophy with type II diabetes and deafness; protein: leucine tRNA 1 (UUA/G), nt 3230-3304 [LocusLink]	sequencing; one of two mitochondrial leucine tRNAs; often caused by heteroplasmic A3243G mutation; other mutations can	Bonte 97; Harrison 97; Massin 95; van den Ouweland 92

			cause a similar disease	
MTATP6, NARP; 516060, 551500	mitochondrion	RP with developmental and neurological abnormalities; Leigh syndrome; LHON; protein: complex V ATPase 6 subunit, nt 8527-9207 [LocusLink]	sequencing; symptoms include developmental delay, neuropathy, ataxia and RP, with or without optic atrophy; RP found primarily with T8993G (Leu156Arg) mutation	Holt 90; Lamminen 95; Santorelli 93; White 99
MTTH; 590040	mitochondrion	pigmentary retinopathy and sensorineural hearing loss; protein: histidine tRNA, nt 12138-12206 [LocusLink]	sequencing; Italian family with heteroplasmic mutation and variable additional findings; another MTTH mutation is associated with cardiomyopathy	Crimi 03
MTTS2; 590085, 601850, 180103	mitochondrion	RP with progressive sensorineural hearing loss; protein: serine tRNA 2 (AGU/C), nt 12207-12265 [LocusLink]	linkage mapping, sequencing; one of two mitochondrial serine tRNAs; Irish family; previously mapped to 9q as RP21	Mansergh 99